Determining the Mechanisms of Selective Advantage in Cultures of Human Pluripotent Stem Cells

By:

Christopher John Price

A thesis submitted in partial fulfilment of the requirements for the degree of
Doctor of Philosophy

The University of Sheffield
Faculty of Science
Department of Biomedical Science

March 2019

Acknowledgements

The work contained within this thesis is the culmination of a journey that has only been made possible due to the continual support and guidance from several people whom I cannot thank enough. Firstly, my supervisor Dr Ivana Barbaric. It has been a privilege to be your first PhD student. Your endless passion, enthusiasm and positivity showed me that though at times things can get tough, with the right approach you can always find a way through and this is perhaps the most valuable lesson I have learnt.

I would also like to thank Professor Peter Andrews. When I knocked on your office door at the end of my first year of undergraduate study, I never thought our discussion would result in me being where I am today. You provided me with the opportunity to discover what science is truly about and have been selfless with your time ever since, giving advice whenever needed and supporting my attendance at different conferences.

I must thank everyone in the Centre for Stem Cell Biology, members past and present, whom have offered encouragement and critically discussed genetic instability with me during my time in the lab. I am especially grateful to the great group of friends: Jason Halliwell, Dylan Stavish, Tom Frith, Oliver Thompson, and Holly Stainton who have stuck with me through all the highs and the moments of doubt. From this group a special thanks goes to Dylan Stavish for all his advice, support and just generally putting up with me especially during the analysis of the RNA sequencing data. You have all helped make my PhD an incredibly fun and enjoyable time.

To Becky, for all the long skype calls and messages through which you have shared this last year with me. You never failed to make me smile and have kept me grounded

Lastly, I would like to thank my family for their unconditional love and support. You have been with me every step of this journey and have each contributed in many different ways. To my mum, Kathryn, thank you for patiently listening to my all my thoughts during our evening walks. To my Grandma, Christine, your calm approach to finding solutions guided me through many of the challenges that arose along the way as well as the endless supply of cakes and cookies that were desperately needed on long days in the lab. My dad, Stephen, whom was a willing chauffeur on the days I couldn't face driving in. A big thanks to my sister, Vicky, whom despite being incredibly busy with her own PhD always found the time to talk things through and make me laugh. None of this would have been possible without all of you.

Abstract

The observation that human pluripotent stem cells (hPSCs) may acquire non-random genetic changes during prolonged culture is a major concern for their use in regenerative medicine and disease modelling. The predominant genetic changes observed in hPSCs include gains of whole or parts of chromosomes 1, 12, 17 and 20. Genetically variant cells possess a selective advantage over normal hPSCs that drives their ability to overtake normal cells and become the predominant cell within the culture. In this study, I generated a panel of genetically variant cell lines containing gains of individual or multiple karyotypic changes to investigate the mechanisms through which each of the commonly acquired chromosomes confers selective advantage. Using a series of experiments to compare proliferation, apoptosis and differentiation between karyotypically normal and variant cells I show that different chromosomes can confer selective advantage by improving different aspects of hPSC behaviour in culture. Alternatively, some chromosomes can confer selective advantage by affecting the same aspect of hPSC fate, however the genetic mechanisms that mediate the improved cellular phenotype could be different. Acquisition of additional karyotypic changes strengthens the growth phenotype of variant hPSCs. Gene expression analysis to identify potential genes that drive selective advantage in each of the variant hPSC lines revealed that gain of karyotypic abnormalities causes global changes in transcription. In addition, I show that cell competition functions as an extrinsic mechanism of selective advantage that is dependent on normal-variant hPSC interactions. In heterotypic cultures, normal cells are actively eliminated in a density-dependent manner by the presence of variant cells that possess significantly faster growth rates. Finally, I shed light onto potential mechanisms through which competitive cell fate could be determined in hPSCs cultures, providing a platform for future studies that may be used to design culture strategies that minimise the appearance of genetically variant hPSCs.

List of Abbreviations

Abbreviation	Meaning
(g)DNA	(genomic) Deoxyribonucleic acid
(h)ESC	(human) Embryonic Stem Cell
(h)iPSC	(human) induced Pluripotent Stem Cell
(h)PSC	(human) Pluripotent Stem Cell
2-DG	2-Deoxyglucose
ANOVA	One-way Analysis of Variance
APC	Adenomatous Polyposis Coli
ATP	Adenosine Triphosphate
BMP	Bone Morphogenetic Protein
CNV	Copy Number Variant
CPC	Chromosomal Passenger Complex
Ct value	Cycle Threshold value
DMEM	Dulbecco's Modified Eagle Medium
DMSO	Dimethyl sulfoxide
DSB	Double-Strand Breaks
E8	Essential 8
EB	Embryoid Body
EC	Embryonal Carcinoma
EDAC	Epithelial Defence Against Cancer
ER	Endoplasmic Reticulum
FACS	Fluorescence Activated Cell Sorting
FBS	Foetal Bovine Serum
FGF	Fibroblast Growth Factor
GDF	Growth and Differentiation Factors
GFP	Green Fluorescent Protein
GMP	Good Manufacturing Process
GO	Gene Ontology
GSK3	Glycogen Synthase Kinase 3
HR	Homologous Recombination

ISCI	International Stem Cell Initiative
KOSR	KnockOut Serum Replacement
LCR	Low-Copy Repeat
LRP	LDL Receptor-related Protein
MAP	Microtubule Associated Proteins
MAPK	Mitogen-Activated Protein Kinase
MCC	Mitotic Checkpoint Complex
MDCK	Madin-Darby Canine Kidney
MEF	Mouse Embryonic Fibroblast
NAHR	Non-Allelic Homologous Recombination
NF-κB	Nuclear Factor κB
NHEJ	Non-Homologous End-Joining
PBS	Phosphate Buffered Saline
PCA	Principal Component Analysis
PFA	Paraformaldehyde
PGRN	Pluripotency Gene Regulatory Network
PI3K	Phosphaditylinositol-3-kinase
qPCR	Quantitative Polymerase Chain Reaction
RFP	Red Fluorescent Protein
RNA	Ribonucleic Acid
ROCK	Rho-associated, coiled-coil containing protein kinase 1
SAC	Spindle Assembly Checkpoint
SARA	Small Anchor for Receptor Activation
SD	Standard Deviation
SEM	Standard Error of the Mean
SNP	Single Nucleotide Polymorphism
TGFβ	Transforming Growth Factor β
TRR	Toll-Related Receptor
v.hPSC	variant human Pluripotent Stem Cell

Contents Table

Table of Figures

1 <u>Introduction</u>

1.1 <u>Human pluripotent stem cells</u>

Human pluripotent stem cells (hPSCs) are a unique classification of cell that possess two defining properties, the ability to self-renew indefinitely and the potential to differentiate into any cell type of the adult body. These cells can be obtained either by explanting the inner cell mass of the blastocyst, embryonic stem cells (ESCs) (Thomson et al., 1998), or by direct reprogramming of somatic cells into the pluripotent state, induced pluripotent stem cells (iPSCs) (Figure 1.1) (Takahashi et al., 2007). The unique defining properties of hPSCs make them attractive tool for conducting basic biological research into human embryonic development as well as a promising source for use in regenerative applications (Zhu and Huangfu, 2013, Thies and Murry, 2015).

1.1.1 <u>Derivation of hESCs</u>

In 1998, Thomson *et al* successfully generated the first human embryonic stem cells by explanting the inner cell mass from blastocyst-stage human embryos, produced by *in vitro* fertilization, onto mitotically inactivated mouse embryonic fibroblasts (MEFs). In the presence of fibroblast growth factor and activin A, hESCs have the capacity to self-renew for long periods of time and retain the ability to differentiate into all three primary germ layers and are hence termed pluripotent (Thomson et al., 1998). Nearly 20 years since hESCs were first derived, now over a thousand hESCs of diverse genotypes have been registered worldwide, the vast majority of these lines are approved for research use only (Fraga et al., 2011, Seltmann et al., 2016, Kurtz et al., 2018). Translation into clinical applications has been hampered by issues ranging from ethical approval to safety concerns (Volarevic et al., 2018). Human embryonic stem cells for clinical use have to be obtained under stringent ethical guidelines and derived using Good Manufacturing Practice (GMP) (Unger et al., 2008). The original derivation techniques described by Thomson *et al* (1998) used an animal-based substrate and media supplemented with serum components that are difficult to define and risk assess. Advances in the field including, development of feeder-free substrates and fully chemically defined culture medias, have resulted in the evolution of GMP grade xeno-free

culture conditions that have been successfully used to generate high quality clinical grade hESC lines (Ye et al., 2017).

1.1.2 <u>Induced Pluripotent Stem Cells</u>

In 2007 the discovery of human induced pluripotent stem cells was heralded as a major breakthrough for the field of stem cell biology. Shinya Yamanaka and colleagues showed that ectopic expression of four key pluripotency-associated genes; Oct3/4 , Sox2, Klf4 and c-Myc, could reprogram somatic cells to a pluripotent state and thus termed induced pluripotent stem cells (iPSCs) (Takahashi et al., 2007, Takahashi and Yamanaka, 2006). The ability to reprogram cells opened the opportunity to create patient and disease specific stem cells for modelling disease and drug screening, as well as circumvented some of the major ethical issues regarding the sacrifice of human embryos to derive stable pluripotent stem cell lines (Kimbrel and Lanza, 2016).

Nonetheless, use of iPSCs comes with its own unique set of challenges and concerns. Primary amongst these is that the reprogramming process remains poorly understood. The original reprogramming method described by Yamanaka utilised a viral vector that delivered the transcription factors of the key pluripotency-associated genes by integration to the host genome (Takahashi et al., 2007). However, the efficiency of reprogramming was very low, and the use of viral vectors carried an associated tumorigenic risk. A greater understanding of the barriers of reprogramming have resulted in the development of more efficient non-integrating reprogramming methods that overcome many of the obstacles hindering their use in translational applications (Brouwer et al., 2016).

Several studies have compared iPSCs to ESCs to determine if they are identical cell populations. Some of these studies show that iPSCs and ESCs share nearly all of their global gene expression and DNA methylation, the small degree of variation observed was insufficient to distinguish between the two cell populations (Guenther et al., 2010, Bock et al., 2011). Whereas, other studies show that they possess genetic and epigenetic differences that reflect their origin and derivation resulting in a gene expression profile that is very similar but not identical (Chin et al., 2009, Marchetto et al., 2009, Kim et al., 2010). However,

epigenetic heterogeneity has also been shown to exist between different ESC lines as well as bias in differentiation potential (Martinez et al., 2012). Therefore, the current consensus within the stem cell field is that they should be regarded as overlapping cell populations that share distinct defining properties (Omole and Fakoya, 2018).
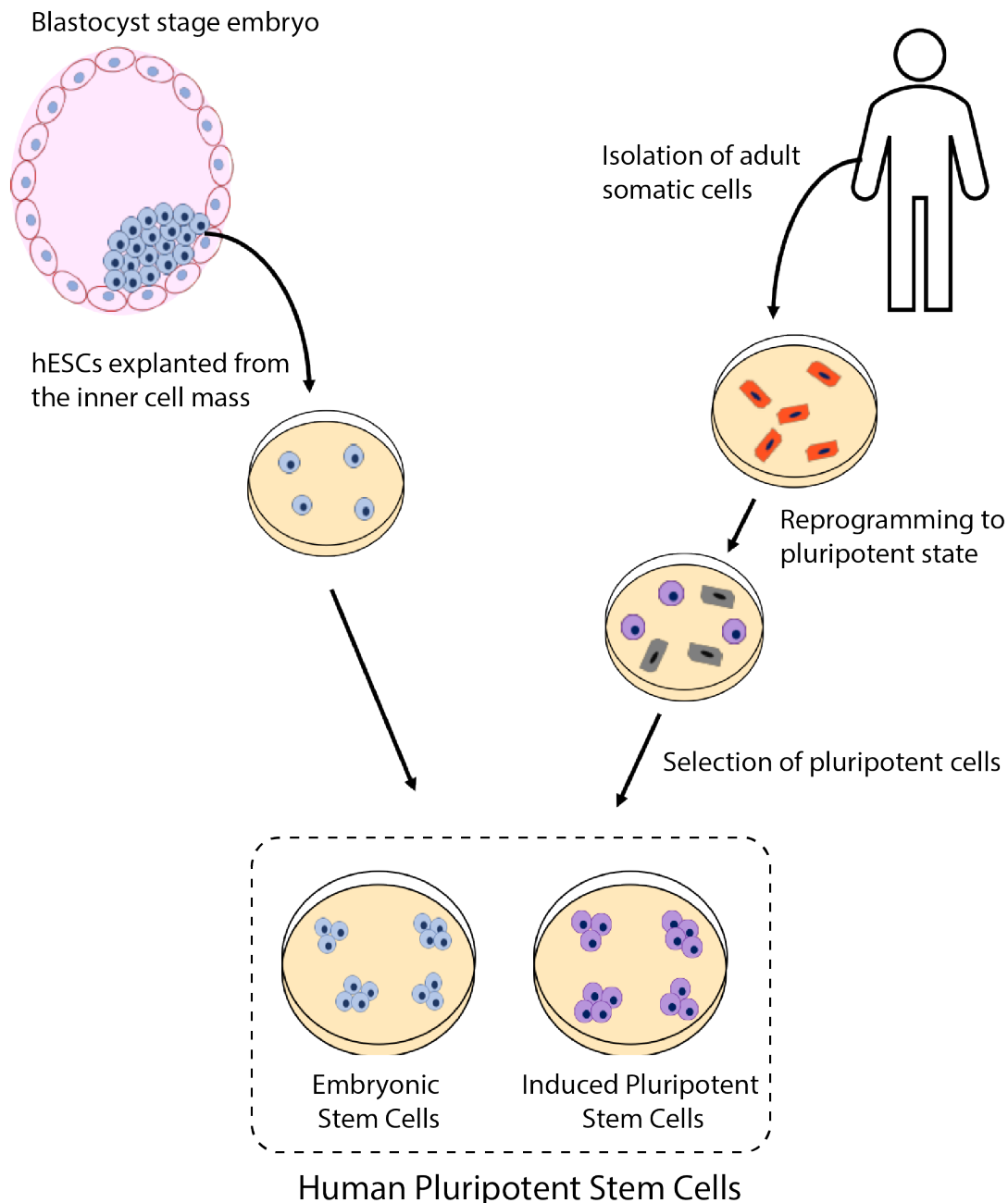
Figure 1.1 Derivation of human pluripotent stem cells.

Human pluripotent stem cells can be derived through two methods. In the first method cells from the inner cell mass of a blastocyst embryo are explanted into culture, hPSCs derived through this method are referred to as embryonic stem cells. Alternatively, adult somatic cells can harvested and then reprogrammed into a pluripotent state by the overexpression of 4 key pluripotency-associated genes; Oct3/4 , Sox2, Klf4 and c-Myc. The reprogrammed pluripotent cells are then selected for in preference to the original somatic cells, hPSCs derived using this method are referred to as induced pluripotent stem cells.

1.1.3 Molecular Markers of undifferentiated hPSCs

Since their discovery the number of hPSC lines has increased vastly worldwide. Numerous lines of different genetic backgrounds have been derived using a variety of techniques. This degree in variation has been proposed to lead the selection of hPSC lines with different properties (International Stem Cell et al., 2007). Generating a requirement for a set of molecular markers to define hPSC identify.

The first study to address this issue was undertaken by the International Stem Cell Initiative, a worldwide collaboration established to compare different hPSC lines and assess their translational potential into clinical applications (Andrews et al., 2005). In 2007, a first phase global study was completed that assessed a total of 59 hESC lines and produced a set of molecular markers consisting of cell-surface antigens and pluripotency-associated genes (International Stem Cell et al., 2007). As the field has developed and our understanding of the pluripotent state evolved this set of markers has been expanded and refined.

The cell surface markers consist of a wide range of antigens that recognise different classes of residues present on the membrane of hPSCs. They were first detected in human embryonal carcinoma (EC) cells; the stem cells of germ cell tumours and have since been used to identify stem cells in both EC and hPSC cultures. Amongst the panel of surface markers are the globoseries glycolipid antigens SSEA3 (Shevinsky et al., 1982) and SSEA4 that recognise sequential regions of the same glycolipid (Kannagi et al., 1983) and the keratin sulfate antigens TRA-1-60 and TRA-181 (Andrews et al., 1984a). These antigens are present on cells of the inner cell mass, the same population of cells within the blastocyst hESC lines are derived (Henderson et al., 2002). Expression of SSEA3 and SSEA4 is rapidly downregulated upon differentiation and typically correlates with loss of pluripotency (Fenderson et al., 1987, Draper et al., 2002, Tonge et al., 2011). Other surface markers include the alkaline phosphatase antigens TRA-2-54 and TRA-2-49 (Andrews et al., 1984b), as well as the protein antigens CD9 (Oka et al., 2002)and Thy1 (Draper et al., 2002).

Genes associated with the pluripotent state can also be used as markers of undifferentiated hPSCs, key amongst these are the transcription factors: *NANOG, POU5F1 (OCT4)* and *SOX2.* Multiple studies have reported their expression in blastocyst and downregulation during differentiation. However, they are also expressed during the differentiation of specific cell types and therefore cannot be used exclusively as markers of undifferentiated pluripotent stem cells and as such are referred to as "pluripotency associated genes". Together they interconnect to form the core components of a network of genes that regulates and stabilizes pluripotency (Boyer et al., 2005).

1.1.4   Molecular mechanisms governing hPSC fate decisions

Pluripotency is maintained by the coordinated activity of three core transcription factors; OCT4, SOX2 and NANOG, that together form the pluripotency gene regulatory network (PGRN). The PGRN cooperatively upregulates expression of other pluripotency factors as well as maintains signalling pathways required for differentiation in a primed yet dormant state. These core transcription factors form autoregulatory and feedforward loops that contribute to pluripotency and self-renewal. This network is modulated by multiple layers of regulatory input including, extrinsic growth factor signalling cues and intrinsic transcriptional and epigenetic modifications reviewed in (Li and Belmonte, 2017, Theunissen and Jaenisch, 2017).

Human pluripotent stem cells require provision of two extrinsic growth factors to maintain pluripotency; transforming growth factor β (TGFβ)/Activin/Nodal and basic fibroblast growth factor (FGF2) (James et al., 2005, Beattie et al., 2005, Xu et al., 2005). Supplied recombinantly, these growth factors allow hPSCs to be maintained without the presence of MEFs and serum based medias (Vallier et al., 2005). In hPSCs, FGF2 and its downstream signalling effectors activate transcription of genes associated with pluripotency and promote proliferation. Binding of FGF to its receptor tyrosine kinases increases the phosphorylation of the receptors intracellular domain which in turn results in the phosphorylation and activation of phosphaditylinositol-3-kinase (PI3K) (Armstrong et al., 2006). FGF activated PI3K/AKT signalling establishes conditions that promotes binding of Smad2/3 to pluripotency targets and induces the expression of NANOG. In contrast, low levels of PI3K/AKT signalling switches the activity of Smad2/3 to cooperate with β-catenin and induce mesoderm differentiation

(Singh et al., 2012). Finally, FGF2 has also been shown to promote proliferation and increase survival of hPSCs but the underlying mechanism has yet to be determined (Rao and Greber, 2017).

The TGFβ superfamily of morphogens is composed of two subgroups; TGFβ/Activin/Nodal family and the Bone Morphogenetic Protein (BMP)/Growth and Differentiation Factors (GDF) family. The signalling pathways of both subgroups are fundamentally important for a variety of roles including; embryonic development, cell growth and determining pluripotent stem cell fate (Moustakas and Heldin, 2009). TGFβ, Activin and Nodal are members of the TGFβ subgroup that have exhibited roles in maintaining the pluripotent state of hPSCs. Signalling of the TGFβ/Activin/Nodal subfamily is mediated by an evolutionary conserved signalling pathway. Binding of extracellular TGFβ ligands to type II TGFβ receptors recruits type I TGFβ receptors forming an activated receptor complex. Ligands of the subfamily bind to different transmembrane receptors, TGFβ bind to TGFBRI (type I) and TGFBRII/ALK5 (type II) receptors whereas Activin and Nodal bind ACVRIIA/IIB (type I) and ALK4/7 (type II) receptors (Huminiecki et al., 2009, Hinck, 2012). In an activated state, the receptor complex phosphorylates the receptor regulated smads (R-Smads), SMAD2/3, which are then released from the Small Anchor for Receptor Activation SARA (SARA) (Tsukazaki et al., 1998). Following release, SMAD2/3 form a trimeric complex with the common-mediator smad (Co-Smad) SMAD4, that translocates into the nucleus. In the nucleus SMAD3/4 are targeted to smad-binding-elements on the DNA where they function as transcriptional regulators that can activate or repress the transcription of downstream target genes (Nakao et al., 1997, Massague et al., 2005). NANOG and OCT4 are key targets of the TGFβ pathway and inhibition of SMAD2/3 phosphorylation in hPSCs downregulates their expression and promotes differentiation (Figure 1.2A)(James et al., 2005, Vallier et al., 2005, Xu et al., 2008, Mullen et al., 2011).
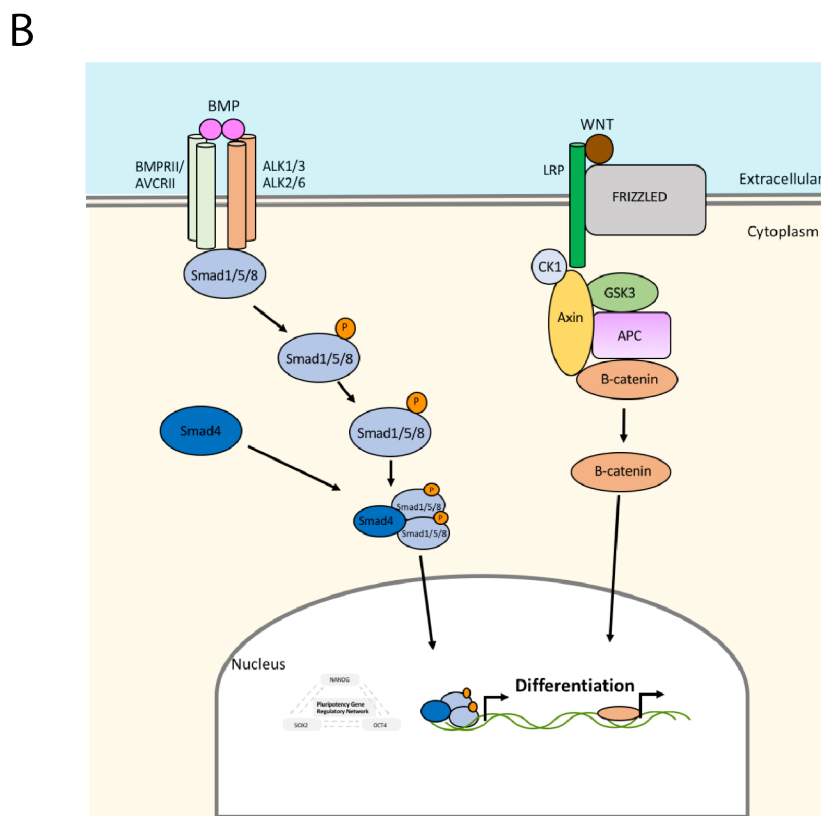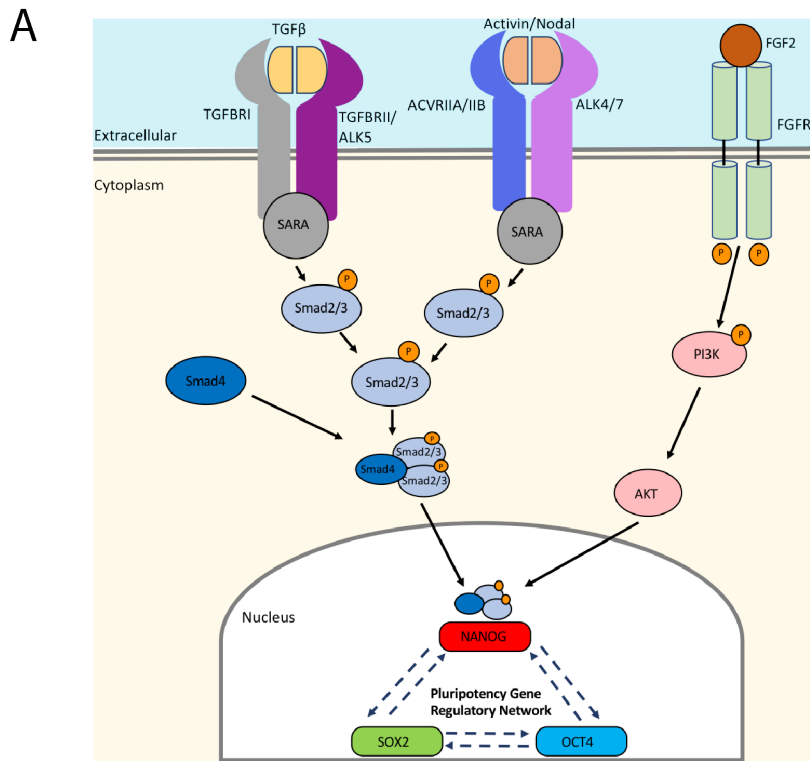
Figure 1.2 Signalling pathways in hPSC fates.

Schematic diagrams of the signalling pathways in human pluripotent stem cells that control (A) pluripotent state; FGF and TGFβ/Activin/Nodal and (B) effect differentiation; BMP and WNT.

The second subgroup of the TGFβ superfamily are the BMPs and GDFs, in contrast to the TGFβ/Activin/Nodal family, this group of ligands functions solely the regulate differentiation in hPSCs. The mechanism of action through which BMP signalling occurs in similar to the TGFβ pathway. BMP ligands binding to type I receptors (BMPRII/ACVRII) and type II receptors (ALK1/3 and ALK2/6) leads to phosphorylation of the R-Smads SMAD1/5/8. Association with SMAD4 forms a trimeric complex that translocates to the nucleus and regulates expression of downstream targets that promote differentiation. A key member of this family is BMP4, signalling mediated by BMP4 functions to repress the PGRN by downregulating core pluripotency genes, in particular SOX2 (Teo et al., 2012). In addition, BMP4 signalling further promotes differentiation by activating expression of genes associated with WNT signalling, in particular WNT3 which induces differentiation towards primitive streak lineages (Kurek et al., 2015).

The effects of WNT signalling in hPSCs has been described to predominantly function through activity of β-catenin in the canonical WNT pathway. In the absence of WNT signal, β-catenin is bound in the cytoplasm by a degradation complex composed of; adenomatous polyposis coli (APC), axin, glycogen synthase kinase 3 (GSK3) and casein kinase 1 (CK1). β-catenin is phosphorylated first by CK1 and then secondly by GSK resulting it its ubiquitylation and degradation. Binding of a WNT ligand to the receptor Frizzled and co-receptor LDL receptor-related protein (LRP) clusters the two receptors and activates WNT signalling. Clustering of Frizzled and LRP receptors recruits to degradation complex to LRP and inhibits the phosphorylation of β-catenin. Unphosphorylated β-catenin accumulates and translocates to the nucleus where it associates with co-activator complexes including; TCF-LEF, SMAD2/3 and SMAD4 and stimulates transcription of WNT target genes (Nusse and Clevers, 2017).

Modulation and crosstalk between the major signalling pathways is required for the differentiation of hPSCs towards specific lineages. Withdrawal of TGFβ and sustained FGF signalling results in neuroectoderm differentiation (Smith et al., 2008, Vallier et al., 2009). In contrast, loss of FGF signalling and continued TGFβ/Activin/Nodal activity is sufficient to promote mesendoderm differentiation, the final cell fate is dependent on the levels of activin A (Kempf et al., 2016). High concentrations of activin A promotes differentiation towards definitive endodermal whereas low concentrations promote mesoderm fate (Gadue et al.,

2006). Endoderm differentiation is also achieved through combined activity of Wnt and BMP signalling, whilst primitive endoderm and extraembryonic trophoblast can be formed through BMP-4 signalling in the absence of FGF or TGFβ (Figure 1.2B)(Teo et al., 2012, Sakaki-Yumoto et al., 2013).

1.2 Genetic Stability of hPSCs

1.2.1 Genetic Changes in hPSCs

Following derivation, hPSCs have a normal diploid karyotype that can be maintained for extended periods of time in culture (Amit et al., 2000, Reubinoff et al., 2000, Thomson et al., 1998). However, in the early 2000's several laboratories reported the acquisition of chromosomal abnormalities in late passage hSPCs lines that had been maintained for prolonged culture periods. The reports were not restricted to a particular cell line or laboratory and suggested that acquisition of karyotypic changes is a phenomenon which all hPSC lines can be subject to during culture (Draper et al., 2004, Cowan et al., 2004, Rosler et al., 2004). The early data reporting genetic changes was compiled by Baker and colleagues and revealed frequent gains in chromosomes 12 and 17 (Baker et al., 2007).

To catalogue the extent and breadth of genetic changes that occur in hPSCs, the International Stem Cell Initiative (ISCI), which was established to compare different hPSC lines worldwide and assess their translational potential into clinical applications, conducted a comprehensive global study to characterise the types of genetic changes and the frequency at which they occur. In this study 125 hESC lines and 11 hiPSC lines obtained from 38 laboratories in 19 countries were screened by either karyotype and/or high-resolution Single Nucleotide Polymorphism (SNP) array. Of the samples submitted, 120 hESC lines were provided at an early and late passage for karyotype analysis to determine whether they had either: acquired a genetic change during culture, remained normal or if they retained a genetic change that had already been acquired. Analysis revealed that the majority of cell lines (79/120 pairs, 66%) remained normal at early and late passage (Amps et al., 2011).

Amongst the remaining cell lines which showed abnormal karyotypes (41/120 pairs, 34%) late passage cells were approximately twice as likely to have a chromosome abnormality as early passage cultures. This data supported the notion that genetic changes are acquired in vitro and do not arise as a result of being abnormal at derivation (Amps et al., 2011).

The appearance of genetic abnormalities has continued to be monitored since the completion of the ISCI study. Overall, from the genetic changes reported gains of chromosomal regions are more common than losses, 73% of all changes involve gains of either a whole chromosome or duplications of specific regions (Baker et al., 2016). Loss of genetic material accounts for 21% of reported changes and the remaining 5% are balanced structural rearrangements in which there is no net gain or loss of genetic material. Aberrations have been observed in all chromosomes however the distribution of changes appears non-random with a higher frequency of abnormalities reported on particular chromosomes (Baker et al., 2016) .

Nearly 50% of all genetic changes include abnormalities in chromosomes 1, 12, 17 and 20. Most common amongst these is gain of chromosome 17, in which both the whole and parts of the chromosome have been reported as amplified. Changes in chromosome 12 are predominantly observed as gain via trisomy. Furthermore, unlike the other commonly altered chromosomes it is the only one in which either loss or balanced rearrangements are yet to be reported. In comparison, chromosome 1 is hardly ever reported as gained via trisomy and more frequently observed as gain of the long arm (1q) via unbalanced structural rearrangement (Baker et al., 2016). The most common change on chromosome 20 is a small structural variant, gain of 20q.11.21 copy-number variant (CNV) (Lefort et al., 2008, Martins-Taylor et al., 2011, Narva et al., 2010, Spits et al., 2008). This genetic change cannot be detected by karyotyping because its size is smaller than the 5Mb detectable resolution of routine G-banding. In the ISCI study, high resolution SNP arrays identified the 20q CNV in more than 20% of the 120 cell lines assessed, of these 22 had previously displayed a normal karyotype (Amps et al., 2011). The length of the 20q.11.21 is variable between different cell lines but always includes a minimal amplicon region spanning approximately 0.6MB that contains the gene BCL-XL which mediates its selective advantage (Avery et al., 2013).

Genetic changes that involve loss of chromosomes are much less common and very rarely occur as whole chromosome (monosomy). Loss via unbalanced structural rearrangements are most frequent and occur predominantly within three regions; 10p13-pter, 18q21-qter and 22q13-qter (Amps et al., 2011, Baker et al., 2016). To date, there are no studies which

have described the selective advantage conferred by loss of chromosomal regions and as such they remain poorly understood.

Furthermore, changes in chromosomes 4, 19 and 21 are rarely reported. It remains unknown why changes in these chromosomes are rarely observed (Baker et al., 2016). One possibility is that most changes involving these chromosomes are severely detrimental to hPSCs and thus upon acquisition cells rapidly undergo apoptosis. Another possibility is that gain or loss of genetic material does not confer any selective advantage to the cells therefore they exist transiently within the culture system and are eliminated upon passaging.

In addition to the large karyotypic and copy number variants described above, hPSCs have been shown to acquire single nucleotide point mutations that provide selective advantage. Detection of these genetic changes cannot be observed using cytogenetic techniques and requires next generation sequencing. In a study which complemented the work by the International Stem Cell Initiative, Merkle and colleagues performed whole-exome sequencing on 140 hPSCs lines at early and late passage obtained from laboratories across the world to identify mutations in the protein-coding genes that had been acquired during culture. In summary, their analysis identified 28 variants that were predicted to alter gene function. Of these 6 were missense mutations in the tumour suppressor gene *TP53* and corresponded to the four sites most commonly mutated in cancer. By monitoring cultures mosaic for *TP53* mutations over a series of passages they showed the proportion of *TP53*-genetically variant hPSCs increases until they constitute the majority of the population demonstrating *TP53* missense mutations also confer selective advantage (Merkle et al., 2017).

1.2.2 Mutation versus selection in hPSC cultures

Establishment of stable genetic changes in culture relies on the occurrence of two sequential events: mutation and selection. Mutation generates genetic change which can potentially provide the hPSC with an advantage over its genetically normal counterparts. This advantage must then be selected for through progressive culture (Figure 1.3).
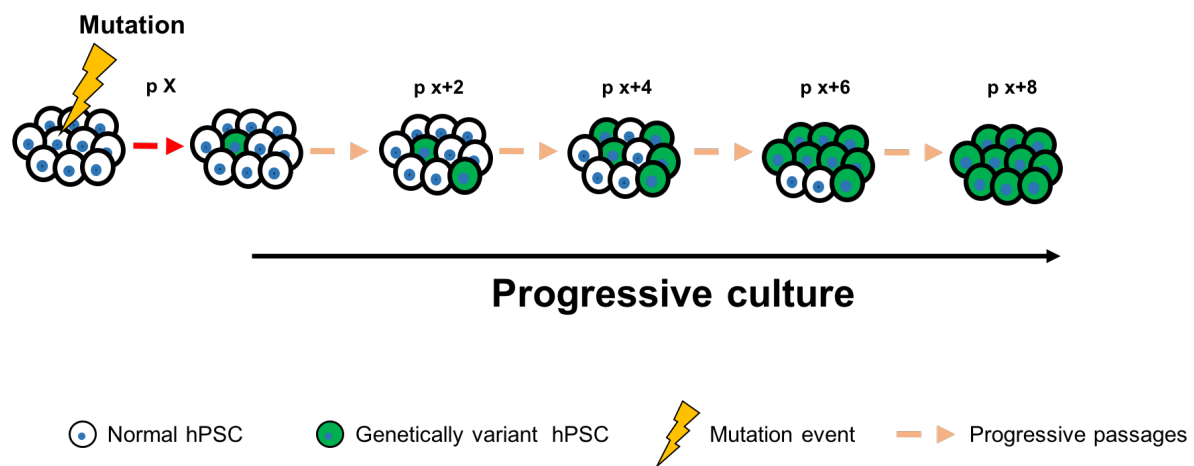
Figure 1.3 Mutation and selection.

During the culture of hPSCs random mutation events can occur that generate genetic changes within a cell. Mutations that provide a growth advantage over normal hPSCs can be selected for during progressive resulting in genetically variant cells overtaking and becoming the predominant cell type within the culture.

In vitro hPSCs are presented with three fate choices: firstly, they can differentiate to produce a specialised cell that is no longer pluripotent. Secondly, they can die, which is a common occurrence and exaggerated by passaging techniques which promote dissociation to single cells (Chen et al., 2010). Finally, they can self-renew to produce two pluripotent daughter cells (Figure 1.4A). A mutation that inhibits differentiation, supports cell survival or increases capacity to self-renew would provide the cell with a selective growth advantage over wild type hPSCs, which is subsequently selected for through progressive passages (Figure 1.4B).
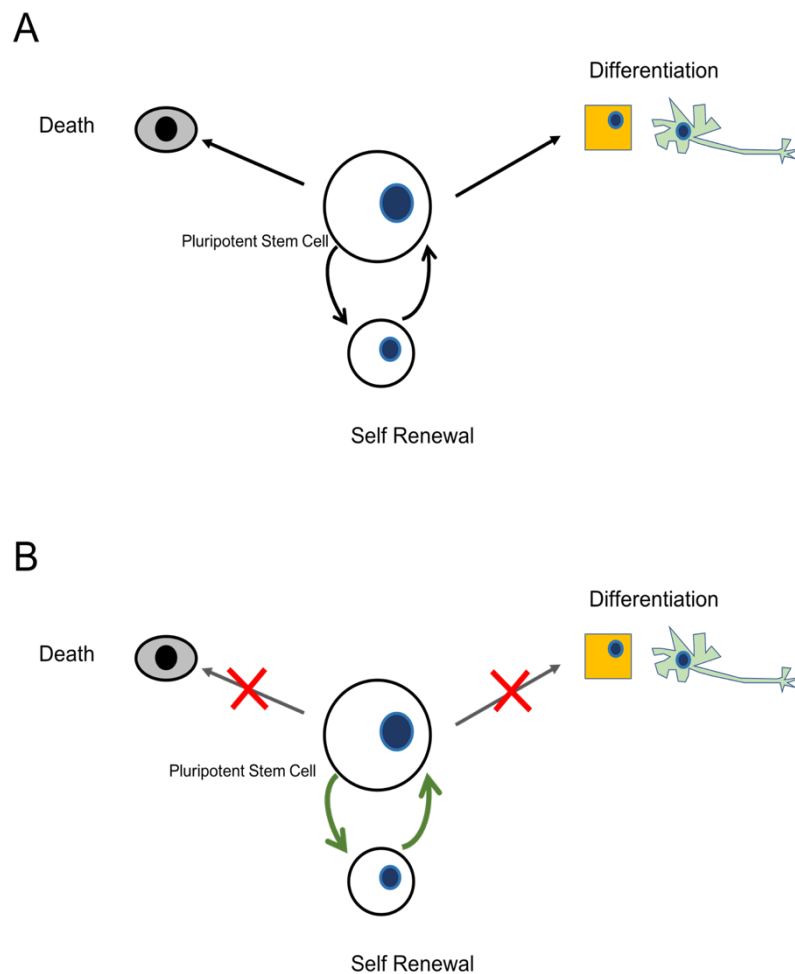
Figure 1.4 Human pluripotent stem cell fates.

(A) Pluripotent stem cells in culture have three possible fate decision; they can either self-renew and produce two equivalent pluripotent daughter cells, differentiate and produce a non-pluripotent cell with restricted differentiation potential or undergo apoptosis and die.

(B) Mutations that could provide pluripotent stem cells with a selective advantage by affecting cell fate would include those which restrict their capacity to differentiate, inhibit cell death or enhance self-renewal.

During culture, hPSCs are exposed to various selection pressures that may be exerted at different stages during their expansion. A significant selection pressure is proposed to occur during passage, hPSCs are typically passaged at low split ratios of approximately 1:3 suggesting that the majority of cells die between passages (Olariu et al., 2010). Genetically variant cells that possess increased resistance to cell death could escape the constraints that restrict expansion of normal cells generating a strong selective advantage that favours the variant hPSC population (Baker et al., 2007, Amps et al., 2011). The selective pressure of hPSC cultures was modelled in a study by Olariu *et al.* , by mixing 1% genetically variant hPSCs into cultures of normal hPSCs they showed that over a series of passages genetically variant cells overtake the normal cells within the culture resulting in a culture population which constitutes predominantly variant cells. Furthermore, the rate at which variant cells overtook the normal hPSC cultures differed upon the passaging technique suggesting that different culture strategies can alter the selective pressures exerted upon hPSCs in vitro (Olariu et al., 2010).

1.2.3   Potential causes of genetic changes in hPSCs

Though the spectrum of abnormalities in hPSCs has been extensively characterised the mechanisms that generate genetic change remain relatively unknown. However, due to the nature of the chromosomal abnormalities it is possible to speculate how they may have arisen. Genomic instability is promoted by two key mechanisms; abnormal mitosis and DNA damage (Ganem and Pellman, 2012). Defects that have been shown to cause whole chromosome gains are all associated with the physical separation of chromosomes during mitosis (Compton, 2011, Gordon et al., 2012). In contrast, translocations and copy number variations arise primarily via non-allelic homologous end joining or errors in DNA repair (Weckselblatt et al., 2015).

1.2.3.1   Translocations and Copy Number Variants

Structural aneuploidies, such as translocation and copy number variants, are a product of either non-allelic homologous recombination (NAHR) or non-homologous end-joining (NHEJ) (Orr et al., 2015). NAHR occurs at specific DNA regions on chromosomes with high levels of similarity called low-copy repeats (LCRs). This high level of sequence similarity can sometimes result in the misalignment of non-allelic copies of the LCRs during mitosis and subsequent cross-over of genetic material. Alignment of two LCRs on the same chromosome and in direct orientation produces duplications and deletions, whereas when LCRs on different chromosomes align this can result in chromosome translocations (Gu et al., 2008).

Structural aneuploidies can also arise as a result of incorrectly repaired double-strand breaks. Double-strand breaks (DSBs) are a severe form of DNA damage induced by collapse of the DNA replication fork or reactive species produced by metabolism (Sancar et al., 2004). Double strand breaks are repaired by either by homologous recombination (HR) which requires the sister chromatid as a template for DNA repair or non-homologous end-joining that directly ligates the damaged DNA ends. Human PSCs preferentially repair DSBs using the high fidelity HR, however because it requires the presence of a sister chromatid it is mostly used during late S/G2 phases of the cell cycle (Mao et al., 2008, Tichy, 2011). NHEJ is active during all stages of the cell cycle but is prone to make errors, these errors include the ligation of broken

DNA ends from different chromosomes to produce chromosome translocations (Figure 1.5) (Iarovaia et al., 2014, Chang et al., 2017, Ghezraoui et al., 2014).
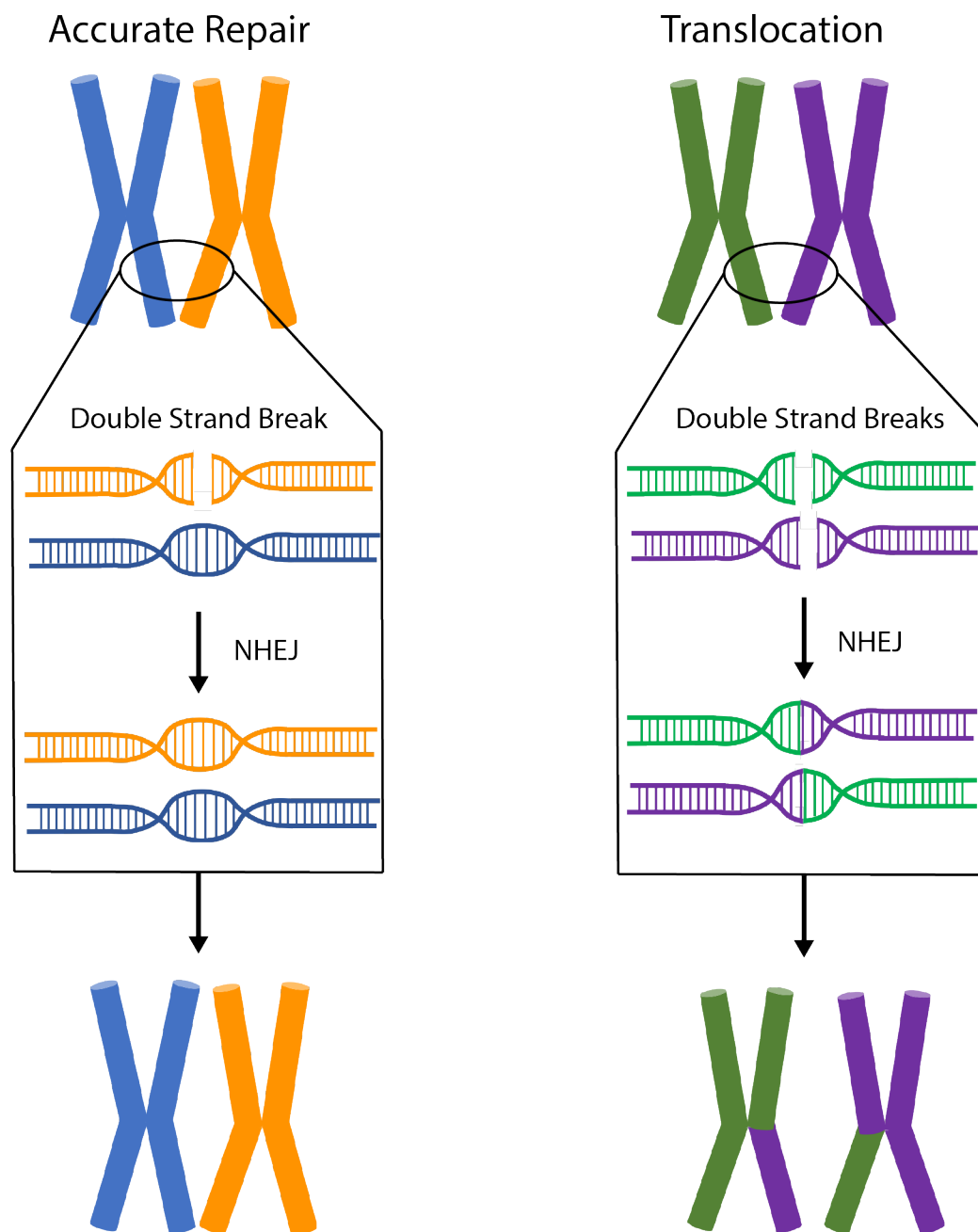
Figure 1.5 NHEJ and chromosome translocation.

Schematic diagram of how NHEJ functions during a single double strand break to accurately repair the damaged DNA. In the event of two double strand breaks occurring on different chromosomes, NHEJ can ligate the broken DNA from different chromosomes resulting in chromosome translocation.

1.2.3.2 Whole Chromosome Aberrations

Cells possess various surveillance mechanisms that monitor and maintain integrity of the genome. Key amongst them are those that function during the cell cycle to ensure the faithful transmission of genetic information from a dividing cell into its daughter progeny.

During mitosis the correct alignment and segregation of chromosomes is monitored by the Spindle Assembly Checkpoint (SAC) (Vleugel et al., 2012). The SAC is composed of two functional components; a sensory apparatus which monitors attachment of chromosomes to the mitotic spindle and an effector system called the Mitotic Checkpoint Complex (MCC) (Musacchio, 2015). The MCC is assembled from three SAC proteins; MAD2, BubR1 and Bub3 (Fraschini et al., 2001, Hardwick et al., 2000, Sudakin et al., 2001). During prometaphase, when chromosomes attach to the mitotic spindle, the MCC is recruited to unattached kinetochores where it binds to and inhibits the function of the active anaphase-promoting complex or cyclosome (APC/C^{Cdc20}). Inhibition is achieved by binding of MAD2 and BubR1 in the MCC to the APC activator Cdc20 (Musacchio, 2015). Following proper attachment of all kinetochores the MCC disassembles relieving its inhibition of APC/C^{Cdc20}, which subsequently promotes the ubiquitination and proteolysis of Cyclin B and Securin, initiating the metaphase to anaphase transition. Separation of sister chromatids is achieved through APC/C^{Cdc20} dependent activation of the cohesion-protease separase (Peters, 2002).

Maintaining the correct levels of proteins within these complexes is important for accurate function. In human cancers, it has been reported that mutations effecting the levels of SAC proteins impact on a cells ability to sustain mitotic checkpoint signalling. Weakened signalling of mitotic checkpoints maintains cell viability but permits the missegregation of chromosomes during division resulting in chromosomal instability and aneuploidy (Weaver and Cleveland, 2005).

Another major regulator of mitosis is the highly conserved Chromosomal Passenger Complex (CPC). The CPC is formed of an enzymatic core (Aurora B kinase) and a localization apparatus composed of the scaffolding protein inner centromere protein (INCEP) and the non-enzymatic subunits survivin and borealin. At different stages of mitosis the CPC is localised to specific regions where it regulates key events. During prometaphase the CPC is localised at

the inner centromere where it ensures the bi-orientation of chromosomes by resolving erroneous kinetochore-microtubule attachments (Carmena et al., 2012). In addition, Aurora B activity during this stage of mitosis also promotes recruitment of the SAC components to the kinetochore (Ditchfield et al., 2003, van der Waal et al., 2012). At the onset of Anaphase the CPC translocates to the cleavage furrow where it regulates the contractile machinery and contributes to axial shortening of chromosomal arms and cytokinesis (Ruchaud et al., 2007). Inhibition of Aurora B causes increased frequency of merotelic attachments; microtubules from opposing spindle poles attach to the same kinetochore (Hauf et al., 2003, Lampson et al., 2004, Knowlton et al., 2006). Merotelic attachments that persist during mitosis cause chromosome lagging which is one of the major mechanisms of aneuploid and chromosomal instability in cancer (Gregan et al., 2011)(Figure 1.6).

Previous work in our lab has shown that hPSCs are prone to mitotic errors and frequently show evidence of chromosome lagging or chromosomal bridges. Treatment of normal and 20q11.21 variant hPSCs with the Aurora B kinase inhibitor AZD1152 caused polyploidy in both lines but survival was predominantly restricted to the variant population (Adam Hirst, data unpublished). These observations suggest that errors in chromosomal segregation are a potential cause of genetic change in hPSCs (Figure 1.6). Furthermore, it is possible that gain of a genetic change that confers increased resistance to apoptosis may predispose hPSCs to acquire further genetic mutations.

Human PSCs have a substantially shorter a cell cycle time than somatic cells which is mainly due to a shortened G1 phase (Becker et al., 2006, Calder et al., 2013, Ghule et al., 2011) . In addition, they also lack function of the G1/S checkpoint that normally functions to prevent cells harbouring DNA damage from entering S phase (Desmarais et al., 2012, Filion et al., 2009). It is proposed that the unique properties of hPSCs make increase their susceptibility to acquire genetic changes. High proliferation rate and shortened cell cycle time provides more opportunity for errors in mitosis and DNA repair, whereas weakened checkpoint signalling permits the missegregation of chromosomes during replication (Weissbein et al., 2014).

A

Accurate Segregation

B

Chromosome Missegregation

whole chromosome
missegregation

Anaphase bridge

meroetelic attachment
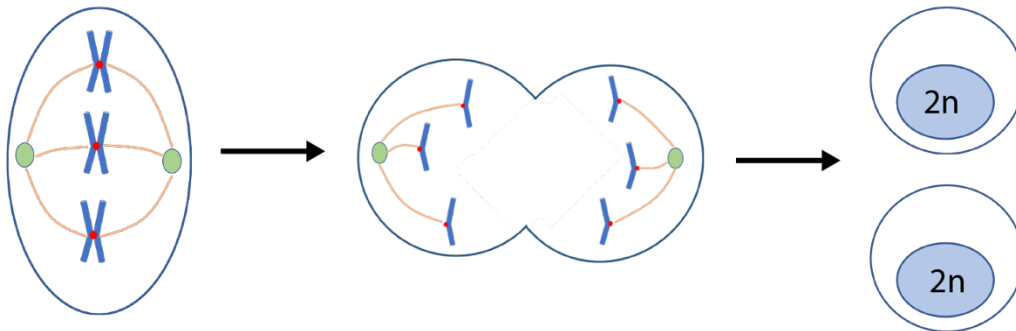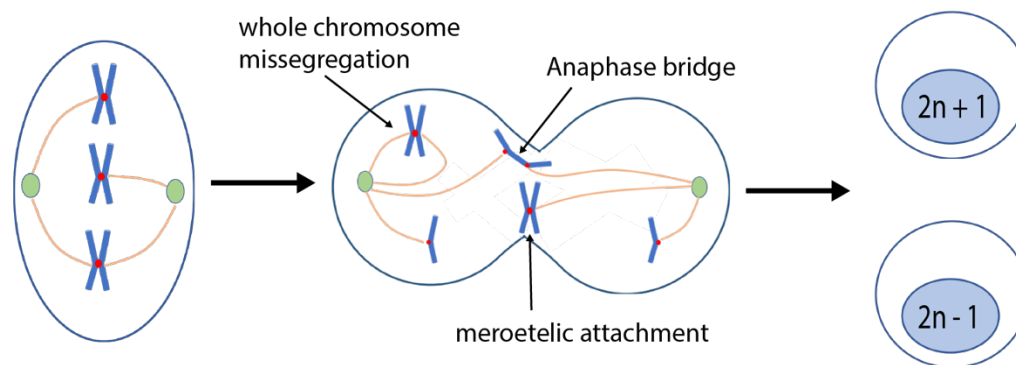
Figure 1.6 Mechanisms promoting whole chromosome aberrations.

Adapted from (van Jaarsveld and Kops, 2016, Santaguida and Amon, 2015) **(A)** During accurate segregation of chromosomes during mitosis, the centromeres of the sister chromatids are attached to the spindle fibres of opposing centrioles and segregated equally between the two future diploid cells (2n). **(B)** Chromosomes missegregation can happen through different errors during mitosis, these include; attachment of microtubules from the same spindle poles to sister chromatids of the same chromosome, merotelic attachment and the formation of anaphase bridges. The resulting mitotic division produces a daughter cell with gain of an additional chromosome (2n+1) and another daughter cell with chromosomal loss (2n-1).

1.2.4 Consequences of frequently acquired genetic changes

As described earlier hPSCs are presented with three basic cell fates during culture; self-renewal, differentiation and cell death. Unsurprisingly genetic variants have been reported in hPSCs that possess altered propensity towards each of these cell fates. These altered cell behaviours could potentially govern the selective advantage of genetically variant hPSCs in culture.

One of the concerns regarding addition of genetic changes for the future applications of hPSCs are reports of variant cells having a different propensity for differentiation towards a particular lineage compared to their normal counterparts. The unique potential of hPSCs to differentiate into any cell type of the adult body makes them a promising source for use in regenerative medicine therapies, disease modelling and drug screening (Corti et al., 2015, Zuba-Surma et al., 2011, Zuba-Surma et al., 2012). However, altered patterns of differentiation, that may reflect a change in the ability of variant cells to make certain derivates, could restrict their translational potential into clinical and pharmaceutical applications.

Altered patterns of differentiation have been reported in most of the commonly acquired variants. For example, gain of chromosome 17q is reported to reduce differentiation capacity towards the endodermal germ line lineage compared to diploid counterparts in an unbiased embryoid body differentiation (Fazeli et al., 2011). More recently directed differentiation of hPSCs to a dopaminergic neuronal fate has been shown to be affected by duplication of chromosome 17q. The authors of this study showed amplification of the WNT3 and WNT9B genes located in this region shifts the balance between the canonical and non-canonical WNT signalling pathways and promotes differentiation of variant cells into mesodiencephalic dopaminergic neurons in contrast to normal hPSCs that are inherently biased to a dorsal telencephalon fate (Lee et al., 2015).

Reports of altered differentiation potential are not restricted to chromosome 17. Gain of chromosome 1p has been linked to diminished *in vivo* differentiation capacity and bias towards ectoderm (Yang et al., 2010). Whilst hPSC cultures mosaic for 1q show enrichment

of the variant population during neural differentiation suggesting that selective advantage can also function during differentiation and is not limited to culture conditions that maintain the stem cell state (Varela et al., 2012).

Regarding self-renewal, some genetic changes have been shown to effect various aspects including proliferation and cloning efficiency. Variant hPSCs harbouring trisomy of chromosome 12 proliferate faster as a result of increased replication and also show greater sensitivity to inhibitors of DNA replication (Ben-David et al., 2014). Furthermore, it has been reported that some variant lines lose their dependency for the essential growth factor bFGF, indicating they can escape some of the constraints governed by the culture environment (Werbowetski-Ogilvie et al., 2009).

The percentage of cells plated that form viable stem cell colonies is referred to as the cloning efficiency. Normal hPSCs have relatively low cloning efficiency, approximately less than 2% (Enver et al., 2005). In comparison, variant hPSCs have been shown to have significantly increased cloning efficiency (Enver et al., 2005, Harrison et al., 2007, Barbaric et al., 2014). Previous work in our lab used time-lapse microscopy to characterise some of the bottlenecks that restrict generation of colonies from single cells. Time-lapse tracking of two normal cell lines and their variant counterparts in cloning assays revealed at least 3 specific bottlenecks: i) survival post-plating, ii) ability of cells to re-enter the cell cycle, and iii) survival of daughter cells following mitosis (Barbaric et al., 2014). The ability of variant cells to progress through these normally restrictive bottlenecks may arise from a reduced tendency to initiate an apoptotic response.

Normal hPSCs maintain components of the proapoptotic machinery in preactivated states and are primed to undergo apoptosis in response to genomic damage (Dumitru et al., 2012). This is proposed to act a quality control mechanism to prevent the propagation of mutated hPSCs, whereas hPSCs with multiple complex genetic abnormalities and variant sublines with gain of chromosome 20q show display reduced propensity to undergo apoptosis during culture (Avery et al., 2013, Yang et al., 2008). Acquired resistance to apoptosis in genetically variant cells is supported by the identification of a gene present in the minimal amplicon region of the common CNV gain 20q11.21. Of the thirteen genes encoded in this region only

3 are expressed in hPSCs; HM13, ID1 and BCL2L1 (Amps et al., 2011). BCL-XL, the predominant isoform of BCL2L1 in hPSCs with known anti-apoptotic function, was the only candidate gene that provided selective advantage to hPSCs when overexpressed. Furthermore, knockdown of BCL-XL in 20q11.21 CNV variant hPSCs abolished their selective advantage (Avery et al., 2013).

It has been proposed that the selective advantage of variant hPSCs is conferred through the overexpression of genes contained within the amplified genomic regions. Different advantageous properties may be conferred to variant cells depending on the function of the overexpressed genes. For example, overexpression of the pluripotency associated gene *NANOG*, located on chromosome 12, may improve the self-renewal properties of hPSCs. On the other hand, the antiapoptotic gene *BIRC5 (SURVIVIN*) is located on chromosome 17 and may provide variant cells with a selective advantage by restricting apoptosis. Identification of BCL-XL as the gene that drives selective advantage of 20q11.21 variant hPSCs supports this hypothesis.

However, the 20q11.21 is a fairly unique mutation with a defined minimal amplicon that contains only 3 the genes expressed in hPSCs. Chromosomal regions gained in the other most common abnormalities are much larger and contain a greater number of genes with the potential to effect cell fate. Evidence of global gene expression changes in cells with chromosome 12 trisomy suggest that selection is not mediated solely by individual or sets of driver genes (Ben-David et al., 2014). But rather, perhaps it is altered activity of molecular pathways, within which these genes function, that controls selective advantage.

A concern for hPSC derived technologies is that many of the commonly acquired genetic abnormalities are frequently observed in various cancers. Human embryonal carcinomas, the stem cells of germ cell tumours and malignant counterpart of hPSCs, always contain amplification of regions on chromosome 12p in addition to gains of other common chromosomes such as 17 (Rodriguez et al., 1993). Amplifications in chromosome 1q are one of the most common genetic changes reported in human neoplasm (Knuutila et al., 1998) and gain of multiple copies is proposed to provide cancer cells with a selective advantage (Puri L, 2014). Adding to concern, the gene expression profile of trisomy 12 hPSCs has been shown

to more closely resemble that of germ cell tumours than normal cells. This similarity is not due to elevated expression of genes located on chromosome 12 but rather global changes in gene expression (Ben-David et al., 2014). The close similarities between genetic changes in hPSCs and those observed in various cancers remains a significant concern for their safety in therapeutic applications.

Although cell preparations for clinical use are being screened for the absence of genetic changes, the difficulty is that the commonly employed methods for detection of genetic changes fail to detect mutant cells when they are present at less than 5-10% of cells in culture (Baker et al., 2016). Hence, the safe progress to therapies will rely on understanding the mechanism of selection in hPSC cultures and how variant hPSC populations that possess improved growth characteristic interact with normal diploid cells in order to optimise culture conditions that minimize the appearance of the mutant cells.

1.3   Cell competition as a mechanism for selective advantage in heterotypic cultures

1.3.1   Cell Competition

Cell competition is an evolutionary conserved mechanism for sensing a cells relative fitness level in comparison to its neighbours. Cells that are less fit ("losers"), although viable, are eliminated in preference to the fitter "winner" population. Following elimination, the winner population undergoes compensatory proliferation to maintain tissue homeostasis. Establishment of winner/loser status is context dependent and relies on the relative fitness levels, not absolute fitness, of the interacting cells. Loser cells when cultured alone in homotypic cultures are viable, but in heterotypic cultures are eliminated through cell competition (Figure 1.7).

Cell competition was initially described and studied in the imaginal wing disks of *Drosophila melanogaster*. In a set of pioneering experiments Morata and colleagues showed a heterozygous mutation in the *Minute* gene, resulting in lowered ribosomal protein levels, produced slowly dividing cells that are eliminated in an apoptotic manner when surrounded by wild type cells (Morata and Ripoll, 1975, Moreno et al., 2002). Manipulating the growth rate of the slowly dividing cells, by using different *Minute* mutants with slower rates of cell division, was shown to alter the intensity of cell competition. *Minute* mutant cells with the slowest growth rate were eliminated the fastest. (Simpson and Morata, 1981).

The relationship between differences in growth rate and cell competition was supported by the description of a supercompetitive paradigm. In supercompetition, acquisition of a mutation that enhances the relative fitness of a cell can result in the removal of surrounding wild-type cells. Comparable to competition, in supercompetition the faster growing cells behave as winners and eliminate the slower growing loser cells, however in the case of supercompetition the mutation confers winner status rather than a loser phenotype. (Johnston, 2014). Supercompetitor status was first described in *Drosophila*, wild type cells are eliminated by overproliferating clones expressing a two-fold increase of the proto-oncogene

dMyc (de la Cova et al., 2004). Furthermore, cells expressing a two-fold increase of *dMyc* behave as losers when confronted by an even faster growing population of cells expressing a four-fold increase in *dMyc* (Moreno and Basler, 2004). These results support the concept that cell competition is highly context dependent and responds to the sensing of relative fitness levels between two populations not absolute fitness (Di Gregorio et al., 2016)

A

Homotypic Populations

or

or

Growth
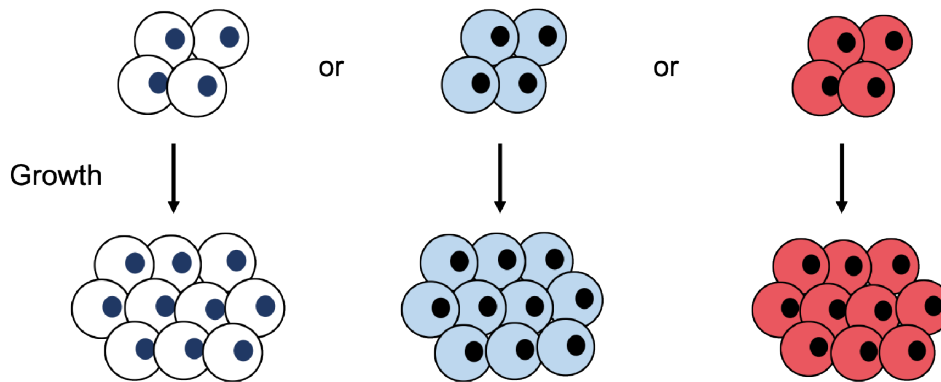
Heterotypic Populations

B

Competition:

Elimination of less-fit cells

Proliferation of fitter cells

C

Supercompetition:

Elimination of wild-type cells

Proliferation of supercompetitor cells

Fitter cell   Less Fit cell   Supercompetitor cell   Apoptotic cell
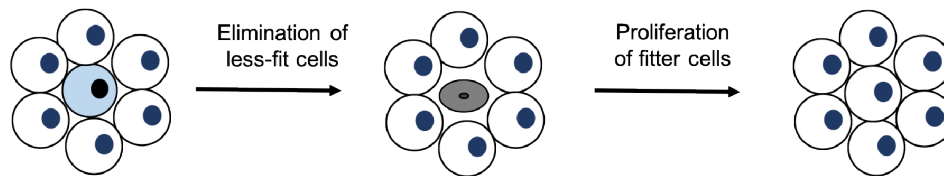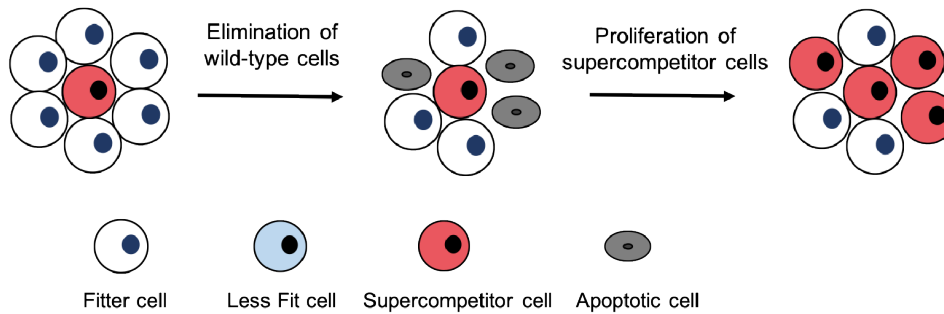
Figure 1.7 Cell competition phenotypes.

(A) In homotypic populations all cells are viable, whereas in heterotypic cultures **(B)** during cell competition less-fit cells (light blue) undergo fitness comparison with fitter (wild-type) cells that lie in close proximity resulting in the elimination of the less-fit population. **(C)** In supercompetition, supercompetitor cells induce apoptosis in neighbouring wild-type cells resulting in expansion of the supercompetitor population.

1.3.2   Cell Competition in Mammalian Systems

Cell competition is an evolutionary conserved mechanism that has also been described in mammalian systems (Madan et al., 2018). Studies on the early stages of mouse embryonic development found that expression levels of c-Myc, the mammalian homolog of dMyc, can affect cell fate in a competition dependent manner (Sancho et al., 2013, Claveria et al., 2013, Diaz-Diaz et al., 2017). Embryonic stem cells defective in BMP signalling are eliminated at the onset of differentiation by establishment of higher c-Myc in the wild-type cells (Sancho et al., 2013). Furthermore, induction of mosaic Myc expression in the mouse embryo promotes the competitive elimination of cells with lower Myc levels without perturbing development (Claveria et al., 2013). Additional in vivo studies report a similar role for cell competition in adult mouse cardiomyocytes. Mosaic overexpression of c-Myc promotes the replacement of wild-type cardiomyocytes (Villa Del Campo et al., 2014). The competitive replacement of cardiomyocytes in the adult heart demonstrates that competitive interactions are not confined to development but also plays a significant role in adult tissue homeostasis. Furthermore, the role of c-MYC expression levels in determining winner and loser phenotype also appears to be conserved between embryonic and adult stages of development.

Cell competition has also been observed during tissue regeneration in rodent studies. The liver has an exceptional regenerative capacity and the underlying mechanisms have been well described. Upon injury or resection, quiescent endogenous hepatocytes are activated and undergo cell division to restore the lost tissue (Forbes and Newsome, 2016). Transplanted fetal hepatocytes in the regenerating liver of adult rats outcompete the endogenous adult hepatocytes to colonise and expand in the regenerating organ. Adult hepatocytes confronted by the transplanted fetal cells undergo apoptosis and are eliminated from the organ (Oertel et al., 2006). Similar observations have been made in other transplantation contexts including the lung and bone marrow (Rosen et al., 2015, Bondar and Medzhitov, 2010). Bondar and Medzhitov showed cell competition is a selective mechanism of hematopoietic stem cells by transplanting a mosaic population containing wild type cells and p53 mutant cells into the bone marrow of irradiated mice. Mutant cells expressing lower p53 levels predominated the tissue whereas outcompeted wildtype cells displayed markers of senescence and reduced proliferation (Bondar and Medzhitov, 2010).

Expansion of one cell population at the expense of neighbouring cells holds many of the hallmarks of tumour growth. Indeed, many of the mutations that affect cell growth have known tumorigenic functions and mediate competitive interactions in mammalian systems. Another gene which causes cell competition in both Drosophila and mammals is the tumour suppressor gene *Scribble*. Mutant scribble cells are eliminated from the epithelium of Drosophila eye imaginal disks by wild-type cells (Brumby and Richardson, 2003). In Madin-Darby Canine Kidney (MDCK) cells knockdown of *Scribble* causes apoptosis in mutant cells when surrounded by normal cells. Apoptosis depends on activation of p38 mitogen-activated protein kinase (MAPK) in the *Scribbe*-knockdown (*Scribble^{kd}*)cells, following death *Scribble^{kd}* cells are independently apically extruded from the epithelium (Norman et al., 2012).

MDCK cells have since been used to demonstrate the role of cell competition as a form of tumour surveillance. MDCK cells constitutively expressing mutant forms of the proto-oncogenes Ras or Src are apically extruded from mosaic epithelia by neighbouring wild-type cells (Hogan et al., 2009, Kajita et al., 2010, Sasaki et al., 2018). In the case of Ras^{V12} mutants cells that are apically extruded remain alive, contrary to previous observations in Scribble mutations. Extrusion of loser cells in an apoptotic independent manner has also been reported in Drosophila (Tamori et al., 2010), suggesting that apoptosis and extrusion are context dependent competitive phenotypes (Kon, 2018). The extrusion of cells harbouring potentially tumorigenic mutations is proposed as protective mechanism called Epithelial Defence Against Cancer (EDAC) (Kajita and Fujita, 2015). Other routinely used mammalian cell lines, the human osteosarcoma line U2OS and 3T3 murine fibroblasts have also been shown to exhibit context dependent competitive phenotype broadening the scope of cell competition in different mammalian systems (Penzo-Mendez et al., 2015).

1.3.3   Mechanisms of Sensing Cell Fitness

To understand how cell competition is triggered it is important to understand how cells present and communicate differences in their cellular fitness.   Various models of fitness sensing have been proposed. Broadly these have been categorised into three mechanisms: (i) competition for growth factors or nutrients, (ii) direct cell-cell fitness comparison, and (iii) sensing of mechanical stress (Figure 1.8) (Di Gregorio et al., 2016).

The first model of cell competition proposed that winner and loser cells compete for limited factors that are required for their survival. This model was supported by observations from two models of competition in Drosophila, the Minute heterozygous mutant and dMyc overexpression. In the Minute model cells compete for the extracellular growth ligand Dpp, the Drosophila homolog of the mammalian BMP2/4 ligands, winner cells have a greater uptake of Dpp than loser cells (Moreno et al., 2002, Deignan et al., 2016). In dMyc mutants, Dpp uptake was not shown to be directly increased, but rather the Dpp/BMP signalling was enhanced in dMyc overexpressing winner cells. In both models, loser cells possess lower expression of Dpp/BMP signalling and rescue requires activation of the Dpp/BMP pathways to prevent elimination by surrounding wild-type cells (Moreno and Basler, 2004, Moreno et al., 2002). However, the role of BMP/DPP levels as a competitive factor is not clear, other studies report that Dpp and BMP levels are unchanged during competition of Minute or dMyc cells (de la Cova et al., 2004, Martin et al., 2009). In other competitive contexts, mouse embryonic stem cells defective for BMP signalling that behave as losers cannot be rescued by addition of BMP ligands (Sancho et al., 2013). Furthermore, other "loser" cells that have normal levels of BMP signalling, such as heterozygous *Minute* mutants in *Drosophila* and autophagy-deficient cells in the mouse, are unable to eliminate BMP defective cells. Other secreted ligands have been reported to influence cell survival, old T-lymphocyte progenitors residing in the thymus and young progenitors derived from the bone marrow compete for the cytokine interleukin 7. Disruption of competition promotes progenitor self-renewal and transformation into T-cell acute lymphoblastic leukemia (Martins et al., 2014). Overall the conflicting results in both Drosophila and mammalian systems has lead to the notion that cells are not just competing for a single growth signal but other survival factors or mechanisms must also feed in to trigger competition (Di Gregorio et al., 2016).

A Competition for Survival Factors

Fit cell

Less-fit cell

B Fitness Sensing

(i) Flower Fingerprint

(ii) Innate immune-like system

Spatzle

TRR

NFkB

Fit fingerprint (Flower^ubi)   UnFit fingerprint (Flower^lose)
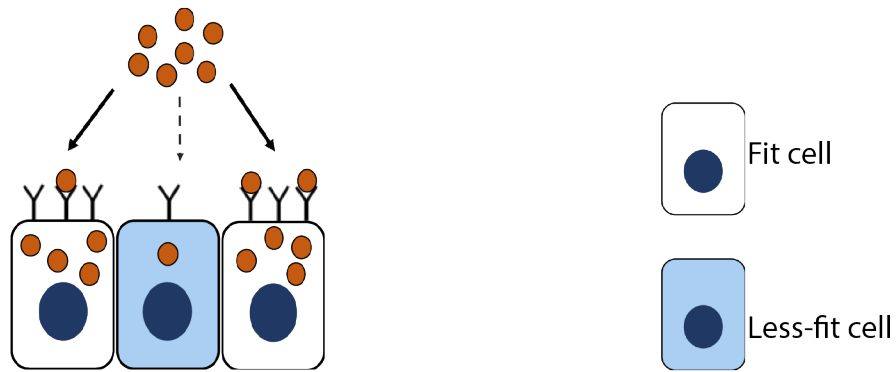
C Mechanical Competition
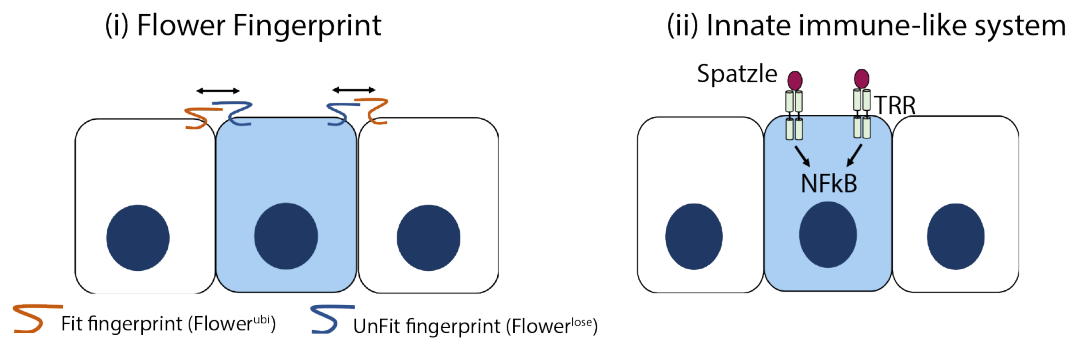
Increase Mechanical Tension
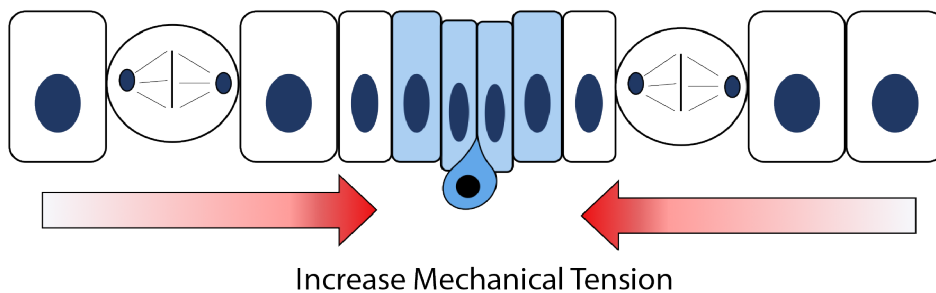
Figure 1.8 Mechanisms of sensing cell fitness.

Adapted from (Di Gregorio et al., 2016) **(A)** Competition for survival factors with limited availability. **(B)** Fitness sensing through **(i)** the Flower fitness fingerprint or **(ii)** innate immune-like system. **(C)** Competition mediated through mechanical stress.

An alternative mechanism of establishing future winner and loser phenotypes is that cells are capable of sensing their own fitness, defined as the ability of a cell to survive and proliferate in its cellular environment, and communicate this through a marker (Merino et al., 2016). Cells display a marker of their fitness state that is recognised by neighbouring cells and used to compare their relative levels of fitness. These markers can either be a short range diffusible signal communicating fitness to cells within the neighbouring proximity or surface markers that require direct contact (Merino et al., 2016, Baillon and Basler, 2014, Di Gregorio et al., 2016). This model was supported by the discovery of a contact dependent signal encoded by the *Flower (Fwe)* gene. Flower encodes several isoforms of a transmembrane protein that are differentially expressed in winner and loser cells. During cell competition of *Minute* mutants of the Drosophila wing imaginal disk, loser cells upregulate expression of either the Fwe^{loseA} or Fwe^{loseB} isoforms whereas the surrounding wildtype winner cells express only the ubiquitous Fwe^{ubi} isoform that is normally found throughout the wing imaginal disk (Rhiner et al., 2010). Furthermore, the Fwe^{loseB} isoform is reported to be involved in comparison of neuronal fitness during brain regeneration and marks neurons that are affected by injury for subsequent elimination (Moreno et al., 2015, Merino et al., 2013). A later study shows it is not just the expression of Fwe^{loseA} or Fwe^{loseB} isoforms but also their relative concentration and the degree of surface contact shared between cells that conveys fitness state and determines winner and loser status (Levayer et al., 2015). Inhibition of *Flower* is sufficient to rescue loser phenotypes in these models however it remains unclear how expression of the different *Flower* isoforms is established (Rhiner et al., 2010, Merino et al., 2013) . Since differential expression of Flower occurs after a cell decides its loser status, it is proposed that another mechanism for sensing fitness must exist upstream of *Flower* that controls the differential expression of its isoforms as an output for signalling winner and loser status (Di Gregorio et al., 2016, Amoyel and Bach, 2014).

In addition to the *Flower* code, the innate immune system has been proposed as another molecular mechanism for sensing fitness between winner and loser populations. Recent work by Meyer and colleagues revealed that loser cell elimination in dMyc and Minute competition models requires signalling through Toll-related receptors (TRRs) and nuclear factor κB (NF-κB) to activate pro-apoptotic genes. Of note, the study reported differences in the combination of TRRs and NF-κB genes activated between Minute and dMyc induced

competition (Meyer et al., 2014). As such, it is proposed that the innate immune system may have evolved to distinguish between different forms of cellular fitness. Further work is required to establish how TRRs are activated and the role of innate immune-like responses as a fitness sensing mechanism in other competitive contexts (Merino et al., 2016, Di Gregorio et al., 2016).

Mechanical sensing was initially proposed as a competitive mechanism in 2005 (Shraiman, 2005). Mathematical modelling of populations with different growth rates within a tissue suggested that the faster growing population would increase local tissue density. Equal sensitivity to density would result in cell death predominantly occurring in the faster growing population thereby limiting expansion of the population. However, if the faster growing population possessed a higher tolerance for density, apoptosis would mostly occur in the slower growing loser population. The density at which cell proliferation of a homotypic population is equivalent to the rate of cell death is referred to as the homeostatic density (Shraiman, 2005). The action of this competitive mechanism was first demonstrated in the *Drosophila* notum, in crowded regions of the tissue a proportion of the cells undergo delamination to make room for the remaining proliferating cells (Marinari et al., 2012). Later studies showed that increasing proliferation of mutant clones compared to wild-type cells, by activating the oncogene *Ras,* induced apoptosis in surrounding wild type cells up to several cell diameters away independently of the *Flower* code (Levayer et al., 2015)

In mammalian systems the role of mechanical stress induced competition has been studied in the *Scribble^{kd}* model. Silencing of the polarity gene *scribble* hypersensitised cells to mechanical stresses triggered by compaction, resulting in basal activation of p53 and lower homeostatic density than wild-type counterparts (Wagstaff et al., 2016). In heterogenous cultures, interaction with wild-type cells causes further compaction activating Rho-associated kinase and p38 which further raises the levels of p53 resulting in apoptosis of *Scribble^{kd}* cells (Wagstaff et al., 2016). A recent study by Bove and colleagues reveal that the competitive interactions of wild-type and *Scribble^{kd}* cells is governed by sensitivity to local density. Wild-type cells that find themselves in areas predominantly populated by losers upregulate their proliferation, increasing the local density that enables them to expand at the expense of the neighbouring loser cells (Bove et al., 2017).

Mechanical forces have also been implicated in other forms of cell competition. In the *Drosophila* wing imaginal disk, cell mixing is required during *dMyc*-induced competition. Elimination of cells with lower *dMyc* levels requires generation and stabilization of winner-looser contacts. Cell mixing is driven by the differential growth rates and tension generated through relative differences in F-actin levels at the interface of winner-looser cell interactions. Overall shifting the percentage of cell-cell contact away from loser-loser interfaces towards a greater proportion of winner-looser interactions (Levayer et al., 2015). These findings suggest that a competitive threshold of winner-loser cell interaction exists and support the conclusion that it is changes within the local environment that determines how cells are presented with competitive cues. Furthermore, the role of cytoskeletal proteins in cell competition is also described in mammalian cancer cells. Winner and loser status have been suggested to be conferred based on the mechanical deformability of tumour cells controlled by *RhoA* and actin-myosin. Downregulation of myosin is required for the engulfment and subsequent death of normal cells by tumour cells with high deformability (Sun et al., 2014).

1.4 **Project Aims**

The overall aim of my work is focused on determining how genetically variant hPSCs overtake normal cells during culture. Initially, I want to test whether different commonly acquired chromosomal abnormalities confer selective advantage through the same or distinct mechanisms. In addition to this, I want to investigate how normal and karyotypically variant cells behave when cultured together to assess the possibility of selection mechanisms that require cell-cell interactions. Finally, I want to explore the genes and signalling pathways that underpin each mechanism of selective advantage. To address these issues the following aims were designed to describe the overall experimental approach I will utilise to achieve this goal:

1. Generate clonal hPSC lines containing individual and multiple genetic changes to assess the effect gaining specific chromosomes has on cell behaviour.

In my first aim I will exploit a resource of cell banks containing mosaic populations to isolate and construct a panel of clonal variant lines containing individual and multiple genetic changes. This will enable me to compare and contrast the behaviour of different variant hPSCs to their normal counterpart and assess how each genetic change effects hPSC cell fate. A key aspect of selection is the advantageous growth properties conferred by altering elements of cell fate to promote self-renewal and restrict differentiation and/or cell death.

2. Characterise the behaviour of normal hPSCs when grown in heterogenous cultures containing variant cells with different genetic changes.

Utilising the cell lines generated in aim one, my second aim will build on the selective properties identified previously to assess if the presence of genetically variant cells can alter the behaviour of normal hPSCs when grown together. Karyotypically variant cells naturally arise in cultures of normal hPSCs and it remains unknown how normal and variant cells behave when sharing a proportion of their cell-cell contact. By generating heterogenous cultures I will be creating a model that is more representative of the naturally occurring events in culture and this will enable me to identify if there are selection mechanism that exist which are dependent on normal-variant hPSC interactions.

2   Materials and Methods

2.1   Human Embryonic Stem Cell Culture

In this study I generated subclonal hPSC lines derived from the H7 embryonic stem cell line, a gift from Professor James Thomson (Thomson et al., 1998). Mosaic populations of normal and karyotypically variant cells that have arisen during the culture of H7 in our lab had been frozen and banked. Karyotypically variant sublines were established from these mosaic banks using a cloning strategy described in Chapter 3 to isolate the genetically variant cells. The karyotypically variant sublines of H7 containing addition of whole or parts of chromosomes 1,17,20 (H7.s6) and 1,12,17,20 (H7.s6-GFP) had previously established within our lab at the University of Sheffield (Draper et al., 2004).

2.1.1   Culture on MEFs

2.1.1.1   Plating of mitotically-inactivated mouse embryonic fibroblasts (MEFs)

Culture vessels were coated with 0.1% (w/v) Gelatin in PBS and incubated at room temperature for a minimum of 20 minutes. MEFs were defrosted and resuspended in DMEM supplemented with 10% foetal bovine serum (FBS) (HyCLone SV30160.03). The gelatin was aspirated from flasks prior to seeding the MEFs. MEFs were seeded at a density of 10,000 cells/cm^2 and placed in an incubator at 37°C in 10% CO_2 overnight prior to their use. MEFs-coated flasks were used within five days of plating.

2.1.1.2   KnockOut Serum Replacement Medium Preparation

For culture of hESCs on MEF feeder cells KnockOut Serum Replacement (KOSR) medium was prepared by supplementing Knockout DMEM medium (ThermoFisher, 10829018) with: 4ng mL^{-1} (Peprotech, 100-18B) , 10µM L-Glutamine (ThermoFisher, 25030081) , 1X Non Essential Amino Acids (ThermoFisher, 11140050) , 200nM 2-Mercaptoethanol (ThermoFisher, 31350010) and 20% KnockOut Serum Replacement (ThermoFisher, 10828028). Medium was filtered using a steritop 0.22µm filter (Millipore) before use.

2.1.1.3 Passaging hESCs on MEFs

Media was aspirated from hESCs and Collagenase IV (Gibco, 17018-029) was added. Cells were incubated between 7 – 10 minutes at 37°C until the edges of the colonies began to lift away from the culture vessel. The collagenase was removed and replaced with fresh media. HESC colonies were gently scraped with a fine tip pastette (Alpha Laboratories, LW4061) to dissect into smaller aggregates. Cells were resuspended in fresh media and divided into new culture vessel at a ratio of 1:3 – 1:6.

2.1.2 Culture on Vitronectin

2.1.2.1 Preparation of Vitronectin coated culture vessels

Vitronectin (VTN-N) (500μg/ml) (A14700, Life Technologies) was thawed and aliquoted upon purchase and then stored at -80°C. Aliquots were thawed at room temperature and diluted in PBS (without Ca+, Mg++) to a final concentration of 5μg/ml. Diluted vitronectin was added to culture vessels and incubated for one hour at room temperature. Vessels were either used immediately or stored at 4°C for up to one week.

2.1.2.2 E8 Medium Preparation

Essential 8 (E8) media was prepared in house using a recipe adapted from Chen et al, 2011 (Table 2.1). In brief, L-glutamine was replaced by Glutamax (ThermoFisher), a thermostable version of glutamine which does not degrade into ammonia during storage or incubation. Large batches of 50X E8 supplement were stored as 10ml aliquots at -20°C. To prepare 1X E8 medium, 10ml aliquots were defrosted overnight at 4°C, added to 490ml DMEM/F12 (Sigma, D6421) and then filtered using a steritop 0.22μm filter (Millipore). For time lapse experiments 50X E8 supplement was added to DMEM/F12 without phenol red (Sigma, D6434).

Table 2.1 Preparation of 50X E8 Media Supplement

Component	50X concentrate	Final concentrations per 1 Litre of E8	Company	Catalogue Number
DMEM/F12	-	-	Sigma	D6421 *or* D6434
L-ascorbic acid	3200mg/L	64mg/L	Sigma	A8960
Sodium selenium	700ug/L	14ug/L	Sigma	S5261
Insulin	970mg/L	19.4mg/L	ThermoFisher	A11382IJ
NaHCO$_3$	27.15g/L	543mg/L	Sigma	S5761
Transferrin	535mg/L	10.7mg/L	Sigma	T0665
Glutamax	50X	10ml/L	ThermoFisher	35050038
FGF2	5mg/L	100ug/L	Peprotech	100-18B
TGFB1	100ug/L	2ug/L	Peprotech	100-21

2.1.2.3   Culture on Vitronectin

Cells grown on vitronectin were passaged using ReLeSR (Stem Cell Technologies, #05873), a non-enzymatic hESC selection and passaging reagent. Media was aspirated from flasks/plates and cells washed once with PBS. ReLeSR was added to the culture vessel and gently washed over the cells for approximately 30 seconds and then aspirated. Cells were left to incubate for 4-6 minutes at room temperature depending on colony density. Following the addition of fresh E8 medium, the culture vessel was gently tapped to detach colonies and the cell suspension was pipetted up and down to break colonies into small clumps. Dissected colonies were seeded into new flasks at various split ratios, ranging from 1:3 - 1:30 depending on the desired confluency and the sub-line used.

2.2 Cell Freezing

For cell freezing, hESCs at approximately 60% confluency were harvested using the methods described in routine culture (2.1.1.3 and 2.1.2.3). The cell suspension was centrifuged for 3 minutes at 1100 rpm and the supernatant aspirated. Cells were resuspended in freezing medium consisting of either 90% FBS supplemented with 10% DMSO (for cells grown on MEFs in hESC medium) or 90% E8 media supplemented with 10% DMSO (for cells grown on vitronectin in E8). Aliquots of 1.0mL cells in freezing medium were pipetted into cryovials and placed into a Mr Frosty (Nalgene) at -80°C overnight. The following day, cyrovials were transferred to liquid nitrogen for long term storage.

2.3 Cell Thawing

Cells were thawed depending on the culture conditions they were growing prior to freezing. Vials were removed from liquid nitrogen and placed into a 37°C water-bath until the cells were fully defrosted. The cells were transferred to a 15ml falcon tube containing 4ml of fresh media and centrifuged at 1100rpm for 3minutes. The supernatant was aspirated and tube flicked to gently dissociate the cell pellet. Cells were resuspended in warm media, either KOSR or E8, depending on the culture conditions prior to freezing and seeded into appropriately coated flasks. To improve viability, cells were seeded with 10μM Y-27632 (Adooq Bioscience).

2.4 Single Cell Dissociation

HESCs were dissociated into single cells using TrypLE Express (Life Technologies, 12604-021). Medium was aspirated from the culture vessel and cells washed one with PBS. Cells were incubated with 100μl/cm^2 for 4 minutes at 37°C and flasks tapped gently to ensure detachment. TrypLE Express was neutralised by dilution through addition of fresh DMEM/F12 at a 4:1 ratio into the culture vessel. Cells were transferred to a 15ml falcon tube and centrifuged at 1100rpm for 4 minutes.

2.5 Antibodies

2.5.1 Primary Antibodies for Immunofluorescence and Flow Cytometry

Table 2.2

Antibody	Details	Dilution	Reference	Supplier
P3X	Mouse Monoclonal IgG	1:10	(Kohler and Milstein, 1975)	In-House Hybridoma
TRA-1-85	Mouse Monoclonal IgG	1:10	(Williams et al., 1988)	In-House Hybridoma
SSEA3	Rat Monoclonal IgM	1:10	(Shevinsky et al., 1982)	In-House Hybridoma
SSEA4	Mouse Monoclonal IgG3	1:100	(Kannagi et al., 1983)	In-House Hybridoma
OCT4A	Rabbit Monoclonal IgG	1:800	-	Cell Signalling Technology (C52G3) #2890
NANOG	Rabbit Monoclonal IgG	1:800	-	Cell Signalling Technology (D73G4) #4903
Cleaved Caspase- 3	Rabbit Polyclonal	1:400	-	Cell Signalling Technology (Asp175) #9661

2.5.2   Primary Antibodies for Western Blot

Table 2.3

Antibody	Details	Dilution	Supplier
P-c-Jun	Rabbit Monoclonal	1:1,000	Cell Signalling Technology (C54B3) #2361
P-SAPK/JNK	Rabbit Monoclonal	1:1,000	Cell Signalling Technology (81E11) #4668
JunB	Rabbit Monoclonal	1:1,000	Cell Signalling Technology (C37F9) #3753
P-JunB	Rabbit Monoclonal	1:1,000	Cell Signalling Technology (D3C6) #8053
P38 MAPK	Rabbit Monoclonal	1:1,000	Cell Signalling Technology (D13E1) #8690
SAPK/JNK	Rabbit Monoclonal	1:1,000	Cell Signalling Technology #9252
P-p38 MAPK	Rabbit Monoclonal	1:1,000	Cell Signalling Technology (12F8) #4631
STMN2	Rabbit Monoclonal	1:1,000	Abcam; ab185956
SRCRB4D	Rabbit Polyclonal	1:1,000	Abcam; ab204496
STMN2	Rabbit Monoclonal	1:1,000	Abcam; ab185943
SUN2	Rabbit Monoclonal	1:1,000	Abcam; ab124916
c-Myc	Rabbit Monoclonal	1:1,000	Abcam; ab32072
p53	Mouse Monoclonal	1:1,000	Santa Cruz Biotechnologysc-126
α-Tubulin	Rabbit Polyclonal	1:1,000	Cell Signalling Technology #2144

2.5.3 Secondary Antibodies

Table 2.4

Antibody	Conjugate	Dilution	Assay	Supplier
Goat anti Mouse AffiniPure IgG+IgM (H+L)	AlexaFluor 647	1:200	FACS, ImmunoFluorescence	Stratech 115-605-044-JIR
Goat anti Rabbit AffiniPure IgG+IgM (H+L)	AlexaFluor 647	1:200	FACS, ImmunoFluorescence	Stratech 111-605-003-JIR
Anti-Rabbit IgG	HRP	1:4,000	Western Blot	Promega W401
Anti-Mouse IgG	HRP	1:4,000	Western Blot	Promega W402

2.6 Immunostaining

Cells were fixed with 4% PFA for 15 minutes at room temperature and subsequently washed with PBS. Cells were either stained immediately or stored at 4°C in PBS to prevent them drying out. For intracellular staining, following fixation cells were permeabilised with PBS supplemented with 0.5% Triton X-100. PBS was aspirated from wells and cells incubated with an appropriate volume of permeabilisation buffer for 10 minutes at room temperature. After fixation and permeabilization, cells were blocked for 1 hour in blocking buffer composed of PBS supplemented with 1%BSA and 0.3% Triton X-100. After blocking, cells were washed once with PBS and stored at 4°C until stained. Primary and secondary antibodies were resuspended in blocking buffer at the concentrations stated in (Table 2.2 and 2.4). Samples were incubated with primary antibodies overnight at 4°C with gentle agitation on an orbital shaker. Cells were subsequently washed twice with PBS before secondary antibody staining. Secondary antibodies were also resuspended in blocking buffer and Hoescht 33342 (1:1,000) (ThermoFisher, H3570) for one hour at 4°C. Cells were again washed twice with PBS before imaging using InCell Analyzer 2200 (GE Healthcare).

2.7 Antibody staining for Flow Cytometry Analysis of surface markers

Cells were harvested to single cells (see 2.4), counted and centrifuged at 1100rpm for 3 minutes. The supernatant was aspirated and cells resuspended in FACS buffer (PBS supplemented with 10% FCS) at 1×10^7 cells/ml. 100µl of sample was placed into 5ml FACS tubes (Falcon 352053) incubated with primary antibody (Table 2.2) for 15 minutes at 4°C . Cells were washed once with 4ml of FACS buffer and centrifuged at 1100rpm for 3 minutes. Supernatant was aspirated and cells dispersed by gently flicking the sample tubes. Secondary antibody was added at the appropriate dilution (Table 2.4) , and incubated for 15 minutes at 4°C in the dark. Cells were again washed in 4ml of FACS buffer and centrifuged t 100rpm for 3 minutes. The supernatant was aspirated and cells resuspended in 300µl FACS and analysed on BD FACS Jazz. Baseline fluorescence was set using the primary antibody control P3X. P3X is a monoclonal IgG1 antigen secreted from the parent P3X63Ag8 myeloma which all in-house antigens were derived and does not show expression on human cells (Kohler and Milstein, 1975)

2.8   Single Cell Deposition by FACS

Heterotypic cultures of hESC were sub cloned using single cell deposition by FACS into MEF coated 96 well pates. MEF plates were prepared (as described in 2.1.1.1), on the day of sorting media from the MEF plates was replaced with 100μl KOSR media containing 10μM Y-27632 and 50μg/ml Gentamycin (LifeTechnologies) to prevent contamination and stored in 5% CO_2 incubator prior to use. Sorts were performed using a BD FACS Jazz, to ensure accurate deposition of single cells machine set up was confirmed by sorting individual fluorescent beads into a 96 well. The plate was imaged at 4x magnification on the InnCell Analyzer 2200 to verify bead number and droplet location was correct. HESCs were dissociated to single cells using TrypLE (see 2.4) and resuspended in an appropriate volume of KOSR medium. Single cells were sorted directly into the wells of the pre-prepared MEF plate, immediately after sorting the plates were centrifuged briefly at 1100rpm for 1 minute to aid attachment of the cells. After 2 days the medium was replaced with fresh KOSR media to remove the Y-27632 and colonies left to develop over the next 12 days.

2.9   qPCR Assay for detecting common genetic changes

2.9.1   gDNA Extraction from 96 well plates

After 14 days or when colonies had reached a substantial size they were passaged as described in 2.1.1.3, half of the cell suspension was placed into a new culture vessel for expansion and the remaining material transferred to a 1.5ml Eppendorf tube and centrifuged at 1100rpm for 3 minutes. Cells were resuspended in 0.4ml cell lysis buffer (Table 2.7) and incubated at 55°C overnight. An equal volume of phenol/chloroform was added and the tube inverted several times to mix. The sample was then centrifuged at 10,000prm for 5 minutes to facilitate phase separation. The aqueous phase was transferred into a fresh Eppendorf tube and 40μl 3M NaAc and 1ml 100% EtOH added, the tube was then inverted 10 times to precipitate the DNA. Sample was centrifuged at 10,000rpm for 30 seconds to pellet the DNA. DNA was gently washed by pipetting 1ml 70% EtOH over the pellet and immediately removing. The sample was centrifuged for a further 30 seconds at 10,000rpm and residual ethanol removed. DNA was resuspended in 30μl TE and left overnight to dissolve. Concentration and purity were analysed on a Nanodrop Lite (ThermoFisher)

2.9.2 <u>qPCR</u>

Relative copy number of commonly identified genetic changes was assessed using the qPCR based approach described in (Baker et al., 2016). In summary, 10µL reactions were set up in triplicate in 384 well plates. Each PCR reaction contained 1X TaqMan Fast Universal Master Mix (ThermoFisher, 4352042), 100nM of forward and reverse primers, 100nm of probe from the Universal Probe Library and 10ng of genomic DNA. PCR reactions were run on a QuantStudio 12K Flex Thermocycler (Life Technologies 4471087) with the following cycle parameters: 50°C – 2mins, 95°C - 10mins, 95°C – 15secs, 60°C – 1min for 40 cycles. Primer sequences and corresponding gene location are described in Table 2.5. Calibrator samples were obtained from cell lines with a diploid karyotype and positive control samples from a cell line possessing gain of all the commonly acquired chromosomal regions; 48,XX, +del(1)(p22p22),der(6)t(6;17)(q27;q1),+12,ish dup(20)(q11.21q11.21), as confirmed by G-banding and fluorescent in-situ hybridisation analysis

Table 2.5 qPCR Primers

Gene	Location	Primer Sequences (5'-3')	Universal Library Probe	Amplicon Size (bp)
NPHP4	1p36	F: ccggcctatcgtactttt R: gccggtgtgtgcagaact	8	60
MDM4	1q32.1	F: gcccccagacctaaatcaat R: tcggtatgacagcaatgtctctt	13	76
RELL1	4p14	F: tgcttgctcagaaggagctt R: tgggttcaggaacagagaca	12	64
DPPA3	12p13.31	F: cgtagcgtcgttgcatca R: tccttttaccgttcctgaca	60	63
LGR5	12q21.1	F: gatatgttggggattgacacg R: tgctcaaagaggacaaccttc	6	60
FLCN	17p11.2	F: tgcagtccacaatgacaagtg R: ccatgagagccgaagactgt	68	74
TK1	17q23.2-q25.3	F: ggtgacagctgcttacagcttag R: actggttgccaccttctcag	60	64
BCL2L1	20q11.21	F: tctgcagaaggctacccta R: tgctgtgtctaagacctctttcat	44	75

2.10 <u>Karyotyping</u>

Karyotyping was performed by a Genetic Technologist and checked by a Clinical Scientist at the Sheffield Diagnostic Genetics Service. Typically, 30 metaphases were analysed by G-banding per sample.

2.11 <u>Competition Assays</u>

2.11.1 <u>Spiking Experiment</u>

Genetically normal H2B-RFP hESCs were spiked with 10% genetically variant cells following dissociation to single cells. A sample of the mixed population was kept for analysis and 1.0×10^6 cells seeded onto vitronectin coated T12.5 flasks containing E8 media supplemented with $10\mu M$ Y-27632. Cells were passaged using ReLeSR (see 2.1.2.3) every 4 days and a sample of the culture placed into a 5ml FACS tube for analysis. ReLeSR passaging produces small clumps of cells which were dissociated to single cells for flow cytometric analysis by treatment with TrypLE for 1 minute. TrypLE was neutralised by dilution through addition of fresh E8 media at a 4:1 ratio. The cell suspension was centrifuged at 110rpm for 3 minutes and resuspended in $300\mu l$ E8 media before analysis on BD FACS Jazz. To set baselines for the normal H2B-RFP and supervariant-GFP lines, the unlabelled normal line was harvested alongside spiked samples.

2.11.2 <u>96 Well Growth Curve Assays</u>

2.11.2.1 <u>Plate Set up</u>

The inner 60 wells of 96 well plates (Greiner, 655090) were coated with $60\mu l$ of vitronectin (see 2.1.2.1) for a minimum of one hour at room temperature. Vitronectin was aspirated and $50\mu l$ E8 media supplemented with $20\mu M$ Y-27632 added per well. The outer 32 wells were filled with $100\mu l$ DMEM/F12 to reduce the edge effect. Plates were incubated at $37°C$ / 5% CO_2 until cells were ready to be seeded.

2.11.2.2 Cell Plating

Single cell suspensions were harvested (see 2.4), counted and centrifuged at 1100rpm for 3 minutes. Cells were resuspended at 1×10^6 cells/ml in E8 media and appropriate volume of cell suspension extracted for further dilution. Genetically normal and variant hESC were mixed at the appropriate concentration and ratio to produce the desired co-cultures described in the individual experiments. The final cell concentration was calculated so that 50μl contained the desired number of cells for plating. 50μl of the samples was seeded per well of pre-prepared 96 well plate resulting in a final concentration of 10μM Y-27632. 24hours post plating the media was removed and wells washed with 100μl E8 to remove the Y-27632 when appropriate. Media was changed daily and replaced with 150μl E8 supplemented either with or without 10μM Y-27632.

2.11.2.3 Plate Fixing and Analysis

The majority of media was removed from 96 well plates leaving ~30μl remaining in each well to prevent cells from detaching upon addition of fixative. Cells were fixed with 100μl 4% PFA containing Hoescht 33342 (1:500) per well for 15 minutes at room temperature in the dark. Cells were subsequently washed four times with PBS and plates either imaged immediately or stored at 4°C until they could be imaged on InCell Analyzer (GE Healthcare). Quantification of cell numbers was performed either by protocols designed in Developer Toolbox (GE Healthcare) or comparable pipelines designed in CellProfiler (Carpenter et al., 2006).

2.12 Clonogenic Assay

Clonogenic assays were performed on MEF coated 24 well plates. Cells were dissociated to single cells (see 2.4), counted and resuspended in KOSR media supplemented with 10μM Y-27632 and plated at a density of approximately 500 cells/cm^2. Cells were incubated for 24 hours to facilitate attachment and the media replaced with standard KOSR medium to remove Y-27632. Colonies were left to grown for a further 4 days with no additional media changes necessary. Prior to fixing wells were washed once with PBS to remove cell debris and then fixed as described in 2.6.

2.13 Embryoid Body Differentiation

The trilineage differentiation potential of normal and karyotypically variant hPSCs lines was assessed using an embryoid body based approach. Cells were dissociated to single cells (see 2.4), counted and resuspended in STEMdiff APEL2 medium (StemCell Technologies, 05270) at 60,000 cells per ml. 50μl of cells were seeded into the inner 60 wells of a 96 well U bottom suspension culture plate (Greiner, 650185). The outer 32 wells were filled with PBS to minimise evaporation from the inner 60 wells. The plate was then centrifuged at 1000rpm for 3 minutes to aggregate the cells. Plates were incubated at 37°C / 5% CO_2 for 7 days, after which the embryoid bodies were collected and transferred to a 15ml falcon tube and centrifuged at 1000rpm for 3 minutes. The supernatant was aspirated and samples stored at -80°C until RNA extraction.

2.14 Statistical Analysis

Statistical analysis of the data presented within this thesis was performed using GraphPad Prism version 7.00 for Mac OS X, GraphPad Software. La Jolla California USA, www.graphpad.com. In the cases where I compared two independent sets of data, an unpaired Students t-test was conducted to determine if there was a significant difference between the mean of the two data sets. The remaining statistical analysis was performed on the data from multiple independent normal and karyotypically variant cell lines, for this analysis a one-way analysis of variance (ANOVA) was used in either one of two ways. Firstly, in the experiments assessing cell cycle time and mitochondrial content analysis, the data from the multiple variant lines was compared against normal hPSCs using a one-way ANOVA followed by Dunnett's test to determine whether there was statistically significant difference between each karyotypically variant and normal hPSCs. Secondly, in the growth rate analysis and the apoptotic resistance experiments I used a one-way ANOVA followed by Tukey's test to compare the means of each independent hPSC line with the mean of all the other cell lines within my panel of normal and karyotypically variant hPSCs to determine if there was a significant difference between each of the cell lines.

2.15 RNA Sequencing

2.15.1 Bulk Cell sorts for RNA

Genetically normal and supervariant hESC were re-isolated from co-cultures using FACS. Cells were harvested to single cell suspension (see 2.4), counted and resuspended at $2x10^6$ cells/ml in E8 media. Sort gates were set using the separate culture unlabelled normal cells as baseline and supervariant-GFP separate cultures as positive gates. $5x10^5$ cells per population were sorted into appropriate collection vessel and post sort re-analysed for a minimum 98% purity. Samples were centrifuged at 1100rpm for 3 minutes, supernatant removed and cell pellets stored at -80°C until RNA extracted.

2.15.2 RNA Extraction

Total RNA was isolated using a Qiagen RNAeasy Plus Mini Kit (Qiagen, 74134) and eluted in ddH$_2$O as per manufacturer's instructions. The concentration RNA was determined using a Qubit 3.0 Fluorometer and purity assessed on a Nanodrop Lite (ThermoFisher).

2.15.3 RNA Sequencing

RNA samples from separate and co-cultures were processed and analysed by Novogene. To summarise, RNA sequencing was performed on a Illumina PE150 machine and sequencing reads were aligned to human genome reference consortium grch38.

RNA samples from separate cultures of normal and karyotypically variant hPSC lines were processed and sequenced by the Wellcome Sanger Institute. RNA sequencing was performed on a Illumina HiSeq 200 machine and aligned to human genome reference grch38. Analysis of differential gene expression was conducted by the Sheffield Bioinformatics Core Facility.

2.16 Transswell Indirect Culture Assay

For indirect co-culture, Millipore Transwell 8.0μm PET membrane inserts (Millipore, PIEP12R48) were used in combination with 24 well plates. Both the insert and lower well were prepared with vitronectin as previously described (see 2.1.2.1). 1.5x10^4 cells were seeded in the lower plate and upper insert. Cells were pre-cultured independently for 24hours in E8 medium supplemented with 10μM Y-27632 to facilitate cell attachment and then washed with DMEM/F12. Inserts were subsequently placed into appropriate wells and fresh E8 media was added to both the lower well and upper transwell insert. Media was changed daily to prevent FGF depletion and samples fixed with 4% PFA at the time points stated in the figure.

2.17 "Fences" Assay

To create a distinct boundary between two different cell populations we used an approach based on the classical wound healing assays. Cells were harvested to single cells and 5x10^4 seeded into the inner compartment of 2 well silicone inserts (Ibidi 80209). 24 hours post plating the silicone inserts were removed leaving a defined 500μm gap between the two cell populations. The cells were washed with DMEM/F12 to remove Y-27632 and replaced with fresh E8 media daily. Cells were left to grow for 4 days until the two opposing cell fronts had been in contact for approximately 24hours. To assess indirect co-culture in this system, two silicone inserts were placed on opposite sides of the well. Cells were seeded into the central facing compartment and cultured as described above. The distance between the silicone inserts prevented the cell populations from coming into contact but allowed them to share the same media environment.

2.18 Time lapse

Time-lapse microscopy was performed at 37°C / 5% CO_2 using a Nikon Biostation CT. Cells were imaged every 10 minutes for 72 hours using 10x or 20x air objective. Image stacks were compiled in CL Quant (Nikon) and exported to FIJI (Image J) for analysis.

2.19 <u>Apoptosis Assays</u>

Apoptosis was assessed by levels of cleaved caspase-3 staining. To collect apoptotic cells which had detached from the flask the old media was added to a 5ml FACS tube and centrifuged at 1400rpm for 5 minutes. The supernatant aspirated and cell pellet flicked to disperse. Remaining cells were harvested with TrypLE (see 2.4) and resuspended in DMEM/F12, the cells suspension was added to the FACS tube containing the previously collected apoptotic cells. The collated sample was centrifuged at 1400rpm for 5 minutes, supernatant aspirated and cells resuspended in 4% PFA for 15 minutes at room temperature. The suspension was then centrifuged at 1400rpm for 5 minutes, and pellet resuspended in permeabilisation buffer (PBS supplemented with 0.5% Triton X-100) and incubated for 5 minutes at room temperature. Cells were centrifuged again at 1400rpm for 5minutes and resuspended in 100μl blocking buffer containing anti-cleaved caspase-3 primary antibody. Samples were gently agitated at room temperature for 1 hour, washed in 1ml of blocking buffer and centrifuged at 1400rpm for 5minutes. Cells were stained with secondary antibody for 1 hour at room temperature in the dark, washed once with 1ml of blocking buffer and centrifuged for a final time at 1400rpm for 5 minutes. Cells were resuspended in 300μl blocking buffer and analysed on BD FACS Jazz. Baseline fluorescence was set using secondary antibody only stained samples.

2.20 <u>ATPlite Assay</u>

ATP levels in normal and karyotypically variant hPSCs was measured using an ATPlite Luminescence Assay system (PerkinElmer, 6016941). Cells from karyotypically normal and variant cultures were harvested to single cells and resuspended in E8 media supplemented with 10μM Y-27632. 30,000 cells were plated per well of a 96 well plate (Greiner, 655090) and incubated at 37°C / 5% CO_2.. After 24 hours, the media from each well was replaced with either; E8 media only, E8 media supplemented with 50mM 2-deoxyglucose (Sigma, D6134), E8 media supplemented with 1μM oligomycin (Sigma, 75351) or E8 media supplemented with 1% DMSO and cells were incubated for 1 hour at 37°C / 5% CO_2.. The cells were then lysed through the addition of 50μl lysis buffer per well and the plate agitated at 7000rpm for 5 minutes as per manufacturers protocol. After lysis, 50μl of substrate solution was added per well and the plate agitated for a further 5 minutes at 7000 rpm. Luminescence of each well

was measured using a Varioskan plate reader. To determine the relative number of cells per well, 50μl of 5X CyQuant NF dye (ThermoFisher, C35007) was added per well and the fluorescence of each well measured using a Varioskan plate reader. ATP measurements were normalised to cell numbers by dividing the luminescence reading per well by its corresponding fluorescence value.

2.21 Western Blot Analysis

2.21.1 Protein Extraction

Protein was extracted from either sorted samples or stock cultures for immunodetection. Cells harvested from culture vessels were washed once with PBS and then placed on ice. 200μl of Laemilli Buffer, pre-warmed to 95°C, was added and the cells harvested by scraping using a fine tip pastette (Alpha Laboratories). Cells isolated by FACS were spun at 1100rpm x 3 minutes and the supernatant aspirated. The tube was gently flicked to dissociate the cell pellet and 200μl of pre-warmed Laemilli Buffer added. Protein lysate was transferred to a 0.5ml Eppendorf and incubated at 95°C for 10 minutes to denature the proteins. Samples were stored at -80°C until future analysis.

2.21.2 Protein Electrophoresis

Protein concentration was determined using BCA quantification (ThermoFisher, 23250) and 10μg of protein sample was loaded per sample. Proteins were resolved using 10 – 15% separating gel run at 120V for approximately 1.5 hours alongside a Page Ruler prestained protein ladder (ThermoFisher, 26616) on a Mini-PROTEAN Electrophoresis cell (Bio-Rad).

2.21.3 Protein Detection

Proteins were then transferred onto a PVDF membrane (Millipore #IPVH00010) using an Electrophoresis Transfer Cell (Bio-Rad). The membrane was blocked in 5% milk for one hour and washed three times with TBST. The membrane was transferred to a 50ml falcon tube and incubated with primary antibody diluted in 5% milk overnight at 4°C on a rotating platform.

The membrane was washed 3 times for 10 minutes in TBST and placed into a 50ml falcon tube containing secondary antibody diluted in 5% milk. The blot was incubated with secondary antibody for 1 hour on a rotating platform and again washed 3 times in TBST for 10 minutes. Immunoreactivity was visualised using ECL Prime (GE Healthcare, RPN2232) and signal captured on a CCD-based camera.

2.22 Solutions and Buffers

PBS (without Ca²⁺ or Mg²⁺)

10X concentrate stock was purchased (Sigma D1408) and 50ml diluted in 450ml double distilled water to make a 1x working solution. The final 1x solution was autoclaved before use and stored at room temperature.

4% PFA

4% PFA was made in 1L batches and used within 6 months of preparation. 40grams of Paraformaldehyde powder (Sigma 158127) was dissolved in 800ml of PBS by stirring and heating to approximately 60°C. To fully dissolve the pH was raised slowly through addition of 5M NaOH until the solution was clear. The volume was adjusted to 1L by addition of an appropriate volume of PBS and the pH corrected to 6.9 by adding small volume of concentrated HCl. The final 4%, pH 6.9 solution was filter sterilised using a steritop 0.22μm filter (Millipore) into 50ml aliquots and stored at -20°C.

Cell Lysis Buffer

1 Litre of stock Lysis solution (without Proteinase K) was made as per Table 2.6. Proteinase K was stored independently at -20°C as a 20mg/ml stock by resuspending 100mg of Proteinase K in 5 mL 50 mM Tris pH 8.0, 10 mm CaCl$_2$. A final lysis buffer was made by adding Proteinase K to the stock lysis solution as per Table 2.7.

Table 2.6

Stock Solution	Vol per Litre	Final Concentration
20% SDS	25ml	0.5%
0.5M EDTA pH 8	20ml	10mM
1M Tris-HCl pH 7.4	10ml	10mM
5M NaCl	2ml	10mM
dH$_2$O	943ml	-

Table 2.7

Component	Vol per 5ml	Final Concentration
Proteinase K	100μl	400μg/ml
Stock Lysis buffer	5ml	-

Permeabilisation Buffer: PBS supplemented with 0.5% Triton X-100

2.5ml of Triton X-100 (Sigma T8787) added to 500ml of PBS, 50ml aliquots were made and stored at -20°C.

Blocking Buffer: PBS supplemented with 1% BSA and 0.3% Triton X-100

5 grams of BSA (Millipore, 82-100-6) was dissolved in 500ml of 1x PBS containing 1.5ml of Triton X-100.

FACs Buffer: PBS supplemented with 10% Foetal Bovine Serum

50ml of Foetal Bovine Serum (HyCLone SV30160.03) added to 450ml of PBS.

Laemilli Buffer: 4% SDS, 20% Glycerol, 0.125M Tris HCl, 0.004% bromphenol blue

50ml of 2X Laemilli buffer was prepared as per Table 2.8 and stored as 1ml aliquots at -20°C. 2X buffer was defrosted and diluted to 1X by adding and equal volume of double distilled H$_2$0.

Table 2.8

Stock Solution	Vol per 50ml	Final Concentration
0.5M Tris-HCl pH6.8	10ml	0.125M
20% SDS	5ml	4%
Glycerol	10ml	20%
Bromphenol blue	2µl	0.004%
dd H_2O	25ml	-

Tris Buffered Saline (TBS): 1.5M NaCl, 200mM Tris

10X TBS was made by dissolving 24g Tris Base and 88g NaCl in 900ml of distilled H_2O. The pH adjusted to 7.6 by addition of concentrated HCl and appropriate volume of distilled H_2O added to a final volume of 1L.

TBST: Tris buffered saline supplemented with 0.1 % Tween 20

100ml of 10X TBS was mixed with 900ml of distilled H_2O and 1ml of Tween 20 to make TBST buffer.

5% Milk:

For 100ml; 5 grams of Milk Powder was dissolved in 100ml of TBST (see above).

Protein Sample Buffer:

4X Protein Sample Buffer was purchased from Bio-Rad (#161-0791), before use 50µl β-mercaptoethanol (BDH, 4414331) was added per 450µl 4X buffer.

Protein Electrophoresis Running Buffer: 0.25M Tris, 1.92M Glycine, 1% SDS

10X running buffer was made by dissolving 30.28g Trizma Base, 144.13g Glycine and 1g SDS in 1L of distilled H_2O and stored at room temperature.

Protein Electrophoresis Transfer Buffer: 0.025M Tris, 0.192M Glycine, 25% Methanol.

5 Litres of 1X transfer buffer was made by dissolving 56.25g Glycine, 15.13g Trizam Base in 1L of Methanol and 4L distilled H_2O.

3   Constructing and characterising a panel of clonal hPSC lines containing genetic changes.

3.1   Introduction

Genetic changes in hPSCs arise during prolonged culture and are detectable using common laboratory or cytogenetic techniques when they reach 5-10% mosaicism (Baker et al., 2016). The predominant genetic changes observed in hPSCs include gains of whole or parts of chromosomes 1,12, 17 and 20, which are also frequently gained in embryonal carcinoma cells, the stem cells of germ cell tumours (Baker et al., 2016, Amps et al., 2011). Genetically variant cells possess different growth characteristics compared to normal cells including improved survival and proliferation capacity (Ben-David et al., 2014, Avery et al., 2013). Over progressive passages variant hPSCs overtake the normal population to become the predominant cells, demonstrating they possess a selective advantage within culture (Olariu et al., 2010). Though acquisition of genetic changes in hPSCs has been well established, the mechanism by which different genetic changes exert their selective advantage remains poorly understood. One possibility is that variant cells possess altered growth properties that allow them to expand more rapidly in culture. Abnormalities that promote self-renewal fate and restrict differentiation and cell death would enable variant cells to overtake normal hPSCs during culture (Amps et al., 2011).

Selective advantage in hPSCs cultures can be tested by spiking homotypic populations of normal cells with variant cells to generate heterotypic cultures. The proportion of each cell type in the heterotypic culture is monitored over progressive passages. This form of analysis has been used to model the effects of advantageous growth properties and key culture parameters that influence the rate at which variant cells overtake normal hPSCs, including population size and passaging technique (Olariu et al., 2010). In a study using two normal embryonic stem cell lines, H7 and H14, as well as their variant counterparts, Olariu and colleagues demonstrated that variant cells containing different genetic abnormalities overtook their counterpart normal hPSCs at different rates. These observations suggest that the strength of selective pressure can differ between variant hPSCs and could depend on the

advantageous properties conferred by the amplified genomic regions. Furthermore, they demonstrated that variant cells overtook normal H14 cells more rapidly in cultures that were passaged using Trypsin, an enzymatic reagent that promoted single cell dissociation compared to collagenase treatment and manual scraping of colonies which favour larger clumps, suggesting that culture conditions can influence the selective pressures exerted during passage and effect the rate at which abnormal hPSCs arise (Olariu et al., 2010). Spiking experiments have also been used to demonstrate the driver gene function and selective advantage of different mutations. During investigation of the 20q11.21 CNV amplification, hPSCs overexpressing one of three candidate genes were mixed with normal cells and monitored over progressive culture. Only overexpression of the BCL-XL gene provided cells with the ability to overtake normal cells demonstrating its role as the gene driving selective advantage in 20q11.21 CNV variants (Avery et al., 2013). Additionally, within heterogenous cultures containing cells harbouring *TP53* mutations the proportion of mutant cells increases over progressive passages demonstrating that mutations in TP53 can provide cells with a positive selective advantage over normal hPSCs (Merkle et al., 2017).

Normal human pluripotent stem cells have two defining functional properties; the ability to self-renew indefinitely and the capacity to differentiate into all cells of the adult body (Thomson et al., 1998). These properties can be tested through a series of experiments that examine different aspects of stem cell fate. Through assessment of these properties in variant hPSC lines and comparing against counterpart normal cells, previous studies have reported gains of different chromosomes to alter various aspects of cell behaviour (Nguyen et al., 2013, Keller et al., 2018).

The self-renewal state of hPSCs can be assessed through a variety of assays that examine different aspects of stem cell function. Proliferation is typically assessed using a standard growth rate assay design that involves seeding a set number of cells into a culture vessel and counting the total number of cells on each day over a set culture period without passaging. Comparison of the number of cells between two days enables the calculation of population doubling rate which can be used as a measure of how rapidly a cell line proliferates. Growth rate assays have been used to show that different variant hPSCs, including chromosome 12 trisomy and the complex gain of both chromosomes 1 and 17, increases the proliferation of

hPSCs (Ben-David et al., 2014). However, the rate of proliferation is dependent on two key parameters: time taken for cells to divide and the rate of apoptosis. Mutations that cause a shortening of time between cells divisions would result in a higher total number of cells between consecutive days just as abnormalities that restrict apoptosis would increase the total cell count by increasing the number of surviving cells. A limitation of previous studies that have reported increased proliferation rates for variant hPSCs is that they do not examine which of these two key parameters is affected (Ben-David et al., 2014, Avery et al., 2013, Enver et al., 2005).

Molecular markers such as cell surface antigens are a convenient way of monitoring the stem cell state. Expression of the antigen SSEA3 is strongly associated with pluripotency and rapidly lost upon differentiation (Fenderson et al., 1987, Draper et al., 2002). Isolation of cells using intensity of SSEA3 expression has shown that hPSCs segregate into subpopulations that exhibit functional differences. Human PSCs with high SSEA3 expression are proposed to exist in a more pristine undifferentiated stem cell state whereas cells with low expression more readily progressed into a differentiated state. Commitment to differentiation is suggested to occur when cells have lost expression of SSEA3 but retain expression of lineage associated transcription factors (Tonge et al., 2011, Allison et al., 2018). A sensitive test of the stem cell state is the ability of a single hPSC to expand and create a colony of pluripotent daughter cells. The cloning efficiency is defined as the number of colonies generated versus the number of single cells plated. Using SSEA3 as a discriminator between undifferentiated and differentiated cells, Enver et al 2005 showed that in SSEA3 positive cells normal hPSCs exhibit a lower cloning efficiency than variant cells possessing gains of chromosomes 1 and 17. The ability of normal hPSCs to clone is nearly abolished upon loss of SSEA3. In contrast, though the cloning efficiency of SSEA3 negative variant hPSCs is reduced compared to SSEA3 positive cells, the efficiency remains higher than SSEA3 positive normal hPSCs (Enver et al., 2005). Single cell transcriptome analysis of SSEA3 positive and SSEA3 negative revealed that patterns of differentiation are altered in variant hPSCs. Normal SSEA3 negative hPSCs show upregulation of genes associated with differentiation, whereas the gene expression of variant SSEA3 negative cells mapped closely to the stem cell compartment alongside SSEA3 positive normal and variant hPSCs (Gokhale et al., 2015). Demonstrating the relationship between

SSEA3 and the stem cell state is altered upon acquisition of certain genetic abnormalities and genetic changes may influence the propensity of hPSCs to differentiate.

The ability to differentiate into the three embryonic germ layers is one of the defining properties of hPSCs (Thomson et al., 1998). Differentiation can be tested through several assays. For example, cells grown on monolayers can be exposed to a cocktail of different cytokines and chemical compounds designed to modulate the activity of distinct signalling pathways that direct cells towards a particular cell type. These are often added progressively to transit cells through the hierarchical progenitor states towards to terminally differentiated state (Terryn et al., 2018). A limitation with this form of assessment is that it only tests a cell's capacity to differentiate towards a single lineage. Other lineages are restricted because of the requirement for different compounds and activity of alternate signalling pathways. Furthermore, differentiation during embryonic development cell fate is influenced by spatial and geometric inputs that occur only in 3D. Another test of differentiation capacity that mimics the 3D nature of the embryo is the formation of embryoid bodies (Martin and Evans, 1975, Ng et al., 2005). Embryoid bodies are spheroid aggregates of hPSCs that undergo spontaneous differentiation into the three germ layers without requirement for addition of growth factors and signalling molecules that would bias cell fate towards a particular lineage. The ability of embryoid bodies to differentiate into the three embryonic germ layers can be quantitatively assessed using gene expression profiling on a defined panel of 96 genes called the pluripotency scorecard (Bock et al., 2011, Tsankov et al., 2015). Pluripotency scorecard approach currently provides the best quantitative approach to assessing the differentiation capacity of hPSCs, however it is insufficient to provide insight into the malignancy potential of variant cells. Previous studies have demonstrated that variant hPSCs can possess altered patterns of differentiation with regards to specific lineages, the effect this resistance may have on the safety of a stem cell based therapeutic is yet to be determined (Keller et al., 2018). Malignancy potential of hPSCs can only be assessed using the teratoma assay (International Stem Cell, 2018). Teratomas generated from variant hPSC lines containing trisomy chromosome 12 abnormality have been shown to possess gene expression profiles distinct from their diploid counterparts as well as enriched for genes associated with cancer-related pathways (Ben-David et al., 2014). Analysis of teratomas for undifferentiated stem

cells and presence of malignant tissue elements can provide an indication as to tumorigenic potential of different hPSC lines (Bouma et al., 2017, Damjanov and Andrews, 2016).

Based on the observations that changes to all aspects of cell fate have been reported in variant hPSCs. The following chapter will address whether different genetic changes confer selective advantage through the same or distinct mechanisms. Utilising the experimental approaches described above I sought to investigate the particular elements of stem cell behaviour that are altered in commonly observed abnormalities as well as how the addition of further genetic changes impacts cell fate.

3.2 Results

3.2.1 Generation of Clonal Cell Lines

Our lab has extensively worked with the hPSC line H7 and in 2004 published one of the first reports of recurrent karyotypic changes in hESCs, the changes reported included gains of chromosomes 17q and 12 in H7 hESCs (Draper et al., 2004). Since the initial report our lab has continued to monitor cultures for karyotypic changes, during this time different genetic variants have spontaneously arisen in cultures of H7 hPSCs. Some of these variants were established into stable lines that have been used in various studies (Harrison et al., 2007, Barbaric et al., 2014, Gokhale et al., 2015). Whereas the other variants were frozen and banked as mosaic populations, a detailed schematic drawing of the culture history of the variant hPSC lines is present in appendix Figure 9.1. I decided to utilise this resource of mosaic and established variant cultures to generate a panel of subclonal lines containing different genetic changes within the same genetic background (Figure 3.1).
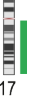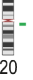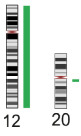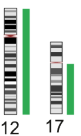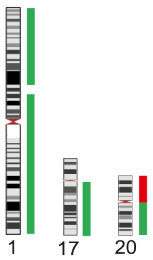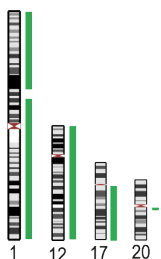
To isolate the variant populations from within the mosaic cultures I used a single cell cloning strategy. Mosaic banks were defrosted and sent for cytogenetic analysis to confirm the genetic changes documented (Figure 3.2A). Following confirmation, I performed single cell sorting into 96 well plates containing MEFs. The sorted cells were left to grow for between 2-3 weeks and establish colonies. Wells containing stem-like colonies were harvested, with half of the cellular material isolated for gDNA extraction and the remaining half passaged for further expansion. Genomic DNA from all the harvested clones was screened by qPCR to determine the relative copy number of the genetic abnormality mosaic in the starting population (Figure 3.2B). Post screening; clones with the desired genetic changes which survived passaging were further expanded and frozen to create master and working cell banks for future use (Figure 3.2C). To confirm the genotype and screen for any other abnormalities that may have arisen during the cloning process, at the time of banking material from each of the clonal lines was sent for karyotyping and qPCR analysis of all the common genetic changes (Figure 3.2D).

I successfully used this strategy to create the clonal lines with individual karyotypic changes: 1q, 20q and 17, as well as the 12,17 line containing two of the most common karyotypic

changes documented in hPSCs. The 12,20 line was sub-cloned from a vial of H7 cells obtained from WiCell reported mosaic for trisomy chromosome 12. In all the trisomy 12 clones I obtained from single cell deposition duplication BCL2L1 at 20q11.21 was also reported during characterisation and I was unfortunately unable to generate a clonal line containing solely chromosome 12. Variant lines 1,17,20 and 1,12,17,20 had previously been established within the lab, stocks of these were obtained and karyotypic changes confirmed before addition to the panel.

Figure 3.1 Panel of clonal hPSC sublines containing genetic changes.

Table detailing the variant hPSC sublines used in this study. Ideogram depicts the chromosomal changes in each of the different genetically variant hPSCs sublines, the bars denote the chromosomal region changed and are colour coded; dark green, gain of a chromosomal region via trisomy, or a structural chromosomal rearrangement (unbalanced transloaction or interstitial duplication); red, loss via a structural chromosome rearrangement (unbalanced transloaction or interstitial deletion).

Ideogram	Description	Karyotype Result
	Duplication of the long arm of chromosome 1 including the possible minimal amplicon 1q32.	46,XX,dup(1)(q21q42)
	Translocation between the long arms of chromosome 6 and 17 resulting in an extra copy of chromosome 17 and derivative chromosome 6.	46,XX,der(6)t(6;17)(q27;q11.2)
	Gain of BCL2L1	46,XX,ish dup(20)(q11.21.q11.21)
	Trisomy chromosome 12 and duplication of BCL2L1.	47,XX,+12, ish dup(20)(q11.21q11.21)
	Addition of chromosome 17q resulting from a derivative chromosome 6 and trisomy for chromosome 12	47,XX,der(6)t(6;17)(q27;q11.2) +12
	Additional chromosome 1 that has an interstitial deletion at 1p22. Gain of 17q via an unbalanced translocation with chromosome 6. Isochromosome of the long (q) arm of chromosome 20. Duplication of BCL2L1 on chromosome 20q 11.21.	47,XX ,+del(1)(p22p22), der(6)t(6;17)(q27;q1), t(12;20)(q13;q11.2),i(20)(q10), ish dup(20)(q11.21q11.21)
	Additional chromosome 1 that has an interstitial deletion at 1p22. Gain of 17q via an unbalanced translocation with chromosome 6, trisomy chromosome 12 and duplication of BCL2L1.	48,XX, +del(1)(p22p22), der(6)t(6;17)(q27;q1),+12, ish dup(20)(q11.21q11.21)

A

Cell Line Karyotype and FISH Report

Result: 46XX , der(6)t(6;17)(q27;q11)[30]/
47XX, der(6)t(6;17)(q27;q11) +12 [2]

BCL2L1: No evidence of duplication
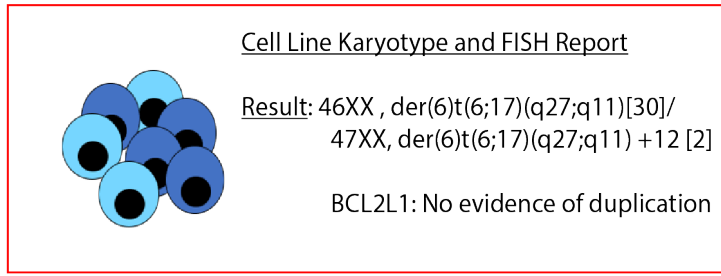
Single Cell Deposition
by FACS
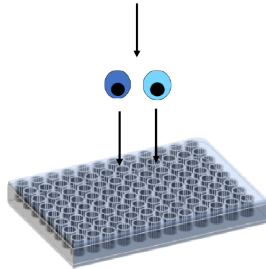
Expansion of clones
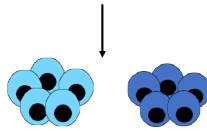
B

qPCR screening
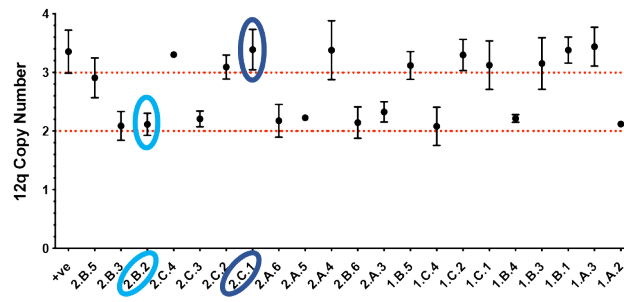
Banking of sub-clonal lines
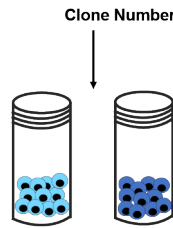
Karyotype and qPCR
characteristaion of banks

C

cl. 2B2

cl. 2C1
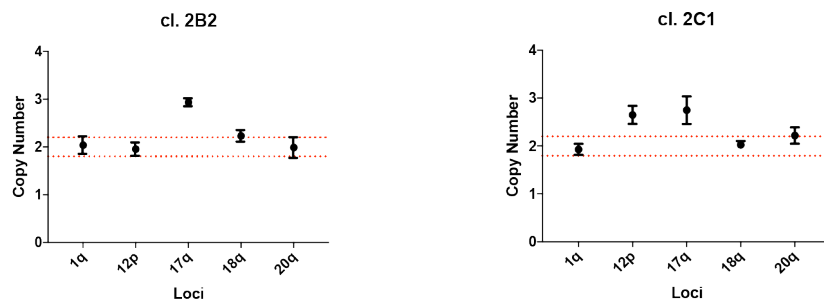
Result: 46XX , der(6)t(6;17)(q27;q11)[30]   Result: 47XX, der(6)t(6;17)(q27;q11) +12 [30]

Figure 3.2 Cloning strategy for generating hPSC sublines containing genetic changes.

Schematic diagram of the cloning strategy approach used to generate the panel of sublines using the 17 and 12,17 lines as an example. **(A)** Heterotypic cultures were identified by karyotype and single cells from these cultures were sorted using BD FACS JAZZ into single wells of a 96 well plate. (**B)** Copy number values for the 12q target gene LGR5 for each clone that was expanded following single cell deposition. Plotted values are means of copy numbers $\pm$ SD relative to H7 karyotypically normal calibrator sample. Positive control values, +ve, are the copy number values for a H7 hPSC line confirmed karyotypically to possess chromosome 12 trisomy. Light blue circle indicates clone 2.B.2 with a copy number value of 2. Dark blue circle indicates clone 2.C.1 with a copy number value of 3. **(C)** qPCR and karyotype results of the banks of clones 2.B.2 and 2.C.1. qPCR graphs show relative copy number for targets genes at the loci of commonly aberrant chromosomal regions. Red lines in all qPCR graphs represent the cutoff levels for a normal diploid result based on the assays detection sensitivity of 10%.

In addition to the panel of variant lines I also made a fluorescently labelled normal line that could be used to distinguish the normal population in experiments that required mixing of variant and normal cells. The variant line 1,12,17,20 already expressed a constitutively active GFP reporter therefore I used a H2B-RFP vector. In the pCAG-H2B-RFP-IRES-PURO vector expression of H2B fused to RFP is driven by a pCAG promoter that has previously shown sustained expression in human PSCs (Liew et al., 2007). The pCAG promoter simultaneously drives neomycin resistance through an IRES conferring antibiotic selection (Figure 3.3A).

The pCAG-H2B-RFP-IRES-PURO vector was electroporated into a normal subline of H7;H7S14 and cells selected for puromycin resistance. A single colony survived selection, this was expanded banked and characterised for any genetic changes. Karyotype and FISH analysis showed no genetic abnormalities (Figure 3.3B) and these results were confirmed by qPCR analysis (Figure 3.3C). To ensure behaviour of the normal-RFP line was comparable to the parental H7S14 line I first assessed their growth rates over a standard 4 day culture period and observed no significant difference between the number of cells counted on each day (Figure 3.3D). Secondly, using flow cytometry analysis I confirmed expression of the RFP and the stem cell associated surface markers SSEA-3 and SSEA-4 providing evidence the normal-RFP line possessed characteristics of PSC (Figure 3.3E).

Figure 3.3 Production of a H2B-RFP normal hPSC line.

(A) The H2B-RFP vector used to generate the H2B-RFP reporter normal hPSC line consists of a pCAG promoter which drives the expression of H2B fused to RFP. Constitutive expression of puromycin resistance through an IRES allowed for selection of successfully transfected cells. **(B)** Karyotype report for the Normal-H2B-RFP line generated showing representative images from G-banded metaphase spreads and reporting a normal karyotype of 46,XX and no evidence of BCL2L1 (20q) duplication by FISH. **(C)** qPCR screening of Normal-H2B-RFP line, plotted values are means of copy numbers $\pm$ SD, red lines represent the cutoff levels for a normal diploid result based on the assays detection sensitivity of 10%. **(D)** Growth curves of normal (blue) and normal-RFP (red) hPSCs. Error bars represent SD from three independent experiments. **(E)** Representative flow cytometric histograms for RFP, positive control staining TRA-185 and pluripotency associated surface antigens SSEA3 and SSEA4. In all graphs the blue plot represents the negative control, and the red plot either the H2B-RFP reporter fluorescence or the antibody staining as denoted above the graph.

A

CAG-H2B-RFP-TRES-Puro
6286 bp

CAG
H2B
RFP
TRES
Puro
Amp
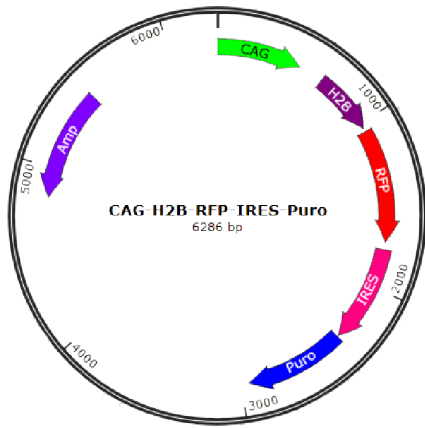
B

Cell Line Karyotype Report

Name	H7S14 PCAG-H2B-RFP P2+4+4+3+3/5
Result	46,XX[30]
	BCL2L1: No evidence of duplication

Comments:

Female karyotype. No abnormality detected. (30 cells examined, 95% chance of detecting a 10% population).

FISH analysis of 100 interphase cells has shown no evidence of BCL2L1 duplication.

C

Copy Number vs Chromosome (1q, 12p, 17q, 18q, 20q). Gain, Normal, Loss.

D

Cell Number vs Days in Culture (Day 0, Day 1, Day 2, Day 3). Normal, Normal-RFP.

E

RFP   TRA-185   SSEA3   SSEA4

Count vs Flourescent Intensity
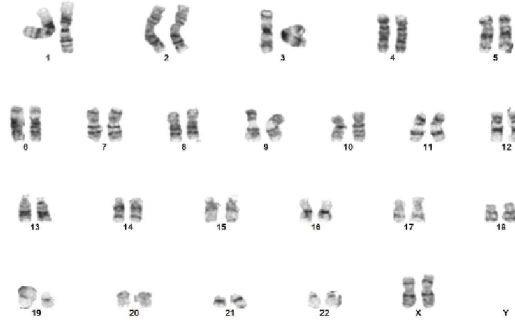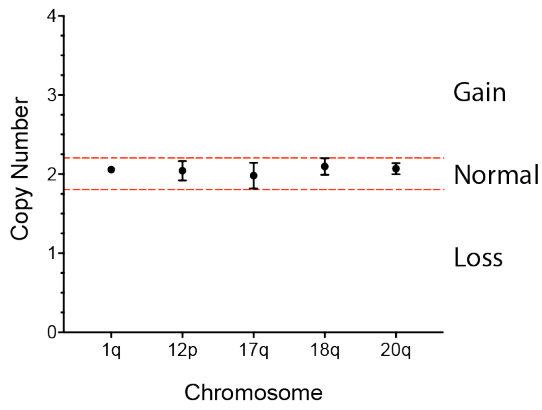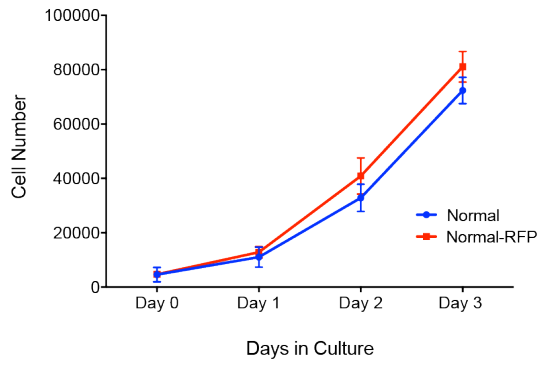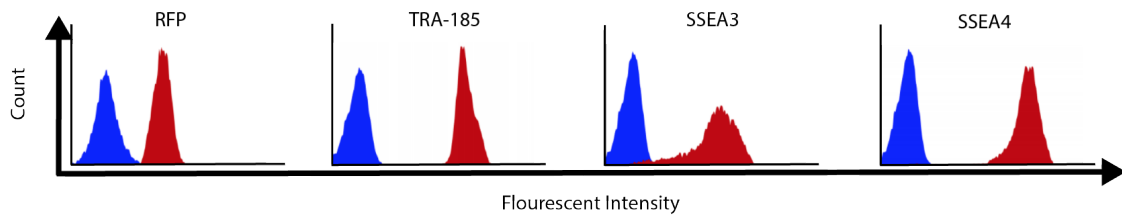
3.2.2 Expression of Stem Cell Associated Surface Markers

I used the expression of the stem cell associated surface markers SSEA-3, SSEA-4 and TRA-1-81 to characterise the undifferentiated state of my panel of variant hPSCs. All the lines showed similar expression to the normal line, demonstrating that acquisition of genetic changes does not alter the proportion of undifferentiated cells or increase levels of differentiation during routine culture (Figure 3.4).

Figure 3.4 Expression of stem cell-associated surface markers.

Flow cytometric histograms for positive control staining TRA-185 and pluripotency associated surface antigens; SSEA3, SSEA4 & TRA-181 against the panel of sub-clonal genetically variant hPSC lines. In all cases the blue plot represents the negative control P3X, and the red plot the antibody staining.
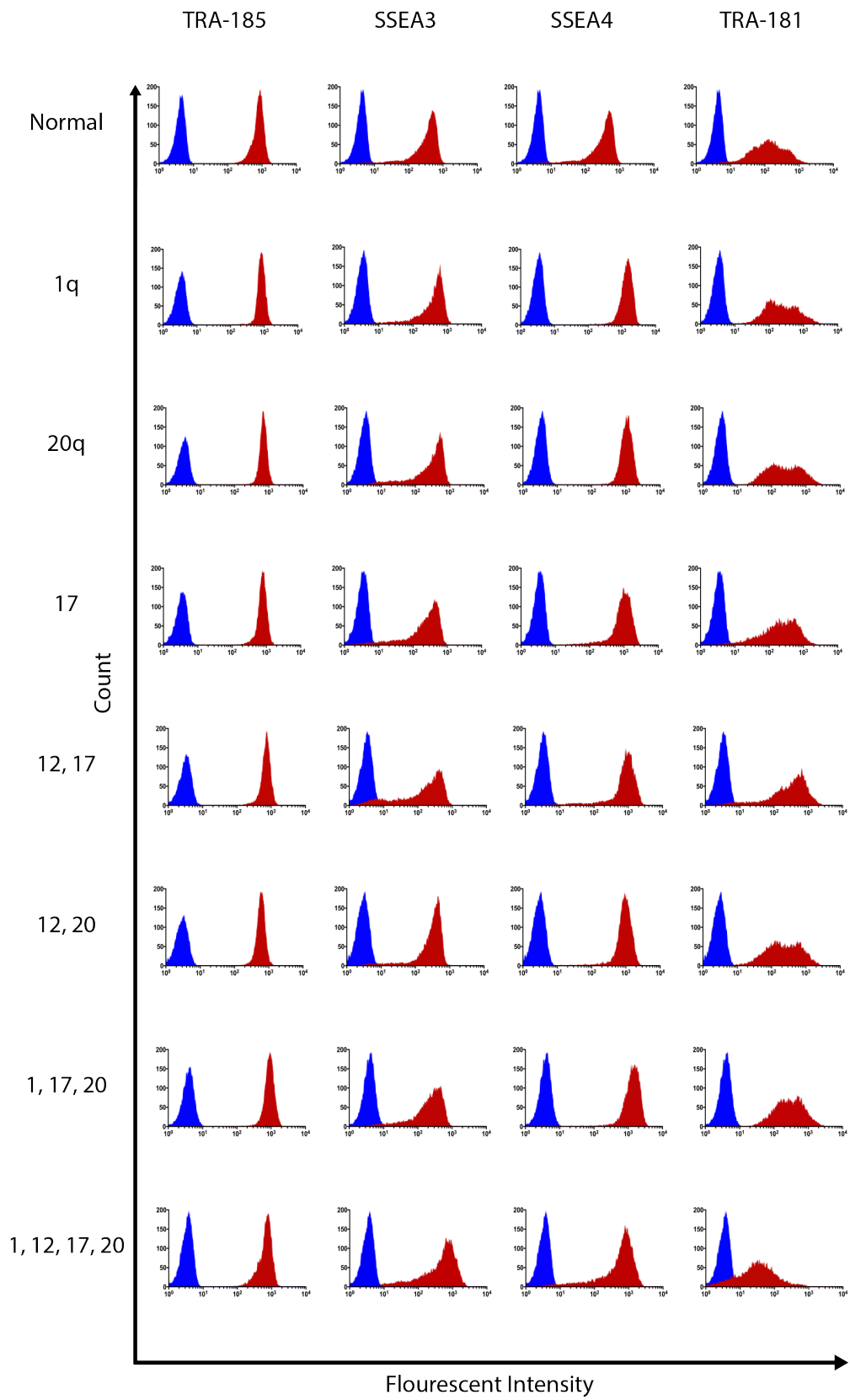
3.2.3   Genetically variant cells overtake normal cells during culture

To establish if all the different genetically variant lines possess selective advantage and assess the rate at which they overtake normal cultures, I performed spiking experiments. Variant and control normal hPSCs were mixed with normal-RFP cells at a level of 10%, equivalent to sensitivity level for detection using common laboratory or cytogentic techniques (Baker et al., 2016). Mosaic cultures were passaged using standard vitronectin culture protocol ever 4 days for a period of 5-10 passages and the proportion of each cell type at each passage was determined using flow cytometry. I observed that all variant lines overtook the cultures whereas the ratio of normal: normal-RFP was maintained.

Analysis of the percentage variant cells also showed differences in the rate at which they overtook the normal cells. The 1,12,17,20 v.hPSC was fastest to reverse the mix ratio to 1:9 taking only 3 passages, whereas the other lines took between 5-7 passages (Figure 3.5A). Furthermore, the gradient of the curves of all variant lines, except 1,12,17,20 v.hPSCs, between passage 1-4 are comparable indicating they overtake normal hPSCs at a similar rate. By passage 10 all variant lines constituted nearly the entire culture (Figure 3.5A).

To show overtake of variant cells was not due to individual culture technique, a second independent experiment was set up and the cultures maintained by a colleague following the same passaging protocol. All variant lines overtook normal hPSCs rapidly over the first 2 passages and by passage 5 constituted nearly the entire culture. Whereas, control normal-RFP did not overtake despite rising from the 11.3% seeded to 23.5% between passages 1-5 (Figure 3.5B).
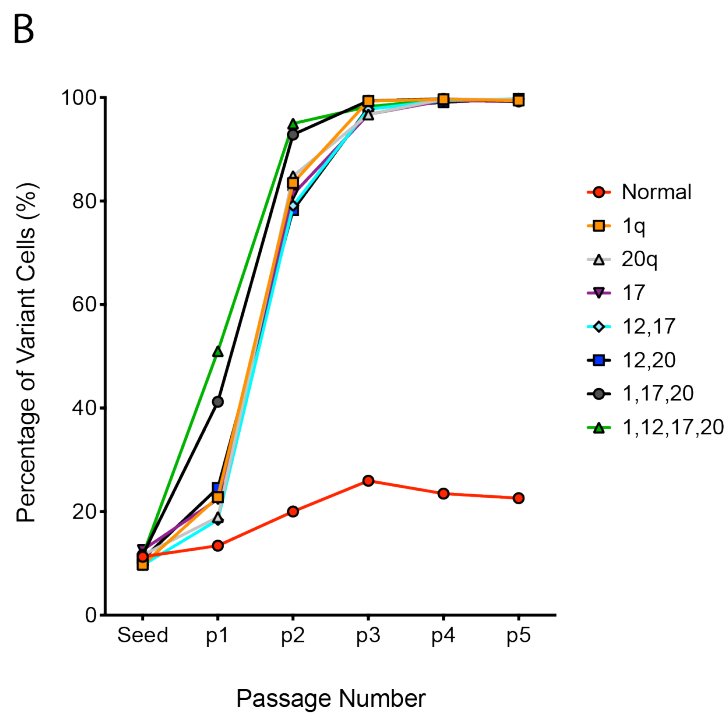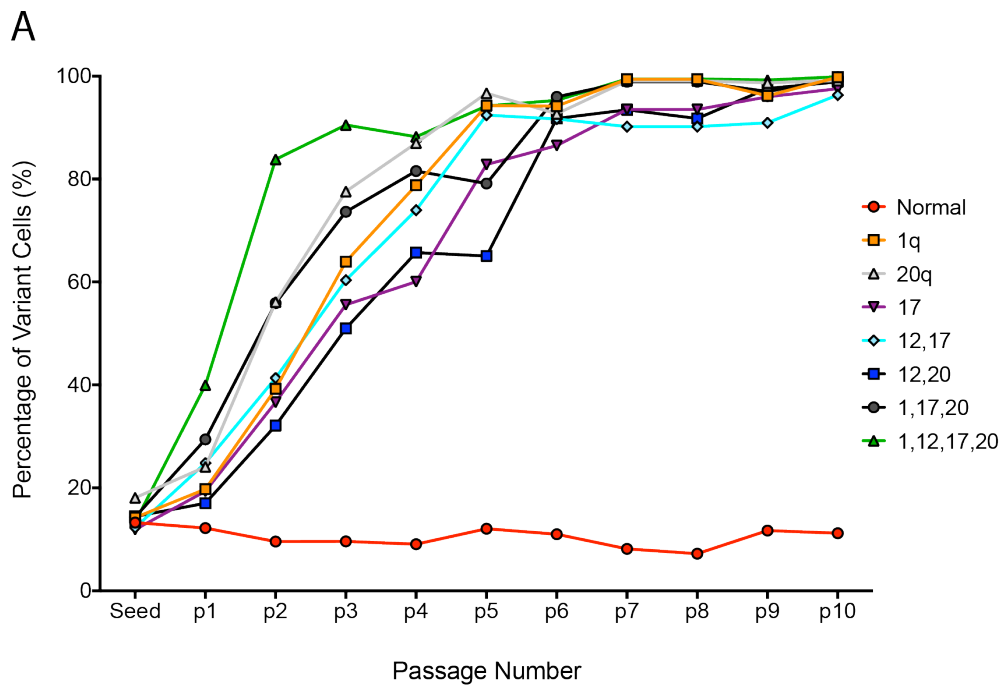
Figure 3.5 Genetically variant hPSCs overtake normal hPSCs over progressive passages.

Genetically variant and control unlabelled normal hPSCs were spiked into normal H2B-RFP cultures at a level of 10%. Cells were passaged every 4 days for 5-10 passages and the percentage of variant and control cells assessed by flow cytometry. **(A)** Results from 1st independent experiment **(B)** results from 2nd independent experiment in which cells were passaged by a colleague following the same passaging protocol.

3.2.4   Effect of genetic change on the growth behaviour of hPSCs

Having demonstrated that genetically variant cells from my panel of hPSC lines containing karyotypic abnormalities possess selective advantage over normal hPSCs and overtake the culture, I next wanted to determine which exact behavioural changes of each variant line enabled them to outcompete the normal hPSCs. Firstly, I analysed the proliferation rates over a standard 4 day culture period. All variant lines, except the 20q v.hPSCs , proliferated faster than the normal cells. Proliferation of the 20q line was similar to normal hPSCs, despite a small significant difference at Day 2, by the end of the experiment there was no significant difference between the total number of cells in each line.

Of the lines carrying an individual genetic change, the 17 v.hPSC line proliferated the fastest in comparison to normal cells. Variant cells with gain of 1q proliferated faster than normal cells but had the lowest level of significance at the end of the experiment. The variant line with the most genetic changes, 1,12,17,20 v.hPSC, had the fastest growth rate. Its proliferation rate displayed a linear increase between days 1-3 whereas all the other cell lines exhibited a quadratic growth curve. Differences in cell number were also observed at day 2 in all of the variant lines compared to normal hPSCs however the degree did not always match that calculated on day 3.

I also assessed the growth of each variant relative to the other lines. All variant lines, except 1q v.hPSC, showed a significant increase in cell number compared to 20q v.hPSCs. But only the 12,17 v.hPSC and 1,12,17,20 v.hSPC grew significantly better than 1q v.hPSCs. The variant lines containing two or more genetic changes and the individual 17 v.hPSC line do not show any significant difference between their total number of cells at day 3 (Figure 3.6).

A

1q

20q

17

12,17

12,20

1,17,20

1,12,17,20
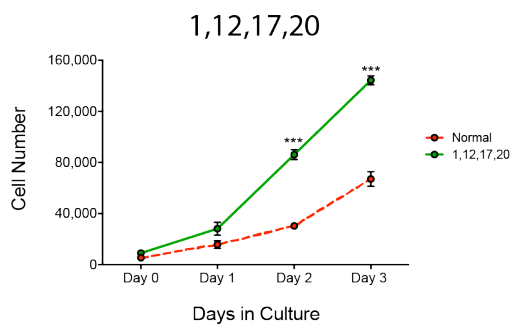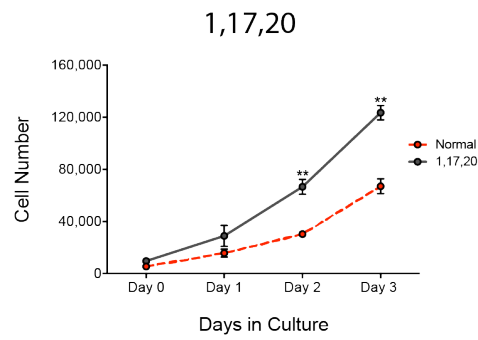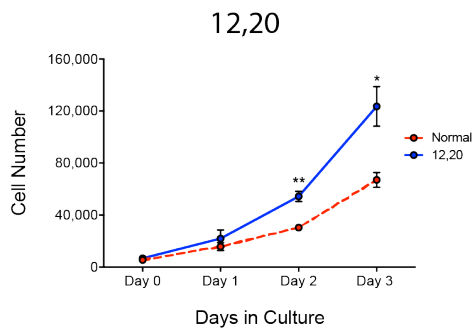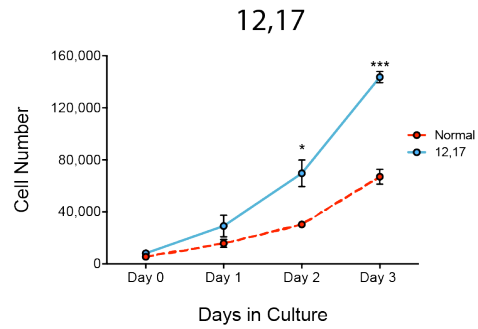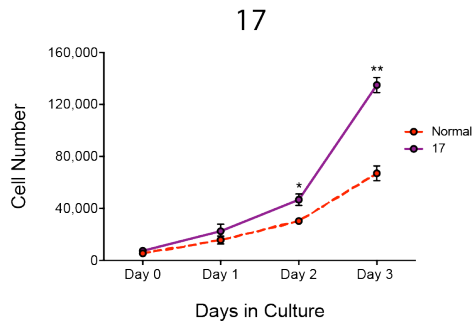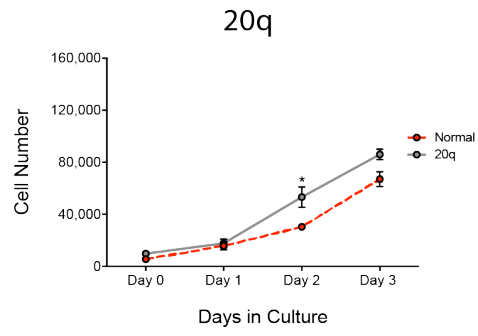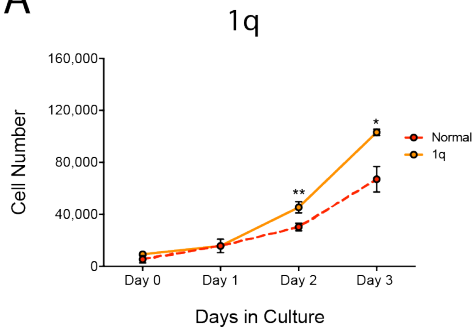
B
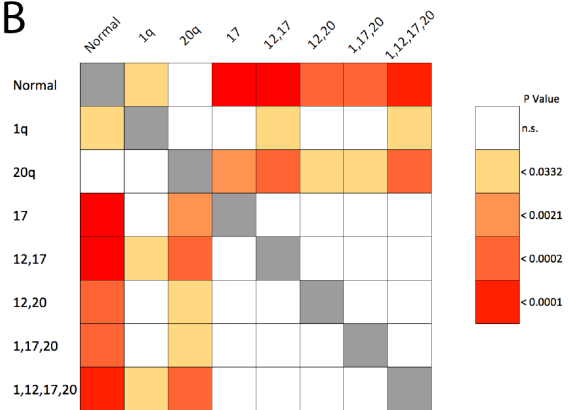
Figure 3.6 Growth rate of variant cells.

(A) Growth curves of normal and variant hPSCs over a 4 days culture period. In all cases the dotted red line represents the normal hPSCs and the solid coloured line denotes the variant hPSCs. Results are the mean of three independent experiments $\pm$ SD. * $p<0.032$, **$p<0.0021$, ***$p<0.002$. P-values obtained by two tailed student's t test.

(B) Statistics matrix of the results from a one-way analysis of variance (ANOVA) followed by Tukey test on the number of cells at Day 3. Boxes are coloured on a scale depending on their significance value from low significance (yellow) to high significance (red). White boxes indicates no significant difference between lines.

3.2.5 <u>Cell Cycle Time</u>

An increased growth rate can result from either a faster cell cycle and/or decreased rate of cell death. To investigate which of these mechanisms determines the growth advantage of each variant line, I first used time-lapse microscopy and measured the time between cell divisions to determine cell cycle time.

Cells were plated at low density and filmed at 10 minute intervals for 72 hours. hPSCs were manually tracked from first to second division and the cell cycle times calculated (Figure 3.7A). To ensure only undifferentiated stem cells were included in the analysis at the end of imaging, cells were fixed and stained with SSEA3 as a marker of undifferentiated state (Figure 3.7B). Only cells that gave rise to SSEA3 positive colonies were included in the analysis.

Cell cycle times ranged from between 10hours – 23hours and some variant lines such as 1q v.hPSC and 12,20 v.hPSC displayed greater variability than the other lines. Lines containing gain of chromosome 17 all displayed a significantly shorter cell cycle time. On average time between 1st and 2nd division was 14 hours, 2 hours $\pm$ 0.4hours less than normal hPSCs, whereas no significant difference was observed between the other variant lines. However, this difference is not solely sufficient to explain the observed growth advantage in the variant lines possessing chromosome 17, nor does it elucidate the mechanism which underlie the selective advantage of 1q v.hPSCs and 12,20 v.hPSCs, indicating that the level of cell death that occurs within cultures must play an important role (Figure 3.8). The equation used to model the exponential growth of two populations with different cell cycle times as well as a detailed table of the results is described in appendix Figure 9.2.

A

Start   1st Division   2nd Division

B

Phase   SSEA3   Merge   2ndry only

C

Time from 1st Division until 2nd Division (h)

Normal | 1q | 20q | 17 | 12,17 | 12,20 | 1,17,20 | 1,12,17,20

Cell Line

n.s.   n.s.   n.s.   ***   ***   n.s.   ***   ***
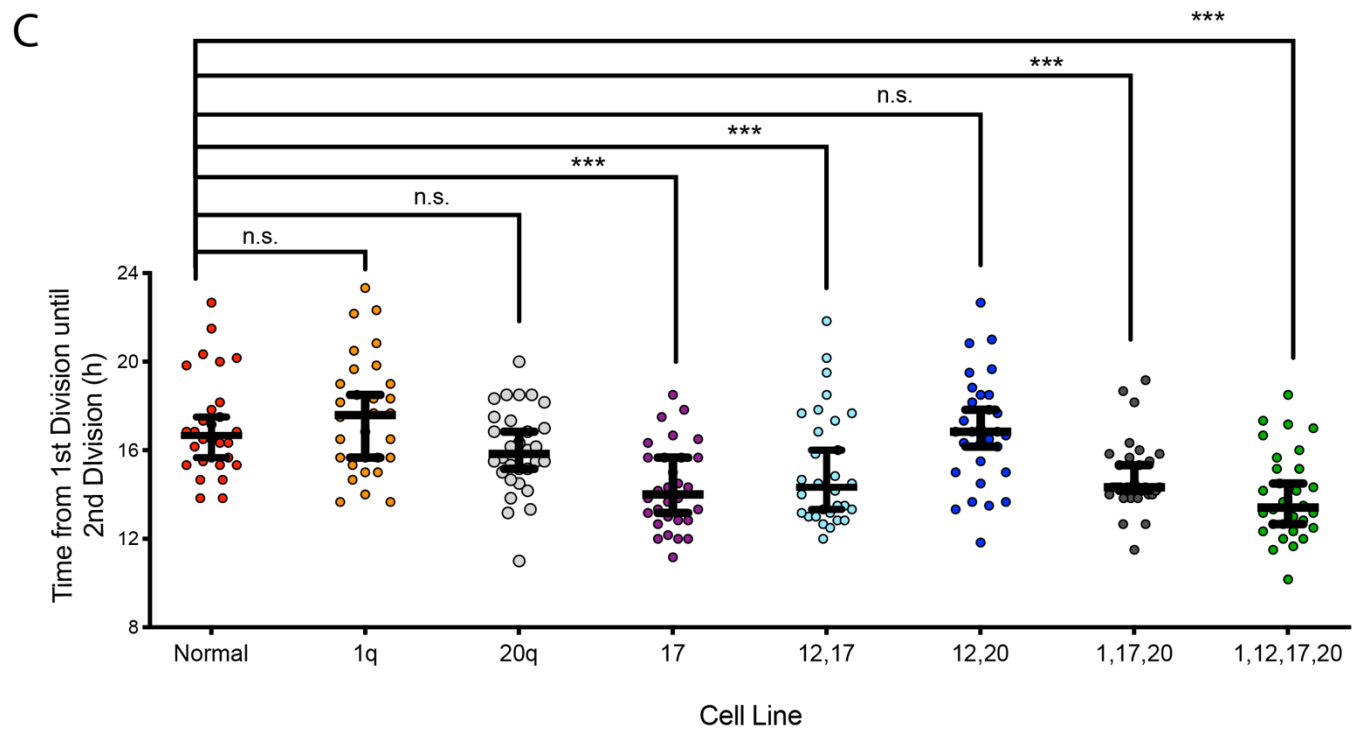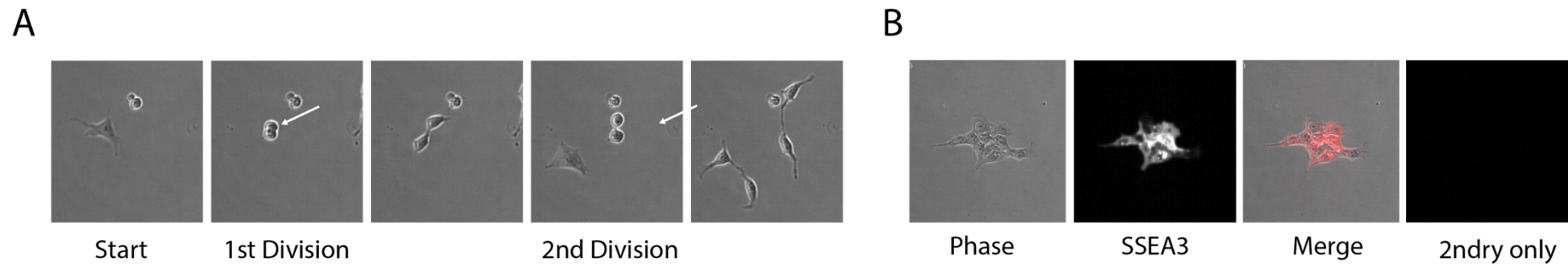
Figure 3.7 hPSC sublines with gain of chromosome 17 have a faster cell cycle time.

(A) Phase contrast images at 10x of hPSCs undergoing division post plating, the point at which two daughter cells are clearly visible (indicated by white arrows) were recorded to calculate time from 1st division until 2nd division. **(B)** Representative phase contrast and immunofluorescence images of SSEA3 staining of the resulting colonies from dividing cells.

(C) The cell-cycle time for normal and variant sublines was measured by manually tracking individual cells from 1st division to 2nd division; each circle represents a single division. Data consists of 30 cells per line with median line and 95% confidence intervals. *** $p<0.002$; a one-way analysis of variance (ANOVA) followed by Dunnett's against normal hPSCs.
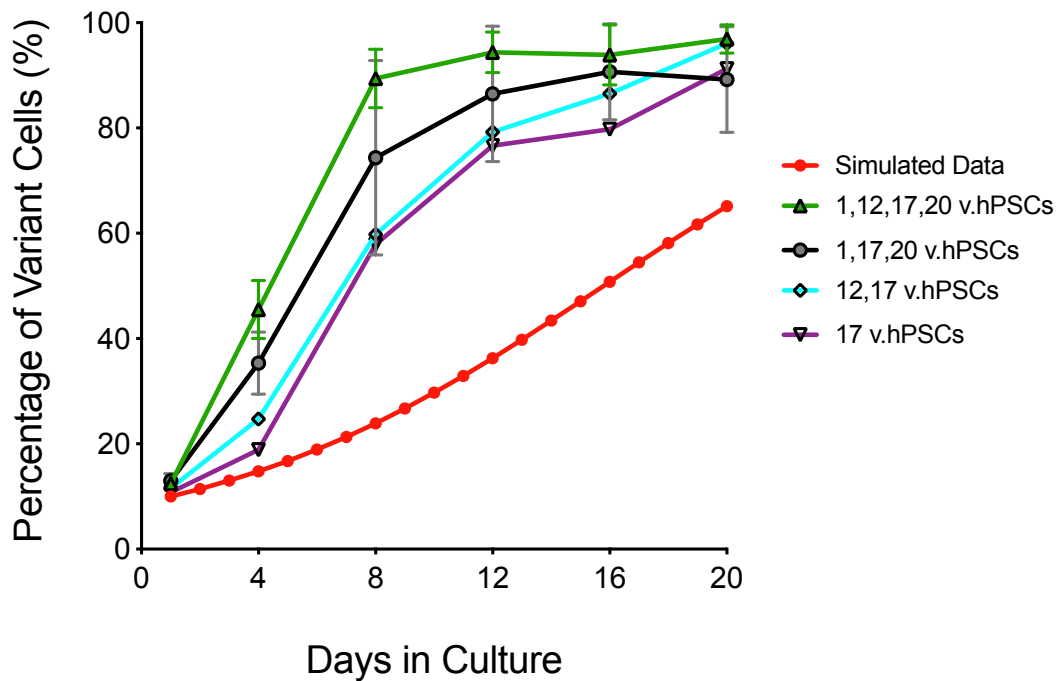
Figure 3.8 Cell cycle time alone is insufficient to explain the growth advantage of variant lines with gain of chromosome 17.

Simulated data for how fast variant cells with a two hour shorter cell cycle time would overtake normal cells, excluding passage and assuming no cell death in both the normal and variant population. For comparison, the average percentage of variant cells from both experiments in Figure 3.5 for the karyotypically variant hPSC lines possessing gain of chromosome 17.

3.2.6   Assessing Apoptotic Resistance

Our lab has previously reported that the selective advantage of variant cells with CNV amplification of chromosome 20q11.21 is mediated through overexpression of the anti-apoptotic gene BCL-XL (Avery et al., 2013). BCL-XL is a member of the BCL-2 family of proteins that have key roles regulating commitment to apoptosis (Shamas-Din et al., 2013). Another member of the BCL-2 family with known anti-apoptotic roles in embryonic development is MCL-1 (Rinkenberger et al., 2000). The MCL-1 gene is located on chromosome 1q21.2 region which is amplified in all of the variant lines carrying gains of chromosome 1. I hypothesised that gain of either or both of these regions would confer a degree of apoptotic resistance to variant hPSCs and contribute to their selective advantage.

Firstly, I harvested protein from 50-60% confluent cultures of normal and variant lines growing under standard vitronectin conditions. Variant lines with gain of chromosome 1 had visibly higher levels of MCL-1 protein than normal hPSCs and variant lines that did not possess chromosome 1 abnormalities (Figure 3.9). In comparison, variant lines with duplication of BCL2L1 appeared to have higher levels of BCL-XL than normal cells and variants lacking 20q11.21 CNV. Cell lines harbouring genetic changes in both 1q and 20q11.21 showed increase levels of both MCL-1 and BCL-XL proteins. Another of the anti-apoptotic proteins, BCL2 appeared to be expressed to a similar level in all cell lines (Figure 3.9).

Secondly, I assessed the level of cell death that occurs during culture in E8 medium on vitronectin. I found that all the variant hPSC lines had lower levels of positive staining for the cleaved form of caspase-3, a measure of early apoptosis, representative flow cytometric histograms are present in appendix Figure 9.3. This included the 17 v.hPSC and 12,17 v.hPSC that didn't appear to have increased levels of MCL-1 and BCL-XL protein. In general, variant lines with the greatest number of genetic changes showed the lowest levels of cleaved caspase-3 positive staining and the greatest degree of significance compared to normal cells. The variant line with the most complex genetic changes, 1,12,17,20 v.hPSC showed the lowest levels of staining and was also significantly lower than 1q v.hPSCs (Figure 3.10A).
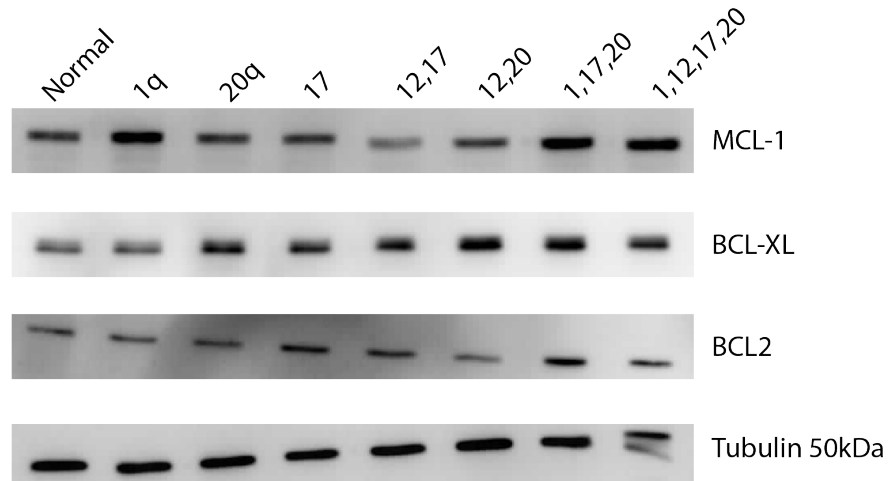
Figure 3.9 Level of anti-apoptotic factors.

Western blot analysis of 20μg total protein from normal and karyotypically variant hPSCs for the BCL-2 family of anti-apoptotic proteins obtained from cells grown under standard culture conditions. Tubulin was used as a loading control.

Next, I chose to challenge the cells with compounds that induce an apoptotic response. BCL-XL is known to provide selective advantage to cells with 20q11.21 CNV (Avery et al., 2013). Therefore, I initially treated cells with ABT-737 (ABT), a small molecule that specifically inhibits BCL-XL (Oltersdorf et al., 2005), to see whether this ablates apoptotic resistance in 20q11.21 CNV lines. Upon treatment with 1μM ABT the levels of cleaved caspase-3 rose in all cell lines compared to E8 conditions. Cleaved caspase-3 levels in the 20q v.hPSC line was similar to the other variant lines, except those possessing 3 or more karyotypic abnormalities.

The variant lines containing 3 or more karyotypic changes, 1,17,20 v.hPSCs and 1,12,17,20 v.hPSCs, were the only cell lines that showed significantly lower caspase levels than normal hPSCs. Furthermore, the levels of cleaved caspase-3 were significantly lower in 1,17,20 v.hPSCs and 1,12,17,20 v.hPSCs than the 12,20 v.hPSC variant line (Figure 3.10B). Variant lines 1,17,20 v.hPSC and 1,12,17,20 v.hPSC are unique because they are the only variants that showed increased levels of both BCL-XL and MCL-1 (Figure 3.9).

Finally, cells were treated with thapsigargin to induce apoptosis in a manner independent of specifically targeting the mitochondria associated BCL-2 family proteins. Thapsigargin inhibits the function of Ca^{2+}-dependent ATPase in the endoplasmic reticulum (ER) causing ER stress and induction of apoptosis (Lytton et al., 1991, Oslowski and Urano, 2011, Sano and Reed, 2013). All cell lines showed increased levels of cleaved caspase-3 compared to E8 conditions upon treatment with thapsigargin. However, compared to normal hPSCs the levels of staining was significantly lower in all variant lines (Figure 3.10C). Furthermore, a greater degree of significance was noted in all the variant lines harbouring duplication of BCL2L1 in comparison to normal cells, suggesting that BCL-XL is providing the strongest anti-apoptotic phenotype of all the karyotypic abnormalities assessed. In addition, cleaved caspase-3 levels were also significantly lower than those found in 1q v.hPSCs in variant lines where gain of BCL2L1 was accompanied by another genetic change. Greatest amongst these were the lines that showed increased levels of both BCL-XL and MCL-1; 1,17,20 v.hPSC and 1,12,17,20 v.hPSC (Figure 3.10C).

A

E8

B

1uM ABT Treatment

C

100nM Thapsigargin Treatment
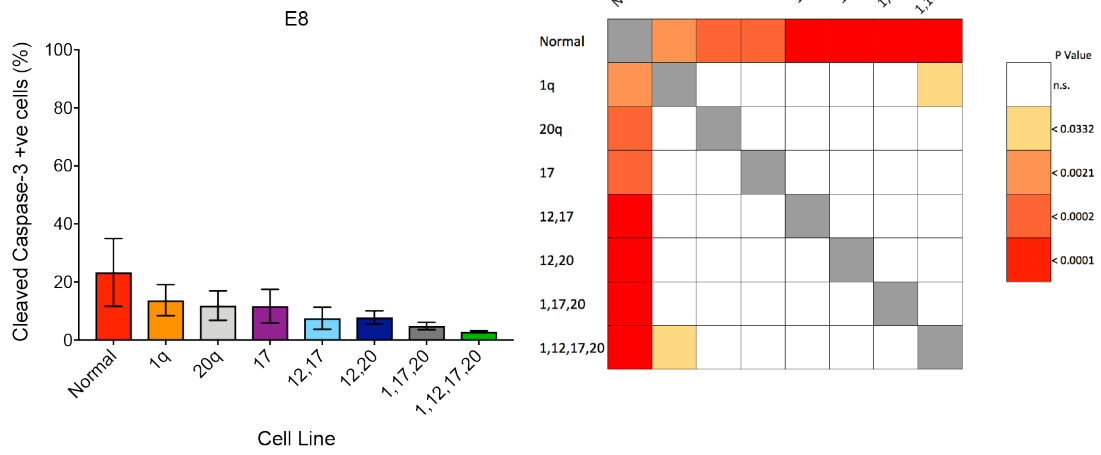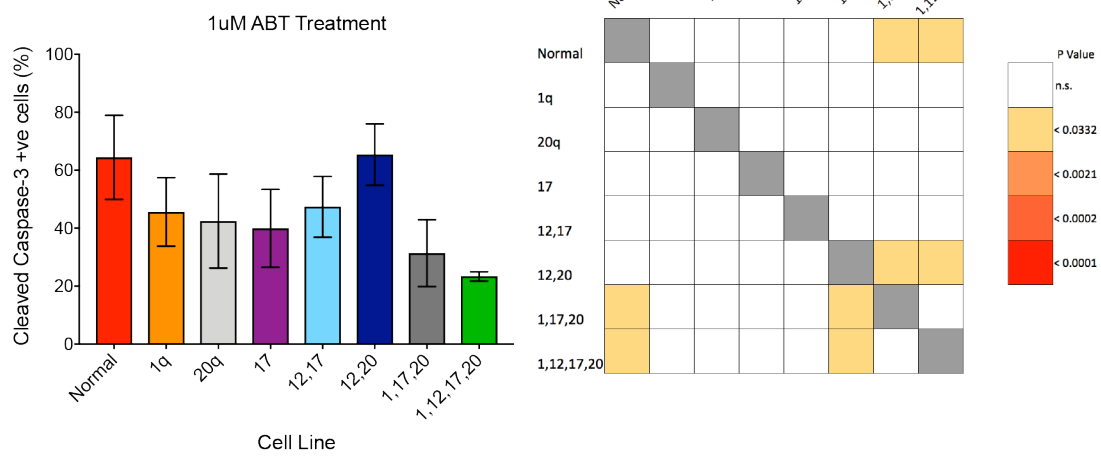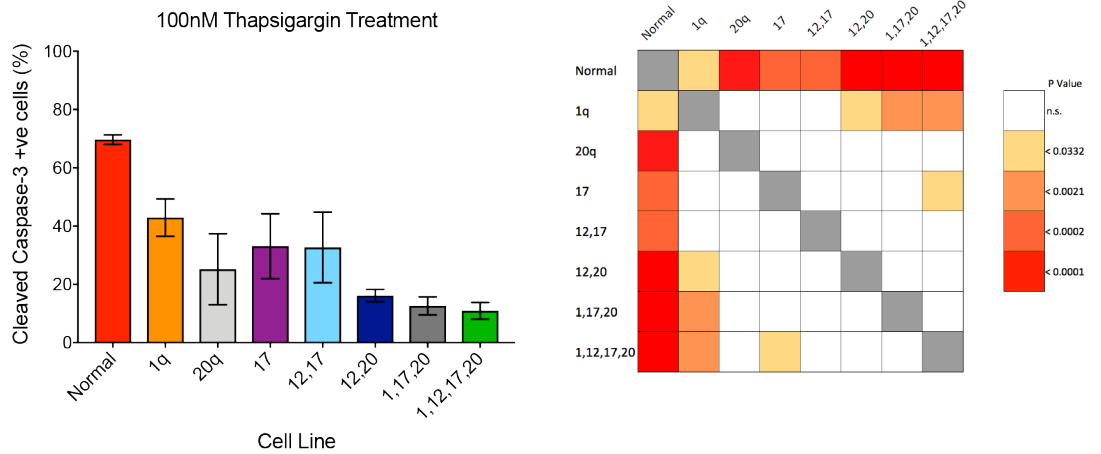
Figure 3.10 Apoptosis levels in normal and variant hPSCs.

Percentage of cleaved caspase-3 positive cells for each hPSC sub-line grown in **(A)** standard E8 conditions **(B)** in the presence of 1uM ABT and **(C)** 100nM Thapsigargin for 24 hours. A minimum of three independent experiments were performed and the mean ± SD plotted. Statistics matrix of the results from a one-way analysis of variance (ANOVA) followed by Tukey test are shown next to data from each culture condition. Boxes are coloured on a scale depending on their significance value from low significance (yellow) to high significance (red). White boxes indicates no significant difference between lines.

 (B) Statistics matrix of the results from a one-way analysis of variance (ANOVA) followed by Tukey test on the number of cells at Day 3. Boxes are coloured on a scale depending on their significance value from low significance (yellow) to high significance (red). White boxes indicates no significant difference between lines.

3.2.7   Cloning efficiency of different variants

Having established that the different variant lines possess altered proliferation and apoptotic responses I wanted to investigate these functional differences in self-renewal at the single cell level. I performed quantitative high content clonogenic assays to assess differences in self-renewal capacity. Cultures of normal and v.hPSC lines were harvested and stained for the surface antigen SSEA-3, associated with the undifferentiated state. Only single cells from populations that were ≥85% SSEA3 positive were seeded to ensure plating of undifferentiated stem cells (Figure 3.11A). Human PSCs were plated onto MEF based culture conditions because the vitronectin culture system did not support clonogenic growth. The resulting colonies were counted and cloning efficiency calculated.

In the variant hPSC lines with a single karyotypic change I only saw a significant increase in cloning efficiency compared to normal cells in cells containing chromosome 17 gain. The lines 1q.v.hPSC and 20q v.hPSC displayed similar cloning efficiencies of 3.5% (±1.1%) and 6.3% (±3.1%) respectively. The two lines carrying a pair of genetic changes, 12,20 v.hPSC and 12,17 v.hPSC were both significantly greater than normal cells but also showed similar patterns of cloning efficiency of 11.8% (±4.3%) and 12.5% (±4.4) respectively. Variant lines with the three of more karyotypic changes were the most clonogenic, 1,17,20 v.hPSCs cloned at 23.74% (±2.4) and 1,12,17,20 v.hPSCs at 34.8% (±9.1%) (Figure 3.11B).

Next, I stained the colonies by immunohistochemistry for either of the pluripotency associated markers OCT4 or NANOG (Figure 3.11C). I then performed a detailed analysis of the total number of cells and the percentage of OCT4 or NANOG positive cells within each colony from every cell line. The variant cell lines with a higher cloning efficiency than normal hPSCs tended to generate colonies containing a significantly greater number of cells. An exception to this observation were colonies formed from 17 v.hPSCs and 12,20 v.hPSCs (Figure 3.11D). Following on from this observation, I next decided to assess the distribution of the total number of cells per colony to further assess the relationship between cloning efficiency and colony size. Normal hPSCs formed relatively small colonies, the upper limit of the standard deviation was approximately 100 cells/colony, whereas the variant lines 17 v.hPSC and 12,20 v.hPSC generated a greater number of colonies containing 100 cells or

more. The variant lines possessing two or more genetic changes exhibited the greatest range of colony size and highest frequency above 100cells/colony (Figure 3.11D').

Normal cells exhibited the lowest average percentage of OCT4 positive cells per colony as well as large standard deviation (39.8%) indicating a high degree of variability in OCT4 positive cells per colony. Analysis of individual genetic changes showed that 20q v.hPSCs and 17 v.hPSCs have a greater number of colonies with high OCT4 expression. In comparison, colonies from 1q v.hPSC have a slightly higher average OCT4 expression than the normal cells but a similar degree of variability (32.5%). Colonies from variant lines containing two or more karyotypic changes displayed comparably higher average percentages of OCT4 expression than normal cells, in addition to a greater frequency of high proportion OCT4 expressing colonies indicated by the smaller standard deviations (13.2%-23.6%)(Figure 3.11E-E').

I performed the same analysis on colonies stained with NANOG from each of the different cell lines, where I saw the same trend as OCT4. Normal and 1q v.hPSCs produced colonies with the lowest average NANOG positive cells per colony and the greatest deviation. In contrast, the other variant lines have a higher percentage of NANOG positive cells and a greater number of colonies expressing high levels of NANOG (Figure 3.11F-F').
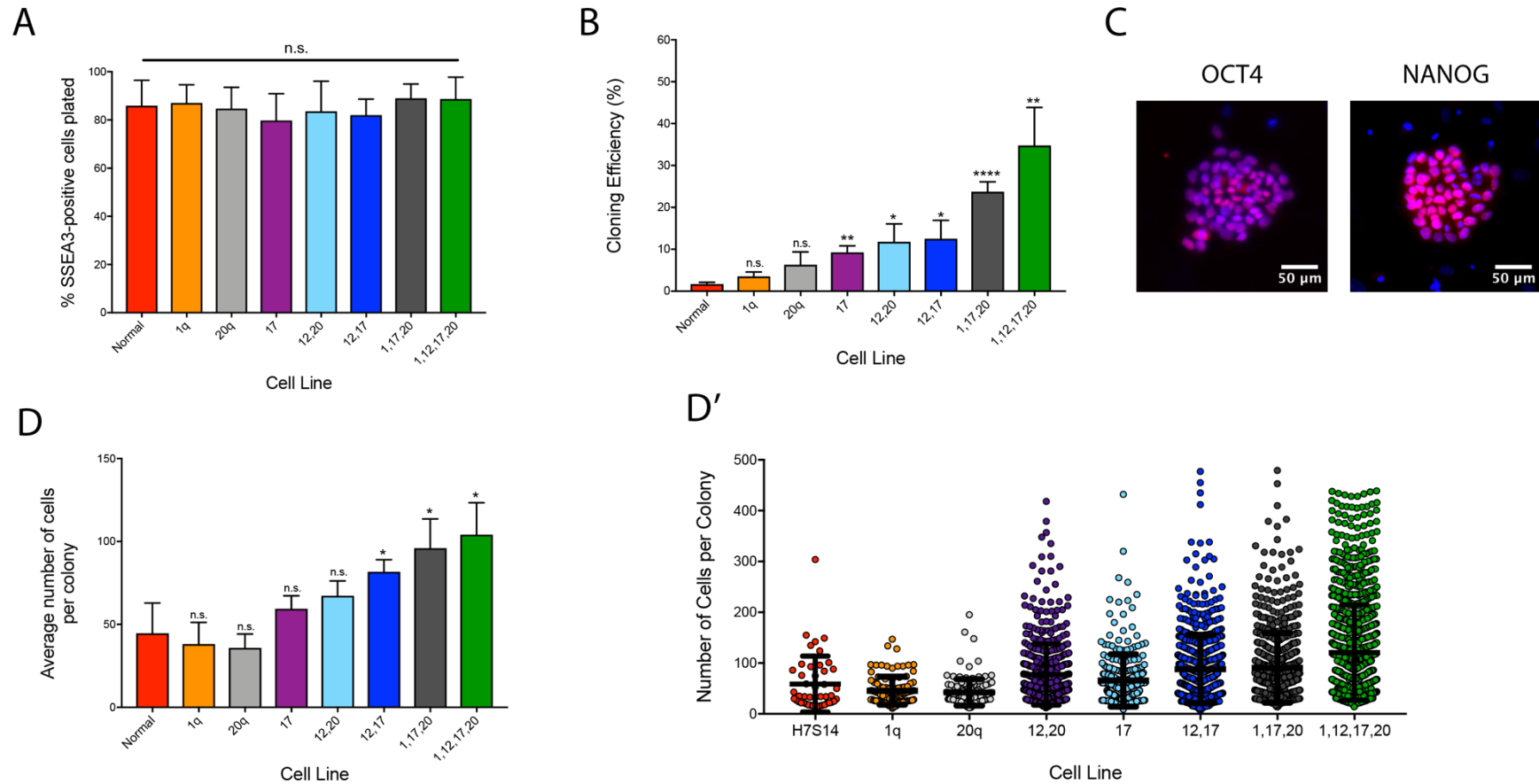
Figure 3.11 Assessment of clonogenic capacity.

Cultures of normal and genetically variant hPSCs were dissociated to single cells and seeded at clonogenic density, after 5 days the resulting colonies were stained for either OCT4 or NANOG. **(A)** The populations harvested were analysed for the pluripotency associated marker SSEA3. **(B)** Absolute cloning efficiencies show variant hPSC sublines clone better than normal hPSCs. **(C)** Immunofluorescence images of colonies stained with Hoescht (blue) and either OCT4 or NANOG (red).
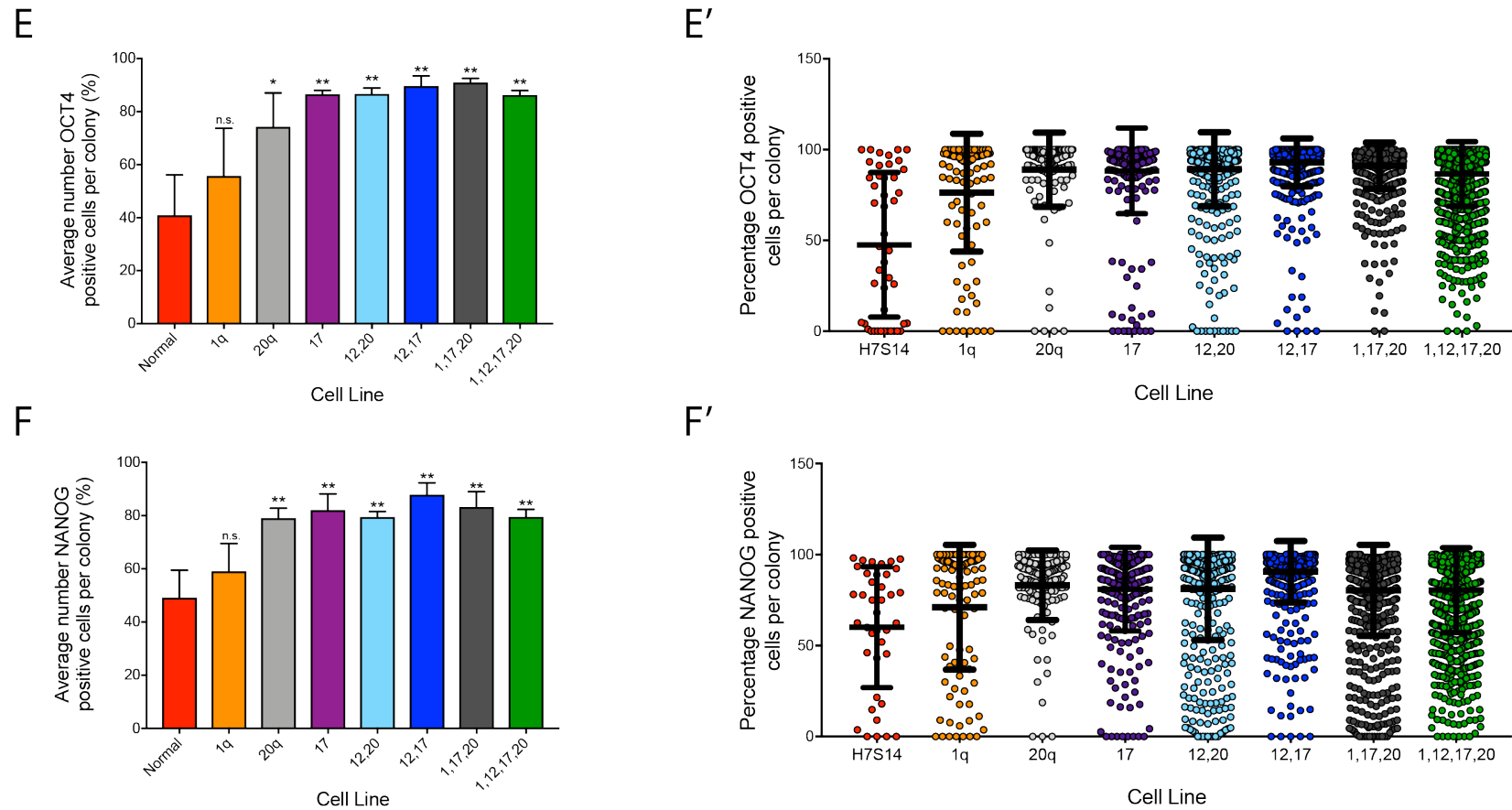
Figure 3.11 Assessment of Clonogenic Capacity cont.

(D) The average number of cells per colony and (D') distribution from a representative experiment. (E) Percentage of OCT4 positive cells per colony and (E') a representative distribution for each cell line. (F) Percentage of NANOG positive cells per colony and (F') a representative distribution for each cell line. N= three independent experiments. * p< 0.032, ** p< 0.021, **** p< 0.0001 , Students Paired t test.

3.2.8   Differentiation capacity of different variants

The final aspect of stem cell fate we wanted to assess was differentiation potential. Various reports have implicated gain of particular genetic changes with loss of differentiation capability in respect to a certain lineage. I thus wanted to test my normal and variant hPSC lines to determine their trilineage potential and whether they exhibited bias to a particular germ line fate in a "Neutral" Embryoid Body (EB) assay.

Cultures of normal and variant hPSC were dissociated to single cells and assessed by flow cytometry for their proportion of undifferentiated stem cells using the surface markers SSEA3 and SSEA4. Only cultures that were $\geq$85% SSEA3 were used to ensure plating of undifferentiated hPSCs (data not shown). To generate EBs, I plated 3,000 cells per well of a 96 well plate in APEL 2 media supplemented with 10μM Y-27632 and incubated for 7 days (Figure 3.12A). The EBs from the various lines differed greatly in size from each other but retained an overall spherical shape (Figure 3.12B). Normal and 17 v.hPSCs formed the smallest EBs however there was less evidence of cell debris in the 17 v.hPSC samples. Whereas, the other variant lines made substantially larger EBs but also exhibited morphologically differences. EBs made from lines possessing gain of 20q11.21, except the 1,12,17,20 v.hPSC line, showed a dense, compact morphology and highly spherical. In comparison, in addition to a region of high density EBs from the 1q v.hPSC , 12,20 v.hPSC and 1,12,17,20 v.hPSC lines also had an outer layer of less dense cells suggesting a slight difference in structural organisation (Figure 3.12B).

Next EBs were harvested and run on TaqMan hPSC scorecards from ThermoFisher that are designed to quantitatively determine the pluripotency and trilineage potential of hPSCs. Normal hPSCs harvested from the same cultures used to make EBs were run as the undifferentiated control. Resulting qPCR data was analysed using ThermoFisher's scorecard analysis software. The software calculates an algorithm score for each germ line lineage and self-renewal based on the expression values of genes associated with the respective lineage. Algorithm values were normalised to undifferentiated controls and plotted for each cell line (Figure 3.12C).

EBs derived from normal cells exhibited a down regulation of self-renewal associated genes and upregulation of ectoderm associated genes. In contrast, there was very little upregulation of genes associated with mesoderm and endoderm. The algorithm score for both lineages was less than the threshold value of 1 at which the software denotes a lineage as being upregulated. The 17 v.hPSC line which formed EBss of a similar size and morphology to normal cells displayed a similar pattern of gene expression; high upregulation of ectoderm associated genes and very little upregulation of mesoderm and endoderm associated genes. However, they also displayed a stronger down regulation of self-renewal associated genes compared to EBs from normal hPSCs (Figure3.12C).

Comparing the algorithm scores, another pair of lines with striking similarity were 20q v.hPSC and 12,20 v.hPSCs. EBs formed from these lines upregulated ectoderm associated and mesoderm associated genes but the algorithm score for endoderm, though greater than normal hPSCs, fell below the threshold value for upregulation. These lines also showed similar morphological characteristics to each other (Figure 3.12C).

EBs derived from 1q v.hPSCs had higher upregulation of the genes associated with the differentiation lineages than normal hPSCs. However only the score for the ectoderm lineage was greater than the threshold, mesoderm and endoderm values fell just below; 0.98 ($\pm$0.2) and 0.80 ($\pm$0.7) respectively.

Variant line 12,17 v.hPSC line was one of two lines that showed a positive expression signature for all the differentiation lineages. Algorithm scores showed strong down regulation of self-renewal associated genes, whilst upregulation of mesoderm associated and endoderm associated genes occurred to a similar degree. Genes associated with ectoderm were upregulated to a slightly higher level than the other differentiation lineages (Figure 3.12C).

The other cell line from which the EBs derived showed expression of genes from all three differentiation lineages was 1,12,17,20 v.hPSC. However, the pattern of expression was different to the previously discussed lines. EBs from this line display a higher upregulation of mesoderm associated genes than the other differentiation lineages. Genes associated with

endoderm were also strongly upregulated to levels not seen in the other lines. In addition, ectoderm associated genes were upregulated to a similar level observed in EBs from the other cell lines.

The only cell line to produce EBs that did not show upregulation of any of the differentiation lineages was 1,17,20 v.hPSC. Algorithm scores for ectoderm associated, mesoderm associated and endoderm associate genes were below threshold value for upregulation. Furthermore, they exhibited upregulation of self-renewal associated genes compared to undifferentiated control (Figure 3.12C).

Figure 3.12 Assessing the tri-lineage differentiation potential of variant hPSCs.

(A) Schematic of the 7 day EB differentiation protocol. **(B)** Representative phase contrast images taken at 4x of EBs from all hPSC sub-lines on Day 0 and Day 7 of EB differentiation. **(C)** A bar chart of the algorithm score from ThermoFisher's human PSC scorecard analysis for self-renewal and the differentiation lineages; ectoderm, mesoderm and endoderm.

The scores are calculated based on the qPCR values of the genes within each lineage set and baselined to the average value of the undifferentiated normal hPSC samples. Results are the mean of three independent experiments $\pm$ SD.

A

Day 0   APEL 2 Media   Day 7

hPSC   Embryoid Body

B

Normal   1q   20q   12,20

Day 0

Day 7

17   12,17   1,17,20   1,12,17,20

Day 0

Day 7

C

Algorithm Score

Cell Line

Self Renewal
Ectoderm
Mesoderm
Endoderm
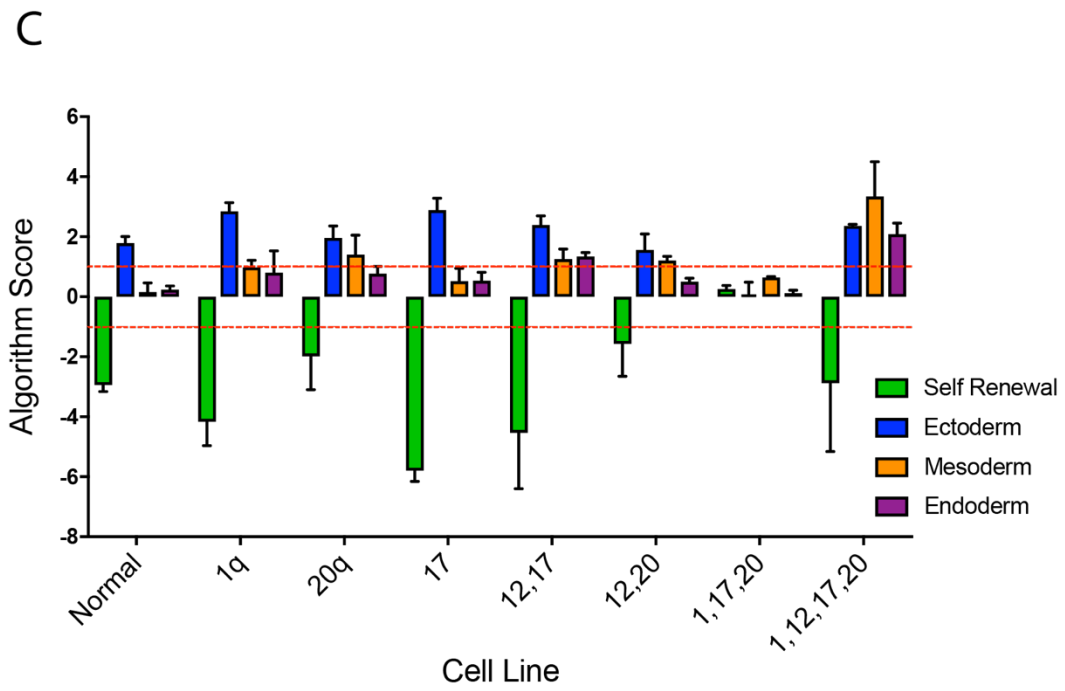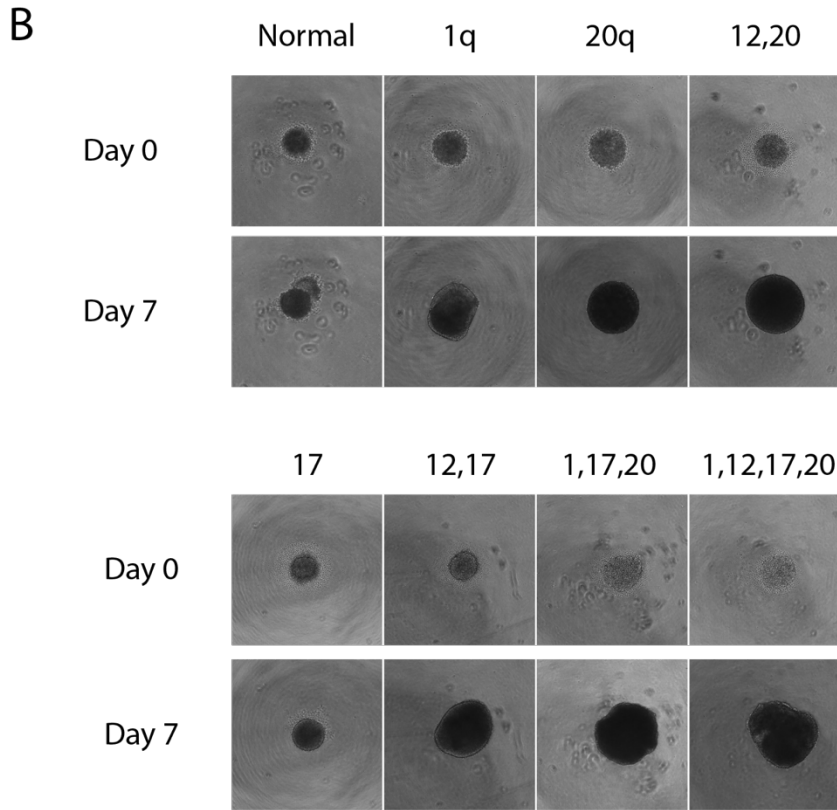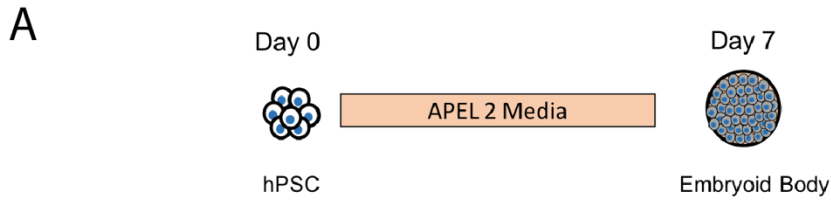
To investigate the variation seen between EBs derived from the panel of cell lines, I utilised the gene expression data from the TaqMan hPSC scorecards. I normalised the Ct value of each gene to the house keeping gene *Actin Beta (ACTB)* for every sample and performed hierarchical clustering on the entire gene set (Figure 3.13).

Hierarchical clustering segregated the cell lines into two main clusters. The first cluster contained all the normal hPSC undifferentiated samples and 1,17,20 v.hPSC EB samples as well as the first repeats of the 20q v.hPSC and 12,20 v.hPSC EB samples. Cells from these samples had high expression of self-renewal associated genes such as *NANOG* and *POU5F1*, whereas genes associated with differentiation had predominantly low expression. However, I also observed high expression of markers associated with both self-renewal and differentiation, such as *LEFTY1* and *GDF3*.

The second cluster contains EBs derived from all the other cell lines and can be further segregated into two clear sub-clusters. The first sub-cluster contained EBs derived from the Normal, 1q v.hPSC, 17 v.hPSC and 12,17 v.hPSC lines. This sub-cluster displayed downregulation of self-renewal associated genes and strong upregulation of ectoderm associated genes. Expression of *SOX2,* a key gene in the regulation of pluripotency and neural ectoderm marker, was also strongly upregulated. Some upregulation was observed in a few genes associated with either an endoderm, mesendoderm or mesoderm fate. However, most genes within these gene groups were lowly expressed.

The remaining sub-cluster encompassed the EBs derived from the 20q v.hPSC , 12,20 v.hPSC and 1,12,17,20 v.hPSC lines. Samples from this cluster displayed upregulation of genes associated with two or more differentiation lineages as well as expression of the self-renewal associated gene *NANOG* in most samples. Within this cluster two samples, 12,17 r1 v.hPSC and 1,12,17,20 r1 v.hPSC, showed expression of both self-renewal associated genes and upregulation of genes associated with each differentiation lineage.

Analysis of differentiation capacity using TaqMan hPSC scorecards demonstrates differences between the EBs generated from each cell line. It also showed some degree of similarity between lines containing the chromosome 20q11.21 amplification. As well as demonstrating that one cell line 1,17,20 v.hPSC formed EBs which retained a self-renewal associated gene expression pattern similar to undifferentiated hPSCs.
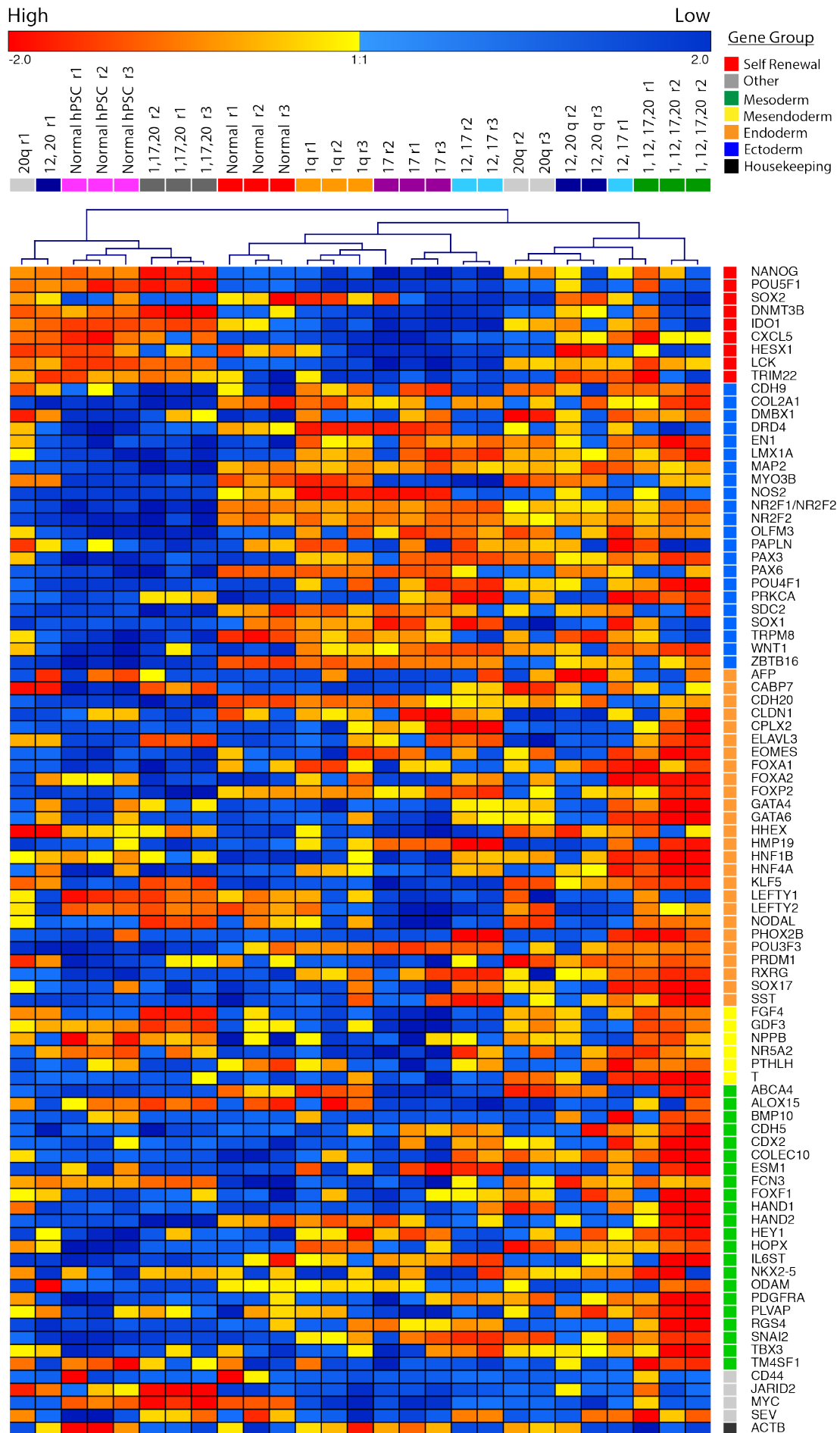
Figure 3.13 Heatmap analysis of embryoid body differentiation.

Heatmap of hPSC sublines differentiated for 7 days as EBs and assessed by ThermoFisher's human PSC scorecard. The Ct values of each gene are normalised to the housekeeping gene *ACTB*. Genes are colour coded and ordered according to their corresponding gene group. Heatmap colour scaling was done after mean centring the genes from all sublines and hierarchical clustering was based on the entire gene set. Repeats of each cell line from the three independent experiments are denoted by name of the cell line followed by r1, r2 or r3 respectively. Overall the data clustered into 2 main subsets, cluster one predominantly contained the undifferentiated normal hPSCs and 1,17,20 samples. The second cluster consisted of all the other hPSC sub-lines.

3.2.9 Assessing the metabolic activity of different variants

I have shown that variant hPSCs exhibit altered aspects of cell fate compared to normal cells. To continue from this, I next wanted to investigate whether they also possessed differences in their metabolic activity. Mitochondria function and metabolic activity have been shown to control proliferation and influence early differentiation in hPSCs (Mandal et al., 2011). Previous studies have shown metabolism in hPSCs occurs mostly through aerobic glycolysis which generates ATP a faster rate, produces less reactive oxygen species than oxidative phosphorylation and generates nucleotides needed for proliferation (Folmes et al., 2011, Panopoulos et al., 2012, Vander Heiden et al., 2009).

Firstly, I performed live staining of normal and variant hPSCs with MitoTracker Green to measure the abundance of mitochondria in each lines. MitoTracker Green was used because it localises with mitochondria independent of mitochondrial membrane potential. However, I was unable to use MitoTracker Green in the 1,12,17,20 v.hPSC line because it constitutively expresses a GFP reporter. As shown in Figures 3.13A and 3.13B, most variant lines had the same level of mitochondrial fluorescence as the normal hPSC lines. In comparison, significantly lower staining intensity was seen in the 12,20 v.hPSC and 1,17,20 v.hPSC lines indicating less abundance of mitochondria in these lines.

Secondly, I measured the steady-state ATP level in standard culture conditions and normalised to cell numbers. While there was a trend for increased ATP levels in all the variant lines, this trend was not significantly different in the 20q v.hPSC and 1,17,20 v.hPSC lines (Figure 3.14A). Next, ATP levels were also measured after incubation with the metabolic inhibitors, oligomycin (ATP synthase inhibitor) and 2-deoxyglucose (2-DG) (glycolysis inhibitor). Treatment with oligomycin showed no significant effect on the amount of ATP produced per cell line indicating the majority of intracellular ATP is not supplied by oxidative phosphorylation, whereas incubation with 2-DG caused comparable decreases in the proportion of ATP production (Figure 3.14B).
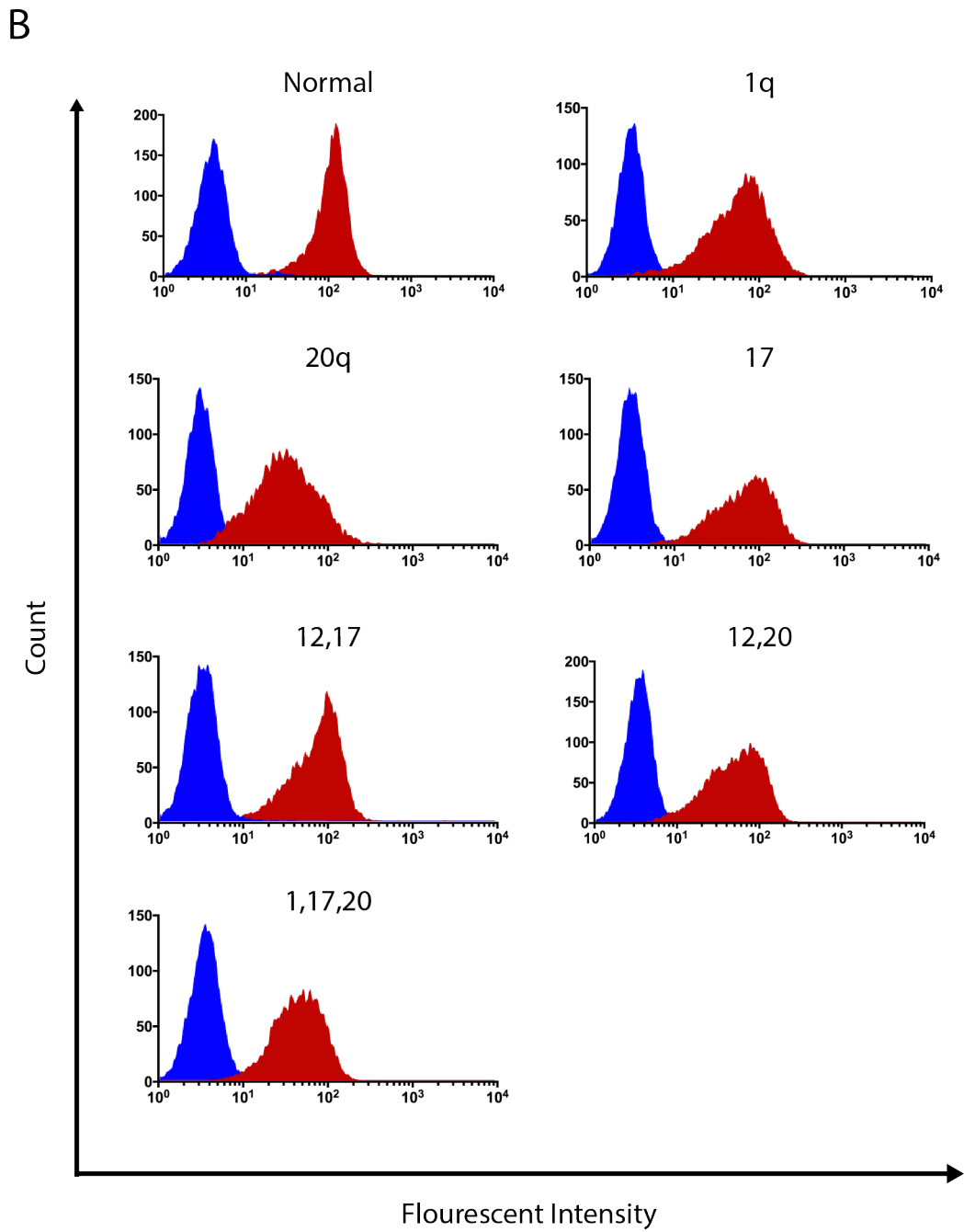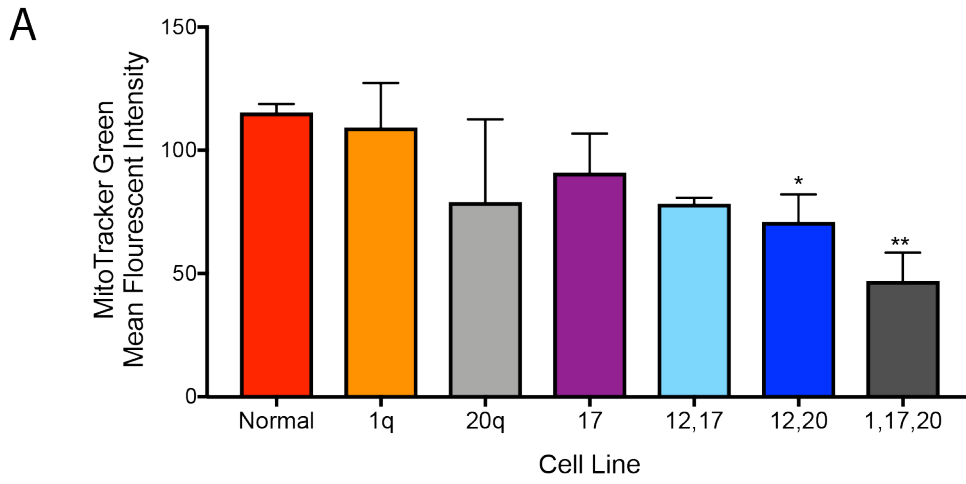
Figure 3.14 Mitochondrial content in hPSC sublines.

(A) Data shown represents the mean $\pm$ SD of the mean fluorescent intensity of Mitotracker Green staining per hPSC subline from three independent experiments. [*] p<0.032, [**] p<0.002; a one-way analysis of variance (ANOVA) followed by Dunnett's against normal hPSCs.

 (B) Representative flow cytometry analysis of Mitotracker Green staining against the panel of sub-clonal genetically variant hPSC lines. In all cases the blue plot represents the negative unstained control, and the red plot Mitotracker Green staining.
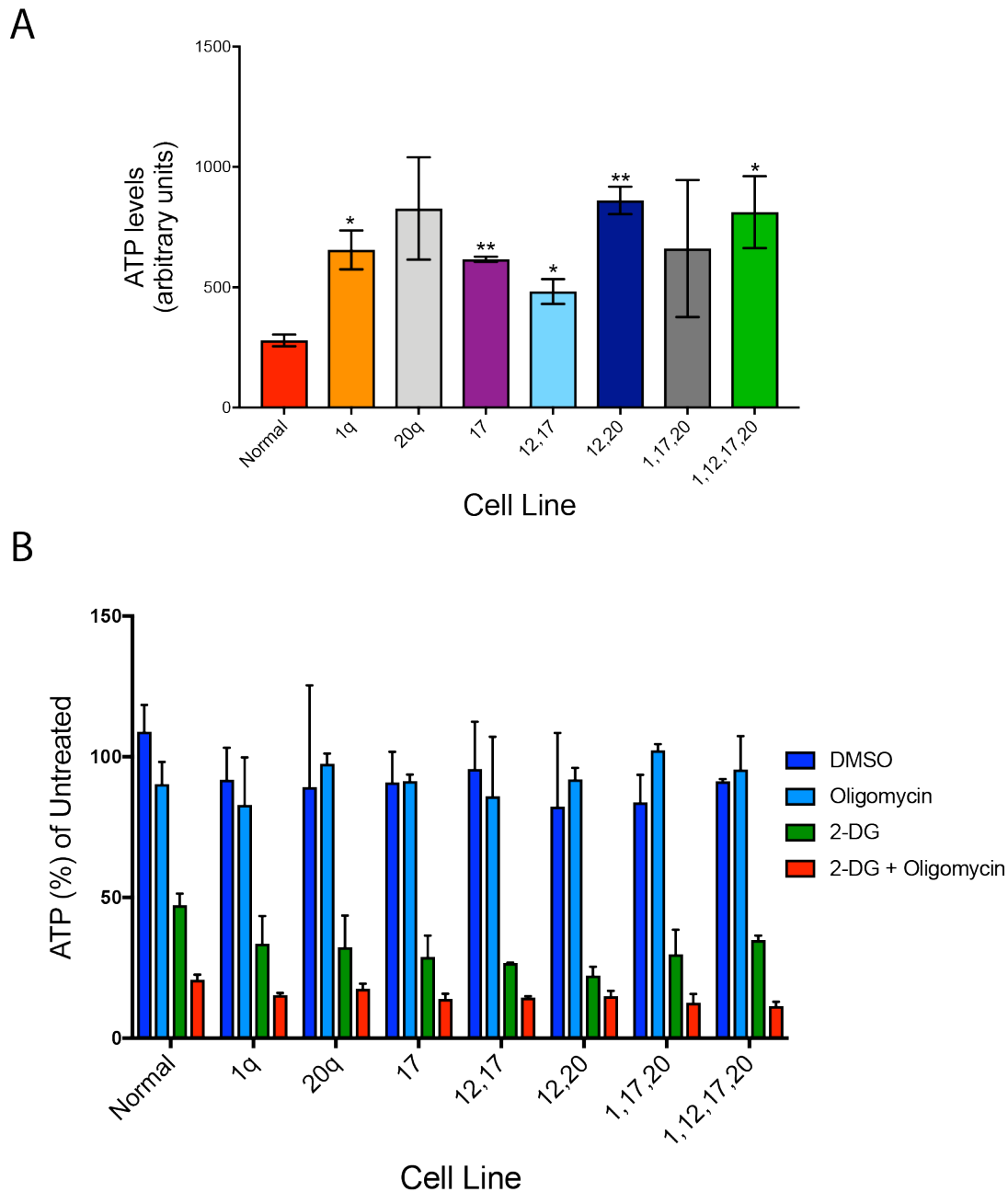
Figure 3.15 ATP production in hPSC sublines.

 (A) Steady-state ATP under basal conditions and **(B)** after the addition of the metabolic inhibitors oligomycin (1uM) , 2-deoxyglucose (2-DG, 50mM) or a combinationof them both (2-DG + Oligomycin). ATP was measured in quadruplicate wells containing equal numbers of cells from two independent experiments which were averaged. All data shown represents the mean ± SD. p<0.032, ** p<0.002; Students t-test.

3.2.10 <u>Transcriptional analysis of genetically variant hPSC lines</u>

To determine the genes and networks that are altered upon acquisition of genetic changes I used RNA-sequencing analysis. RNA was harvested from standard cultures of each variant line and normal-RFP hPSCs. Quality control analysis of the RNA sequencing data for each of the normal and karyotypically variant hPSCs samples is detailed in appendix Figure 9.4.

Firstly, to examine how the different variant lines clustered in comparison to the normal cells and each other I compared the global expression signatures. Principal Component Analysis showed the 20q v.hPSCs mapped closest to the normal, separation between the samples seemed to be based on principal component 2, that accounts for the least variance between the samples. Whereas, the variant lines containing three or more karyotypic changes, 1,17,20 v.hPSC and 1,12,17,20 v.hPSC clustered the furthest from the normal hPSCs. The 17 v.hPSC, 12,17 v.hPSC and 12,20 v.hPSC samples clustered in close proximity to each other and mapped between the normal hPSCs and the variant lines containing three or more genetic changes. Variant 1q v.hPSCs also mapped between the normal cells and variant lines with multiple genetic changes, however apart from cluster of samples composed of; 17 v.hPSC, 12,17 v.hPSC and 12,20 v.hPSC. Comparing the samples based solely on principal component 1, the variant lines with abnormalities involving chromosome 1 seemingly separate the furthest from normal hPSCs (Figure 3.16A).

To examine whether the differences between variant lines is the result of overexpression of the genes that reside on the amplified chromosomes, or from a global change in gene expression that is caused by the influence the genetic changes might have on other chromosomes as previously reported for chromosome 12 trisomy by Ben-David et al. 2014, I repeated the PCA analysis excluding the genes located on chromosomes; 1, 12, 17 and 20. Removal of the genes on the amplified chromosomes did not effect the overall clustering of the normal and karyotypically variant lines, suggesting that gain of additional chromosomal regions effects the global expression of variant lines (Figure 3.16B).

Secondly, the samples were analysed by Pearson correlation and subjected to hierarchical clustering. Both Pearson Correlation hierarchical clustering and PCA showed similar clustering

of normal and variant hPSC lines. Furthermore, all the cell lines are molecularly very similar to each other; 0.006 range correlation coefficient (Figure 3.16C).

A

B

PCA without Chr. 1,12,17 & 20

C
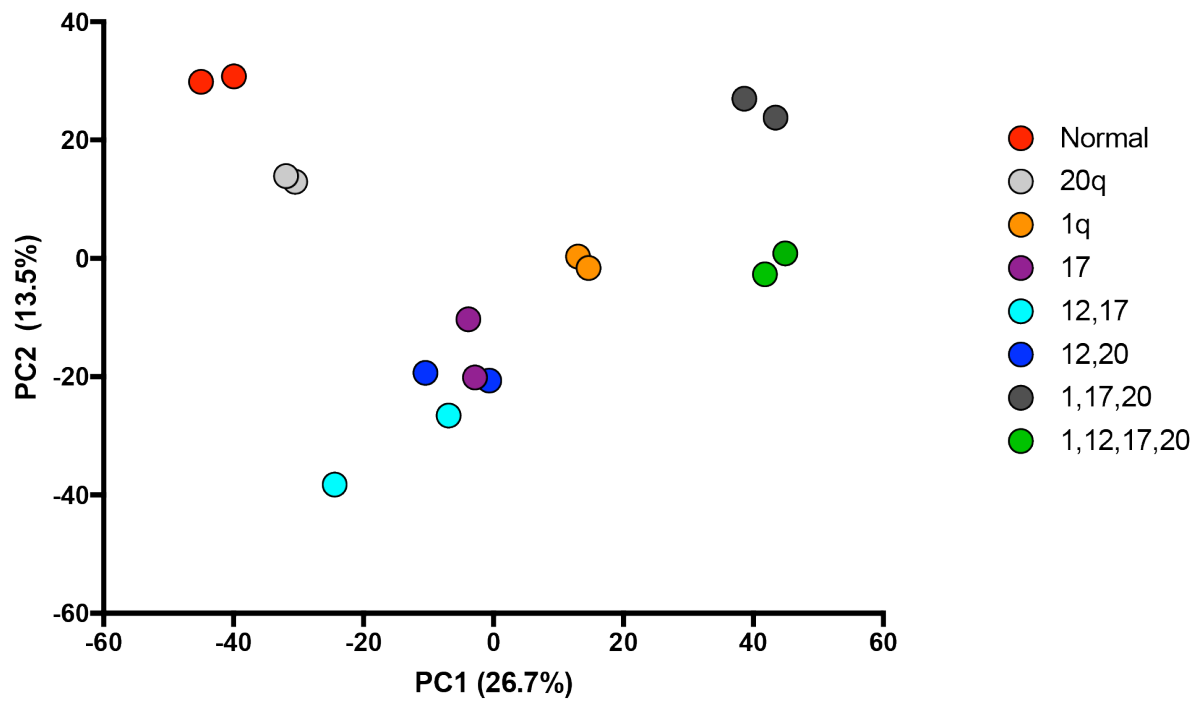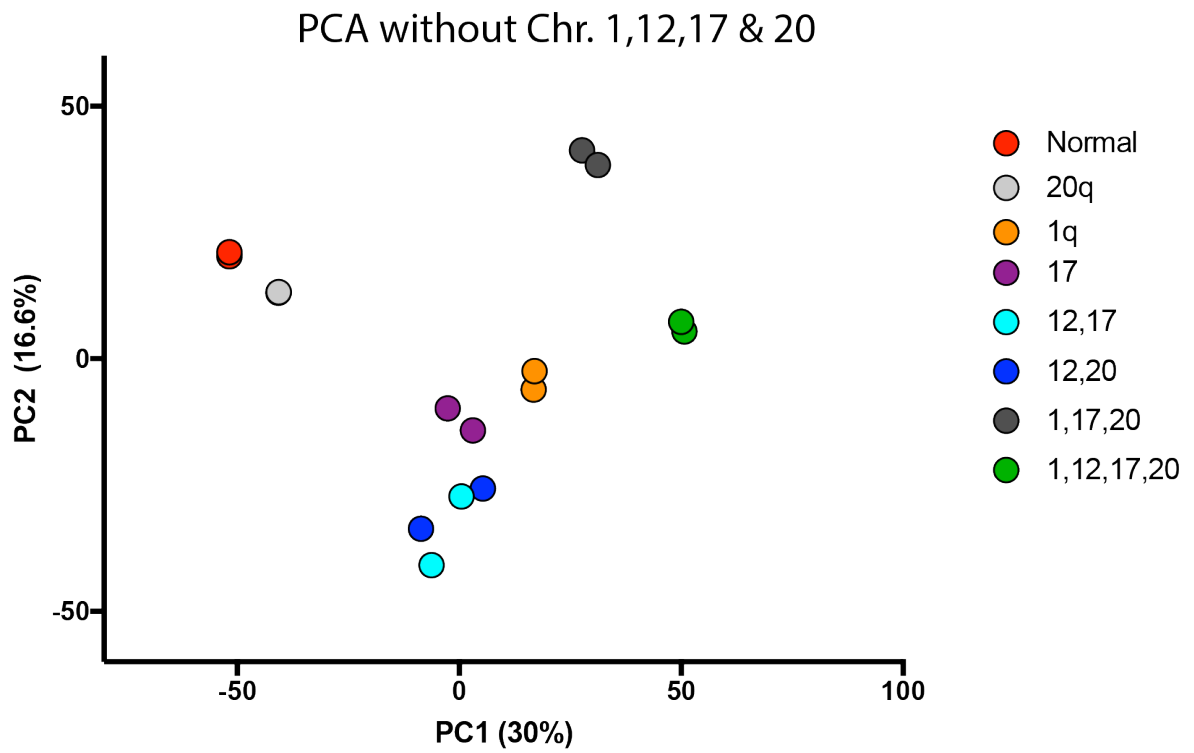
Pearson Correlation
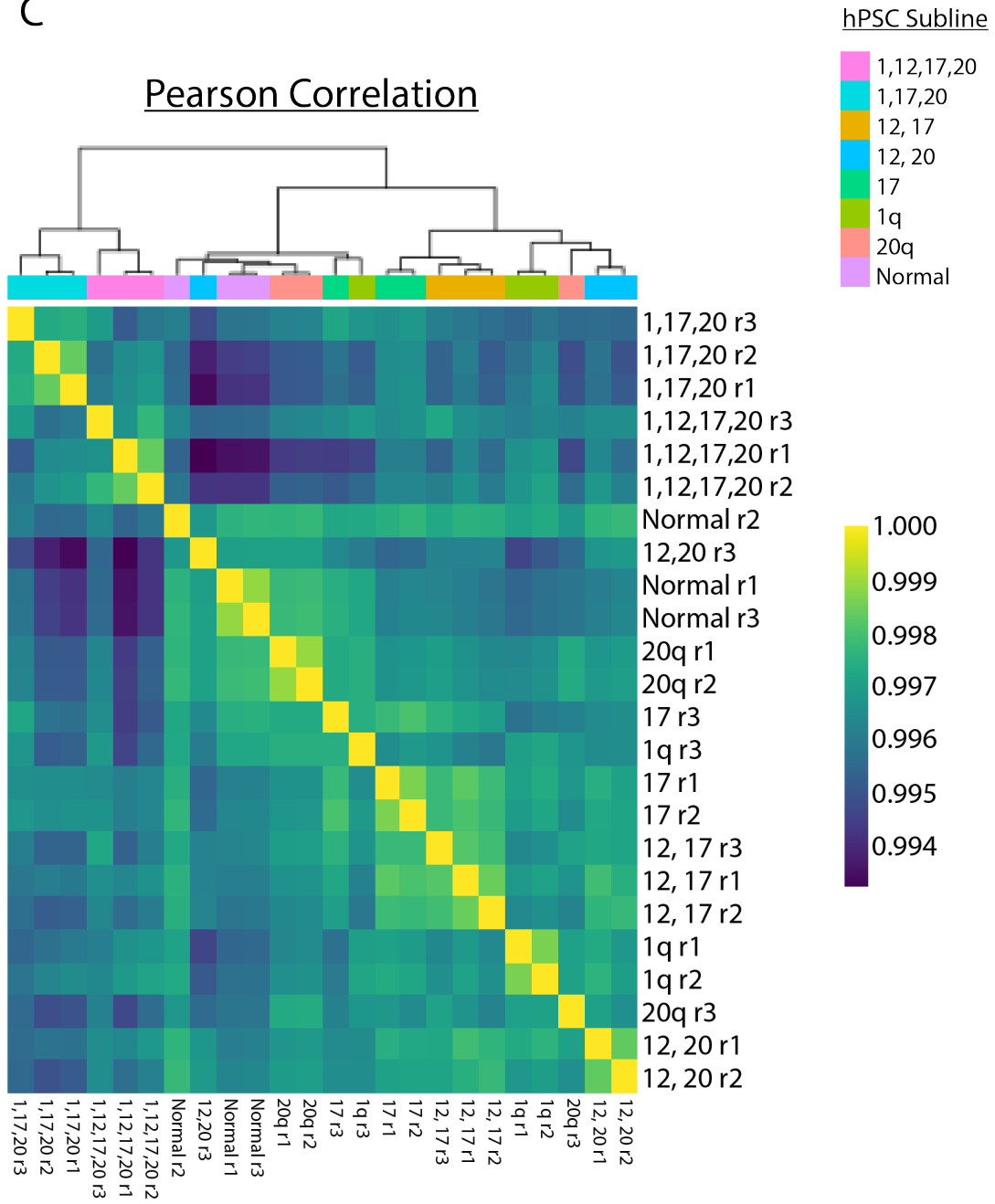
Figure 3.16 RNA sequencing comparison of normal and variant hPSCs.

Principal component analysis of normal and variant hPSCs grown under standard culture conditions **(A)** including all chromosomes and **(B)** excluding the amplified chromosomes 1,12,17 and 20. **(C)** Pearson Correlation analysis and hierarchical clustering based on the transcription profile of the different cell lines. Overall the data clustered into 3 main subsets, cluster one exclusively contained the variant lines possessing three or more genetic abnormalities. The second cluster consisted predominantly of normal and 20q v.hPSCs. The final cluster contained mostly all of the remaining variant lines.

Next, I attempted to identify candidate genes that drive the selective advantage in each of the variant sublines. Due to the large size of the karyotypic changes and the vast number of genes that reside on the amplified chromosomal regions of variant hPSCs I rationalised that comparing the expression levels of each gene within the amplified regions against the expression levels in normal hPSCs would be an inefficient approach to identify potential candidate genes. Based on my previous finding that acquisition of karyotypic changes causes global changes in gene expression (Figure 3.16 A-B), I hypothesised that a potential explanation for this observation is expression of certain biological pathways, that have key genes located on amplified chromosomal regions, with the potential to provide hPSCs with a selective advantage are upregulated in variant hPSCs. I therefore decided to perform pathway enrichment analysis to compare the normal and karyotypically variant lines and then if appropriate follow on by identify potential candidate genes within the enriched pathways.

Firstly, I compared the genes from each of the variant sublines against the normal hPSCs to generate lists of genes that are differentially expressed for each variant line. The DEG lists were substantially long so I then applied a ≥ 2 Log2 Fold Change cutoff value to the list for upregulated genes and $\leq$ -2 Log2 Fold Change cutoff value for downregulated genes to assess only the genes that were substantially up/down regulated in each of the variant cell lines. These lists were then submitted for gene ontology (GO) enrichment analysis to reveal the key molecular and biological processes present within groups. PANTHER (Mi et al., 2017) classification system was used to perform a statistical overrepresentation test of the genes submitted. This assigns each gene from the list to a GO term category and then assess whether a particular category is overrepresented or underrepresented, the resulting p-values for each category indicate whether the probability that co-expression of genes within each list were drawn randomly or not. The resulting list was then refined using REViGO (Supek et al., 2011) to remove redundant GO terms. A final list of terms is plotted in semantic space, where correlated GO terms cluster in proximity to each other (Figure 3.17).

Analysis of the list of downregulated genes, $\leq$ -2 Log2 Fold Change, for each variant line compared to normal hPSCs showed no GO term enrichment suggesting that no specific processes or pathway are downregulated. Furthermore, removal of the $\leq$ -2 Log2 Fold Change threshold did not affect the analysis. Assessing the upregulated genes, ≥ 2 Log2 Fold

Change, GO analysis produced a list of terms for only 3 of the variant lines; 1 .vhPSC , 17 v.hPSC and 12,20 v.hPSC. Comparison of these lists revealed a common set of highlighted biological processes. First, a cluster of terms pertained to differentiation including, ectoderm and mesoderm development. Secondly, cell adhesion, biological adhesion processes and finally cell-cell signalling and cell growth were enriched (Figure 3.17).

Examining the lists of upregulated genes from the variant hPSC lines that produced no GO overrepresented terms showed two opposing scenarios. In the case of 20q v.hPSCs the list of genes submitted for GO analysis was very short, only 76 genes compared to 265 (average of variant lines that generated a list of GO terms), suggesting there is very little difference between the normal and 20q v.hPSCs which is consistent with the PCA and Pearson correlation analysis. In comparison, the 12,17 v.hPSC , 1,17,20 v.hPSC and 1,12,17,20 v.hPSC produced lists of an average size of 636 genes, much greater than the other lines suggesting that these lines have global upregulation across the genome.

1q

17

12, 20
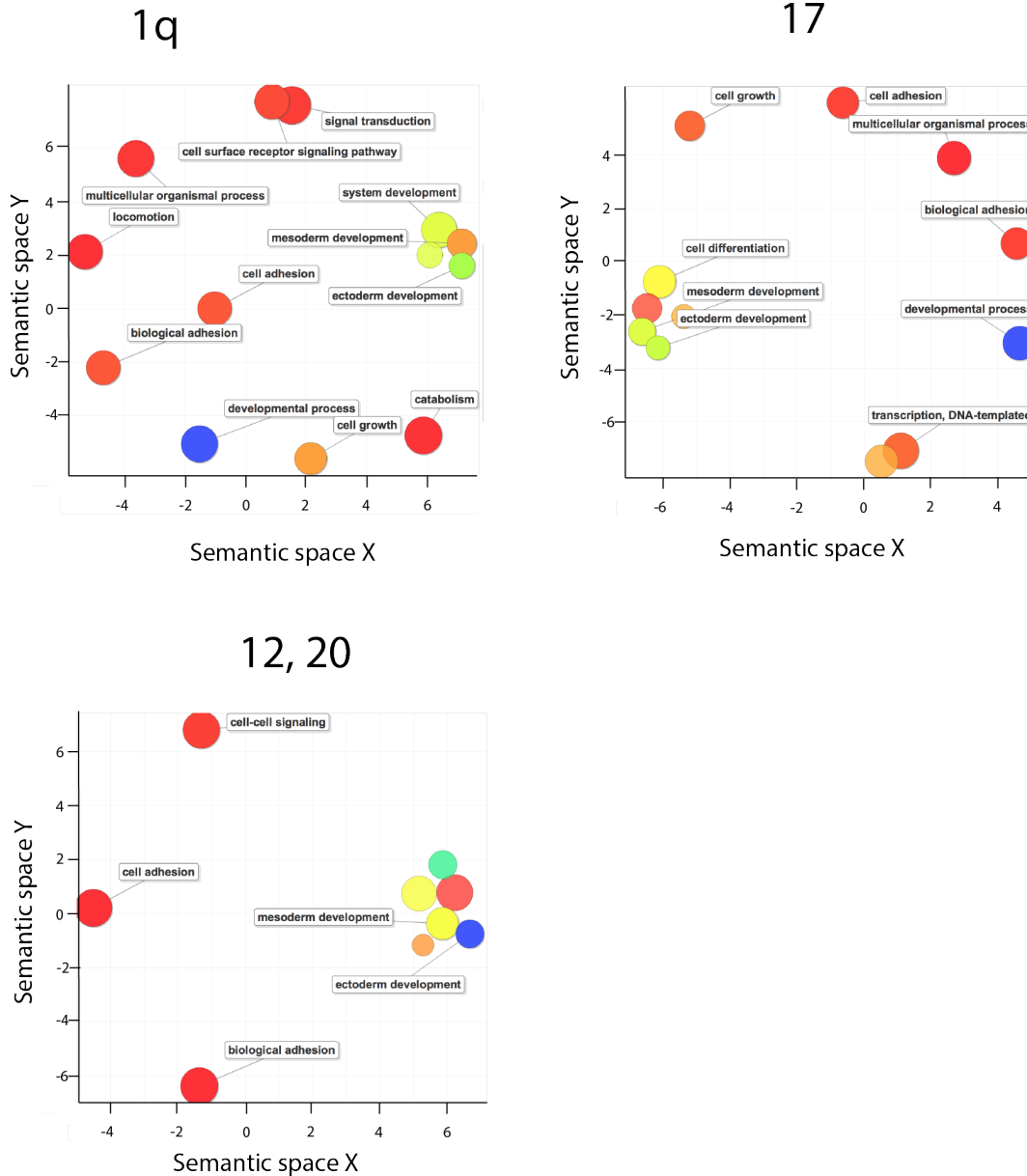
Figure 3.17 Biological pathway enrichment of upregulated genes in variant hPSCs.

Gene Ontology terms of molecular function for the upregulated genes in variant hPSC lines. Terms are positioned in semantic space by ReviGO based on the correlation between biological process. Term size is based on the log size p-value, higher (bigger) and lower (smaller) and coloured based on their Log10 p-value, higher p-values (Red) and lower p-values (Blue) both as calculated by ReviGO.

Finally, I wanted to examine whether the differentially expressed genes from variant lines with multiple genetic abnormalities are a sum of the individual mutations that they are composed of or whether the mutations act synergistically to produce an altered pattern of gene expression. To perform this analysis, I used the lines containing individual mutations; 1 v.hPSC, 17 v.hPSC and 20 v.hPSC and the line 1,17,20 v.hPSC. Though the mutations from the individual variant lines on chromosome 1 and 20 do not involve the gain of the entire regions observed in the multiple 1,17,20 v.hPSC line they share the minimal amplicon regions 1q25-q41 and 20q11.21 (Baker et al., 2016). The lists of differentially expressed genes compared to normal hPSCs from the 4 lines was compiled and for every variant line each gene was assigned a value depending on its expression compared to normal hPSCs. Genes were assigned the corresponding values; 1 - overexpressed, 0 - not differentially expressed in that line or, -1 -downregulated and the results plotted as a heatmap (Figure 3.18)

Heatmap analysis demonstrates that the differentially expressed genes from variant lines with individual genetic changes are not co-observed in the 1,17,20 v.hPSC line. The differentially expressed genes form clusters predominantly unique to each line. There are small regions of overlap between two or more of the variant lines with individual changes but the pattern of up/downregulation does not coincide with the 1,17,20 v.hPSC line. Furthermore, there are two large clustering's of differentially expressed genes that are unique to the line with multiple karyotypic changes.
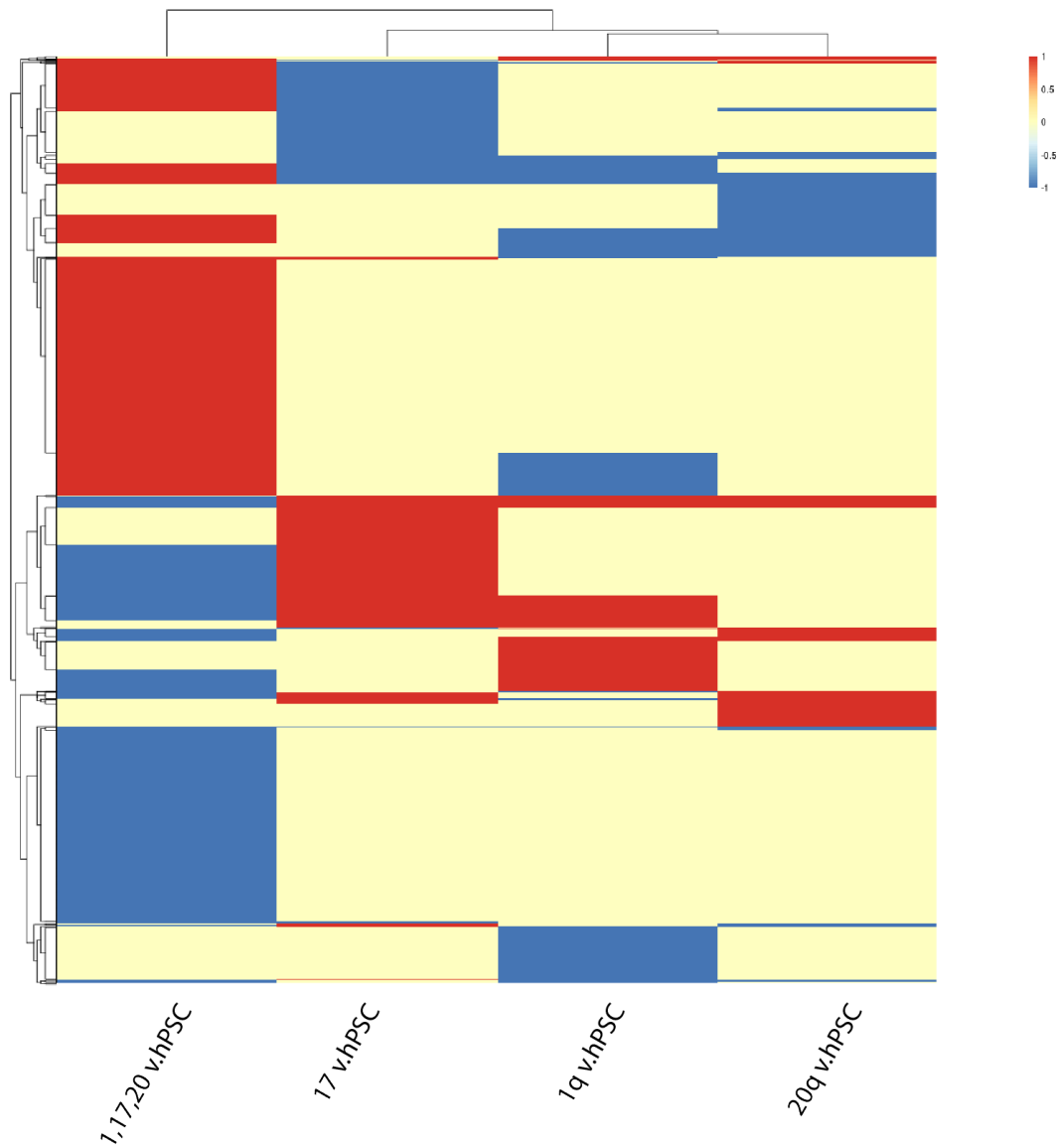
Figure 3.18 Comparison of gene expression changes between individual and complex variant hPSC lines.

Heatmap of differentially expressed genes for variant lines 1q v.hPSC , 17 v.hPSC and 20q v.hPSC containing individual changes versus the complex variant line 1,17,20 v.hPSC. Genes are colour coded depending on whether they are upregulated (red), downregulated (blue) or not differentially expressed (yellow) compared to normal hPSCs.

3.3 Discussion

Different genetic changes have been associated with altered aspects of hPSC fate. In this study I have generated a panel of clonal sublines containing the most commonly observed genetic changes acquired in hPSCs in culture. Generation of lines with individual and multiple karyotypic changes allowed me to explore how selective advantage evolves upon the acquisition of two or more abnormalities. Furthermore, by creating the variant lines from the same H7 background I was able to circumvent the issue of intrinsic differences between hPSC lines that has hindered the comparison of genetic variants in other studies.

Through monitoring cultures of normal cells spiked with different variant lines I have shown that all the genetic changes interrogated confer selective advantage over diploid hPSCs. The first experiment I conducted suggested the rate at which different variants overtake normal hPSCs may vary depending on the abnormalities possessed. However, the second experiment in which cells were maintained by a colleague the variant cells overtook normal hPSCs in a shorter culture period and I did not observe a clear difference in rate of overtake between lines. This may be due to differences in individual culture technique and that could have enhanced particular selective pressures during passage. Previous studies have described how different culture techniques can influence the rate genetic abnormalities appear during long term culture (Olariu et al., 2010). The state of dissociation in which hPSCs are seeded into new culture vessels during passage appears to be a critical factor, furthermore previous work in our lab has demonstrated that some variant cells are able to overcome the selective bottlenecks that are imposed by extensive dissociation of hPSC colonies (Barbaric et al., 2014). It remains to be shown if certain culture techniques promote or diminish the selective advantage of particular genetic abnormalities. Though not explored in this study this panel of variant lines has the potential to be an effective tool in the assessment of different culture platforms and techniques to establish a guide on recommended culture practices for limiting appearance of genetic variants over progressive passages.

Utilising the panel of variant lines, I assessed each aspect of cell fate to identify how genetic abnormalities confer selective advantage. The proliferation, apoptosis and clonogenic studies revealed that different genetic changes confer altered growth properties to particular variant lines (Figure 3.19).

Variant hPSC line	Proliferation	Cell Cyle Time	Resitance to Apoptosis	Cloning Efficiency	Differentiation Capacity	Metabolic Activity
1q v.hPSC	↑		↑			↑
20q v.hPSC			↑			
17 v.hPSC	↑	↓	↑	↑		↑
12,17 v.hPSC	↑	↓	↑	↑		↑
12,20 v.hPSC	↑		↑	↑		↑
1,17,20 v.hPSC	↑	↓	↑	↑	↓	↑
1,12,17,20 v.hPSC	↑	↓	↑	↑		↑

Figure 3.19 Summary of cell fate phenotypes possessed by variant hPSC lines.

Table of the different variant hPSC sublines and their phenotype in the assays described within Chapter 3 that tested the different aspects of cell fate. Arrow direction indicates either increase (up) or decrease (down). Arrow size and colour represents the degree of significance in change relative to normal hPSCs; small and light blue arrows represent a small degree change, larger and dark blue arrows represent a greater degree of change.

Variant cells with the individual gain of 1q proliferate faster than the normal cells, but this proliferative advantage is not due to a shorter cell cycle time. Rather, the selective advantage is more likely to be linked to an increased level of apoptotic resistance. It remains unclear at what stage of culture this is advantage is exerted, results from the apoptosis assays suggest that this may be during the growth phase and in response to environmental stress.   However, the small but insignificant rise in cloning efficiency hints at an additional weaker role in supporting survival of single cells.   The apoptotic advantage of 1q variant hPSCs could potentially be mediated by the anti-apoptotic gene, *MCL-1,* contained within the amplified region and expressed at higher levels in not only the 1q variant line but also in lines with addition of nearly the entirety of chromosome 1. Although a role for other genes within this region cannot be excluded, *MCL1* offers a likely mechanism that could be readily investigated.

Similar to the 1q abnormality gain of 20q11.21 in my studies appeared to provide variant cells with an apoptotic resistance which correlates with the anti-apoptotic function of the known driver gene BCL-XL (Avery et al., 2013). Comparable to the findings of Avery and colleagues 20q variant hPSCs overtook normal cells over a series of successive passages and this does not appear to be dependent on a difference in time between cell divisions. However, in contrast to their study I did not observe a significant increase in the growth rate of the 20q variant line by counting the total number after 4 days. This can potentially be explained by a major difference between the two experimental set ups, in my assay Y-27632 is included for the first 24hours to support cell survival and set equivalent starting numbers restricting any selective advantage that may exerted during plating. A potential hypothesis, which requires experimental validation, is that 20q primarily exerts its selective advantage during the plating stage of cell culture supporting cell survival at low density and upon dissociation towards single cells. Treatment with Y-27632 under these culture conditions may restrict the selective advantage of 20q variant hPSCs.

Variant hPSCs containing solely the addition of chromosome 17q proliferate the fastest of all the individual variant lines. This proliferative advantage is due not only to decreased apoptosis in culture but also a potentially faster average cell cycle time of the population. The reason for this decreased average cycle time is not clear but is likely either a result of altered cell cycle checkpoint regulation that permits variant cells to progress more rapidly through

division (Shaltiel et al., 2015) or alternatively a greater proportion of variant cells survive following division which lowers the average cycle time of the population sampled. It will thus be interesting to further track and compare the lineage trees of cells with and without gain of chromosome 17 taking into consideration not only the daughter cells that survive post division but also those that die in order to determine whether cell cycle time is indeed altered in certain variant hPSCs. Further to this, analysis of the clonogenic assays showed 17q variant hPSCs have the greatest cloning efficiency but also produce larger colonies with higher expression of stem cell associated markers. I was able to conclude that of the individual genetic changes assessed, gain of chromosome 17 confers the strongest growth advantage.

A few candidate genes have been proposed to contribute to driving selective advantage in variant hPSCs that have gained parts of chromosome 17, including the anti-apoptotic gene *BIRC5 (SURVIVIN)* (Draper et al., 2004). A possibility is that *SURVIVIN* might provide variant hPSCs with a selective advantage in a similar manner to BCL-XL, by stopping apoptosis (Altieri, 2015). However, the contribution of *SURVIVIN* to the selective advantage of genetically variant hPSCs harbouring gains of chromosome 17q have yet to be established. Regions of chromosome 17 are also frequently gained via structural rearrangements in a variety of human cancers, genes encoded within the amplified regions have been proposed to underlie the neoplastic growth of abnormal cells (Mitelman et al., 1997, Orsetti et al., 2004, Zhang and Yu, 2011). Of note, topoisomerase IIα (*TOP2A)* a gene located at 17q21.2 that has an important role in DNA remodelling during transcription and replication, is a key target for chemotherapy drugs in multiple forms of cancer (Heestand et al., 2017). *TOP2A* has recently been shown to be highly expressed in hPSCs and is required for undifferentiated cell survival (Ben-David et al., 2015). One possibility is that overexpression of oncogenes, with essential functions in hPSCs, may also drive aspects of the selective advantage conferred by gain of chromosome 17. Identifying genes such as TOP2A, with known roles in hPSCs, as well as oncogenic properties should help to identify candidate genes and pathways that can best investigated to determine the mechanisms that drive selective advantage in particular karyotypic variants.

Whilst my data on chromosome 12 only comes from variant lines harbouring additional genetic abnormalities, by comparing the paired abnormality lines 12,17 v.hPSC and 12,20 v.hPSC to the individual variant lines with corresponding genetic change I am able to report

on some of the phenotypic effects trisomy chromosome 12 may confer. My growth rate studies revealed that 12,20 v.hPSCs proliferate faster than 20q v.hPSCs as well as have a greater cloning efficiency. The broadly similar apoptotic responses between the individual and paired variant lines implies that chromosome 12 does not confer any additional apoptotic resistance. Supporting the notion that chromosome 12 provides mostly a proliferative advantage and consistent with other reports assessing the effects of additional chromosome 12 on hPSCs (Ben-David et al., 2014). Of note, this increase in proliferation was not observed between 17 v.hPSCs and 12,17 v.hPSCs. How multiple genetic abnormalities which confer similar phenotypic properties drive selective advantage in the same cell remains unclear. One possibility is that they both exert their proliferative effects predominantly through the same pathway(s) and that further addition of either chromosome only raises the already heightened activity a little further. This may explain why though 12,17 v.hPSCs have a similar cloning efficiency to 17 v.hPSCs they also produced more colonies of a greater size.

Additional genetic abnormalities seemingly correlated with stronger growth properties, variant lines containing three or more chromosomal gains possessed the fastest growth rates, lowest levels of apoptosis and highest cloning efficiencies. For a genetic abnormality to become fixed in culture it must provide the cell with a selective advantage (Amps et al., 2011, Avery et al., 2013). In line with this principle in variant lines already carrying a genetic change the new abnormality acquired must provide an additional advantage otherwise it would not persist in the variant population. The elevated resistance to apoptosis and increased proliferative capacity can be mapped back to properties described in the individual mutant lines but whether they function as simply the sum of all the properties acquired from each individual mutation or a result of their combined interaction would require further interrogation.

Having shown different genetic abnormalities confer altered growth properties to variant hPSCs, the next question I sought to address was whether they also effect the cells differentiation potential. Using normal hPSCs and my panel of variant lines I assessed the differentiation potential of all lines under neutral EB conditions. In contrast to the normal hPSCs which generated EBs with a strong ectoderm bias, nearly all of the variant lines produced EBs with upregulation of genes associated with all three germ line lineages but

maintained an ectoderm bias, except for 1,12,17,20 v.hPSCs which displayed a more even level of gene upregulation between germ line lineages. The only line that exhibited any resistance to differentiation and maintained a strong pluripotency associated gene expression signature was 1,17,20 v.hPSC. The ability of the 12,17 and 1,12,17,20 v.hPSC lines, with whom the genetic abnormalities of 1,17,20 v.hPSCs match closest, to differentiate suggest that this result is not a consequence of those amplified regions. Unique amongst the panel of variant lines, the genetic abnormality on chromosome 20 in the 1,17,20 v.hPSC line is an isochromosome of the long arm (q) in addition to the duplication of *BCL2L1*. Loss of genes from the short arm presumably is the cause for the restricted differentiation potential of this line. This region contains genes known to be important in embryonic development and differentiation such as *BMP2* and *JAG1*, key members of the BMP and NOTCH signalling pathways respectively. Understanding which pathways underpin this restriction of differentiation capacity may assist in identifying other regions of the genome that if perturbed can negatively impact on the function of hPSCs. My findings show that genetic changes can not only support differentiation but may also restrict it. Together, this suggests the potential effects of genetic changes in hPSCs destined for use in applications that require subsequent differentiation will have to be assessed on an individual basis.

The metabolic activity of hPSCs is uniquely regulated by multiple pathways and has been linked with changes in gene expression in variant hPSCs carrying trisomy chromosome 12 (Ben-David et al., 2013, Folmes et al., 2011, Ben-David et al., 2014). My studies revealed that genetically variant hPSCs have increased levels of ATP produced mostly by the glycolytic pathway. I postulate the reason for this raised metabolic state may reflect increased energy demands on the cells brought on by stronger growth phenotypes. Further studies are required to characterise the metabolic profile of normal and variant hPSCs, and to examine if changes in metabolic activity are co-ordinated by genes located on amplified chromosomes. Finally, I used RNA sequencing to assess the genes and networks that are altered in genetically variant cells. Principal component analysis and hierarchical clustering provided some intriguing results, the clustering of the variant lines indicates that in my culture conditions differentially expression of genes on chromosome 1q separate the different variant populations. The close clustering of variant lines 17 v.hPSC , 12,17 v.hPSC and 12,20 v.hPSC implies the gain of chromosomes 12 and/or 17 renders variant hPSCs more transcriptionally

similar to each other and may be reflected in the similar growth phenotypes discussed earlier. GO enrichment analysis was employed and convergence on some shared biological processes was observed in the variant lines which yielded a list of terms. It will thus be interesting to further compare the differentially expressed genes associated with these terms between samples, in order to identify specific sets of genes that may be important in conferring elements of certain forms of selective advantage to variant hPSCs. Enrichment analysis was unable to determine significantly upregulated biological processes in the variant samples that produced extensive list of differentially expressed genes; 12,17 v.hPSC, 1,17,20 v.hPSC and 1,12,17,20 v.hPSC. Together with the positional distribution of these lines in both PCA and hierarchical clustering analysis this data indicates a global upregulation of gene expression across the genome.

Using the analysis of differentially expressed genes, I lastly show that in variant lines containing multiple genetic abnormalities the combination of genetic changes act synergistically to induce expression changes that shift the transcriptional programme away from that of the individual variants. A caveat to this analysis was the genetic changes of chromosomes 1 and 20 were not exact matches between the individual variant lines and 1,17,20 v.hPSCs. However, if the hypothesis that a complex variant line is a sum of the individual variants held true than overlapping sections of differentially expressed genes would have still been observed.

In summary, the data presented within this chapter demonstrates that the selective advantage of commonly acquired karyotypic changes in hPSCs can be conferred through acquisition of enhanced growth properties. Different genetic changes can confer different growth properties, whilst other genetic changes can confer similar growth properties that may be driven by different genes or pathways. Analysis of variant lines containing two or more karyotypic changes shows that acquisition of further genetic changes improves the growth behaviour of variant cells. Seemingly, as the complexity of the karyotypic abnormalities possessed by variant hPSCs increases so does the advantageous growth phenotype. The ability of karyotypic changes to alter aspects of hPSC fate suggests that part of the mechanisms that drive selective advantage in hPSC cultures are intrinsic and function by enhancing variant cell growth behaviour.

4 Characterising the behaviour of diploid hPSCs in the presence of variant cells.

4.1 Introduction

Selection of variant hPSCs occurs following the acquisition of an advantageous genetic change. Over progressive passages the proportion of variant hPSCs increases due to strong selective pressures that favour expansion of variant cells with improved growth properties. Mutations that promote self-renewal and restrict apoptosis and/or differentiation would generate a more robust growth phenotype capable of escaping the normal restrictions imposed on diploid cells during culture (Amps et al., 2011, Baker et al., 2007, Barbaric et al., 2014).

Different genetic abnormalities can alter various aspects of cell fate, as reviewed and described in earlier chapters, which may exert their selective advantage at different stages during culture. Studies examining the effect of genetic change in hPSCs to determine selective advantage have been predominantly performed by comparing homotypic populations of variant cells against counterpart diploid lines. This form of analysis has enabled the identification of selection mechanisms that exist during the post plating stage of culture. In 2D culture of hPSCs, cells are grown on top of a supporting substrate within a defined growth area. Cells proliferate and expand, reducing the available space for future daughter cells. Once hPSCs reach a high level of confluency they are passaged by detaching cells from the surface of the culture vessel and re-plating a proportion of hPSCs into a new culture vessel. After passaging, hPSCs must first survive post-plating before they enter the growth phase of culture. During these different stage of culture various selective pressures could be exerted on normal and variant hPSCs.

Tracking of two variant hPSCs lines with multiple genetic changes and their counterpart normal cells by time-lapse imaging revealed that selection mechanisms present during post-plating are composed of at least 3 bottlenecks. The first bottleneck is the initial survival of re-plated cells; variant hPSCs showed significantly higher levels of survival after 12 hours in

comparison to normal cells. Secondly, the ability of cells that survived initial re-plating to re-renter the cell cycle is improved in variant hPSCs, as normal cells are less likely to undergo division following the 12 hour re-plating period. The final bottleneck is survival of daughter cells post-division. In the populations of normal hPSCs cell fate was strongly biased towards death of either one or both of the daughter cells. In contrast, daughter cells of the first mitosis post-plating in variant populations both had a higher probability of survival than cell death (Barbaric et al., 2014). This was the first study to identify and describe selective mechanisms that exist during the culture of hPSCs.

Although comparison of normal and variant populations is able to provide insight into the advantageous growth properties of variant hPSCs as well as elucidate some of the selection pressures during routine culture, a major issue with this form of experimental design is that is does not accurately recapitulate the emergence of variant cells. Following the mutation event that generates a variant hPSC and during selection, normal and variant hPSCs co-exist within the same culture environment, thereby sharing the same culture conditions as well as a proportion of their cell-cell interactions.

Cell-cell interactions are critical for development and tissue homeostasis; they allow cells to produce coordinated responses to a wide variety of extracellular and intracellular signals as well as communicate differences in cellular identity (Barnes et al., 2017). During cell competition the ability of cells to communicate their relative fitness levels is required for establishment of future "winner" and "loser" status. This interaction is important for the detection and elimination of polyploid embryonic cells in vivo and in vitro. Tetraploid (4n) cells can persist in the epiblast until 6.5dpc following which they are progressively lost from the developing embryo (Eakin et al., 2005). In vitro studies show 4n mouse ESC are eliminated by diploid (2n) cells suggesting this loss is due to a competitive disadvantage of tetraploid cells (Sancho et al., 2013). These observations suggest that cells are capable of detecting differences in their relative levels of genomic material and depending on the properties conferred determine winner and loser phenotypes.

Very little is known about how normal and variant hPSCs interact or respond in the same culture environment. A single study by Werbowetski-Ogilvie (2011) examined the effect of co-culturing colonies of normal and variant hPSCs containing amplification of 20q11.1-11.2. In their experiments, they observed that normal hPSCs exhibited a shift in their growth phenotype to resemble the variant population. Normal hPSCs displayed enhanced self-renewal and niche independence as well as a shift in global gene expression during co-culture with variant cells. The data from this study suggests that variant hPSCs can transmit their neoplastic growth properties to normal hPSCs when co-cultured together (Werbowetski-Ogilvie et al., 2011). However, in their co-culture system cell-cell contact was restricted to the periphery of normal and variant hPSC colony interface. Heterogenous colonies composed on normal and variant hPSCs were not formed restricting any investigation into the effect of normal cell–variant cell interactions on cell fate.

The following chapter will address how normal and variant hPSCs behave in each other's presence as well as whether there are selection mechanisms that depend on direct cell-cell interactions between the two populations.

4.2 Results

4.2.1 Growth of Normal hPSCs is restricted in co-culture with supervariant hPSCs

To assess if there are any selective pressures exerted on normal hPSCs by the presence of variant hPSCs, I first grew normal and variant cells either separately or in co-cultures at a ratio of 50:50. I selected the variant line 1,12,17,20 v.hPSC to mix with normal cells because it possessed karyotypic changes in the most commonly reported chromosomal regions. In addition, the 1,12,17,20 v.hPSC line constitutively expressed a green fluorescent reporter allowing for the two cell populations to be distinguished from each other. In further text, to reflect the multiple genetic abnormalities, the 1,12,17,20 v.hPSC line is referred to as supervariant hPSCs.

Co-culture assays were set up by harvesting homotypic populations of normal and supervariant hPSCs to single cells. Following dissociation an equal amount of normal and supervariant cells were mixed at 50:50 ratio to generate a heterogenous population that was seeded into 96 well plates at a fixed density of 15,000 cells per well ($\sim$45,000cells/cm^2). Maintenance of hPSCs in culture is supported by high cell densities (Thomson et al., 1998, Barbaric et al., 2014). Within the co-culture population it could be considered there are two densities to consider; the number cells in either normal or supervariant population, and the total cell number of normal and supervariant hPSCs. Therefore, separate culture controls of normal and supervariant hPSCs were seeded at two densities. Firstly, the "separate culture high density" in which the density of homogenous cultures was equal to the total number of cells in the co-culture condition. In the second density control, the number of normal or supervariant cells plated was equivalent to the amount of the respective population in co-culture (7,500 cells), this is the density referred to as "separate culture" in the following figures and text (Figure 4.1A).

To minimise the effect of selection mechanisms that occur during the post-plating period cells were plated in the presence of Rho-associated, coiled-coil containing protein kinase 1 (ROCK) inhibitor Y-27632 which has been shown to significantly alleviate to selective bottlenecks that occur during plating (Barbaric et al., 2014). After 24 hours post-plating (designated as Day 0), Y-27632 containing media was removed from the culture and replaced with standard E8 for

the remaining culture period (Figure 4.1B). At both densities, separate cultures of normal and supervariant hPSCs cells grow exponentially, I observed supervariant cells proliferate faster than normal hPSCs confirming the observations made in chapter 3 (Figure 3.6)(Figure 4.1C-D).

To count the number of cells of each population in separate and co-cultures I utilised an automated image-based approach. On each day of the 4-day culture period cells were fixed and stained with a fluorescent DNA dye, the resulting images were processed using the quantification software Cell Profiler (Carpenter et al., 2006). I generated a set of analysis pipelines that firstly identified all cells within each well using a DNA stain. Normal and variant cells were next identified using the constitutively expressed fluorescent reporters, supervariant-GFP or normal-RFP cells depending on which normal and variant hPSCs had been mixed together in co-culture. Finally, the total number of cells and the number of GFP/RFP positive cells were counted to calculate the number of normal and variant cells for each culture condition (Figure 4.2).

A

	Normal	Normal HD	Co-culture	S.Variant	S.Variant HD
Nº Normal cells per well	7,500	15,000	7,500		
Nº S.Variant cells per well			7,500	7,500	15,000
Total Nº cells per well	7,500	15,000	15,000	7,500	15,000

B

E8 + 10uM Y-27632	E8

Seed Cells

Day -1 | Day 0 | Day 1 | Day 2 | Day 3

C

Separate Culture High Density

D

Separate Culture Low Density

Normal hPSCs
Supervariant hPSCs

145
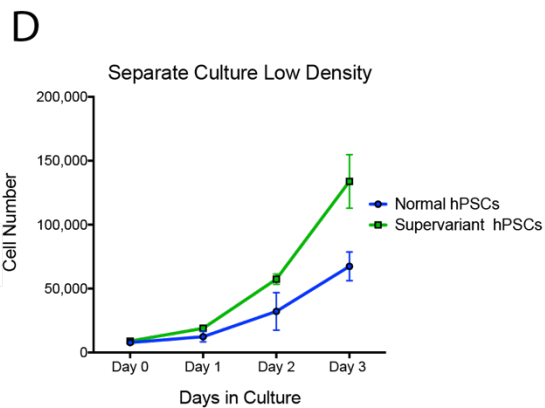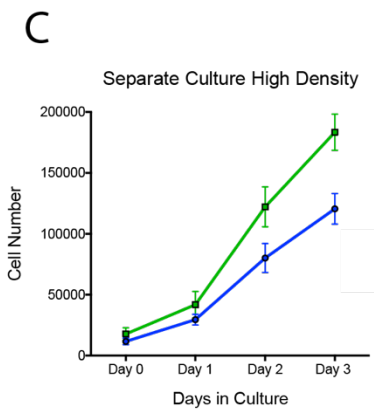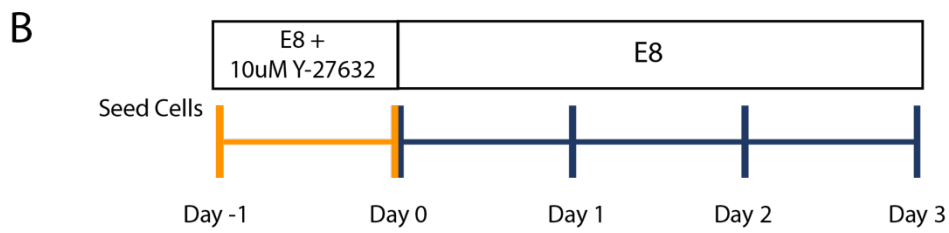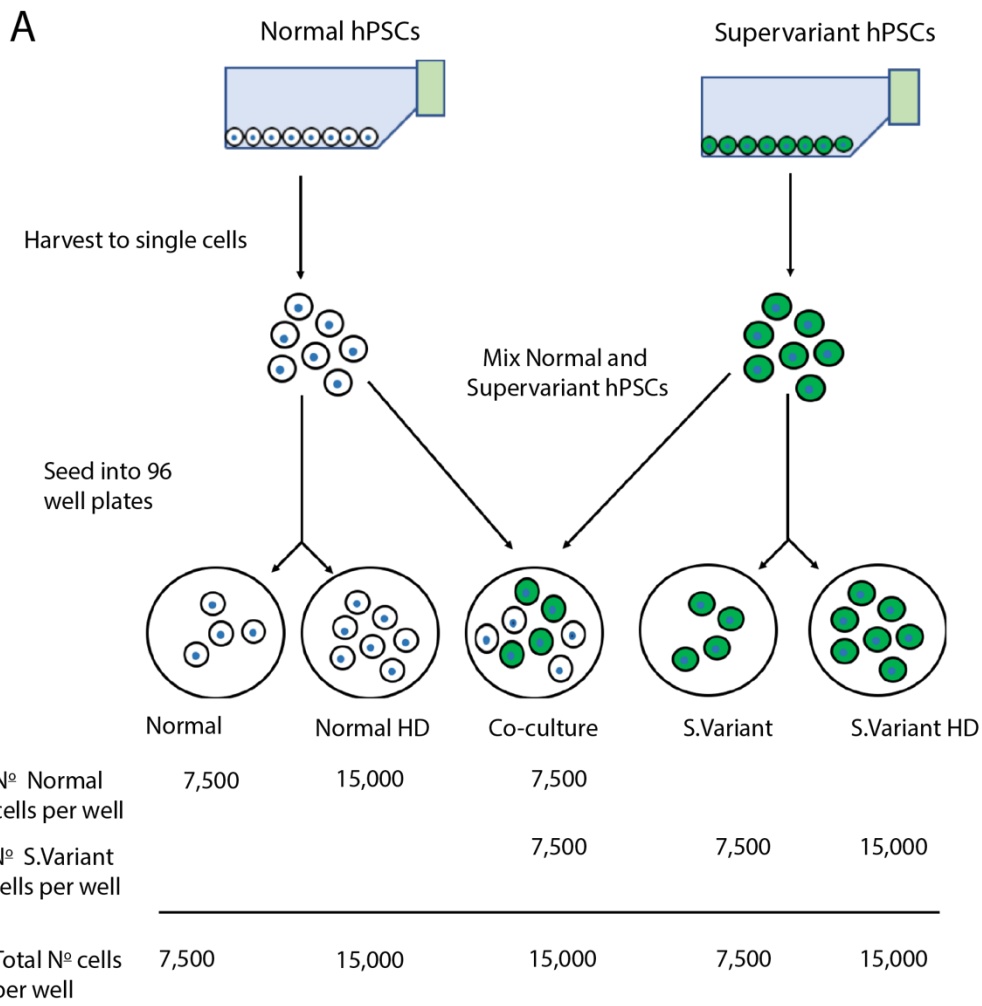
Figure 4.1 Establishing the co-culture assay.

(A) Schematic diagram of the assay to assess growth of normal and supervariant hPSCs in separate or co-culure **(B)** Schematic timeline of the assay showing the media conditions during the post-plating period (yellow line) and the growth period (blue line). **(C)** Growth curves of normal and supervariant hPSCs grown at high density. A minimum of three independent experiments were performed and the average ±SD was plotted.

1. Identify cells using DAPI signal

2a. Identify GFP +/- ve cells

Threshold GFP +ve signal

overlay nuclei onto GFP +ve signal

2b. Identify RFP +/- ve cells

Threshold RFP +ve signal

overlay nuclei onto RFP +ve signal

3. Count Cells

Total Number of cells

Number GFP +/- ve cells
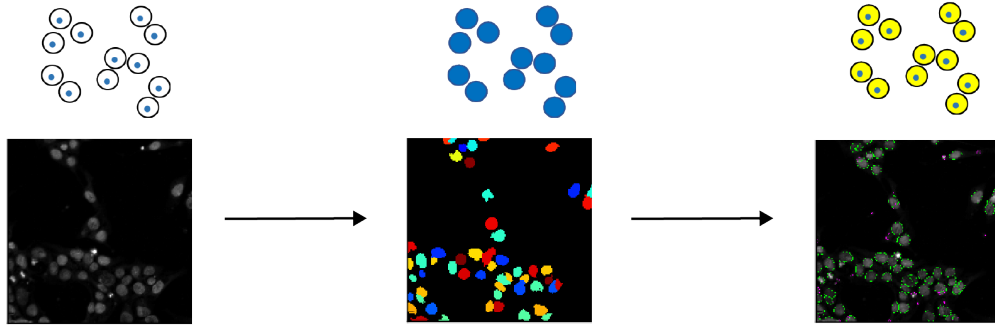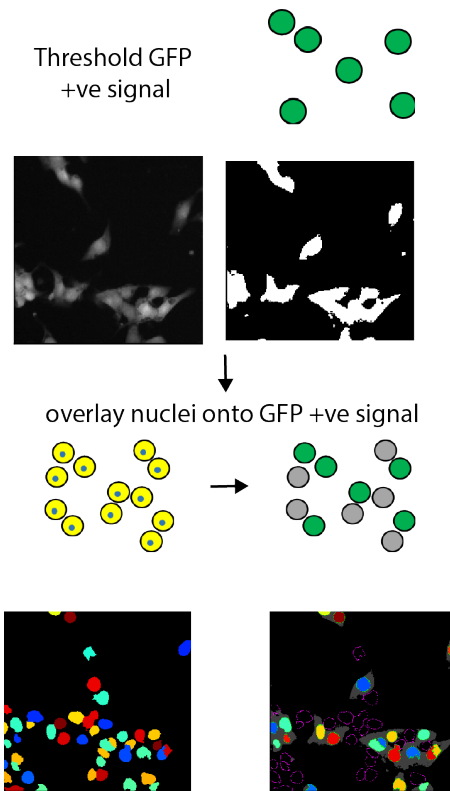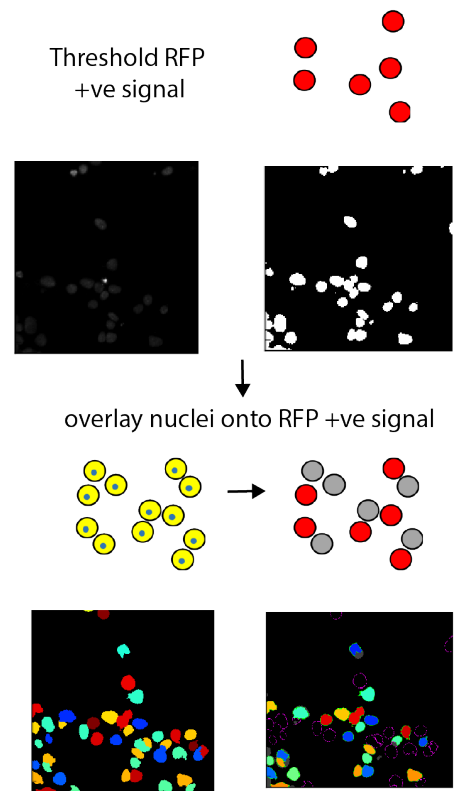
Number RFP +/- ve cells
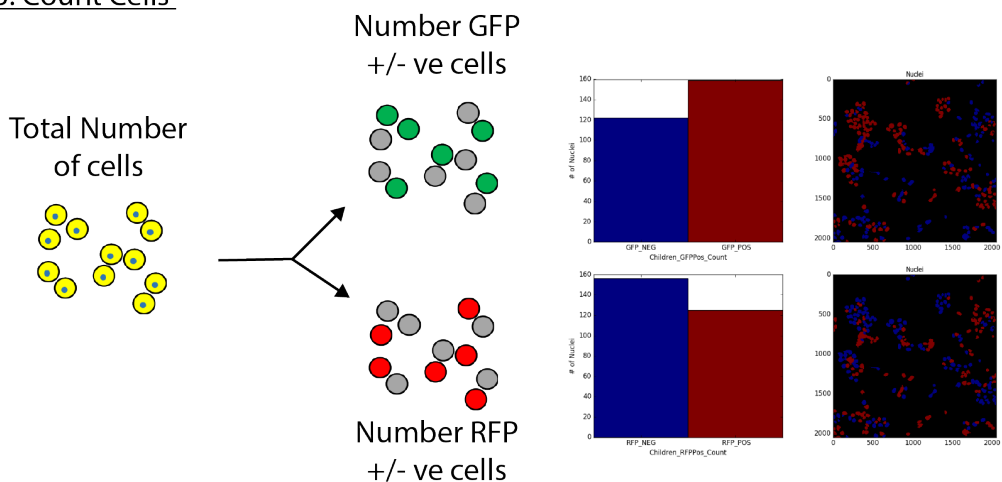
Figure 4.2 Quantification pipeline for counting normal and variant hPSCs.

Schematic diagram of the high throughput approach used to count normal and variant hPSCs in separate and co-cultures. All cells can be identified using a ubiquitous DNA stain, the number of normal-RFP or supervariant-GFP cells can then be identified based on their fluorescent signal. The cell number for RFP/GFP negative cells is determined by subtracting the count for the fluorescent population from the total number of cells.

Time-course images were taken over a standard 4 day culture period and revealed co-culture generated heterogenous colonies. However, the proportion of normal cells present was dramatically different between the homogenous and heterogenous cultures (Figure 4.3A). Utilising the time-course images the final cell number for each population was determined and used to generate growth curves for normal and variant cells in separate and co-culture conditions. Analysis of the growth curves in separate culture show that supervariant hPSCs proliferate faster than normal hPSCs (Figure 4.3B). This higher proliferation rate is reflected in the ratio of supervariant:normal hPSCs which starts at 1:1 and increases over progressive days in culture (Figure 4.3C). Comparison of growth curves and ratio supervariant to normal hPSCs showed that from day 2 the number of normal hPSCs is significantly decreased in co-culture with supervariant hPSCs. In contrast to this, the growth of supervariants is unaltered by co-culture with normal hPSCs (Figure 4.3B&C). This decrease was determined to be due to cell death because normal cells in co-culture showed significantly higher levels of cleaved caspase-3 staining than separate cultures (Figure 4.3D).

To confirm the effects of co-culture with supervariant hPSCs on normal cells, I repeated the experiment using the normal-RFP described in chapter 3. When normal-RFP and supervariant hPSCs were cultured either separately or together, I observed that, from day 2 of culture the growth of normal-RFP hPSCs decreased specifically in co-culture whereas the growth of supervariants was once again unaffected (Figure 4.4A-C). The growth behaviour of normal and normal-RFP hPSCs in co-culture with supervariant cells was comparable over the culture period (Figure 4.4D).

Figure 4.3 Normal hPSCs are eliminated in the presence of supervariant hPSCs.

(A) Time-course images of normal hPSCs grown separately or in co-culture with supervariant-GFP hPSCs. **(B)** Growth curves of normal and supervaraint hPSCs grown separately (left) and in co-culture (right).**(C)** Ratio of supervariant hPSCs to normal hPSCs grown in separate and co-cultures. **(D)** Cleaved caspase 3 levels in separate and co-culture. A minimum of three independent experiments were performed and the average ±SD was plotted. *** p< 0.005, Students Paired t test.

A

Separate Culture / Co-culture

Day 0   Day 1   Day 2   Day 3

B

Separate Culture   Co-Culture

Normal hPSCs
Supervariant hPSCs

C

Separate Culture
Co-culture

D

Separate Culture
Co-culture

A

Separate Culture

Co-culture

Day 0   Day 1   Day 2   Day 3

B

Separate Culture   Co-Culture

Normal-RFP hPSCs
Supervariant hPSCs

C

Normal hPSCs
Normal-RFP hPSCs

Separate Culture
Co-culture

D

Co-Culture with Supervariant hPSCs

Normal hPSCs
Normal-RFP hPSCs
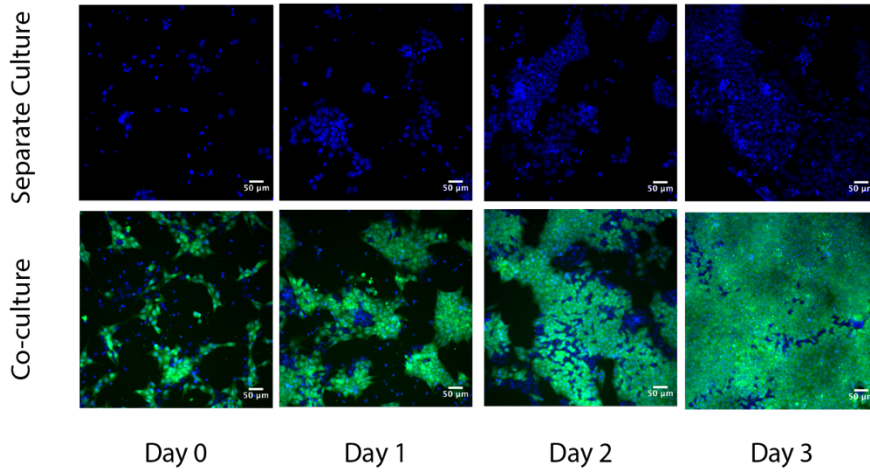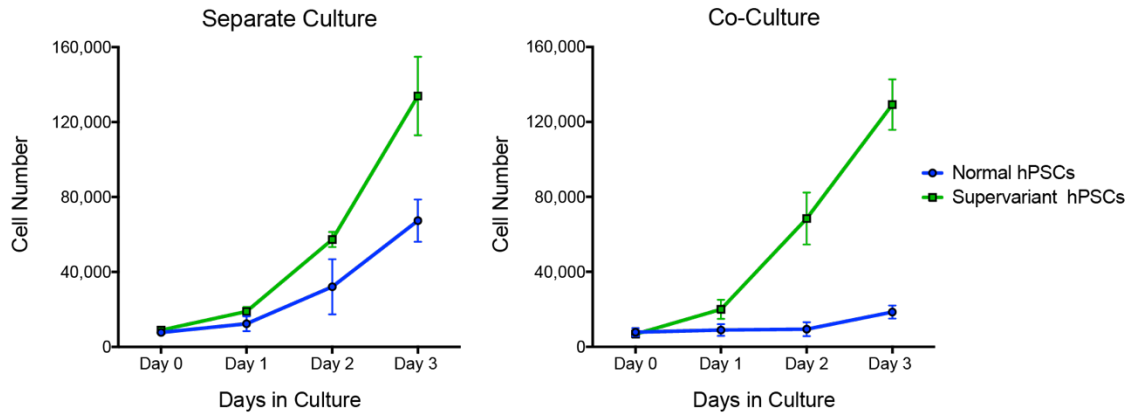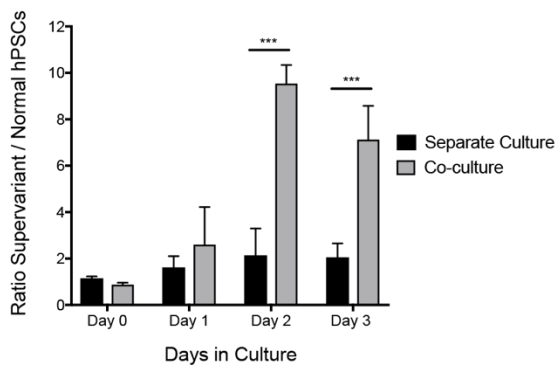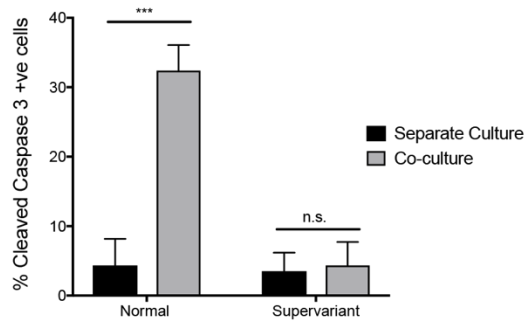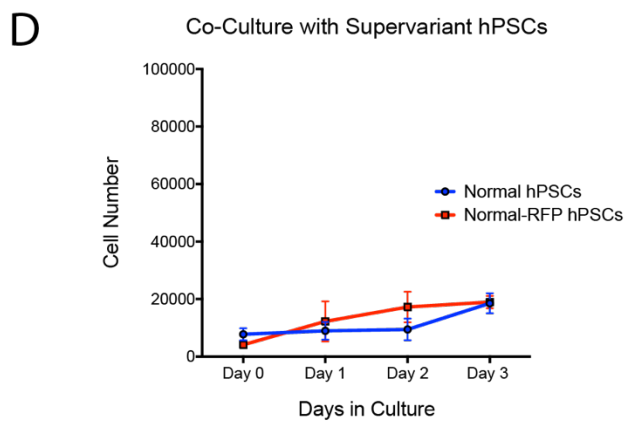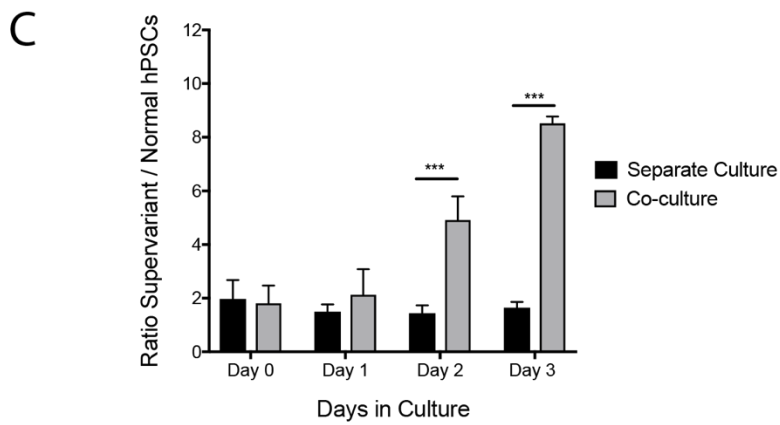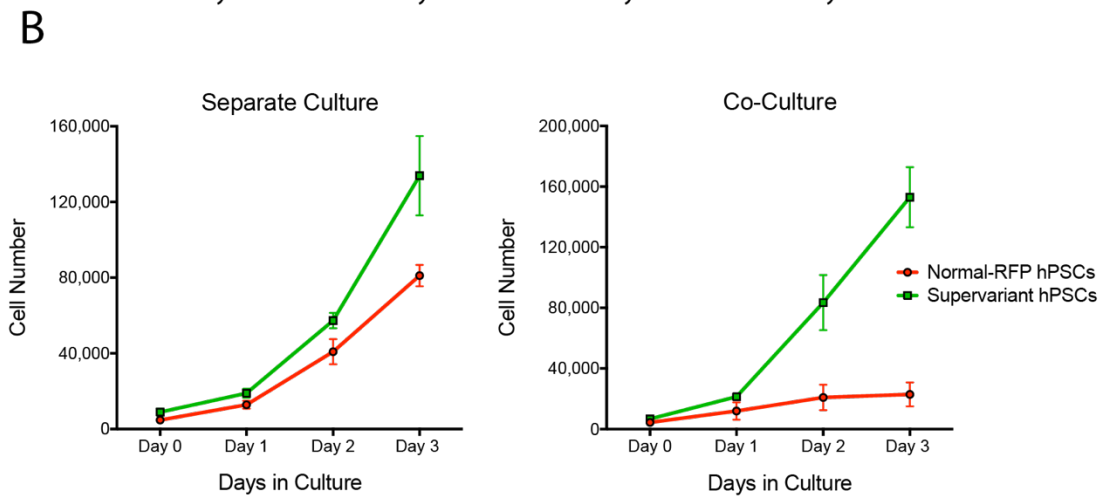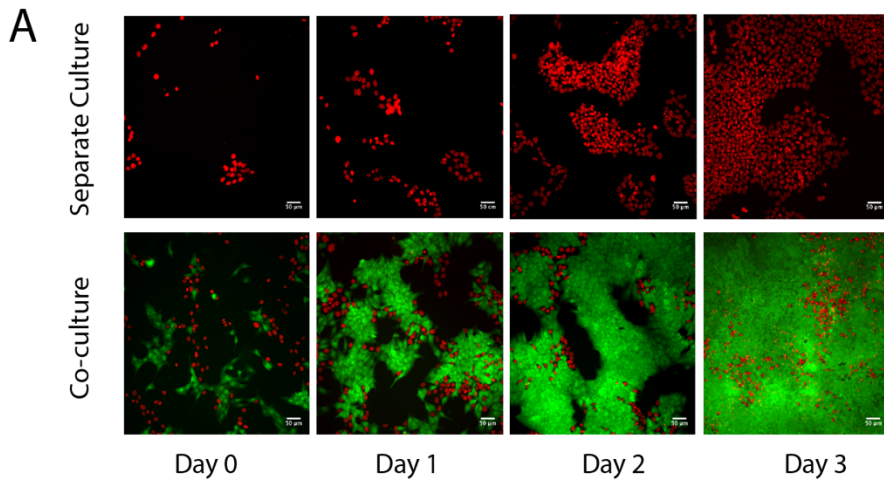
Figure 4.4 Normal-RFP hPSCs are eliminated in the presence of supervariant hPSCs.

(A) Time-course images of normal-RFP hPSCs grown separately or in co-culture with supervariant-GFP hPSCs. **(B)** Growth curves of normal-RFP and supervaraint hPSCs grown separately (left) and in co-culture (right).**(C)** Ratio of supervariant hPSCs to normal hPSCs grown in separate and co-cultures. **(D)** Growth curves of normal and normal-RFP hPSCs grown in co-culture with supervariant hPSCs.

A minimum of three independent experiments were performed and the average ±SD was plotted. *** p< 0.005, Students Paired t test.

4.2.2 1q and 20q variant hPSCs behave as losers in co-culture with supervariant hPSCs

My findings that normal hPSCs are eliminated by supervariant cells prompted me to investigate whether this also occurred in variant cells that also possessed a significantly lower growth rate compared to supervariant hPSCs. Cells in heterogenous populations possessing significantly lower growth rates have previously been shown to be eliminated by the faster growing population (Morata and Ripoll, 1975, Moreno and Basler, 2004). Variant line 20q v.hPSC possess a growth phenotype very similar to normal hPSCs and no significant difference between the final cell number over a 4 day culture period. In contrast to 20q v.hPSC, 1q v.hPSC cells proliferate significantly faster than normal cells, but also have a significantly lower growth rate compared to supervariant cells (Figure 3.6).

When 1q and supervariant cells were cultured together, I observed that the growth of 1q v.hPSCs decreased compared to separate culture. The decrease occurred from day 2, consistent with previous data from normal hPSCs (Figure 4.5A-B). Furthermore, I found the decrease in cell number to be due to apoptosis, as 1q v.hPSCs showed significantly higher levels of cleaved caspase 3 staining in the co-culture condition compared to separate culture (Figure 4.5C). Once again, the growth rate and apoptosis levels of supervariant cells was unchanged when cultured separately or in combination with another.

I saw a similar pattern of growth when I co-cultured 20q v.hPSCs with supervariant hPSCs. Growth of 20q v.hPSCs in co-culture with supervariant cells was significantly reduced compared to separate culture. However, unlike normal and 1q v.hPSCs ratio growth was only significantly lower on Day 3, this is because of the greater degree of variation in the total number of supervariant cells at Day 2 in separate culture between individual experiments (Figure 4.6). Overall the growth of supervariant hPSCs in co-culture with lines possessing significantly lower growth rates was unaffected compared to when they were cultured separately.
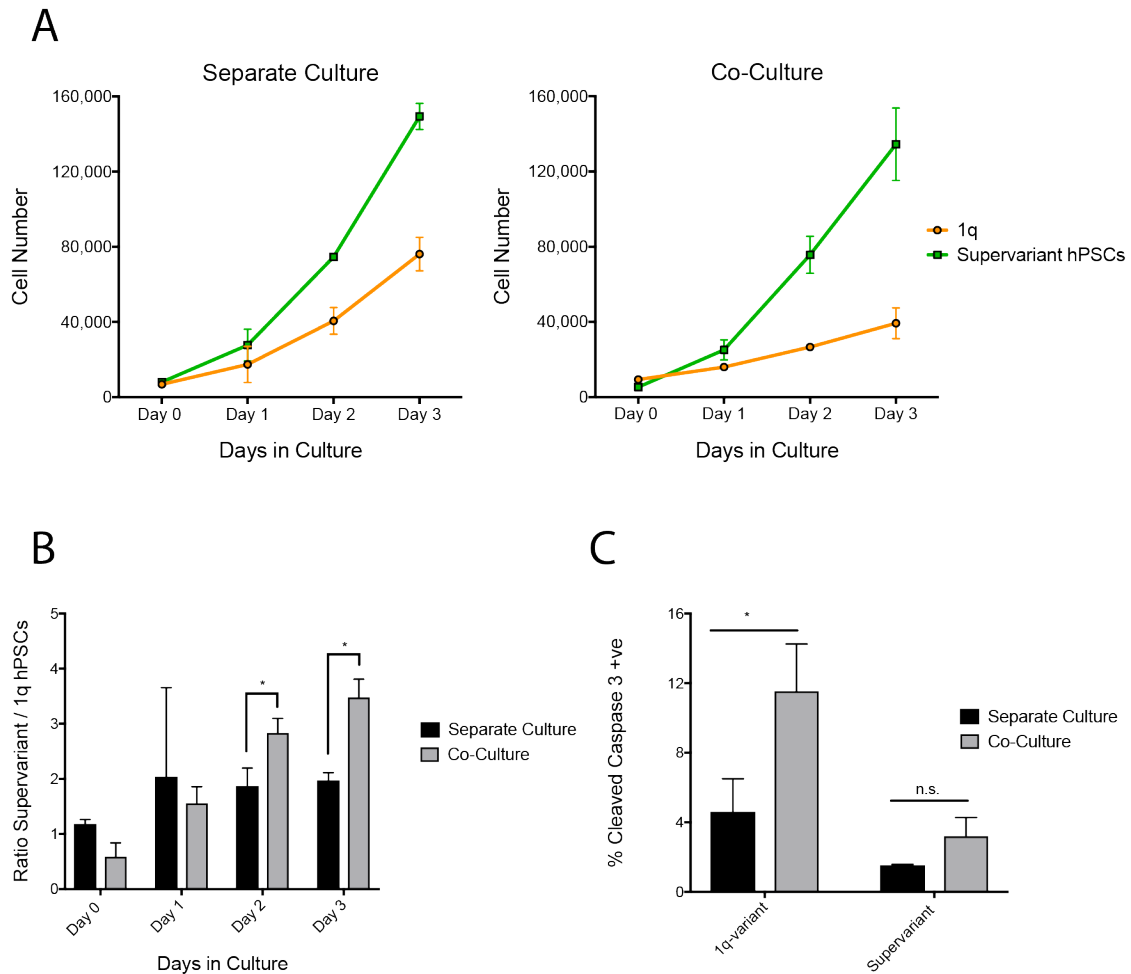
Figure 4.5 1q v.hPSCs are eliminated in the presence of supervariant hPSCs.

(A) Growth curves of 1q v.hPSCs and supervariant hPSCs grown separately (left) and in co-culture (right).**(B)** Ratio of supervariant hPSCs to 1q v.hPSCs grown in separate and co-cultures. N= 2 independent experiments and the average ±SEM was plotted. * p< 0.05, Students Paired t test. **(C)** Cleaved caspase 3 levels in separate and co-culture. A minimum of three independent experiments were performed and the average ±SD was plotted. * p< 0.05, Students Paired t test.

A
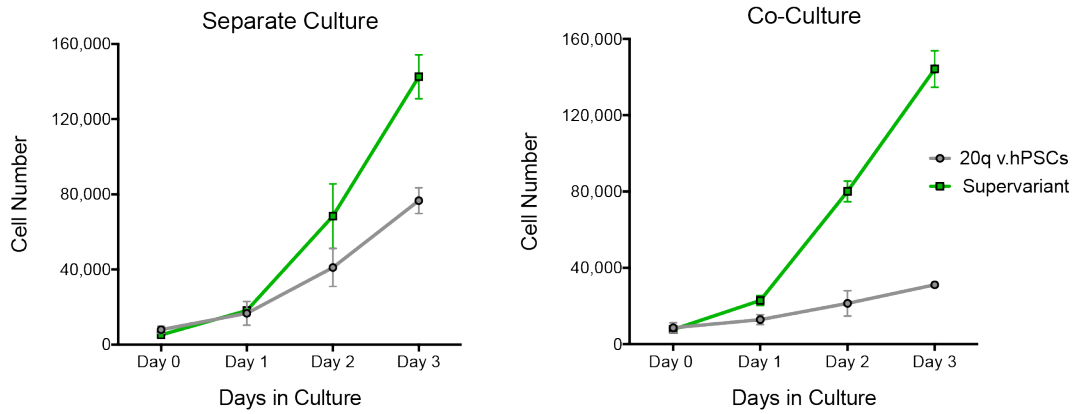
B
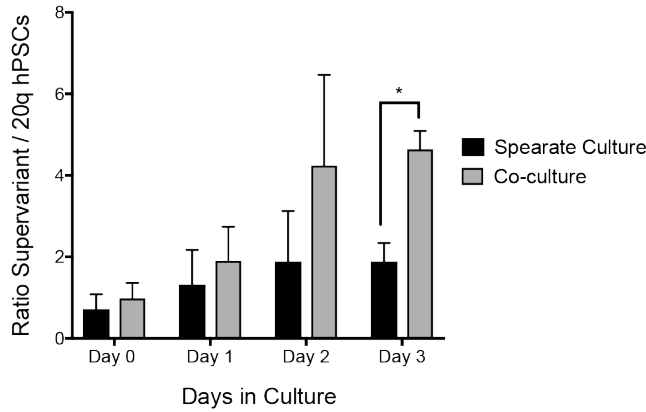
Figure 4.6 Growth of 20q v.hPSCs is restricted in co-culture with supervariant hPSCs.

(A) Growth curves of 20q v.hPSCs and supervariant hPSCs grown separately (left) and in co-culture (right).**(B)** Ratio of supervariant hPSCs to 20q v.hPSCs grown in separate and co-cultures. N= 2 independent experiments and the average ±SEM was plotted. * p< 0.05, Students Paired t test.

4.2.3 Co-culture of normal and variant hPSCs with similar growth rates does not restrict their growth phenotype

Given the observations that the growth of normal and some variant hPSCs was restricted in co-cultures with the significantly faster growing supervariant hPSCs, I next asked how cell lines with similar growth rates behave in co-culture. For this, I mixed normal-RFP hPSCs with normal hPSCs, 1q v.hPSCs and 20q v.hPSCs and analysed their growth behaviour in co-culture.

Normal hPSCs and 20q v.hPSCs do not grow significantly faster than normal-RFP cells when cultured separately, whereas 1q v.hPSCs grow slightly faster between days 2 and 3 (Figure 3.3D, Figure 3.6 and Figure 4.7). I observed that the grow of all of these lines was not significantly different when grown in co-culture with normal-RFP hPSCs compared to when they were cultured as homogenous populations. Furthermore, growth of normal-RFP cells is similarly unaffected by co-culture with each of the respective lines. This data indicates that the growth of normal hPSCs is not restricted when grown with cells of similar growth rate, neither does the higher total cell density within co-culture provide any additional support to either cell population.
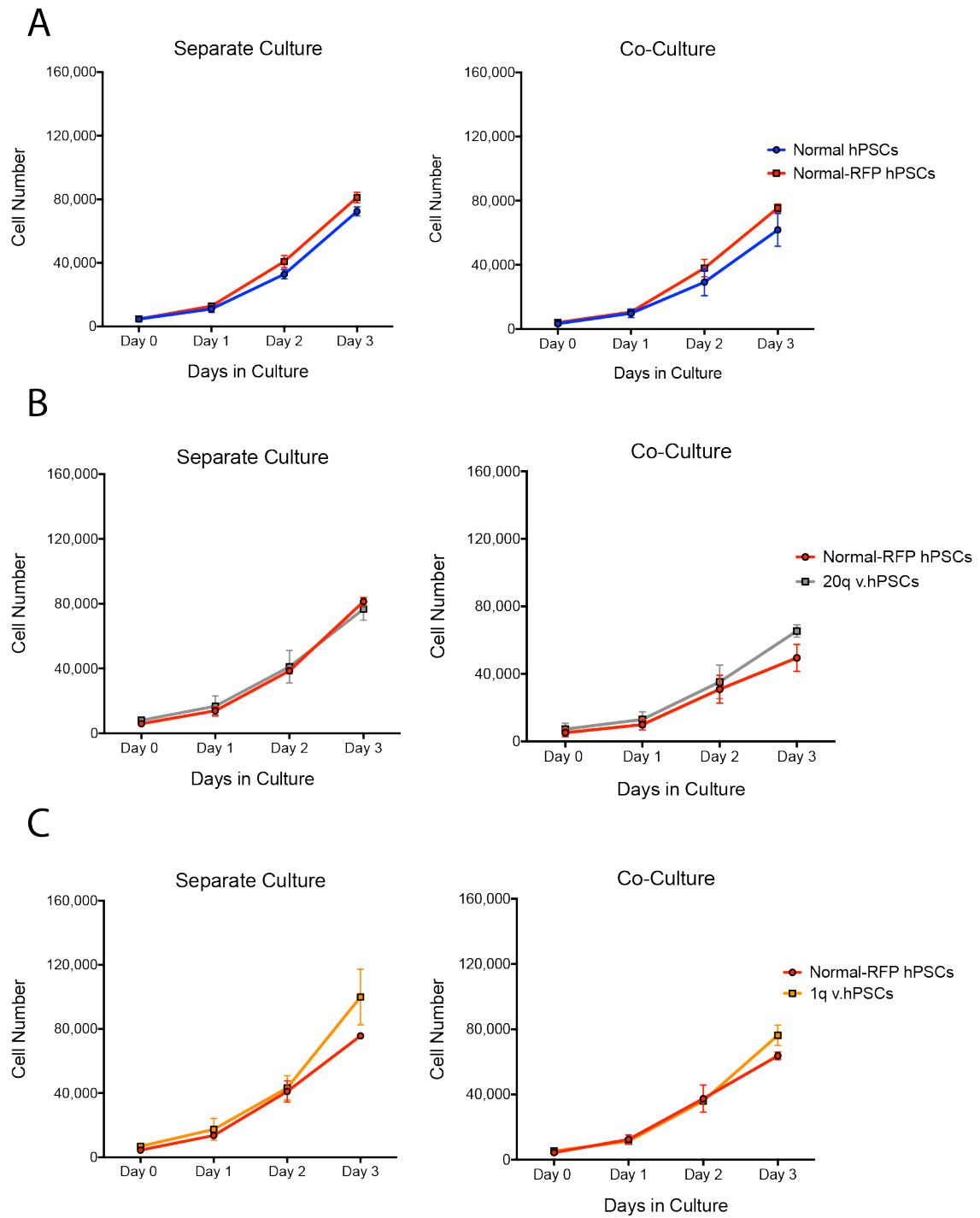
Figure 4.7 Growth of normal-RFP hPSCs is unaffected by co-culture with lines of similar growth rates.

Growth curves of separate and co-culture of Normal-RFP hPSCs and **(A)** Normal hPSCS, independent **(B)** 20q v.hPSCs and **(C)** 1q v.hSPCs. The growth rate of all lines is similar between separate and co-culture indicating they are not eliminated in each others presence. N=3 independent experiment for Normal hPSCs and N=2 for 20qv.hPSCs and 1q v.hPSCs. All graphs are plotted using the average ±SEM.

Following on from the experiments using cell lines with similar growth rates to normal-RFP hPSCs, I then went onto investigate how a variant hPSC line with a similar growth rate would respond to co-culture with supervariant hPSCs. For this, I selected 1,17,20 v.hPSCs from the remaining panel of variant lines because it is the most similar to supervariant hPSCs with regards to the genetic changes both lines possess. In separate culture 1,17,20 v.hPSCs and supervariant hPSCs have equivalent growth rate (Figure 3.6, Figure 4.8A). In co-culture, I observed the growth rate of both cells lines was equal, although the total cell number for both cell lines was significantly lower than when grown separately (Figure 4.8A-B). I found this was because co-cultures of supervariant and 1,17,20 v.hPSCs reached very high level of confluency at day 2 with little free growth area in the wells for cells to expand into between days 2 and 3. To address this issue, I cultured the cells separately and together at half the density of the original assay: co-culture, ~22,500cells/cm^2, 3,500 cells of each genotype per well; separate culture, ~11,250cells/cm^2, 3,500 cells per well. At lower density, I observed no significant difference between the growth rate of 1,17,20 v.hPSCs and supervariant cells. Furthermore, both cell lines grew at equivalent rates when cultured separately or with each other (Figure 4.8C). Together, these data suggest that the expansion of hPSC lines with similar growth rates is not restricted when cultured together, whereas when cultured with cells that proliferate significantly faster the growth of the slower growing population is restricted.

A

Separate Culture

Co-Culture

B

C

Separate Culture Low Density

Co-Culture Low Density
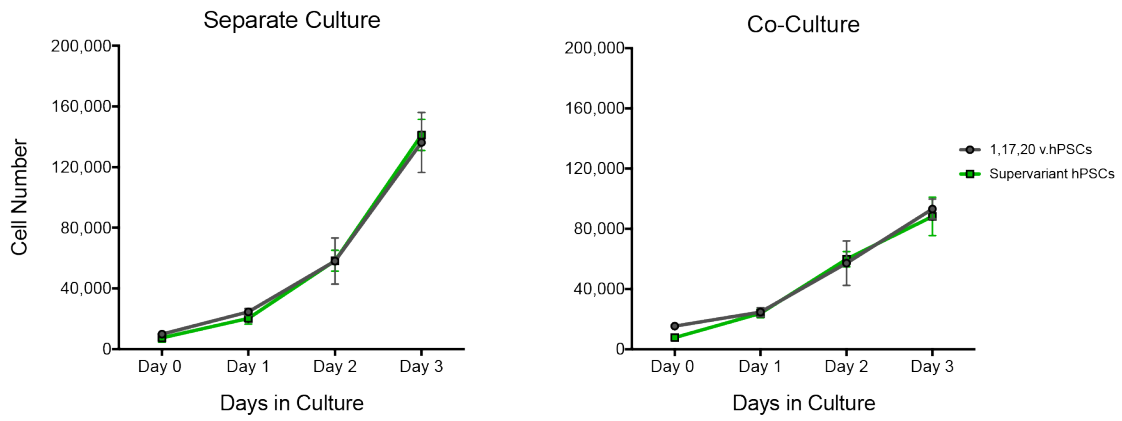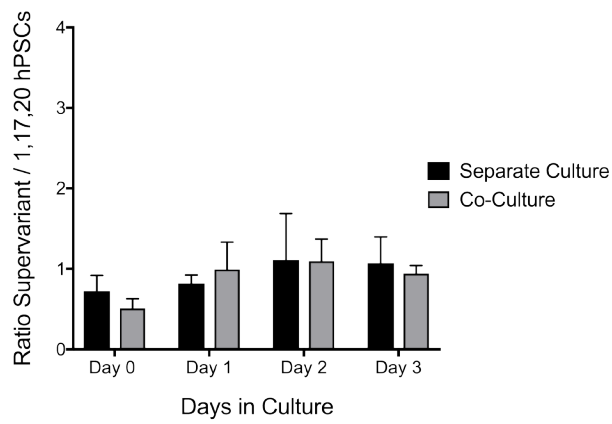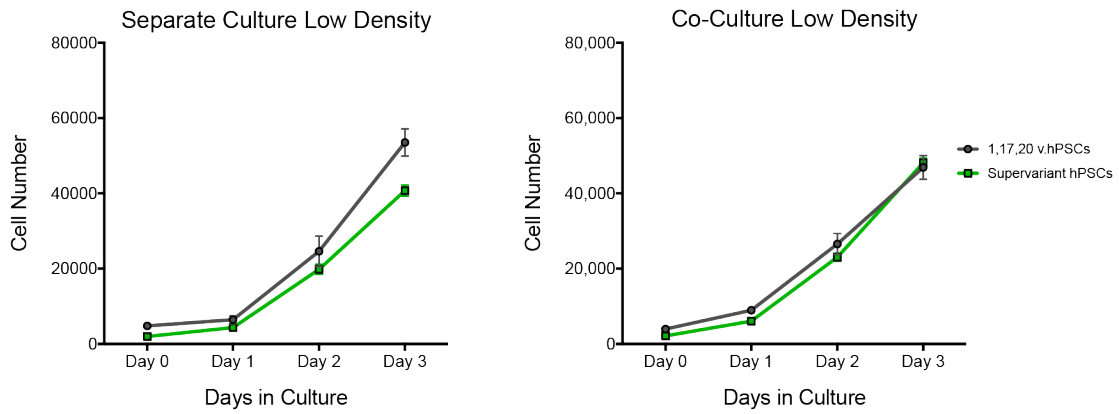
Figure 4.8 Supervariant hPSCs do not restrict the growth of variant hPSCs with similar growth rate.

(A) Growth curves of 1,17,20 v.hPSCs and supervariant hPSCs grown separately (left) and in co-culture (right).**(B)** Ratio of supervariant hPSCs to 1,17,20 v.hPSCs grown in separate and co-cultures. A minimum of three independent experiments were performed and the average ±SEM was plotted. **(C)** Low density growth curves of 1,17,20 v.hPSCs and supervariant hPSCs grown separately (left) and in co-culture (right). Results are the mean of 6 wells from the same experiment ±SEM.

4.2.4 Growth of Normal hPSCs is restricted in co-culture with 1,17,20 v.hPSCs

To further test this hypothesis, I grew normal-RFP cells separately or in co-culture with 1,17,20 v.hPSCs. The variant line 1,17,20 v.hPSC was previously shown to have a significantly faster growth rate than normal cells (Figure 3.6) and possess similar growth properties to supervariant hPSCs (Figure 4.9). For these reasons, I asked if the growth of normal cells could also be restricted when cultured with 1,17,20 v.hPSCs. Analysis of their growth rate and of the ratio of 1,17,20 v.hPSCs to normal-RFP revealed the total number of number of normal-RFP cells decreased from day 2. This led to a significantly lower number of normal-RFP cells in co-culture, compared to the separate population. The growth of 1,17,20 v.hPSCs was unaffected by culture with normal-RFP cells, similar to the observations made on supervariant hPSCs when mixed normal-RFP hPSCs (Figure 4.9).
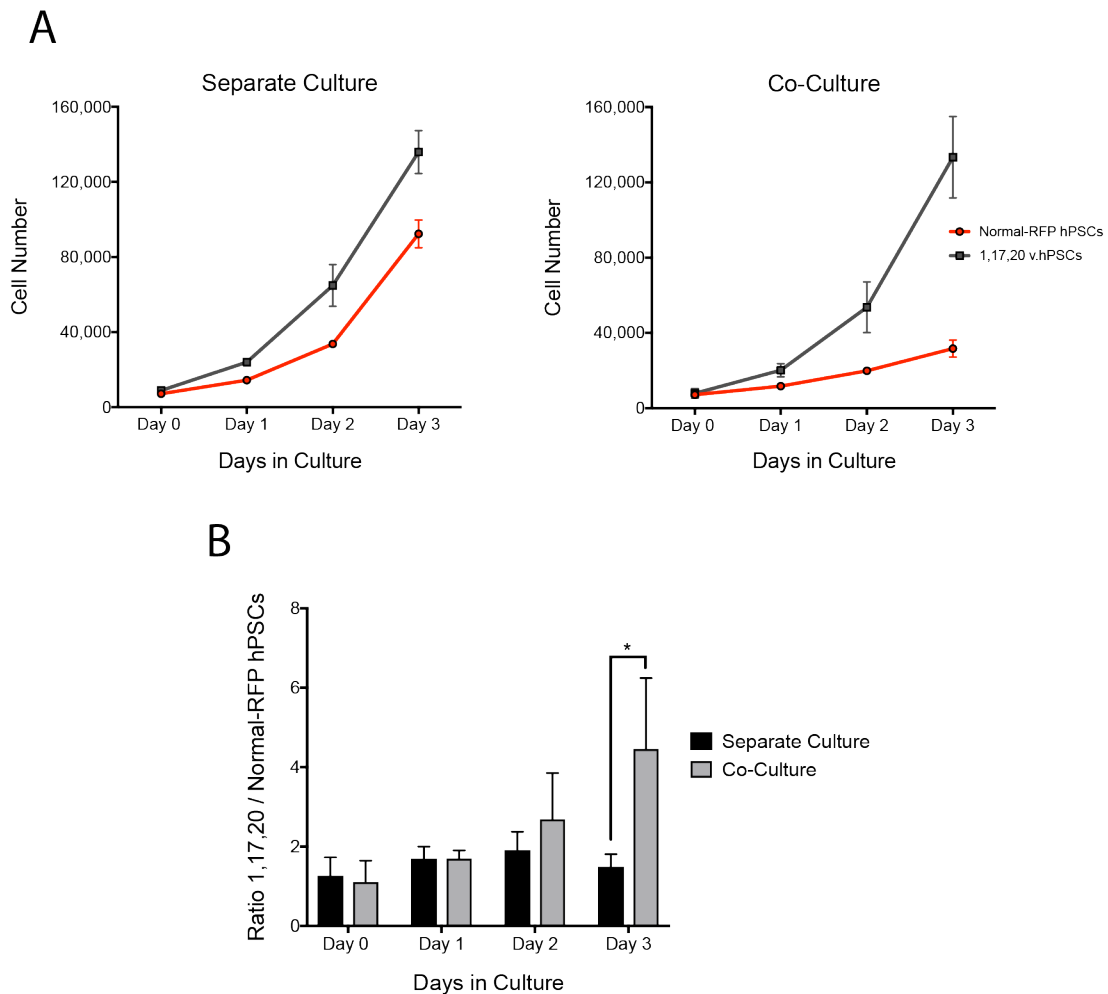
Figure 4.9 Growth of normal-RFP hPSCs is restricted in co-culture with 1,17,20 v.PSCs.

(A) Growth curves of normal-RFP hPSCs and 1,17,20 v.hPSCs grown separately (left) and in co-culture (right).**(B)** Ratio of supervariant hPSCs to 20q v.hPSCs grown in separate and co-cultures. A minimum of three independent experiments were performed and the average ±SEM was plotted * p< 0.05, Students Paired t test.

4.2.5 Determining whether elimination is mediated through contact-dependent or contact-independent mechanisms?

The increased death rate of normal cells in the presence of supervariants could be mediated either through cell-cell contacts or by cell-secreted diffusible factors, or the combination of both. To address these possibilities, I first assessed the levels of cleaved caspase-3 staining in co-cultures using Transwell systems which spatially separates the two populations but allows exchange of secreted factors in the culture media. I found that the levels of cleaved caspase-3 positive staining in normal and supervariant hPSCs was not affected by co-culture with the opposing cell type (Figure 4.10). This potentially indicates that secreted factors are not sufficient to mediate normal hPSC elimination.
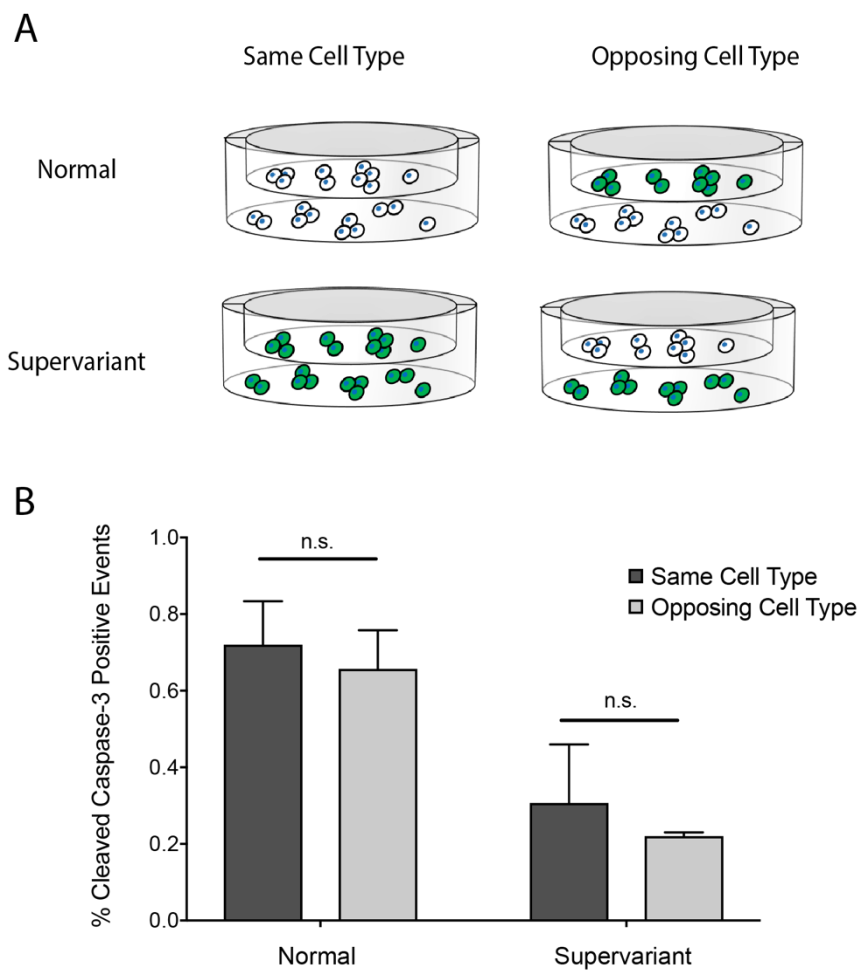
Figure 4.10 Normal hPSCs are not eliminated by contact-independent mechanisms.

(A) Schematic drawing of Transwell assay showing how populations of cells are cultured in the same well but spatially separated. **(B)** Assays using Transwell inserts indicate that the levels of apoptosis are not altered when cells are grown with overlying hPSCs of the same or opposing cell type. A minimum of three independent experiments were performed and the average ±SD was plotted. n.s , Students Paired t test.

Next, I manipulated the levels of normal-supervariant cell interactions by increasing the percentage of supervariants at plating. I established co-cultures with increasing proportion of supervariant hPSCs and corresponding separate culture controls (Figure 4.11A). I observed, that when I varied the percentage of supervariant hPSCs in the starting population of co-cultures, at the end of the standard experimental culture period heterogenous cultures that consisted of 30% or greater supervariant hPSCs at the time of plating showed significant reduction in the number of normal hPSCs compared to separate culture (Figure 4.11B). This result indicates a threshold level of supervariant hPSCs must be present in the heterogenous culture following post-plating to restrict the growth of normal hPSCs.

Increasing the proportion of supervariant cells also correlated with a greater overall cell density within co-culture conditions. To investigate the importance of cell density within co-cultures I generated a heterogenous population containing an equal proportion of normal and supervariant or normal-RFP hPSCs that I plated at increasing densities, finishing at the density used in the previous experiments that show elimination of normal hPSCs (Figure 4.1 and Figure 4.3). As plating density increased, co-culture of normal cells with supervariants exhibited a threshold like response that resulted in reduced growth of normal hPSCs around 26,500 cells/cm^2 plated (Figure 4.11C). Analysis of the higher densities showed that the number of normal cells in co-culture with normal-RFP hPSCs continued to increase as well as total number of cells in normal:supervariant co-cultures (Figure 4.11C). The further increase of total number of cells in co-cultures containing normal and supervariants at higher plating densities, as well as the decrease in the number of normal hPSCs at these densities, indicate that elimination of normal hPSCs is mediated by density-dependent cell contact.
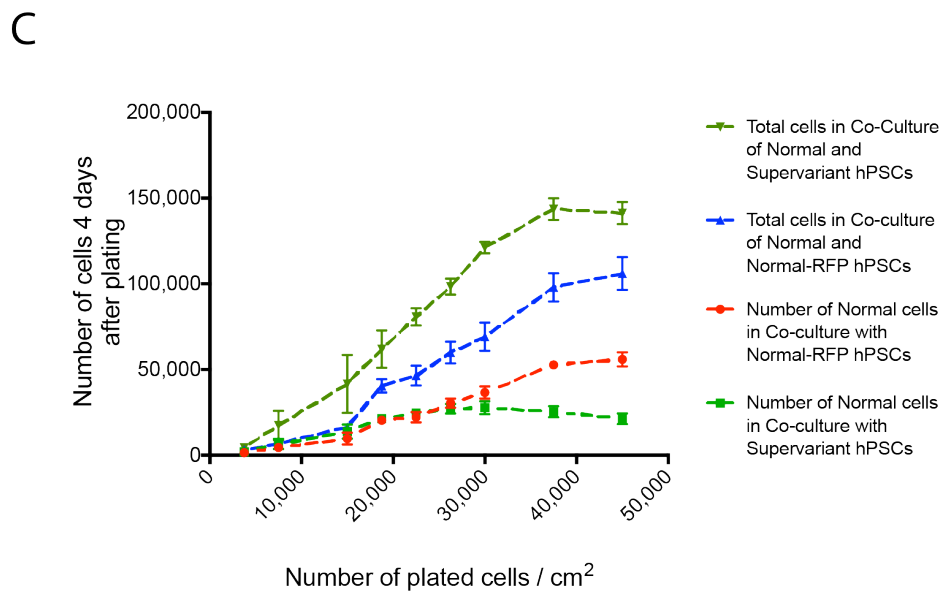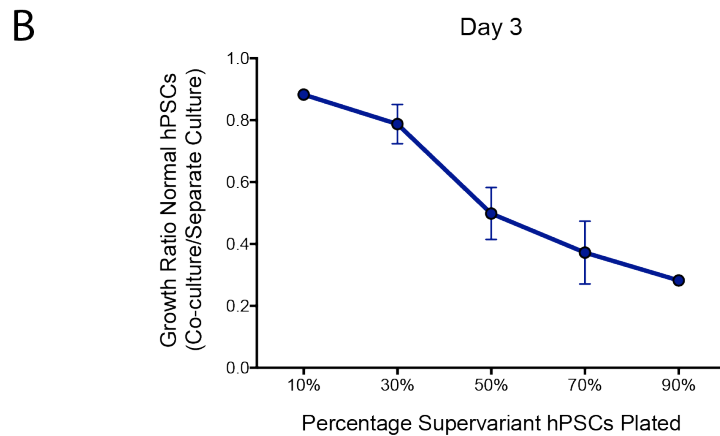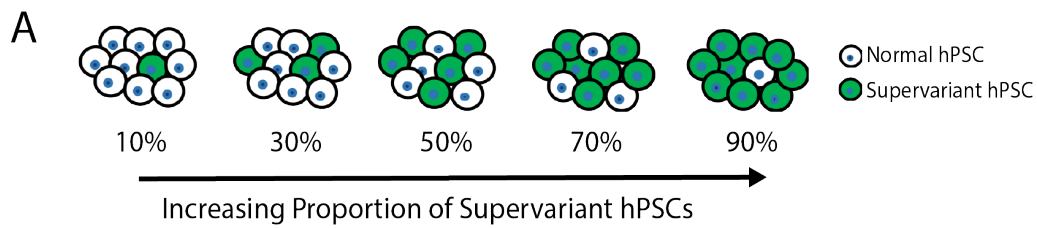
Figure 4.11 Elimination of normal hPSCs is dependent on cell-contact.

(A) Schematic diagram of co-cultures with increasing percentage of supervariant hPSCs. **(B)** Plot of the ratio of normal cells when co-cultured with increasing percentage of supervariants at the time of plating against separate culture controls. Results are the mean of 2 independent experiments ±SEM. **(C)** Effect of increasing cell plating-density on the number of normal hPSCs when grown in co-culture with control normal-RFP or supervariant cells and the total number of cells in each heterogenous population. Results are the mean of three independent experiments ±SEM.

4.2.6 <u>Time-Lapse Analysis of normal and supervariant hPSC interactions</u>

Having demonstrated that cell contact and density are important components of the mechanism(s) that mediate normal cell elimination during co-culture with supervariant cells, I next utilised time-lapse imaging to assess regions of co-cultures in which normal cell survive and regions where they are eliminated to determine how interactions with supervariant hPSCs changes between these two scenarios. Co-cultures were established using the plating density of 45,000 cells/cm^2 that has been standardly used in most of the mixing experiments described earlier in this chapter and at which elimination of normal hPSCs is greatest (Figure 4.11C). Images were captured every 10 minutes between days 2 and 3, the period during which the greatest decrease in cell numbers compared to separate culture is observed (Figure 4.3).

In regions where normal hPSCs survived by the end of day 3 I observed several common features. Firstly, there were less cells overall within the field at the start of imaging suggesting that the starting density was low. Secondly, normal cells appeared in more homogenous regions of the expanding colony and seemingly shared more cell-cell contacts with other normal cells than supervariant hPSCs. As the colonies expanded these homogenous regions generally persisted. Neighbouring supervariant cells did not appear to extensively migrate into them but rather grew around them. Finally, these homogenous regions tended to occur at the edge of mixed colonies with one side facing a portion of cell-free culture area that the normal cells were able to expand into (Figure 4.12A).

Conversely, in areas that I observed elimination of normal hPSCs, the fields contained more cells in general indicating a higher density. Composition of the colonies appeared more heterogenous with greater mosaicism of normal and supervariant hPSCs. Homogenous regions of normal hPSCs were small and tended to be situated in the middle of the heterogenous colony surrounded by supervariant hPSCs. Additionally, more evidence of supervariant hPSCs migrating into the regions of normal cells could also be observed. Finally, cells that underwent apoptosis detached from culture surface and could be observed in the culture media (Figure 4.12B).

A

00:00 h 02:00 h 04:00 h 06:00 h 08:00 h 10:00 h 12:00 h

14:00 h 16:00 h 18:00 h 20:00 h 22:00 h 24:00 h 26:00 h
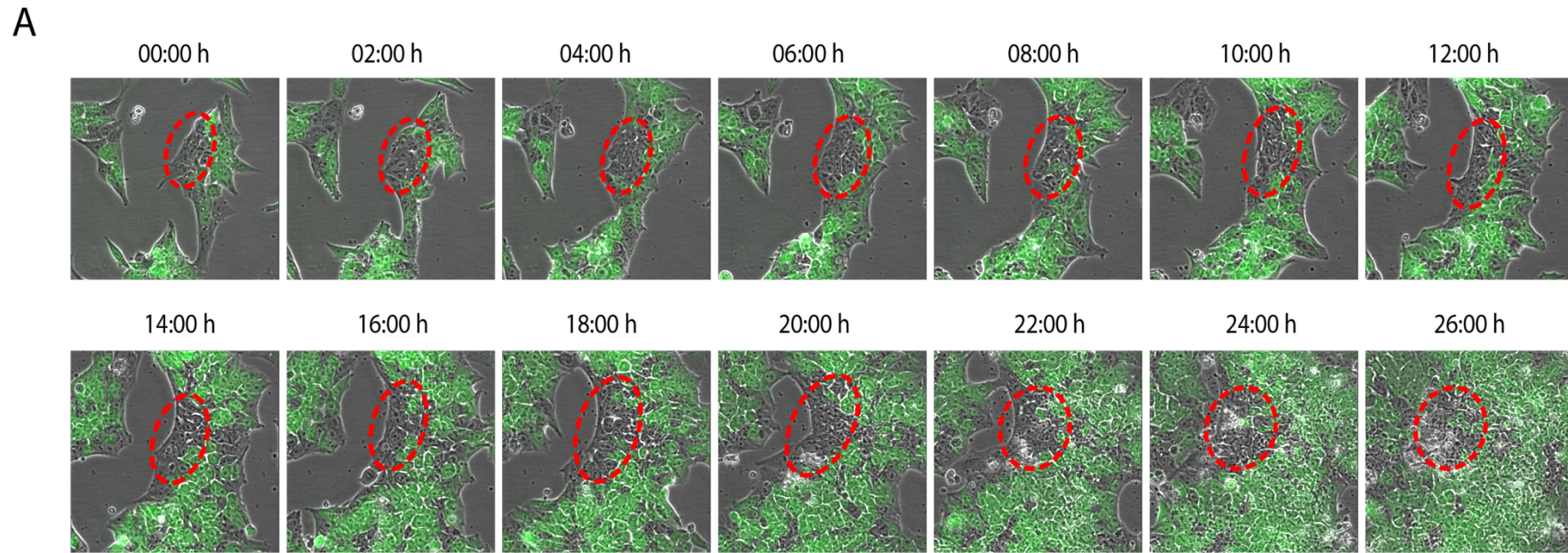
Figure 4.12 Time-lapse analysis of cell-contact dependent elimination of normal hPSCs

Time-lapse images showing regions of **(A)** normal cell survival in co-cultures with supervariant occurs at the cell-free edges of heterogenous colonies with low degrees of mosaicism and **(B)** elimination of normal hPSCs in the centre of larger colonies containing a large proportion of supervariant hPSCs. Regions of normal cell survival and elimination are denoted by the red circle.

B

00:00 h 02:00 h 04:00 h 06:00 h 08:00 h 10:00 h 12:00 h

14:00 h 16:00 h 18:00 h 20:00 h 22:00 h 24:00 h 26:00 h
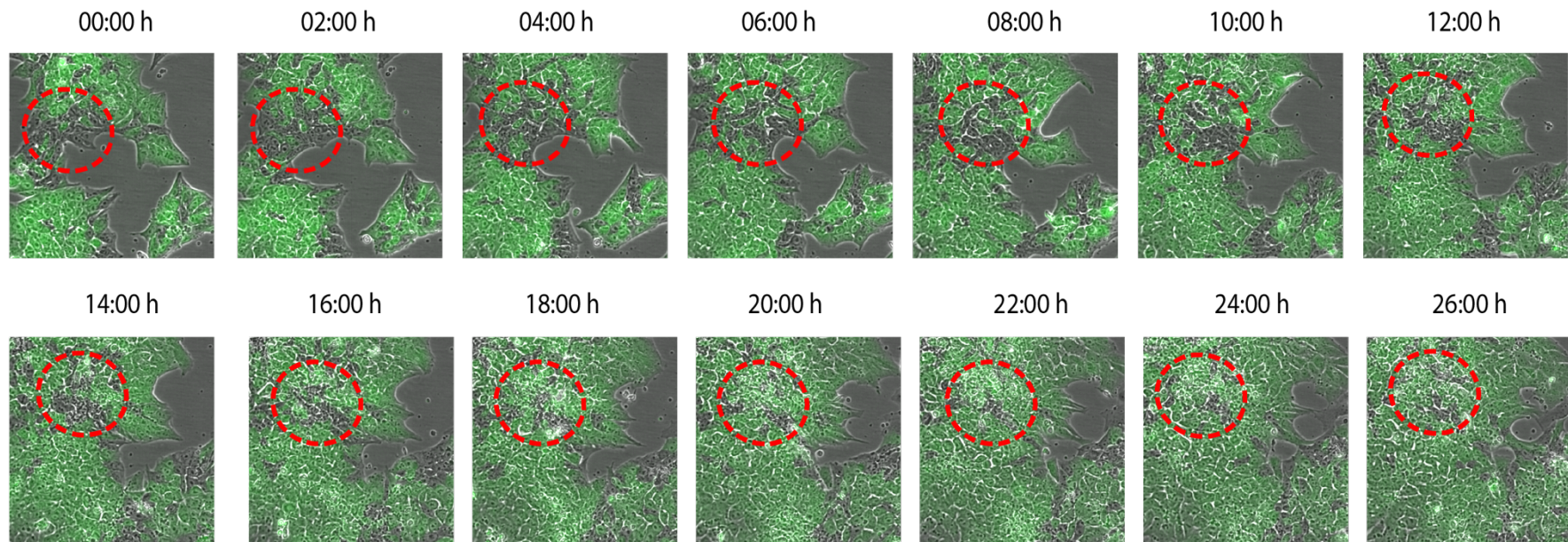
An attractive model to explain the density contact-dependent elimination of normal hPSCs is that normal hPSCs are more sensitive to increases in mechanical forces as heterogenous colonies expand (Wagstaff et al., 2016). To assess whether normal and supervariant cells exhibit different responses to being confronted by the opposing cell type at high density, I plated normal and supervariant cells on microslides with separate chambers and allowed the cells to grow into contact with each other (Figure 4.13A). After the cells had come into contact they were cultured for a further 48 hours and the position of each cell front was tracked using the constitutively expressed fluorescent proteins.

In conditions where normal cells were plated alongside normal-RFP hPSCs, both cells populations grew and met each other in the middle of frame creating a boundary line (Figure 4.13B). After 8 hours in contact, I observed a band of apoptotic cell debris which lay along the border where the two cell lines met, however the position of the boundary had not moved. Over the following 40 hours, the boundary at which the two populations met remained in a stable position (Figure 4.13B).

To enable more accurate tracking of the border of genetically normal hPSCs, normal hPSCs were substituted with normal-RFP cells and cultured alongside supervariant hPSCs. The two populations grew together and met in the middle of frame at a similar position to the boundary of normal and normal-RFP hPSCs. Following contact, the normal-RFP hPSC boundary is pushed back by the advancing supervariant population, by 48 hours post contact the normal-RFP population had nearly been pushed out of view. In addition to the retreating normal-RFP hPSC boundary I also observed the appearance of apoptotic cell debris. Firstly, between 8 and 16 hours post contact the cell debris was predominantly observed over the normal-RFP population. As the culture period progressed, between 32 hours and 48 hours, cell debris appeared over both populations of hPSCs (Figure 4.13C). Together, these findings indicate supervariant hPSCs possess enhanced mechanical properties that allow them to tolerate higher densities as well as migrate in an invasive-like manner into the normal hPSC population.
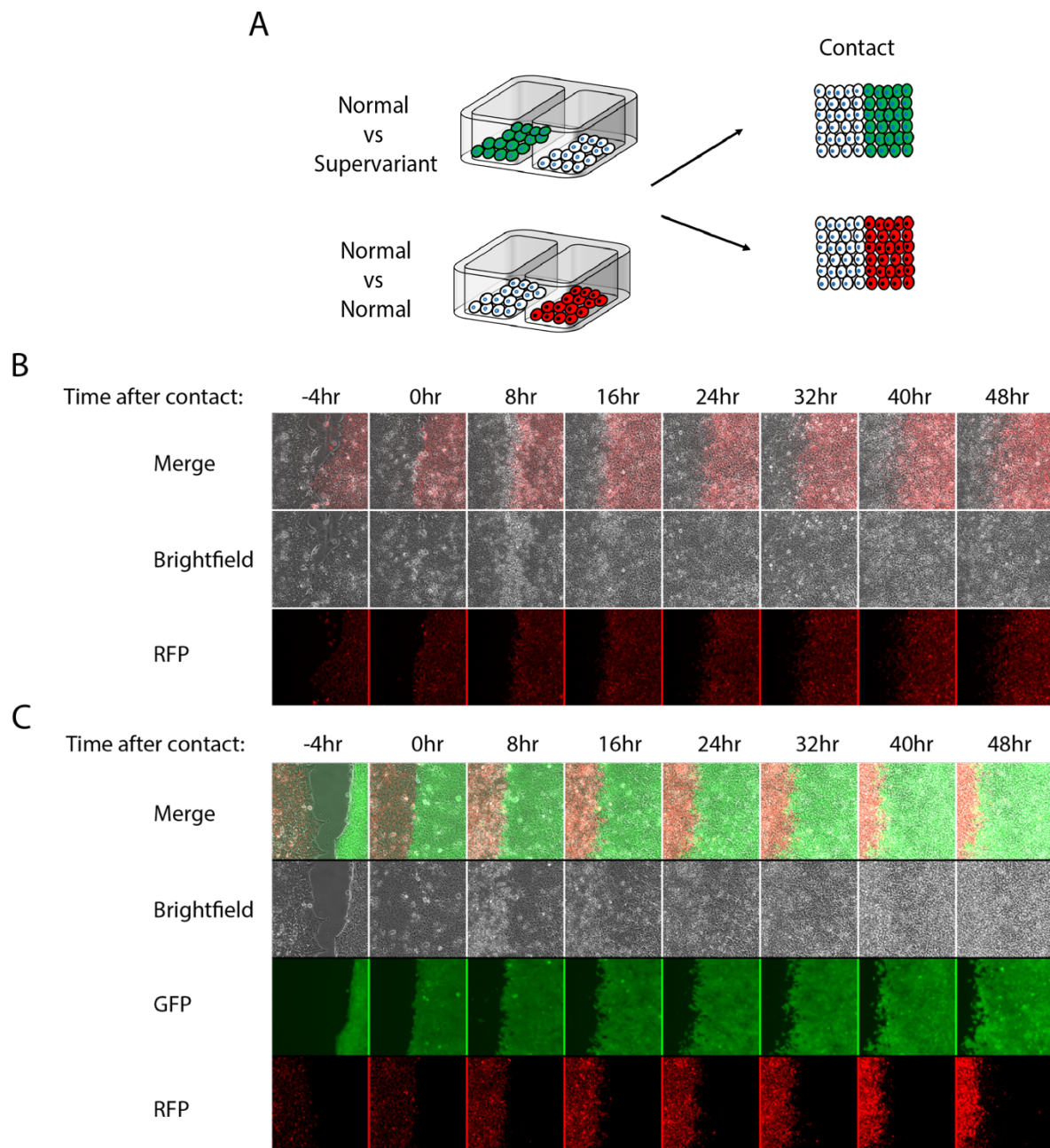
Figure 4.13 Supervariant hPSCs are mechanically superior than normal cells

(A) Schematic diagram of mechanical stress assay, cell populations are seeded on opposite halves of the chamber and left to attach. The chamber is then removed leaving a 500μm cell free gap for the populations to grow over and into contact with each other. Time-course images of **(B)** normal-RFP cells coming into contact with normal hPSCs, in the 48 hour culture period post contact the position of the cell boundary remains fixed. **(C)** Normal-RFP come into contact and are pushed backwards by supervariant hPSCs.

4.3 Discussion

Selection mechanisms in hPSC cultures drive the overtake of normal diploid cells by genetically variant hPSCs. My previous work highlighted the advantageous properties conferred by different chromosomes to variant hPSCs that provide a growth advantage by altering their propensity towards particular cell fates. One possibility is that the improved growth properties of variant cells allow them to passively overtake normal hPSCs by promoting self-renewal fate and restricting differentiation and cell death. Previous work has demonstrated these growth properties may exert their selective function at bottlenecks in standard culture practice (Barbaric et al., 2014). Here I took a different approach and focused on the behaviour of normal and variant hPSCs when cultured together to characterise selection mechanisms that are present during the co-existence of both populations. Through recapitulating the composition of hPSC cultures with an emerging variant population and alleviating the selection bottlenecks that occur during plating, I have identified an active mechanism of selection whereby the presence of particular genetically variant lines exerts a direct effect on normal hPSCs that influences their fate and causes apoptosis.

Firstly, I assessed the growth rates of normal and supervariant cells in homogenous and heterogenous cultures. I found that the growth of normal hPSCs was restricted in co-culture with variant compared to separate culture whereas the growth of supervariants is unaffected. This observation was confirmed on normal-RFP hPSCs. There was a significant increase in cleaved caspase-3 levels of normal hPSCs showing this elimination occurs by apoptosis. I then looked at the behaviour of variant hPSC lines 1q v.hPSC and 20qv.hPSCs that also possess significantly lower growth rates than supervariant hPSCs. My data shows that growth of these two variant lines is suppressed in a similar manner by the presence of supervariant hPSCs. In conclusion, these results indicate that a common mechanism exists within cultures of hPSCs that mediates the elimination of slower growing cells when in the presence of faster growing hPSCs.

I then went on to compare the behaviour of hPSCs when cultured alongside lines that possess similar proliferation rates. This was done firstly in the slower growing normal populations and then in the faster supervariant hPSCs. When I compared the growth of normal-RFP cells in separate and co-cultures with other normal cells and the variant lines 1q v.hPSC and 20q

v.hPSC, I saw there was no overall change in the growth rate of either population. A similar effect was seen in the faster growing cultures containing supervariant hPSCs and 1,17,20 v.hPSCs. Finally, I tested the effect of co-culturing 1,17,20 v.hPSCs with normal-RFP hPSCs. Based on the previous observations that normal-RFP hPSCs were eliminated by faster growing supervariant cells and 1,17,20 v.hPSCs have similar growth properties to supervariant cells , I hypothesised 1,17,20 v.hPSCs would also restrict the growth of normal-RFP cells. I found that the total number of normal-RFP cells was significantly lower on day 3 of co-culture whereas growth of 1,17,20 variant hPSCs was unaffected. When comparing the ratio of 1,17,20 v.hPSCs to normal-RFP I only saw a significant difference between separate and co-culture on day 3, whereas in supervariant cultures a difference is also observed on day 2. This difference is because the total number of normal-RFP cells in co-culture is higher in cultures containing 1,17,20 v.hPSCs than supervariant cells.

The elimination of slower growing cells hPSCs when confronted by a faster growing population mode of elimination shares several common features with the phenomena called cell competition(Morata and Ripoll, 1975, Moreno and Basler, 2004, Madan et al., 2018); for this reason, I propose cell competition may be a selection mechanism in hPSC cultures. Various mechanisms for sensing cell fitness during cell competition have been described in Drosophila and mammals. It has been proposed that cells compete for limited factors required for their survival (Moreno et al., 2002). A possible limiting factor in hPSC cultures is fibroblast growth factor 2 (FGF2), an essential component in culture media for maintaining undifferentiated stem cells (Levenstein et al., 2006). FGF2 levels decline during culture at 37°C which is why media is usually replaced daily (Lotz et al., 2013). It is plausible that a faster growing population reduces the amount of available FGF2 more rapidly than slower growing cells. Variant hPSCs have also been shown to exhibit growth factor independent growth suggesting they would less likely be negatively affected by low levels of survival factors (Werbowetski-Ogilvie et al., 2009). However, it is probably unlikely that the elimination of normal hPSCs is mediated by this mechanism because I found that culturing normal and supervariant cells in the same media environment but spatially separated has limited effect on the levels of apoptosis in both populations. This result could indicate that competition between normal and supervariant hPSCs is mediated by cell-contact dependent mechanisms.

Previous studies have indicated that the establishment of future winner and loser fate is dependent on the proportion of winner and loser cells and initial seeding density (Bove et al., 2017). My data confirms that manipulation of these two variables can alter the competitive fate of normal and supervariant hPSCs. I manipulated the proportion of supervariant hPSCs in co-cultures but maintained overall plating density and saw that elimination of normal hPSCs exhibited a dose-like response. Conditions with the highest starting percentage of supervariants produced the greatest reduction in normal hPSC growth. In addition, I also demonstrated elimination of normal hPSCs is dependent on starting density. Time-lapse imaging was used to explore how different degrees of normal-supervariant interactions and density could mediate elimination of normal hPSCs. I noted that elimination of normal hPSCs was seemingly prevalent in areas of high density predominated by supervariant hPSCs, which would suggest competition in hPSC cultures is mediated either through a cell surface fitness marker, mechanical stress or both. The limitation of these observations is that the local density and cell contacts of individual cells are constantly changing and evolving as cells migrate, undergo division and die. It is therefore difficult to track the population dynamics and determine the time and culture state at which loser fate is specified. Further experimental work will be required to develop a quantitative approach that can be used to investigate how local density and proportion of normal-supervariant contacts govern the competitive outcome in cultures of hPSCs.

My observations that increased cell density during co-culture with supervariant hPSCs enhances cell death is also of great importance because it partially contradicts the findings of previous studies that show high cell density supports survival and establishment of hPSC colonies post plating (Thomson et al., 1998, Barbaric et al., 2014). My data suggest that the effect of density on hPSC culture must be considered in an additional context. During the growth phase of culture, the presence of a rapidly expanding population with greater tolerance for density can raise the local density above the homotypic level for normal hPSCs, generating an environment that is detrimental to survival of normal cells. I cannot exclude the possibility that the improved properties of variant hPSCs may generate conditions that support normal cell growth. For example, the ability of variant hPSCs to overcome post-plating bottlenecks could raise the density of hPSCs that would intern support normal hPSC survival during this period of culture. This hypothesis requires further experimental validation

but supports the notion that growth of normal hPSCs can also be enhanced by the presence of genetically variant cells (Werbowetski-Ogilvie et al., 2011). Collectively this data highlights the requirements for cell survival during culture are context dependent and may change as different populations emerge during hPSC expansion.

To explore the differences in tolerance of normal and supervariant hPSCs to mechanical stress I developed an assay that assessed their mechanical properties, by seeding cells on opposing sides of and letting them grow together to form a distinct border I was able to track the movement of either population from the point of contact. I found that, normal-RFP hPSCs are progressively forced backwards by the advancing supervariant hPSCs. This data suggests that supervariant hPSCs have a higher tolerance for mechanical stress, indicating mechanical cues are a predominant component of competition in hPSCs. It remains to be determined how the presence of supervariants influences signalling pathways in normal hPSCs and these change depending on the local cell density and proportion of interactions between the two cell populations.

5   Molecular mechanisms of cell competition in hPSCs

5.1   Introduction

Cell competition is a process that assess and compares the fitness levels of a cell to neighbouring cells within the local environment and results in the elimination of the less fit population. The relative fitness of a cell is detected and compared by a set of mechanisms that interpret short-range biochemical signals or long-range mechanical cues. Upon determining relative fitness levels and establishing winner/loser fate competing cells must communicate this information via downstream signalling pathways to execute cell fate. Loser cells are actively eliminated from the tissue or experimental culture by apoptosis and in some situations the "winner" population undergoes compensatory proliferation to replace the lost cells. The mechanisms that govern compensatory proliferation have so far remained elusive. Whereas, multiple pathways have been implicated as the effectors of loser cell elimination, predominant amongst these are the cellular stress response pathways; p53, JNK and NK-$_k$B.

In the first model of mechanical cell competition, Shraiman predicted that the mechanical force exerted by the faster-growing population upon loser cells could cause compression of the slower growing population that would be sufficient to induce apoptosis (Shraiman, 2005). A later study proposed that in addition to compression another mechanical force to consider in epithelia is stretching pressure. Deformation and stretching of slow growing loser cells was proposed to be caused by the mechanical force exerted by the rapidly expanding winner cells and trigger apoptosis (Vincent et al., 2013). Cell stretching has predominantly been described as a force that stimulates cell proliferation (LeGoff and Lecuit, 2015). A strong candidate pathway that links mechanical force and regulation of cell growth is the Hippo-YAP signalling pathway (Gumbiner and Kim, 2014). Cell stretching has been shown to promote translocation of YAP/TAZ to the nucleus where it upregulates transcription of genes that promote cell growth (Aragona et al., 2013). The Hippo pathway has previously been implicated as both a trigger and a mediator of cell competition but not in a mechanical context (Bras-Pereira and Moreno, 2018). A common feature in both proliferation and apoptosis contexts is that cells detect the mechanical stimuli and coordinate a cellular response through downstream signalling pathways. Understanding the interplay between mechanical forces and the

signalling pathways that control both proliferation and apoptosis can provide an approach to determine the molecular mechanisms that determine aspects of cell competition.

Mechanical competition was first described as a mechanism of cell competition in mammalian systems in a study assessing the elimination of loss of polarity mutants in MDCK cells (Wagstaff et al., 2016). Compression forces were shown to be required and sufficient to induce cell death in both homotypic and heterotypic cultures. Knockdown of *Scribble* raises the baseline level of p53 higher than wildtype cells, hypersensitising *Scribble^{kd}* mutants to compaction. In homotypic cultures, the authors seeded *Scribble^{kD}* MDCK cells as a monolayer onto a stretched polydimethylsiloxane substrate that when released caused cell compression, this induced cell death in *Scribble^{kD}*, whereas wild type cells were unaffected. In heterotypic cultures of MDCK cells, wild type cells surround *Scribble^{kd}* cells raising the local density and exerting a mechanical stress across both populations. The rise in density causes compression of the cells that is sensed by the cytoskeletal regulator ROCK. In response, ROCK phosphorylates its downstream target p38, a member of the stress-activated MAP kinases (MAPK). Phosphorylation of p38 leads to elevation of p53 levels that is sufficient to induce apoptosis in the hypersensitised *Scribble^{kd}* mutant cells. In this study the authors used both a genetic manipulation and chemical inhibitor approach to determine the function of each component within the mechanical competitive pathway. Treatment of heterotypic cultures with the ROCK inhibitor Y-27632 reduced the levels active phosphorylated p38 in *Scribble^{kd}* and rescued them from elimination. The role of p53 as the executor of cell death in this competitive context was demonstrated using p53 knockout cells. Manipulation of the basal levels of p53 is sufficient to alter the competitive fate of wild-type cells. Co-culture of wild type and p53 knockout cells alone is insufficient to induce cell competition, however addition of Nutlin-3, a small chemical inhibitor that induces low-level p53 activation, transforms the competitive landscape and results in elimination of wild-type cells. Collectively this demonstrates that p53 acts in a dose-dependent manner, with conditions that raise p53 above a threshold level sufficient to induce apoptosis (Wagstaff et al., 2016).

JNK signalling was first identified as a molecular mechanism of cell competition in cells with different growth rates, however it has not currently been shown as a molecular mechanism involved in the models of mechanical cell competition described in the literature so far (Bras-Pereira and Moreno, 2018). In other competitive contexts such as the Drosophila wing imaginal disk, JNK signalling has been shown to control loser cell fate in both a competitive and supercompetitive context. In Minute$^{+/-}$ competition, slower growing mutant cells are eliminated by wild-type cells, whereas in dMyc overexpression mediated supercompetition wild-type cells are eliminated by the faster growing mutant population. JNK signalling inhibits the growth of loser cells and inhibition of the signalling pathway rescues the elimination of the loser population in both contexts (Moreno et al., 2002, Moreno and Basler, 2004, Kucinski et al., 2017).

The role of JNK signalling in cell competition has also been observed in different tissues at later stages of development as well as cancer. Adenomatous polyposis coli is a tumour suppressor gene that regulates canonical WNT signalling through the degradation of β-catenin and is frequently mutated in colorectal cancers (Zhang and Shay, 2017). APC mutants in the Drosophila midgut over-proliferate and outcompete neighbouring wild-type cells. JNK signalling is hyperactivated in the APC supercompetitors and is required for their cell growth, inhibition of JNK signalling in both APC mutants and surrounding wild-type cells reduces the growth APC cells demonstrating JNK signalling has a role in coordinating cell fate in both winner and loser cells. JNK signalling is required in winner APC mutants to promote proliferation and loser wild-type cells to control their elimination (Suijkerbuijk et al., 2016). During tumour development, competition for space can control the expansion of oncogenic cells (Tsuboi et al., 2018). Compressive forces play a key role in governing cell fate during tumour expansion, in this context the mechanical forces that induce cell death are proposed to be an alternative mode of supercompetition termed mechanical supercompetition (Levayer et al., 2016). Therefore, it is possible that mechanical competition could also contribute to a cell competition phenotype within a variety of context where the effect of mechanical forces has not been assessed.

In contrast to these observations, other groups studying the same competitive contexts did not observe an effect on Minute$^{+/-}$ competition and dMyc driven supercompetition when JNK signalling was inhibited. Leading to the suggestion that JNK signalling functions as an enhancer of cell competition and not as a molecular trigger of competitive behaviour (Vincent et al., 2013). Since its initial description, a role for JNK signalling has also been identified in competition driven by loss of epithelial polarity. Winner and loser cell fate is mediated by activity of JNK signalling in both populations. In loser cells JNK signalling is required for cell death, inhibition prevents apoptosis in the loser population. Activity of JNK in winner cells has been shown to impact different aspects of cell behaviour. Engulfment of loser cells in the Drosophila imaginal epithelia is mediated by JNK signalling in the surrounding winner population. Activated JNK results in the overexpression of the platelet derived growth factor/vascular endothelial growth factor receptor, PVR, which in turn activates the phagocytic pathway in neighbouring winner cells, removing loser cells from the epithelia by engulfment (Ohsawa et al., 2011). Lastly, JNK signalling has been shown to drive compensatory proliferation of winner cells in Drosophila. In the wing imaginal disk, JNK activity during the competitive elimination of *Rab5* mutant cells depresses WNT/Wg signalling which in turn stimulates proliferation (Ballesteros-Arias et al., 2014). Whereas during *Minute$^{+/-}$* competition in the adult midgut, JNK signalling increases expression of the JAK-STAT ligand Unpaired-3 in loser cells. The secreted Unpaired-3 binds to its receptor Dome on neighbouring wild-type cells and stimulates their proliferation by upregulating JAK-STAT signalling (Kolahgar et al., 2015).

5.2 <u>Results</u>

5.2.1 <u>ROCK inhibitor does not alleviate suppressed growth phenotype</u>

The ROCK inhibitor Y-27632 has previously been shown to restrict the elimination of loser cells during mechanical competition as well as relieve the selection mechanisms present during post-plating (Watanabe et al., 2007, Barbaric et al., 2014, Wagstaff et al., 2016). I therefore decided to test whether the continual presence of Y-27632 in the culture media was able to rescue the elimination of normal hPSCs from co-culture with supervariant hPSCs. Interestingly, I observed that Y-27632 had little effect on the growth of normal and supervariant hPSCs in both separate and co-culture. Lower numbers of normal hPSCs in co-culture were counted from Day 2 whilst growth of supervariant hPSCs remained unaffected (Figure 5.1A-B). Comparison of separate and co-cultures with and without Y-27632 revealed that ROCK inhibitor did not alter the of the ratio of supervariant to normal hPSCs on any day over the culture period (Figure 5.1C-D). This suggests that Y-27632 does not provide additional support for cell growth passed its dissociation-induced apoptosis protection. Neither is it capable of rescuing the elimination of normal hPSCs by supervariant hPSCs.

Figure 5.1 ROCK inhibition does not restrict competitive behaviour of supervariant hPSCs.

(A) Growth curves of normal and supervariant hPSCs grown separately (left) and in co-culture (right) in the presence of 10μM Y-27632. **(B)** Ratio of supervariant hPSCs to normal hPSCs grown in separate culture with and without 10μM Y-27632. Ratio of supervariant hPSCs to normal hPSCs grown in **(C)** separate culture and **(D)** co-culture with and without 10μM Y-27632. A minimum of three independent experiments were performed and the average ±SEM was plotted. n.s; Students t-test.
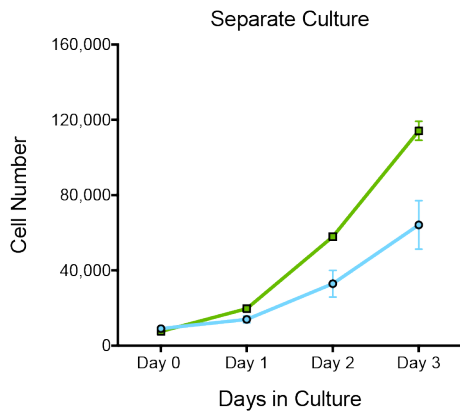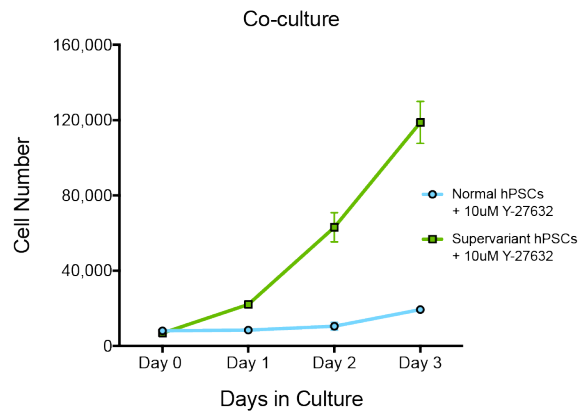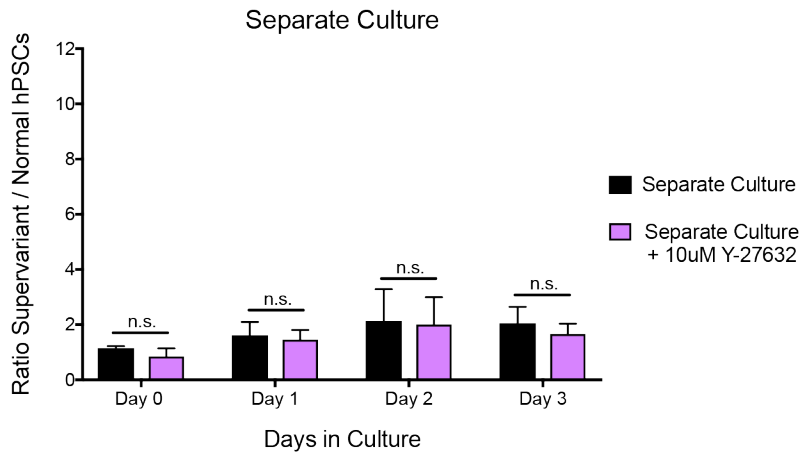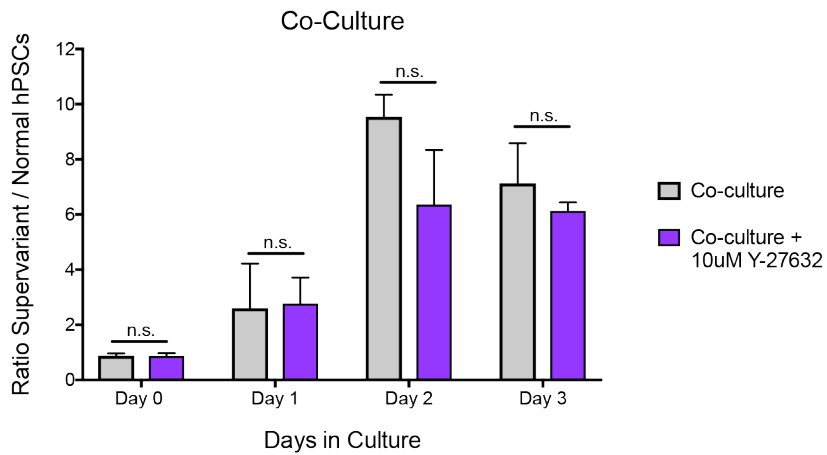
5.2.2 Inhibition of p53 does not alleviate suppressed growth phenotype

In mechanical competition p53 has been described as the molecular mechanism that functions downstream of ROCK and mediates loser cell elimination (Wagstaff et al., 2016). Though inhibition of ROCK did not rescue the competitive phenotype in my cultures, is it possible that mechanical stress is detected by other mechanotransducers and cell fate is coordinated by the same molecular mechanism. Therefore, I decided to investigate whether p53 could be involved in the competitive elimination of normal hPSCs. Firstly, I assessed the levels of p53 in separate and co-cultures of normal and supervariant cells. Immunofluorescent analysis shows normal hPSCs in co-culture have higher levels of p53 than cells grown in separate culture (Figure 5.2A). In contrast, the levels of p53 in supervariant cells were unaffected by co-culture (Figure 5.2B). Next, I treated separate and co-cultures with Pifithrin-μ, a p53 inhibitor that has previously been shown to improve the survival of hPSCs (Qin et al., 2007). Similar to my observations with Y-27632, I saw that pifithrin-μ had no discernible effect on the growth of normal and supervariant cells in separate or co-culture. In co-culture, the number of normal cells were lower than those counted in separate culture, whereas the number of supervariant cells were unaffected (Figure 5.2C-D). Analysis of the ratio of supervariant:normal hPSCs confirmed that treatment with pifithrin-μ did not affect the growth of normal and supervariant cells in separate culture (Figure 5.2E). Furthermore, pifithrin-μ was unable to rescue the elimination of normal cells in co-culture with supervariant hPSCs (Figure 5.2F). Collectively, this data suggests that p53 is not the molecular mechanism that mediates elimination of normal cells during cell competition.

Figure 5.2 Pifithrin-μ does not restrict competitive behaviour of supervariant hPSCs.

Quantification of p53 staining of **(A)** normal hPSCs and **(B)** supervariant hPSCs grown in either separate or co-culture. Red bars = mean $\pm$SD, [***] p<0.0002, Students t-test **(C)** Growth curves of normal and supervariant hPSCs grown separately (left) and in co-culture (right) in the presence of 10μM pifithrin-μ. **(D)** Ratio of supervariant hPSCs to normal hPSCs grown in separate culture with and without 10μM pifithrin-μ. Ratio of supervariant hPSCs to normal hPSCs grown in **(E)** separate culture and **(F)** co-culture with and without 10μM pifithrin-μ. Result of 3 wells from the same experiment $\pm$SEM. n.s : Students t-test.

A — Normal hPSCs
B — Supervariant hPSCs
C — Separate culture
D — Co-culture
E — Separate Culture
F — Co-Culture
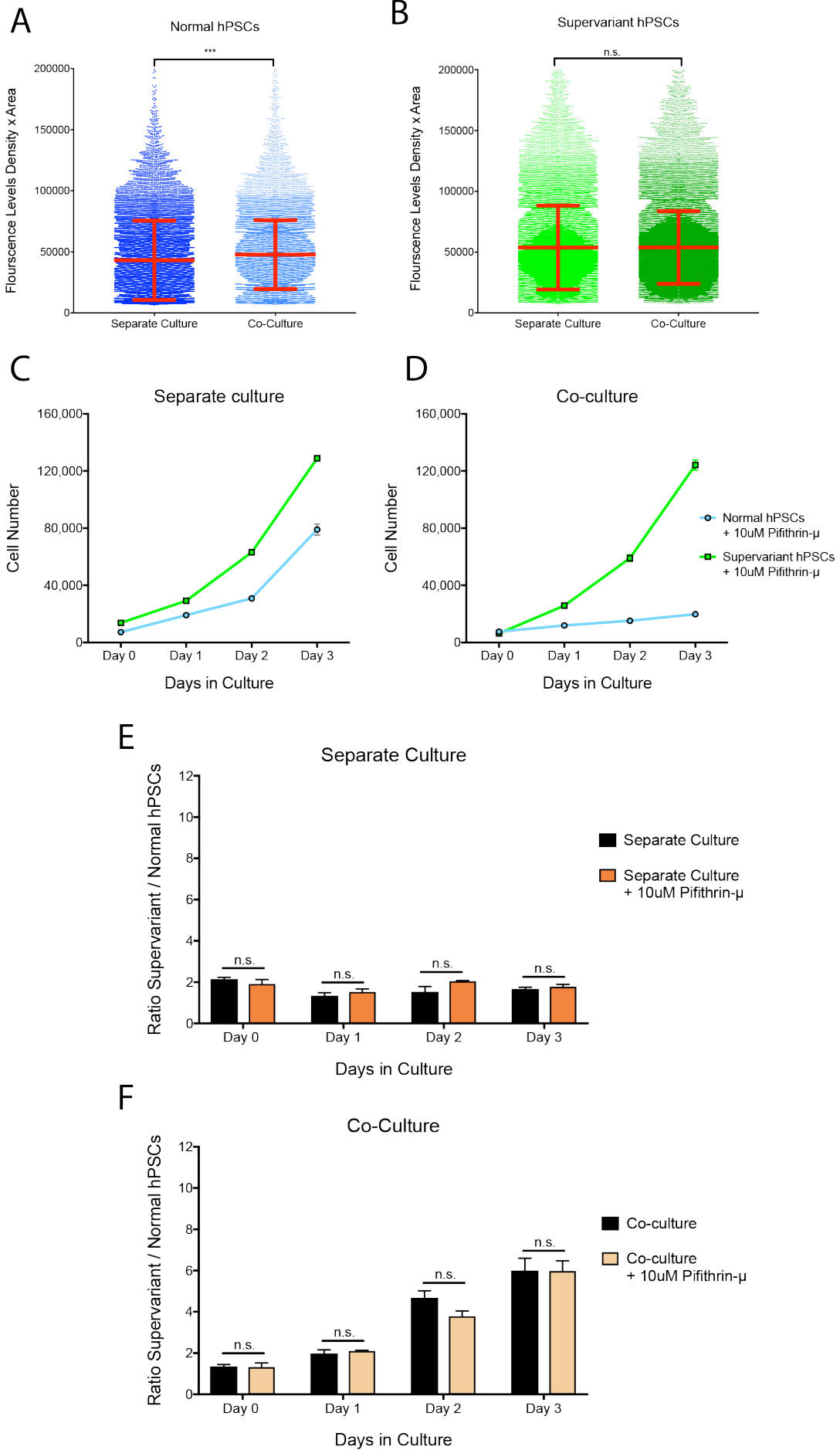
5.2.3   Treatment with Z-VAD-FMK does not alleviate suppressed growth phenotype

Having demonstrated that the mechanisms previously described in mechanical competition of MDCK cells do not appear to mediate the competitive phenotype in normal and supervariant hPSC cultures, I next decided to test if inhibition of caspase activity can rescue normal hPSC elimination. I have previously shown that the levels of cleaved caspase-3 are increased in normal hPSCs in co-cultures (Figure 4.3D), therefore I treated separate and co-cultures continually with the pan-caspase inhibitor Z-VAD-FMK. Surprisingly, the addition of Z-VAD-FMK did not rescue the growth of normal cells in co-culture (Figure 5.3A-B). Further analysis of the ratio of supervariant:normal cells in separate and co-culture showed that normal cells were still eliminated from co-cultures from day 2 onwards (Figure5.3C-D).

Figure 5.3 Z-VAD-FMK does not rescue elimination of normal hPSCs.

(A) Growth curves of normal and supervariant hPSCs grown separately (left) and in co-culture (right) in the presence of 50μM Z-VAD-FMK. **(B)** Ratio of supervariant hPSCs to normal hPSCs grown in separate culture with and without 50μM Z-VAD-FMK. Ratio of supervariant hPSCs to normal hPSCs grown in **(C)** separate culture and **(D)** co-culture with and without 50μM Z-VAD-FMK. A minimum of three independent experiments were performed and the average ±SEM was plotted. n.s; Students t-test

A — Separate Culture

Cell Number vs Days in Culture (Day 0, Day 1, Day 2, Day 3)

Normal hPSCs + 50uM Z-VAD-FMK
Supervariant hPSCs + 50uM Z-VAD-FMK

B — Co-culture

Cell Number vs Days in Culture (Day 0, Day 1, Day 2, Day 3)

C — Separate Culture

Ratio Supervariant / Normal hPSCs vs Days in Culture

Separate Culture
Separate Culture + 50uM Z-VAD-FMK

n.s.

D — Co-culture

Ratio Supervariant / Normal hPSCs vs Days in Culture

Co-culture
Co-culture + 50uM Z-VAD-FMK

n.s.
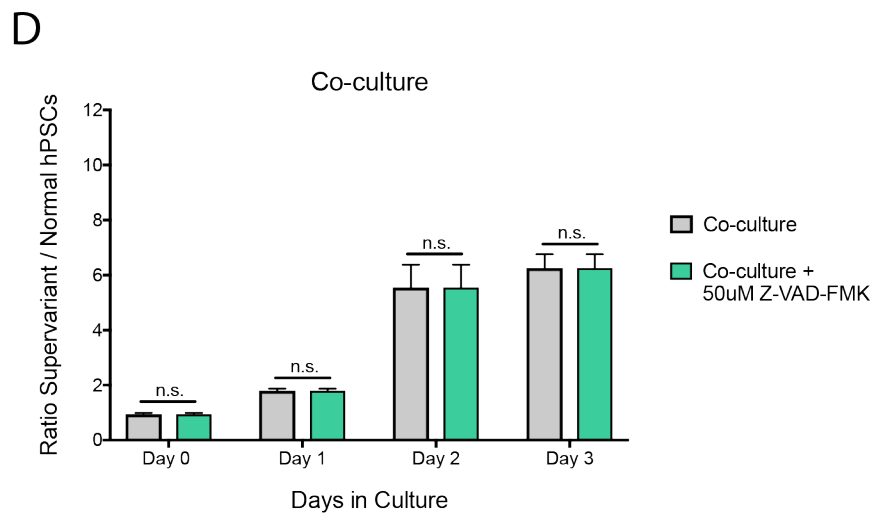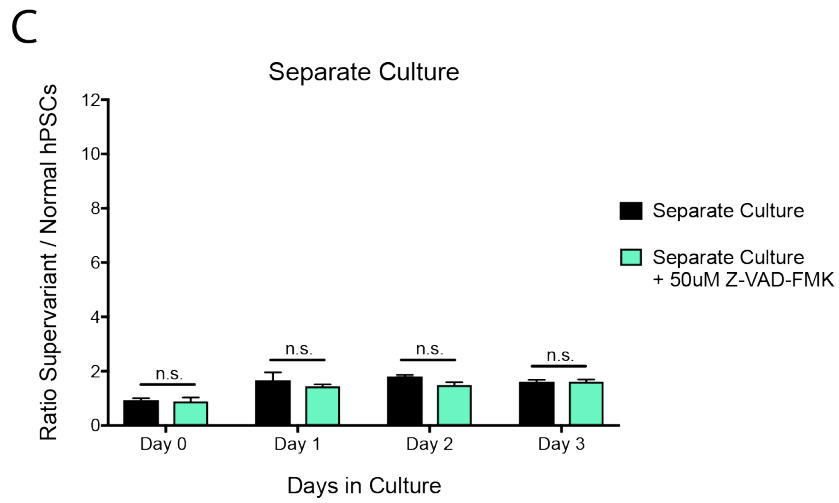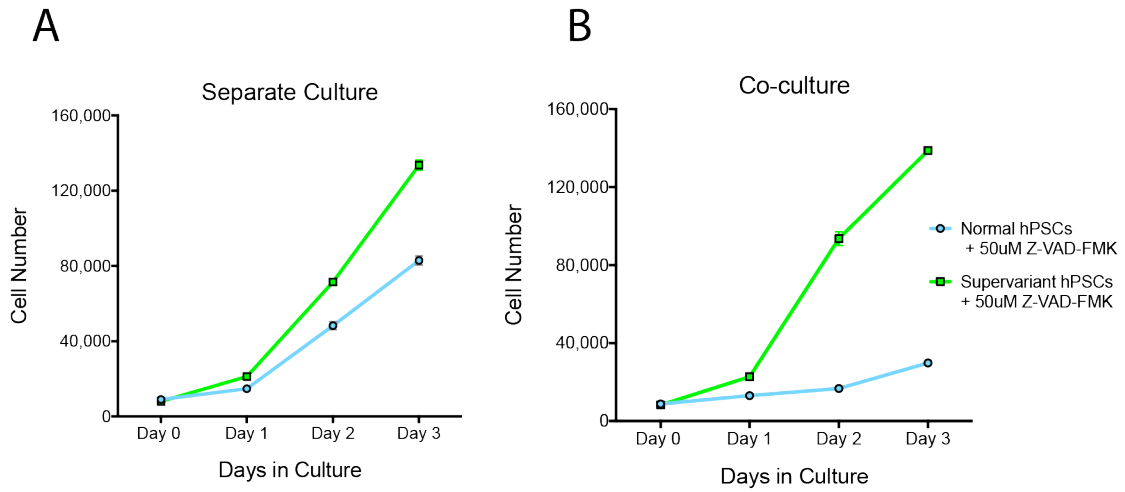
5.2.4   RNA sequencing of winner and loser cells in separate and co-culture

To identify genes and pathway that determine winner and loser status during competitive interactions within hPSC cultures I performed RNA sequencing on cells isolated from separate and co-cultures. I grew winner supervariant cells and loser 1q v.hPSCs separately or together in co-culture until Day 2 of the standard culture period. Winner and loser cells were re-isolated from co-culture by fluorescence-activated cell sorting (FACS) using the constitutively expressed GFP in supervariant hPSCs as the discriminator between the two populations (Figure 5.4A). Separate culture conditions were sorted to set the baseline and population gates for GFP positive and negative cells as well as to expose hPSCs grown in separate and co-culture to the same isolation conditions (Figure 5.4B). In co-culture conditions I observed that the percentage of winner hPSCs in the total population had increased to ~70%, this change in percentage of winner and loser cells was consistent with those observed in previous mixing experiments (Figure 4.5B) and strongly suggested loser cells were being competitively eliminated (Figure 5.4C). Cells from each population were isolated from four independent experiments and RNA sequencing data was obtained for each repeat, the transcriptome of the repeats for each population were pooled and analysed together.

Figure 5.4 Isolation of winner and loser hPSCs from separate and co-cultures.

(**A**) Schematic diagram of the strategy used to isolate winner and loser cells from separate and co-cultures for RNA sequencing. (**B**) Flow cytometry plots of winner and loser cells isolated from separate cultures (**C**) Flow cytometry plots of winner and loser cells in co-culture and the sorted populations isolated for RNA sequencing.

A

Loser hPSCs Winner hPSCs Co-culture

Cells grown in separate or co-culture to day 2

Winner and Loser hPSC populations re-isolated by FACS

RNA isolated and sequenced
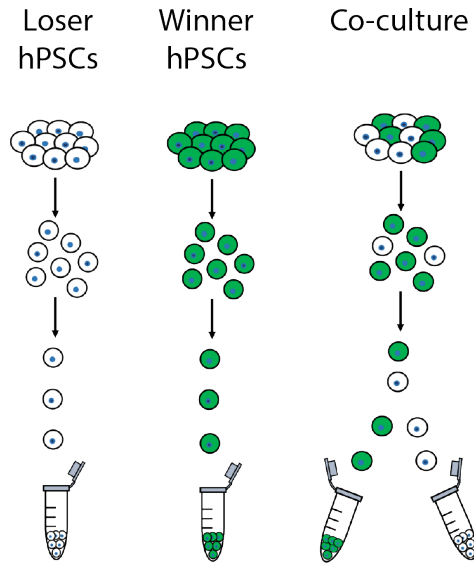
B

Loser hPSCs
Separate culture

Winner PSCs
Separate culture

99.9%

99.9%
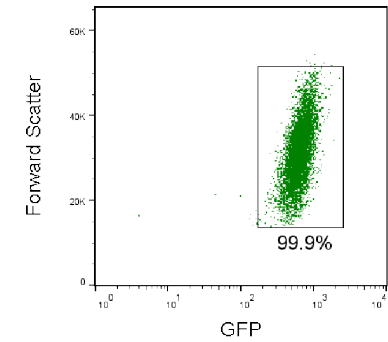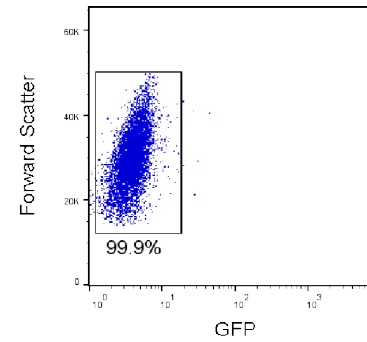
C

Co-culture

Loser hPSCs
Post Sort

Winner hPSCs
Post Sort

31.8 % 67.8 %

99.4 %

99.5%
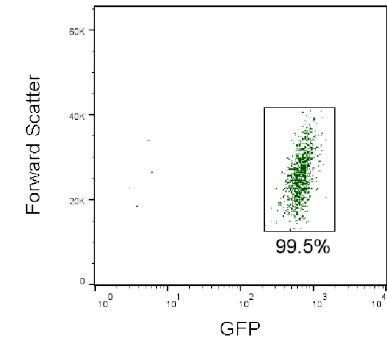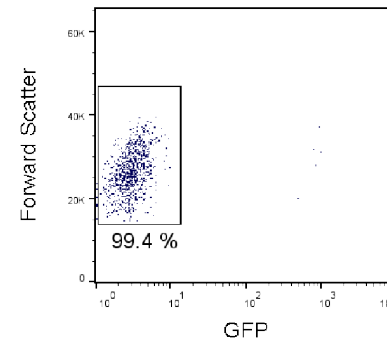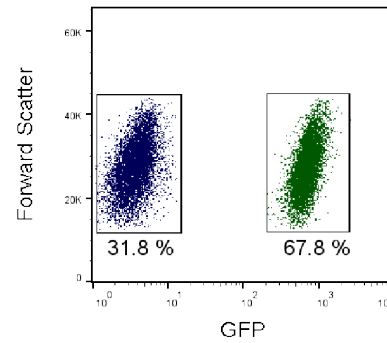
The genes from each sample were normalised to Fragments Per Kilobase per Million Reads (FPKM) and a threshold cut off value of >1 FPMK was applied to generate a list of significantly expressed genes for each population. The resulting gene lists were plotted into venn diagrams to examine the similarities and differences between winner or loser cells grown in separate or co-culture. Firstly, I assessed the presence and absence of gene expression between winner and loser cells grown in separate culture. This analysis showed that winner and loser cells share the majority of their significantly expressed genes; 13,187 (91.4%), however of the remaining genes, 826 (5.7%) were uniquely expressed by winner cells and 409 (2.9%) genes were uniquely expressed by loser cells in separate culture (Figure 5.5A). Next, I assessed differential gene expression between winner cells and loser cells in separate culture by direct comparison and applied a threshold of >1.3 Log_{10} adjusted p-value. In total, 3524 gene were significantly upregulated in winner cells, whereas 3311 genes were significantly downregulated in winner hPSCs compared to loser cells. I subjected the lists of differentially expressed genes that were either up-regulated or down-regulated to GO enrichment analysis and refined the resulting terms using reviGO. Gene ontology analysis showed no enriched terms from the list of upregulated genes. In contrast, the GO analysis on the list of down regulated genes highlighted key biological terms related to metabolic processes and gene expression (Figure 5.5C). To investigate the molecular pathways the differentially expressed genes represent, Kyoto Encyclopedia of Genes and Genomes (KEGG) enrichment analysis was performed (Kanehisa et al., 2010). A threshold of >0.25 corrected p-value was applied to the analysis and the resulting pathways plotted (Figure 5.5D). The most significantly enriched molecular network from the downregulated genes was the ribosomal pathway potentially indicating a change in either the rate or control of translation. The next three most significantly enriched molecular pathways in the downregulated genes were the cell cycle, TGF-β and Hippo pathway, all of these molecular pathways are associated with proliferation in hPSCs and may reflect the previously demonstrated differences in growth rate of winner and loser cells (Figure 5.5D).

Following the analysis of winner and loser cells grown in separate culture, I next performed the same set of analyses comparing winner and loser cells grown in co-culture. Assessment of the number of significantly expressed genes showed that comparable to the separate culture analysis winner and loser cells predominantly express the same genes, 13,558 (93.4%) (Figure 5.6A). Of the genes expressed exclusively by one of the populations, 466 (3.2%) genes were uniquely expressed in winner cells and 497 (3.4%) genes were uniquely expressed by loser cells. Differential gene expression analysis revealed that 2326 genes were upregulated and 1944 genes were downregulated in winner cells grow in co-culture compared to loser hPSCs (Figure5.6B). GO enrichment of the upregulated genes correlates with biological processes associated with cellular transport and localisation (Figure 5.6C), however KEGG analysis showed that no specific molecular pathway was associated with the upregulated genes. Assessment of the downregulated genes using GO analysis showed genes were associated with regulation of DNA transcription, cell adhesion and metabolism. KEGG analysis revealed that the most significantly downregulated molecular pathway was the Hippo signalling pathway. In addition, molecular pathways involved in cell adhesion as well as development of specific cell types were reported (Figure 5.6D).

A

Winner Separate   Loser Separate

826   13187   409

B

Winner Sep. vs Loser Sep.

$-\log_{10}(padj)$

Up regulated:
3524

Down regulated:
3311

$\log_2(\text{fold change})$

C

Gene Ontology Terms

biological adhesion
macromolecule metabolic process
anion transmembrane transport
macromolecule modification
organic acid transmembrane transport
RNA modification
cellular macromolecule metabolic process
metabolic process
primary metabolic process
organic substance metabolic process
nitrogen compound metabolic process
cellular metabolic process
gene expression
biosynthetic process
cellular nitrogen compound metabolic process
homophilic cell adhesion via
plasma membrane adhesion molecules
organic cyclic compound biosynthetic process
regulation of gene expression
aromatic compound biosynthetic process
heterocycle metabolic process
cellular aromatic compound metabolic process
organic cyclic compound metabolic process

Log10(p-value)

D

KEGG Pathway

Steroid biosynthesis
Ribosome biogenesis in eukaryotes
Oocyte Meiosis
RNA transport
Hippo
TGF-beta
Cell Cycle
Ribosome

Log10(p-value)

189

Figure 5.5 Gene expression analysis of winner and loser cells grown in separate cultures.

(A) Venn diagram of the significantly expressed genes present within either winner hPSCs and/or loser hPSCs isolated from separate culture conditions with a FPKM >1. Each circle represents the total number of genes present within a population, overlapping regions correspond to genes that are shared by both cell populations. **(B)** Volcano plot of the differentially expressed genes between winner hPSCs and loser hPSCs in separate culture, downregulated gene (green) are positioned on the left of the plot and upregulated gene (red) are on the right of the plot. **(C)** Gene Ontology enrichment analysis of genes downregulated in winner cells compared to loser cells in separate culture. Analysis of the upregulated genes produced no overrepresented terms. **(D)** KEGG pathway analysis of the downregulated genes showing the molecular pathways with a corrected p-value >0.25 threshold.
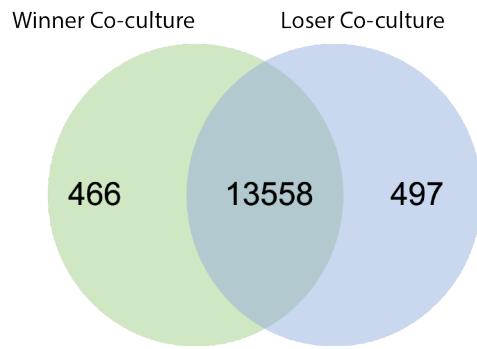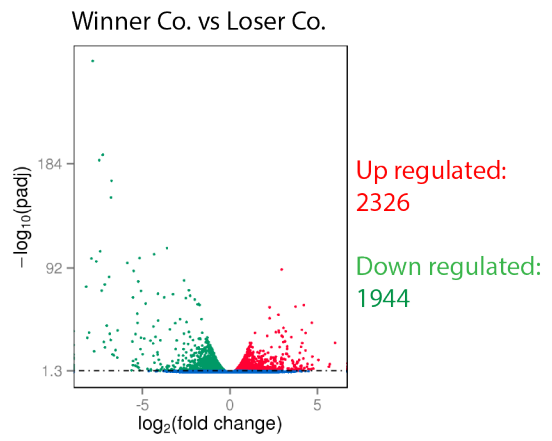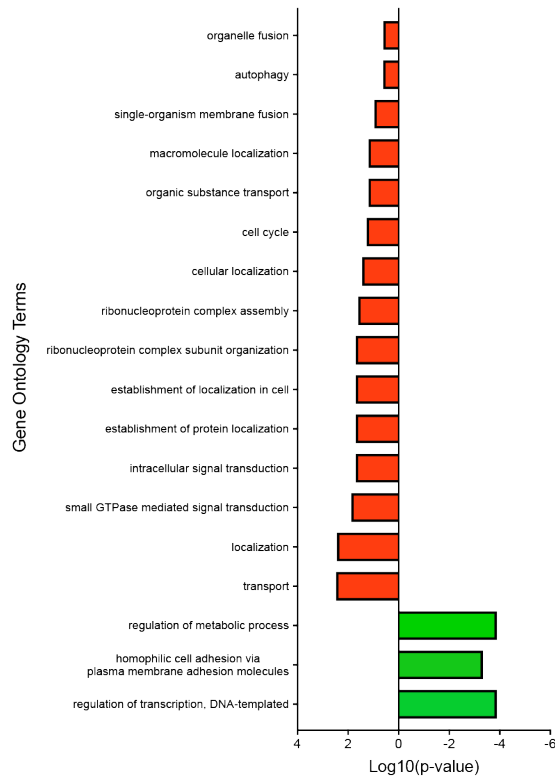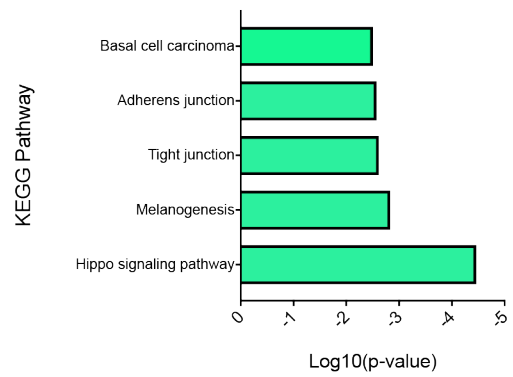
Figure 5.6 Gene expression analysis of winner and loser cells grown in co-culture.

(A) Venn diagram of the significantly expressed genes present within either winner hPSCs and/or loser hPSCs isolated from co-cultures with a FPKM >1. Each circle represents the total number of genes present within a population, overlapping regions correspond to genes that are shared by both cell populations. **(B)** Volcano plot of the differentially expressed genes between winner hPSCs and loser hPSCs in co-culture, downregulated gene (green) are positioned on the left of the plot and upregulated gene (red) are on the right of the plot. **(C)** Gene Ontology enrichment analysis of genes upregulated genes (red) and downregulated genes (green) in winner cells compared to loser cells from co-cultures. **(D)** KEGG pathway analysis of the downregulated genes showing the molecular pathways with a corrected p-value >0.25 threshold. Analysis of the upregulated genes produced no overrepresented terms above the significance threshold.

In the molecular pathway analysis between winner and loser cells, I observed the Hippo signalling pathway was significantly overrepresented in the downregulated genes from both separate and co-cultures. To investigate this observation further I compiled the lists of genes from the KEGG analysis that were associated with Hippo pathway signalling in both separate and co-culture analyses. Utilising the FPKM values from the expression level analysis I performed hierarchical clustering on the Hippo signalling pathway gene list using the samples of winner and loser cells grown in both separate and co-culture (Figure 5.7). Hierarchical clustering segregated the samples in two main clusters. The first cluster contained all the loser hPSC samples, cells in these samples had predominantly high expression of Hippo signalling associated genes including *YAP1* and *TEAD3* that are major transcriptional effectors of the signalling pathway. The second cluster contained the winner hPSC samples, winner cells isolated from both separate and co-culture displayed lower expression of all Hippo signalling associated genes (Figure 5.7).

Figure 5.7 Heatmap analysis of Hippo signalling pathway associated genes.

Heatmap of the differentially expressed genes associated with the Hippo signalling that were identified in KEGG analysis. Heatmap colour scaling was done after mean centring the genes from all winner and loser hPSC populations and hierarchical clustering was based on the entire gene set. Repeats of each population from the four independent experiments are denoted by name of the cell line followed by r1, r2, r3 or r4 respectively. Overall the data clustered into 2 main subsets, cluster one predominantly contained the loser hPSCs grown in either separate or co-culture. The second cluster consisted of winner hPSCs grown in separate or co-culture.
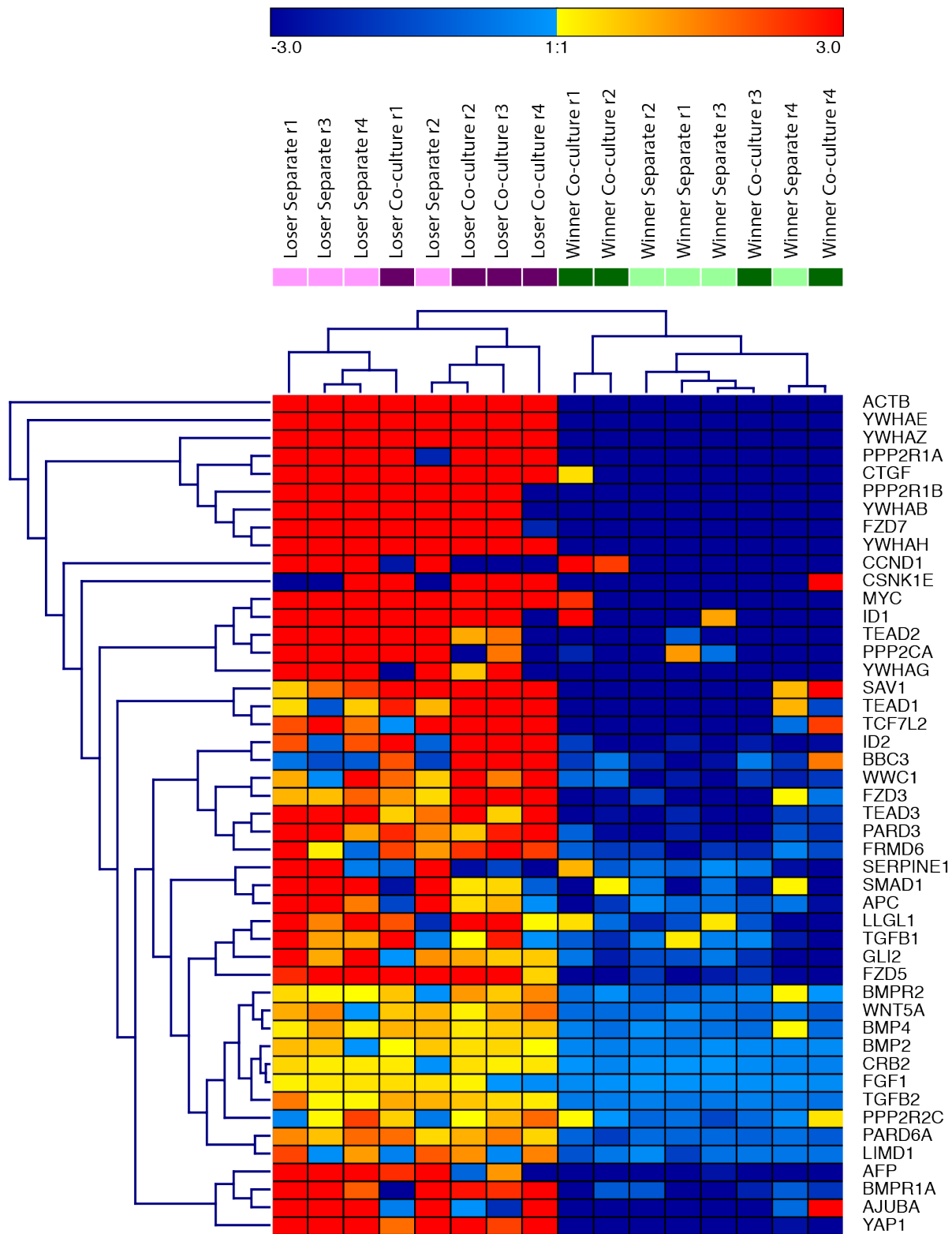
Next, I wanted to investigate how the gene expression of each cell line changes between separate and co-culture to potentially identify genes or molecular pathway that are altered during competition. Firstly, I assessed the differences between winner cells by comparing the number of significantly expressed genes. Winner cells in separate and co-culture share 97% (13,805) of their expressed genes, the remaining genes are split nearly evenly with 219 genes (1.5%) uniquely expressed in co-culture and 208 (1.5%) uniquely expressed in separate culture (Figure 5.8A). However, analysis of the differentially expressed genes from winner hPSCs populations by direct comparison of separate and co-culture conditions revealed that no genes were significantly downregulated in co-culture conditions. Furthermore, only 5 genes were differentially upregulated above the significance threshold of >1.3 Log_{10} adjusted p-value (Figure 5.8B). Further analysis of these few upregulated genes revealed they had varied function and their Log_{10} adjusted p-value was just above the >1.3 threshold applied, but also fell below a threshold of >2 demonstrating the genes were upregulated to a low level of significance (Figure 5.8C). Overall the pattern of gene expression in winner hPSCs is relatively unaltered suggesting that supervariant cells are unaffected by co-culture. This allowed me to focus on genes that are differentially expressed uniquely between loser hPSCs in separate and co-culture.

In loser hPSCs, hPSCs grown in separate and co-culture share the majority of their significantly expressed gene; 13,392 (94.0%). Of the remaining genes, 663 genes (4.6%) were uniquely expressed in co-culture and 204 (1.4%) were uniquely expressed by loser cells grown in separate culture (Figure 5.9A). I then compiled the significantly expressed gene analysis from each of the samples into a single Venn diagram to assess the distribution of gene expression across all the populations (Figure 5.9B). By this analysis, I observed that each of the populations uniquely expresses a set of genes, however this is a small percentage of the total number of genes expressed; approximately between 0.7% - 1.2% respectively. All samples share the majority of their genes expressed, approximately 88.4% of the total number of genes. Therefore, I performed differential gene expression analysis between loser cells grown in co-culture and loser cells grown in separate culture, the differential gene expression for all analyses was then plotted into a venn diagram to assess the distribution (Figure 5.9C). The greatest number of uniquely differentially expressed gene was observed in the comparison of winner and loser cells grown in separate culture.

A

Winner Co-culture   Winner Separate

219   13805   208

B

Winner Co. vs Winner Sep.

$-\log_{10}$(padj)

log$_2$(fold change)

Up regulated:
5

Down regulated:
0

C

Gene Name	-Log10(padj)	Description
FOSB	-1.456	FBJ murine osteosarcoma viral oncogene homolog B
JUND	-1.734	jun D proto-oncogene
PLK2	-1.734	polo-like kinase 2
PHLDA3	-1.734	pleckstrin homology-like domain, family A, member 3
AC004057.1	-1.734	pseudogene

Figure 5.8 Gene expression analysis of winner cells grown in either separate or co-culture.

(A) Venn diagram of the significantly expressed genes present within winner hPSCs isolated from either separate cultures or co-cultures with a FPKM >1. Each circle represents the total number of genes present within a population, overlapping regions correspond to genes that are shared by both cell populations. **(B)** Volcano plot of the differentially expressed genes between winner hPSCs and loser hPSCs in co-culture, downregulated gene (green) are positioned on the left of the plot and upregulated gene (red) are on the right of the plot. **(C)** Table of the differentially expressed genes downregulated between winner cells in isolated from co-culture compared to separate culture.

However, of the total number of differentially expressed genes within the comparison of winner and loser cells in separate culture 47.8% of the genes are also differentially expressed when comparing winner and loser cells in co-culture. This data supports the earlier observations that there are significant differences between winner and loser cells that occur independent of the culture conditions and could be responsible for the different growth properties of the two cell lines. The population with the second highest number of uniquely differentially expressed genes was comparison of loser cells in co-culture and separate culture. In contrast, there were no differentially expressed genes uniquely found in the comparison between winner cells in co-culture and winner cells in separate culture (Figure 5.9C). Cluster analysis of the differentially expressed genes further highlights the similarities between winner cells and differences in loser cells that are grown in separate or co-cultures (Figure 5.9D). These observations support the earlier conclusions that loser cells are affected by co-culture with winner cells whereas winner cells are unaffected by the presence of losers in heterotypic cultures. Next, I wanted to investigate the genes and molecular pathways that are different between loser cells in co-culture and separate that could determine loser cell fate during competition. I subjected the lists of differentially expressed genes that were either up-regulated or down-regulated in co-culture to GO enrichment analysis and refined the resulting terms using reviGO (Figure 5.9E). Gene Ontology enrichment analysis on the genes upregulated upon co-culture highlighted processes involved in cell growth as the top functionally enriched pathways. Interestingly, amongst these processes the MAPK cascade was the only signalling pathway enriched suggesting components of this pathway may play a key role in conferring loser status (Figure 5.9F). Whereas, analysis of genes downregulated in co-culture highlighted a cluster of terms associated with DNA synthesis and integrity as well as other groups associated with cell communication and signal transduction (Figure 5.9G).

A

Loser Co-culture   Loser Separate

663   13392   204

B

Loser Separate   Winner Separate   Winner Co-culture   Loser Co-culture

102   104
15   298   66
125   57   394   171
13056
7   32
42   59
235

C
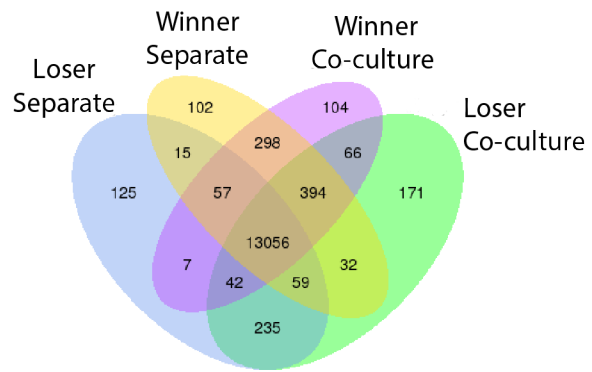
Samples	Nº DEG
A. Loser Co. vs Loser Sep.	4,146
B. Winner Sep. vs Loser Sep.	6,835
C. Winner Co. vs Loser Co.	4,270
D. Winner Co. vs Winner Sep.	5

A.   B.   C.   D.

1850   613
1714   2539   1
1313   729   0   0
388   0   1   2
0   1
1

D

Cluster Analysis of Differentially Expressed Genes

Winner Separate culture

Winner Co-culture

Loser Separate culture

Loser Co-culture

-1   -0.5   0   0.5   1

F

RNA metabolism
translation
cell growth
MAPK cascade
regulation of biological process
cell differentiation
intracellular signal transduction

semantic space Y
semantic space X

log10 p-value

E

Loser Co. vs Loser Sep.

$-\log_{10}(\text{padj})$

$\log_2(\text{fold change})$

Up in
Co-culture

Down in
Co-culture

G

response to external stimulus
intracellular signal transduction
cell-cell signaling
rRNA metabolism
regulation of molecular function
DNA replication
chromatin organization
nuclear transport

semantic space Y
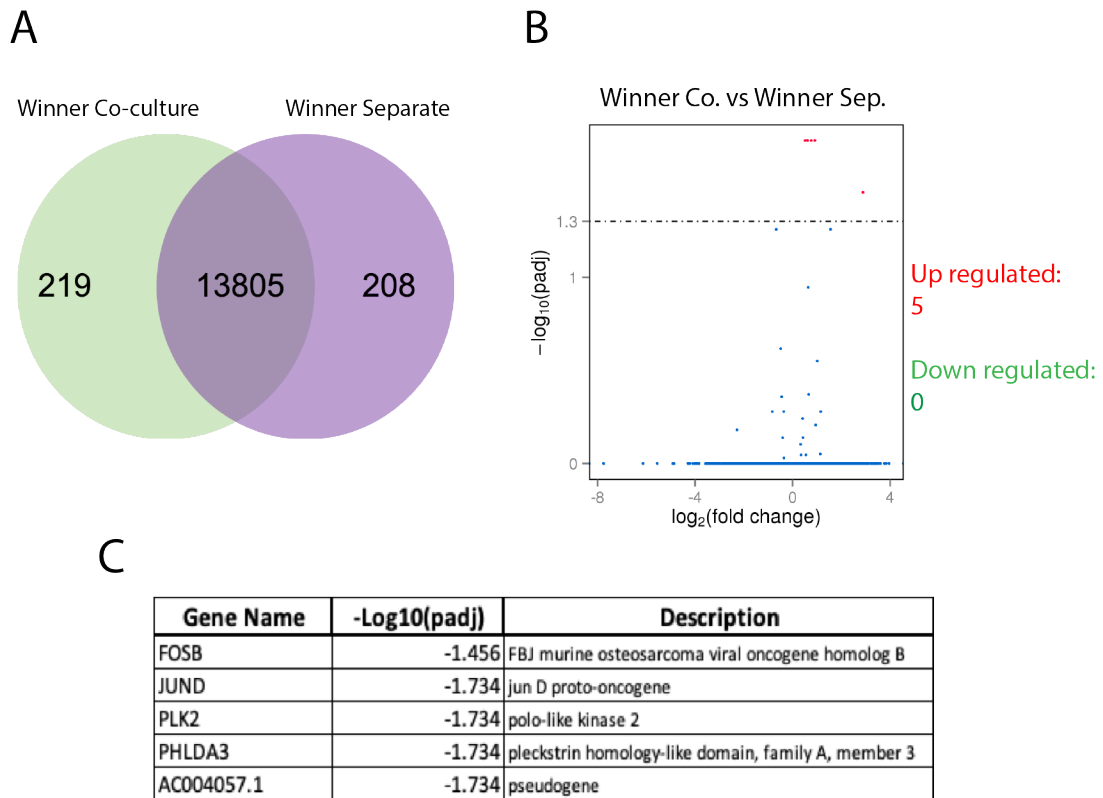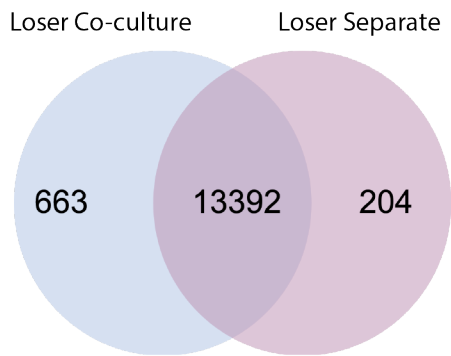semantic space X

log10 p-value
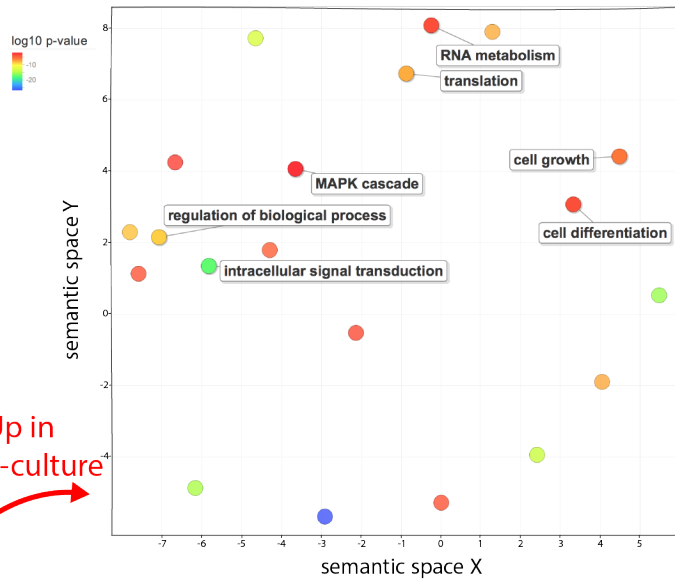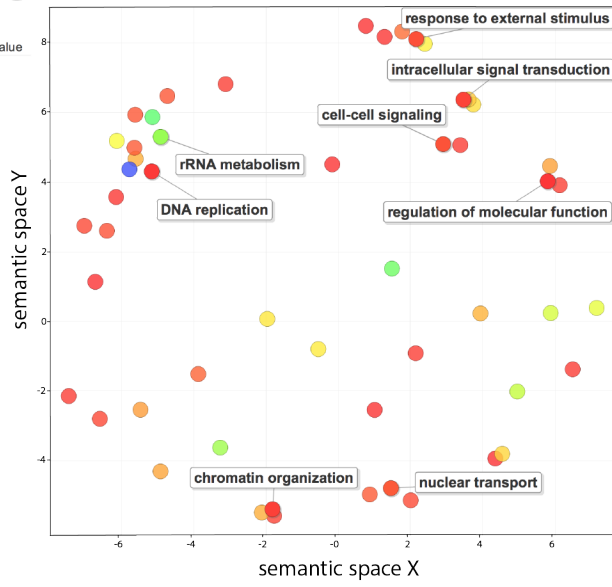
Figure 5.9 Gene expression analysis of loser cells grown in either separate or co-culture.

(A) Venn diagram of the significantly expressed genes present within loser hPSCs isolated from either separate cultures or co-cultures with a FPKM >1. **(B)** Venn diagram showing the significantly expressed genes present within winner and loser cells isolated from either separate cultures or co-culture. **(C)** Venn diagram of the differentially expressed genes present within different comparisons of winner and loser cells that have been isolated from either separate cultures or co-cultures. For all venn diagrams, each circle represents the total number of genes present within a population, overlapping regions correspond to genes that are shared by different populations. **(D)** Unsupervised hierarchical clustering of the winner and loser cells from separate and co-culture based on the differentially expressed genes. **(E)** Volcano plot of the differentially expressed genes between loser hPSCs in separate culture and co-culture, downregulated gene (green) are positioned on the left of the plot and upregulated gene (red) are on the right of the plot. Gene Ontology enrichment analysis of genes **(F)** upregulated in loser hPSCs upon co-culture, and **(G)** downregulated in loser hPSCs in co-coculture with winner hPSCs. Terms are positioned in semantic space by ReviGO based on the correlation between biological processes. Terms are coloured based on their Log10 p-value, higher p-values (red) and lower p-values (blue).

To further investigate how genes of the MAPK pathway are differentially expressed in winner and loser cells during separate and co-culture, I utilised the list of MAPK genes from the GO enrichment analysis and gene expression data to perform hierarchical clustering (Figure 5.10). The data segregated in two main clusters, the first cluster contained the samples isolated from co-culture whilst the second cluster contained the separate culture samples. Within the cluster containing winner and loser cells isolated from co-culture most of the genes associated with the MAPK pathway were highly expressed to a similar degree. In contrast, within the second cluster winner cells from separate cultures show higher expression of MAPK associated genes than loser cells from separate cultures. Winner cells in separate culture showed high expression of some MAPK associated genes, however more genes were highly expressed in the co-culture condition. Overall, loser cells from separate culture showed the lowest expression levels of all the winner and loser cell samples. Of note, the gene *FOS* was uniquely expressed to a high level in the winner and loser cells isolated from co-culture. *FOS* is a component of the transcription factor activator protein 1 (AP-1) complex that regulates gene expression in response to stimuli processed by the MAPK pathway (Figure 5.10). Collectively, this data indicates that the MAPK might be involved in processing the competitive signals present within heterotypic cultures of winner and loser hPSCs.

Figure 5.10 Heatmap analysis of MAPK pathway associated genes.

Heatmap of the differentially expressed genes associated with the MAPK signalling that were identified in KEGG analysis. Heatmap colour scaling was done after mean centering the genes from all winner and loser hPSC populations and hierarchical clustering was based on the entire gene set. Repeats of each population from the four independent experiments are denoted by name of the cell line followed by r1, r2, r3 or r4 respectively. Overall the data clustered into 2 main subsets, cluster one predominantly contained winner and loser hPSCs grown in co-culture. The second cluster consisted of winner and loser hPSCs grown in separate culture.
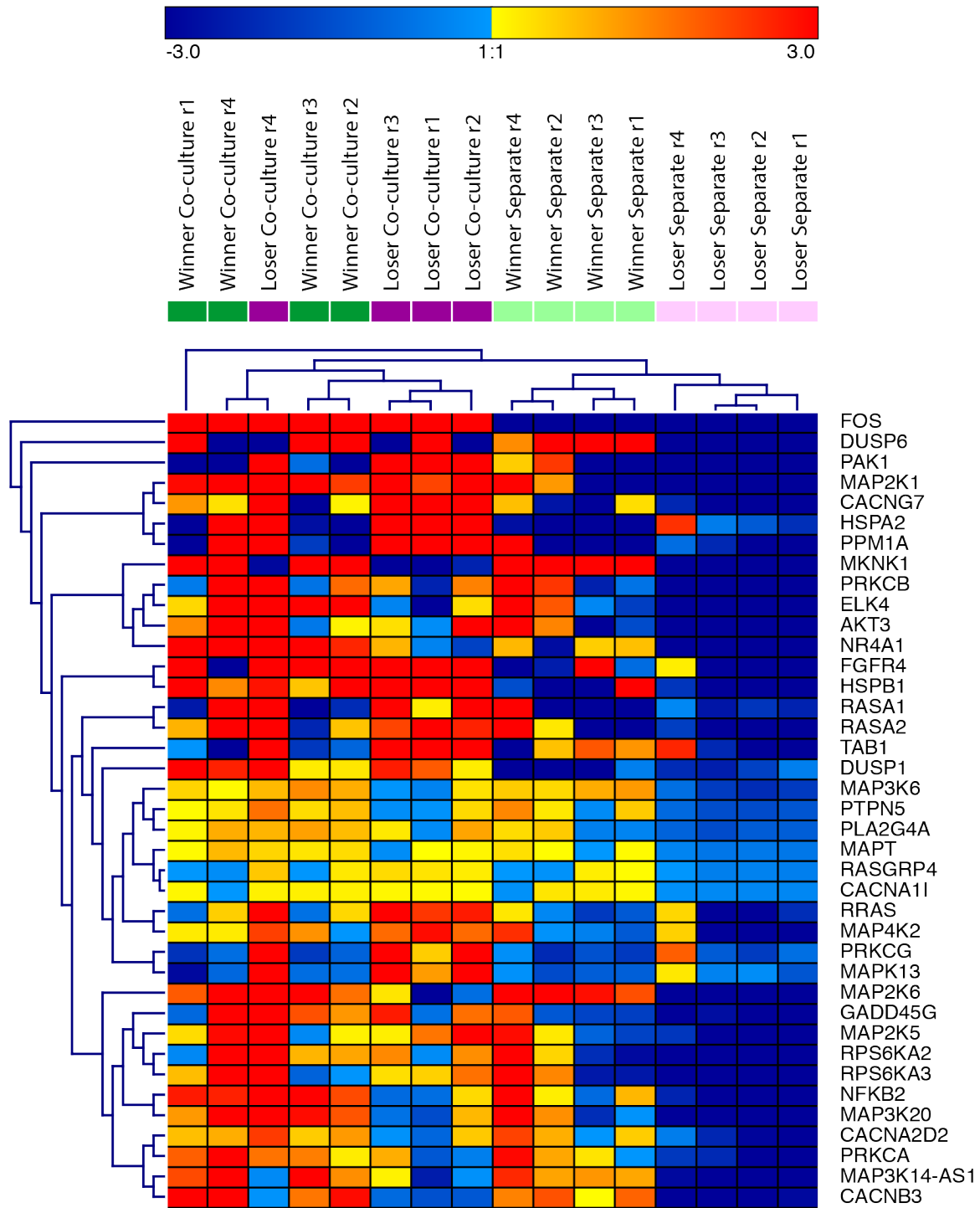
5.2.5 <u>Validation of candidate genes and pathways</u>

To validate the potential candidate genes identified from RNA sequencing I grew loser normal hPSCs and winner supervariant hPSCs in separate or co-culture and re-isolated cells using FACS at Day 2, equivalent to the stage cells were isolated for RNA sequencing. In addition, winner and loser cells were also grown separately at higher density as previously described (Figure 4.3) to control for the overall higher plating density of the co-culture condition. Whole cell lysate protein was harvested from the re-isolated winner and loser hPSC populations for analysis by Western blot.

The MAPK pathway is composed of four subfamilies that respond to a variety of extracellular signals received by a cell. Two of the subfamilies, JNK and p38, are activated by cellular stress and form a group that is referred to as the stress-activated MAPKs. I therefore assessed whether other components of the conventional stress-activated MAPKs are also activated.

The first candidate I assessed was JNK signalling, I observed that the level of JNK is relatively equal across winner and loser hPSCs in both separate and co-culture (Figure 5.11i), however the amount of phosphorylated JNK (p-JNK) is greater in winner cells than loser hPSCs (Figure 5.11ii). Furthermore, the levels of p-JNK in winner hPSCs is greatest in the co-culture condition. Loser hPSCs have relatively low levels of p-JNK that are difficult to detect and discern if there are differences between separate and co-culture (Figure 5.4ii). I then assessed the levels of c-Jun, a component of the AP-1 transcription factor complex, that is activated by JNK in response to cellular stress, enhancing its downstream transcriptional functions. I observed, that c-Jun protein expression was visibly less in normal loser cells grown in co-culture compared with those in co-culture. In contrast, winner cells grown in co-culture appeared to have higher levels of c-Jun compared to separate culture conditions. Overall from the separate cultures, loser cells displayed higher levels of protein expression than winner hPSCs at the corresponding density (Figure 5.11iii).

I next assessed the levels p38, the other stress-activated MAPK pathway. I observed that all winner and loser cell populations possess a similar level of p38 MAPK (Figure 5.11iv). However, the levels of the active phosphorylated form of p38 MAPK (p-p38 MAPK) was higher

in winner samples and didn't appear to be altered between separate and co-culture. In comparison p-p38 MAPK was hardly detected in loser cells but did appear to be increased upon co-culture (Figure 5.11v). Collectively these results indicate that the components of the MAPK pathway are differentially active between winner and loser cells and respond differently to the signalling cues received during co-culture.

Lastly, I compared the levels of two extensively characterised effectors of cell competition that have reported roles in mechanical competition and mammalian PSCs, c-myc and p53. Previously, analysis of immune fluorescence images suggested that p53 levels might be increased between loser cells in co-culture compared to separate culture (Figure 5.2A). Using western blot analysis, I observed that p53 levels are comparably low in all winner and loser cell populations, with the exception of a small increase in the winner high density condition (Figure 5.11vi). The level of c-myc from separate cultures were higher in loser hPSCs than winner hPSCs. In co-culture conditions, the levels of c-myc in loser cells was lower than separate culture controls, whereas there was no discernible difference between winner hPSC separate and co-culture conditions. Overall, levels of c-myc in co-cultures appeared to be slightly lower than those of winner hPSCs (Figure 5.11vii).
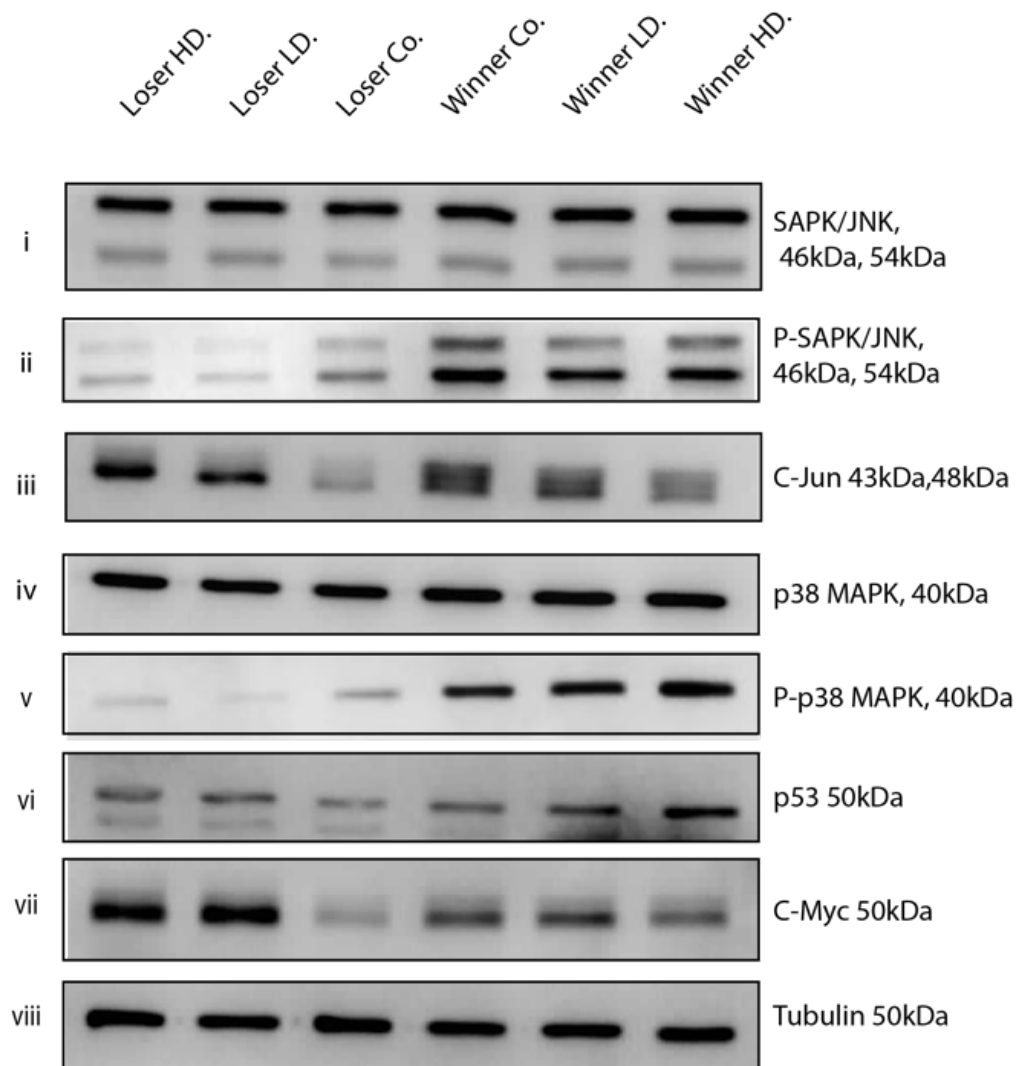
Figure 5.11 Validation of candidate genes.

Western blot analysis of candidate genes obtained from RNA sequencing analysis on winner and loser hPSCs isolated from cells grown in separate culture at either standard or high density as well as co-culture. Tubulin was used as a loading control.

5.3   Discussion

My previous work demonstrated how competitive interactions between supervariant winner hPSCs can restrict the growth of normal and other karyotypically abnormal hPSC lines that possess significantly lower growth rates. Competition between winner and loser cells was shown to be mediated through mechanical stress and modulated by the proportion of supervariant cells and overall cell density. To begin unravelling the mechanisms that determine winner and loser cell fate I first looked at the effect of prolonged ROCK inhibition, as this has previously been shown to inhibit mechanical competition in MDCK cells (Wagstaff et al., 2016). Furthermore, treating cells with the chemical inhibitor Y-27632 has also been shown to alleviate selection bottleneck in hPSCs and restrict the invasive properties of tumour cells (Barbaric et al., 2014, Sahai and Marshall, 2003). In contrast to these observations, my data indicates that continual ROCK inhibition does not rescue normal hPSC elimination, suggesting the involvement of alternative pathways that execute winner and loser cell fate.

I next investigated whether p53 signalling was involved in coordinating the elimination of normal hPSCs. P53 has previously been reported as the mechanisms that functions downstream of ROCK in mechanical competition of MDCK cells but is also a known downstream effector of competition in other forms of cell competition (Wagstaff et al., 2016, Di Gregorio et al., 2016). In my data, despite an indication by immunofluorescence that p53 levels could potentially be elevated in loser cells upon co-culture, by western blot the levels did not appear to change. Furthermore, inhibition of p53 using pifithrin-μ did not rescue normal hPSCs from elimination by supervariant hPSCs. Collectively this data suggests that p53 is probably not the downstream molecular mechanisms that determines cell fate during competition in hPSC cultures.

In addition, I decided to test the role of another gene that has been extensively described as a key component of competitive interactions. Previous studies have shown that c-myc can play critical roles in determining winner and loser cell fate during mammalian cell competition (Sancho et al., 2013, Claveria et al., 2013). In both competition and supercompetition involving c-myc future winner cells possess higher levels of c-myc than the loser population (de la Cova et al., 2004, Moreno and Basler, 2004). In contrast, my data showed that in

separate culture loser cells possess higher levels than winner hPSCs, however these levels decrease in co-culture with winner cells, whereas the levels of c-myc in winner cells appeared unaltered between separate and co-cultures. Additionally, in accordance with observations from previous studies, I observed higher levels of c-myc in the winner hPSCs co-culture conditions compared to loser cells. The difference in c-myc levels between cells in co-culture follows the trend from previous studies and could suggest a potential role as either an effector or marker of cell competition, however the high levels of c-myc in separate cultures of loser cells make it less likely it would function in exactly the same way as in *Drosophila* and other mammalian competitive systems. The limitation of these observations is that the differences in c-myc between future winner and loser cells cannot be measured between individual competing cells. My previous data has demonstrated that not all loser hPSCs will be undergoing competitive elimination, some loser cells can be found in microenvironments that support their survival (Figure 4.12A), in this state these cells could possess different levels of c-myc that support their survival. Diaz and colleagues, utilised time-lapse microscopy and live cell tracking of a fluorescent Myc fusion protein to show that two key factors, time in contact and proportion of contacts between cells of different Myc levels is what drives execution of winner and loser cell fate during Myc-driven competition in mouse ESCs (Diaz-Diaz et al., 2017). Future work, using a similar approach to assess how c-myc levels change in individual winner and loser cells during competitive interactions would assist in determining what role c-myc plays during cell competition in hPSC cultures. In conclusion, the difference in c-myc levels of winner and loser from separate cultures as well as the role of c-myc in competition of hPSCs remains unresolved.

Finally, recent studies have shown that treatment of mouse embryonic stem cells with Z-VAD-FMK can abolish the competitive elimination of loser cells during embryonic development (Sancho et al., 2013, Bowling et al., 2018). In my data, I previously showed that the levels of cleaved capase-3 were significantly higher in loser cells (Figure 4.3D), therefore I attempted to prevent the apoptosis of normal hPSCs by treating cells with the pan-caspase inhibitor Z-VAD-FMK. Surprisingly, addition of Z-VAD-FMK was insufficient to rescue normal hPSCs from elimination within co-culture. Of note, Z-VAD-FMK treatment has been reported to be insufficient in rescuing loser cells that show increased cleaved-capase-3 levels within

mechanical competition of *Scribble^kd* MDCK cells (Norman et al., 2012). One possible explanation is that Z-VAD-FMK-insensitive caspases are involved in the apoptosis of loser hPSCs (Chauvier et al., 2007). An alternative possibility is that inhibition of caspases subsequently induces cell death through alternative caspase-independent pathways ensuring loser cells are eliminated during competition (Tait et al., 2014, Broker et al., 2005).

I was unable to identify the molecular mechanism that determines winner and loser cell fate in hPSC cultures by screening different inhibitors to pathways previously reported in the literature of mechanical competition. Therefore, I used an unbiased RNA sequencing approach to investigate how the gene expression of winner and loser cells changes between separate and co-cultures. I firstly compared the transcriptome of winner and loser hPSCs to assess whether there is an underlying mechanism that confers the ability of winner cells to possess a higher homeostatic density. My analysis between winner and loser cells isolated from either separate or co-cultures revealed that the Hippo signalling pathway is downregulated in winner cells in both culture conditions. In contrast, loser cells display high activation of Hippo pathway associated genes in both separate and co-culture. The Hippo signalling pathway has significant functions in the regulation and control of cell growth, in particular how cells respond to cell contact inhibition during culture (Gumbiner and Kim, 2014). At low density the Hippo pathway is typically inactive, the transcriptional co-activators YAP and TAZ are localised in nucleus and promote cell growth. At high density, the activity of various upstream molecules mediates contact inhibition which results in the phosphorylation of YAP and its exclusion from the nucleus inhibiting cell growth (Gumbiner and Kim, 2014, Meng et al., 2016). The Hippo pathway is dysregulated in various forms of cancers, oncogenic cells do not respond to the environmental cues that normally activate Hippo signalling, instead aberrant activation of YAP/TAZ drives cell proliferation in cancer cells (Stein et al., 2015, Park et al., 2018). An intriguing hypothesis, that requires experimental validation, is that activation of the Hippo signalling pathway is dysregulated in winner hPSCs, this loss of contact-inhibition provides winner cells with the ability to proliferate at higher densities than loser hPSCs resulting in a higher homeostatic density.

Lastly, I compared the transcriptome of winner or loser cells that had either been grown in separate culture or in co-culture to investigate whether a specific molecular pathway is activated upon co-culture that could potentially regulate competitive cell fate. I found that the gene expression of winner cells is unaltered between separate and co-culture suggesting that they do not receive a specific signal that confers winner status. This observation is a possible explanation as to why the growth rate of supervariant hPSCs is unaltered in co-culture conditions and I do not observe compensatory proliferation of winner cells in a similar to manner to that which has been described in other competitive systems (Bowling et al., 2018, Di Gregorio et al., 2016). In conclusion, this data suggests that supervariant winner hPSCs are unaffected by co-culture with loser hPSCs and point to changes in loser hPSC gene expression as being a key determinant of competitive cell fate. I then went on to compare the transcriptome of loser hPSCs in separate culture and those grown in co-culture with winner hPSCs. This was done by firstly performing differential gene expression analysis and then using GO enrichment to identify key biological processes that had been altered between the two culture conditions. There was large scale downregulation of genes associated with cellular homeostatic functions including, DNA and RNA synthesis, DNA integrity and cell-cell signalling. Degradation of DNA is an integral component of apoptosis (Zhang and Xu, 2000) and therefore in this context reduction in the activity of pathways that maintain DNA homeostasis would not be unexpected in loser cells. I then looked at the biological processes over represented in the upregulated genes. My data showed that genes associated with cell growth process, in particular the MAPK signalling, were significantly upregulated. Using a western blot approach, I functionally validated if components of the MAPK pathway were altered between winner and loser cells that had been grown in either separate and co-culture.

The MAPK signalling cascade incorporates a diverse range of extracellular signals to coordinate a range of cellular responses that include cell proliferation and apoptosis (Sun et al., 2015). Furthermore, different elements of the MAPK pathway have been previously implicated in controlling cell fate during cell competition (Di Gregorio et al., 2016, Wagstaff et al., 2016). In my data I found that two signalling cascades of the MAPK pathway, JNK and p38, were differential active between winner and loser hSPCs. In general, I observed that the levels of phosphorylated JNK and p38 were higher in the winner cells from both separate and

co-culture than loser cells which correlated with the higher expression levels observed in the transcriptome analysis. Loser hPSCs typically showed low levels of active JNK and p38, that were elevated in co-culture conditions. A possible explanation for these observations is that during competition the high cell density causes elevation in mechanical tension which in turn increases cellular stress in normal loser hPSCs. The elevated cell stress stimulates JNK and p38 signalling in winner and loser cells which alters the activity of downstream transcription factors including c-jun, and ultimately effecting the expression of genes related to cell survival. The greater resistance to cell death described previously in winner cells may provide a growth advantage that permits their survival despite high levels of cellular stress.

Although I was not able to determine the molecular mechanisms that control cell competition in hPSCs. The data presented within this chapter provides evidence that particular molecular pathways are differentially active between winner and loser cells, as well between loser cells in separate and co-culture. These findings can provide a platform for future studies into how the Hippo signalling pathway is involved in controlling the homeostatic density of winner and loser cells as well as how signalling from the stress-activated MAPK pathways effects impacts the fate of future winner and loser cells during competition within hPSC cultures.

6 <u>Final Discussion</u>

Karyotypically abnormal cells arise during culture of hPSCs and are selected for over several passages, eventually overtaking normal hPSCs to become the predominant cell type within the culture population. The spectrum of karyotypic changes that occur is broad and encompasses every chromosome, however gains of whole or partial chromosomal regions occur more frequently in particular chromosomes. The acquisition of these genetic changes is thought to provide abnormal cells with a selective advantage over counterpart normal hPSCs. Though previous studies have described variant cells to possess improved growth phenotypes the mechanisms through which selection occurs have remained obscure.

In this body of work, I have begun to unravel the mechanisms through which genetically variant cells can exert their selective advantage. The data presented demonstrates that the mechanisms of selective advantage in hPSCS cultures can be categorised into two subgroups. Firstly, the intrinsic mechanisms that enhance growth of variant cells enabling them to passively overtake normal cultures. Secondly, extrinsic competitive cell-cell interactions that actively restrict growth of normal hPSCs.

6.1 <u>Intrinsic mechanisms of selective advantage</u>

The intrinsic mechanisms of selective advantage exert their affect by directly influencing the probability of variant cells to undergo one of the three potential fates presented to hPSCs in culture; self-renewal, differentiation or cell death. Through generating of a panel of clonal karyotypically abnormal cell lines containing individual or multiple genetic changes I was able to compare and contrast the effects different common karyotypic abnormalities have on hPSC fate. This analysis revealed that different genetic variants provide variant cells with different selective growth properties that may be exerted at different stages during culture. Amongst the individual karyotypic abnormalities tested, I found addition of the short arm of chromosome 17 was the abnormality that provided variant cells with the greatest proliferative advantage. Upon further investigation the underlying mechanism was shown to be a combination of decreased rate of apoptosis and potentially reduced cell cycle time which was not observed in the other individual variant hPSC lines. In a 2D culture system where cells

are passaged based on when they reach a particular level of confluency (~80%), an increased rate of proliferation would provide a strong selective advantage by causing the culture population to reach passage confluency faster. This reduces the time available for the normal hPSC population to expand, increasing the proportion of variant cells within the culture population and reducing the number of normal hPSCs that are carried forward into the subsequent passage. Over subsequent passages this mechanism of selection would serially dilute the proportion of normal hPSCs within the population until the cultures consisted of predominantly variant cells.

In the case of the other variant lines containing a single karyotypic change, 1q v.hPSC and 20q v.hPSC, I have demonstrated that their mechanism of selective advantage is most likely exerted by solely restricting cell death. Overexpression the anti-apoptotic gene *BCL-XL* encoded within the amplified region of chromosome 20 has previously been shown to drive selective advantage of variant cells with gain of the CNV 20q11.21 (Avery et al., 2013). In my data I also observe overexpression of BCL-XL in cells with gain of 20q11.21, furthermore these cells show reduced levels of apoptosis during culture that is ablated upon chemical inhibition of BCL-XL. A potential candidate for driving apoptotic resistance in 1q v.hPSCs is the gene, *MCL1,* which belongs to the same family of anti-apoptotic genes as BCL-XL (Rinkenberger et al., 2000). My data from 1q v.hPSCs show they have increased levels of *MCL1* and their selective advantage is most likely related to an increase in apoptotic resistance. Collectively these findings indicate that in some variant cells, that possess different karyotypic abnormalities, the mechanisms of selection may be exerted through the same mode of action but controlled by the expression of different upstream driver genes.

My analysis of hPSC lines with multiple karyotypic genetic abnormalities show that addition of further genetic changes confers additional properties that strengthens the growth phenotype of the variant cells. In general, as the complexity of the genetic changes increased so too did the performance of variant hPSCs in the studies that assessed the self-renewal state. An interesting hypothesis, that requires experimental validation, is that variant hPSCs which acquire an additional genetic change exert their selective advantage over the original variant population using the same mechanisms present in culture that individual variants can use to outcompete normal cells. The ability of variant hPSCs to exert these selection

mechanisms is proposed to be driven changes in gene expression that are a consequence of the additional genomic regions (Amps et al., 2011). In this study, I compared the signature of the differentially expressed genes from a variant line containing multiple genetic abnormalities and those of individual variant lines with the closest matching karyotypic changes, and revealed that the transcriptional profile of karyotypically complex line is not the sum of the individual abnormalities. Rather, variant lines with multiple genetic changes have a unique expression profile that suggests the individual variants act synergistically to create new transcriptional regulatory networks.

Following on from the characterization of variant hPSC behaviour, I next wanted to identify the genes and pathways that control the selective advantage of my different variant lines. Similar to the previously reported effect of genetic abnormalities of global gene expression (Ben-David et al., 2014), I observed that addition of genetic material does not induce expression changes restricted to the amplified region but rather causes a genome-wide change in transcription. These findings suggest that it is not only the activity of potential "driver" genes that control selective advantage but also the transcriptional networks they are integrally involved in. Support for this notion is reflected in my GO enrichment data from most of the variant lines containing two or more karyotypic abnormalities that could not determine significantly overrepresented biological processes due to global upregulation across the genome. GO enrichment analysis did prove effective when I analysed variant lines with individual chromosomal abnormalities and 12,20 v.hPSCs. Amongst the biological terms overrepresented in these cell lines, cell adhesion and cell growth were significantly upregulated. Of note, cellular adhesion is guided by actin microtubule cross talk and several studies have shown that actin-myosin contraction following dissociation of hPSCs at passage causes cell death (Chen et al., 2010, Ohgushi et al., 2010). Treatment with Y-27632, which inhibits phosphorylation of myosin regulatory light chains through ROCK, supports hPSC attachment and survival through the series of culture bottlenecks that occur post plating (Barbaric et al., 2010, Barbaric et al., 2014). Karyotypically abnormal cells with addition of chromosomes 1 and 17 are able to overcome these bottlenecks providing a strong selective advantage at the beginning stages of culture (Barbaric et al., 2014). It is possible modulation of this signalling axis can influence cell fate and upregulation of genes associated with cell adhesion favour survival of hPSCs during the selection mechanisms present post-plating.

Future studies are required to further characterise the gene expression changes observed in karyotypically variant hPSCs, however overexpressed genes associated with these processes could be ideal candidates for identifying genes or sets or genes that drive particular aspects of selective advantage.

6.2 Extrinsic mechanisms of selective advantage

Though the assessment of individual characteristics of variant cells from homogenous cultures allowed me to identify the growth properties that provide these cells with an aspect of their selective advantage. The analysis of homogenous normal and variant cultures did not recapitulate the naturally occurring events that arise when a genetically variant cell appears in culture. Therefore, to investigate the selection mechanism that occur due to cell-cell interactions I used a co-culture approach that generated mosaic cultures in which normal and variant cells shared a proportion of their cell contacts.

In my co-culture conditions I showed that the growth rate of normal-hPSCs was significantly reduced due to active elimination when cultured with supervariant hPSCs that possess a significantly faster growth rate. The active elimination of normal hPSCs demonstrated that a mechanism of selection existed that was dependent on the interaction of normal and variant hPSCs. Furthermore, I demonstrated that this is a conserved selection mechanism in hPSC cultures that also functions in variant hPSC during the acquisition of further genetic changes. The growth of karyotypically variant hPSC lines with significantly lower growth rate than supervariant hPSCs was also shown to be suppressed in co-cultures. Whereas, cell lines with similar growth rates did not affect each other's rate of proliferation when grown in co-culture. This mode of elimination shared several common features with cell competition, and I argue that cell competition is an active mechanism of selective advantage that supresses the growth of hPSCs with a weaker growth phenotype.

Cell competition has not been previously reported in hPSCs and little is known whether the fitness sensing mechanism described in other developmental systems are conserved. In mouse pluripotent stem cells the roles Myc and mTOR have been extensively described as

determinants of cellular fitness (Diaz-Diaz et al., 2017, Bowling et al., 2018). In contrast to those observations, here I found that signalling through the p38 MAPK pathway is important for determining winner-loser cell fate. It is unclear why different signalling pathways are involved between these competitive contexts and may be related to the mechanism for sensing cell fitness. A previous study has reported that p38 signalling controls winner and loser cell fate during mechanical competition of mutant MDCK cells, but other studies have implicated different signalling pathways (Wagstaff et al., 2016, Bras-Pereira and Moreno, 2018). It is possible that in different contexts the relative fitness between the cell populations is being determined by alternative sensing mechanism which in turn activate unique downstream pathways. Distinguishing the mechanism used to compare hPSC cellular fitness will be essential for determining whether human PSCs share common or different competitive interactions to other systems.

In this study I have characterised many of the mechanisms and dynamics by which different variant cells gain growth advantage, however the genetic control of these behaviours remains unknown. The supervariant line used predominantly in this section of work has very complex genetic alterations, it remains unclear what is the contribution of each chromosome to the aspects of altered behaviour observed within these cells and how they may change a cells fitness state. As previously discussed, it has been speculated that different chromosomes confer different properties to hPSCs through overexpression of genes encoded within these regions which provides the selective advantage. One possibility is that amplified expression of genes harboured on these amplified regions is sufficient to alter variant cell growth phenotype and confer winner status. Alternatively, it is plausible that during co-culture normal and variant hPSCs both receive similar levels of pro-apoptotic signals but variants cells, unlike normal hSPCs, possess elevated levels of anti-apoptotic signalling factors that prevent their elimination. Understanding how the different sensing pathways interact in a single competitive context will likely to provide new insights into the downstream mechanisms that regulate cell competition. Future work should address our lack of understanding on the molecular basis of competitive interactions within hPSC cultures which will be essential for designing culture conditions that alleviate selective advantage and minimise the appearance of genetically variant hPSCs during prolonged culture.

6.3 Future Directions and Considerations

As an increasing number of hPSC based therapeutics are entering clinical trials evaluating their safety is critical for the future of regenerative medicine (Martin, 2017). Genetic changes that arise in hPSCs pose several challenges that could impact on various aspects of therapeutic safety. In this study, I have shown that different karyotypic abnormalities confer different intrinsic advantageous properties that affect the fate of undifferentiated hPSCs, however it remains unknown if genetic variants would influence the behaviour of differentiated cells in a similar manner. One of the major safety concerns is the tumorigenic potential of hPSCs (Peterson et al., 2016). Undifferentiated hPSCs are capable of generating teratomas, a tumour composed of somatic ells from all three germ line lineages, when transplanted into immunocompromised mice (Damjanov and Andrews, 2016). The addition of karyotypic abnormalities increases the tumorigenic potential of undifferentiated hPSCs. Human PSCs that have gained chromosomal abnormalities have the potential to generate teratocarcinomas, which in addition to somatic tissue components possess a persisting undifferentiated stem cell population (Damjanov and Andrews, 2016, Ben-David et al., 2014).

Though it is highly unlikely undifferentiated hPSCs would be used as a therapeutic and differentiated populations intended for transplantation are screened for undifferentiated hPSCs, it is not possible to exclude the potential presence of a small number of undifferentiated cells that exist below the detection limit (Tateno et al., 2017). In my data, I reported a particular variant line with gain of isochromosome 20q showed a level of resistance to differentiation. Though this finding requires more investigation to determine the extent of resistance to differentiation, it highlights the possibility karyotypic abnormalities that confer altered patterns of differentiation could raise the probability of undifferentiated cells with teratoma/teratocarcinoma forming potential being present in the final therapeutic increasing the associated risk.

Furthermore, it is possibly malignancy might arise from the differentiated cells. Gain of the karyotypic regions commonly acquired in hPSCs are also observed in various forms of cancer, one example is neuroblastoma. Gain of chromosome 17q is the most frequent genetic abnormality observed in neuroblastoma and is associated with poor prognosis (Theissen et

al., 2014). Genes located on chromosome 17q that are upregulated during neurogenesis have been proposed to play an important role in the progression of neuroblastoma (Saito-Ohara et al., 2003, Uryu et al., 2017). Taken together, it is plausible that hPSCs with gain of 17q are more likely to develop neoplastic properties when differentiated towards a neurogenic fate compared to hPSCs with genetic changes that have not been previously associated with neuroblastoma. It is possible that the risk associated with a karyotypic abnormality may only be observed in a particular differentiated derivative, emphasising the requirement for risk assessment based on the context hPSC derived therapeutics are being used in regenerative medicine. In addition, the underlying causes of neuroblastoma remain unknown therefore the description of genetically variant hPSCs with karyotypic abnormalities that match those found in pathology could open new avenues for disease modelling.

On the other hand, some genetic variants could carry low risk and be beneficial for transplanted cells to possess. One possibility is gain of 20q11.21, from my data and previous studies the 20q11.21 variant appears to provide cells only with an antiapoptotic advantage in the undifferentiated state (Avery et al., 2013). If the karyotypic variant 20q11.21 continued to provide differentiated derivates with a degree of apoptotic resistance whilst not effecting their behaviour and function it could be beneficial for regenerative therapy by enhancing cell survival during transplantation.

An alternative approach is to reduce the probability of genetically variant hPSCs arising during culture. The cultures practices employed to expand hPSCs can significantly affect the rate at which variant cells arise and overtake cultures (Jacobs et al., 2016, Garitaonandia et al., 2015, Olariu et al., 2010). In addition, the current methods commonly used for screening genetic changes in hPSCs have a detection limit of 5%-10% mosaicism, therefore it is possible that an unidentified karyotypically variant population can exist within hPSC cultures that have been defined as "normal" (Baker et al., 2016). Thus, it is also essential to design new strategies that minimise the appearance of genetic variant. My work characterising the mechanisms of selective advantage may provide a platform for designing culture strategies that restrict the appearance of karyotypic variants by alleviating selective advantage.

In conclusion, the safety risks particular genetic variants pose could be heavily dependent on the context cell-based therapeutics are being utilised and would have to be examined on a case by case basis. Finally, the panel of variant hPSCs lines containing commonly acquired genetic changes generated in this study has the potential to become a crucial resource that enables future investigation into the safety of hPSCs for regenerative applications, as well as the mechanisms that underlie various forms of disease.

7   Concluding Remarks

In this study, I sought to determine the mechanisms of selective advantage that exist in cultures of hPSCs, that drive the overtake of karyotypically normal cultures by variant cells possessing gains of the most commonly observed chromosomal regions. By generating a panel of variant hPSC lines containing individual and multiple karyotypic abnormalities I was able to characterise and identify how different chromosomal regions confer selective growth properties, as well as how karyotypic abnormalities act synergistically within lines that possess multiple karyotypic changes to further enhance the growth phenotype of complex variant hPSCs. I found that some karyotypic changes confer selective advantage by altering different aspects of cell fate, whereas other common abnormalities function through the same mode but use different upstream genetic regulation to drive their selective growth properties. Examining the transcriptome of the different variant lines using RNA sequencing showed that gain of chromosomal regions resulted in global changes to gene expression. From this, we can now work to identify the genes and transcriptional networks that drive the selection mechanisms of different common genetic abnormalities and understand how the transcriptional landscape of variant cells evolves upon the addition of further karyotypic changes.

The analysis of homogenous cultures enabled me to identify the intrinsic mechanisms of cell competition, however it was apparent these conditions did not recapitulate the culture environment created as variant cells overtake normal hPSCs. I therefore generated co-cultures of normal and variant hPSCs that I could use to interrogate the selection mechanisms that exist when normal and variant hPSCs directly interact within the same culture environment. Through tracking the growth rate of different normal and variant hPSC lines I was able to show that cell competition is a selection mechanism that restricts the growth of normal and variant hPSCs when grown in heterogenous cultures with variant hPSCs that have a significantly faster growth rate. Furthermore, I have shed light on a potential pathway that mediates this extrinsic competitive selection mechanism. Finally, the characterisation of these selection mechanisms has opened up new avenues of research into the behaviour of normal and variant hPSCs that can be used to assess the impact karyotypic abnormalities may have on the future safety of hPSCs derived therapeutics for therapeutic applications.

8 **References**

ALLISON, T. F., SMITH, A. J. H., ANASTASSIADIS, K., SLOANE-STANLEY, J., BIGA, V., STAVISH, D., HACKLAND, J., SABRI, S., LANGERMAN, J., JONES, M., PLATH, K., COCA, D., BARBARIC, I., GOKHALE, P. & ANDREWS, P. W. 2018. Identification and Single-Cell Functional Characterization of an Endodermally Biased Pluripotent Substate in Human Embryonic Stem Cells. *Stem Cell Reports,* 10**,** 1895-1907.

ALTIERI, D. C. 2015. Survivin - The inconvenient IAP. *Semin Cell Dev Biol,* 39**,** 91-6.

AMIT, M., CARPENTER, M. K., INOKUMA, M. S., CHIU, C. P., HARRIS, C. P., WAKNITZ, M. A., ITSKOVITZ-ELDOR, J. & THOMSON, J. A. 2000. Clonally derived human embryonic stem cell lines maintain pluripotency and proliferative potential for prolonged periods of culture. *Dev Biol,* 227**,** 271-8.

AMOYEL, M. & BACH, E. A. 2014. Cell competition: how to eliminate your neighbours. *Development,* 141**,** 988-1000.

AMPS, K., ANDREWS, P. W., ANYFANTIS, G., ARMSTRONG, L., AVERY, S., BAHARVAND, H., BAKER, J., BAKER, D., MUNOZ, M. B., BEIL, S., BENVENISTY, N., BEN-YOSEF, D., BIANCOTTI, J. C., BOSMAN, A., BRENA, R. M., BRISON, D., CAISANDER, G., CAMARASA, M. V., CHEN, J., CHIAO, E., CHOI, Y. M., CHOO, A. B., COLLINS, D., COLMAN, A., CROOK, J. M., DALEY, G. Q., DALTON, A., DE SOUSA, P. A., DENNING, C., DOWNIE, J., DVORAK, P., MONTGOMERY, K. D., FEKI, A., FORD, A., FOX, V., FRAGA, A. M., FRUMKIN, T., GE, L., GOKHALE, P. J., GOLAN-LEV, T., GOURABI, H., GROPP, M., LU, G., HAMPL, A., HARRON, K., HEALY, L., HERATH, W., HOLM, F., HOVATTA, O., HYLLNER, J., INAMDAR, M. S., IRWANTO, A. K., ISHII, T., JACONI, M., JIN, Y., KIMBER, S., KISELEV, S., KNOWLES, B. B., KOPPER, O., KUKHARENKO, V., KULIEV, A., LAGARKOVA, M. A., LAIRD, P. W., LAKO, M., LASLETT, A. L., LAVON, N., LEE, D. R., LEE, J. E., LI, C., LIM, L. S., LUDWIG, T. E., MA, Y., MALTBY, E., MATEIZEL, I., MAYSHAR, Y., MILEIKOVSKY, M., MINGER, S. L., MIYAZAKI, T., MOON, S. Y., MOORE, H., MUMMERY, C., NAGY, A., NAKATSUJI, N., NARWANI, K., OH, S. K., OH, S. K., OLSON, C., OTONKOSKI, T., PAN, F., PARK, I. H., PELLS, S., PERA, M. F., PEREIRA, L. V., QI, O., RAJ, G. S., REUBINOFF, B., ROBINS, A., ROBSON, P., ROSSANT, J., SALEKDEH, G. H., et al. 2011. Screening ethnically diverse human embryonic stem cells identifies a chromosome 20 minimal amplicon conferring growth advantage. *Nat Biotechnol,* 29**,** 1132-44.

ANDREWS, P. W., BANTING, G., DAMJANOV, I., ARNAUD, D. & AVNER, P. 1984a. Three monoclonal antibodies defining distinct differentiation antigens associated with different high molecular weight polypeptides on the surface of human embryonal carcinoma cells. *Hybridoma,* 3**,** 347-61.

ANDREWS, P. W., BENVENISTY, N., MCKAY, R., PERA, M. F., ROSSANT, J., SEMB, H., STACEY, G. N. & STEERING COMMITTEE OF THE INTERNATIONAL STEM CELL, I. 2005. The International Stem Cell Initiative: toward benchmarks for human embryonic stem cell research. *Nat Biotechnol,* 23**,** 795-7.

ANDREWS, P. W., MEYER, L. J., BEDNARZ, K. L. & HARRIS, H. 1984b. Two monoclonal antibodies recognizing determinants on human embryonal carcinoma cells react specifically with the liver isozyme of human alkaline phosphatase. *Hybridoma,* 3**,** 33-9.

ARAGONA, M., PANCIERA, T., MANFRIN, A., GIULITTI, S., MICHIELIN, F., ELVASSORE, N., DUPONT, S. & PICCOLO, S. 2013. A mechanical checkpoint controls multicellular growth through YAP/TAZ regulation by actin-processing factors. *Cell,* 154**,** 1047-1059.

ARMSTRONG, L., HUGHES, O., YUNG, S., HYSLOP, L., STEWART, R., WAPPLER, I., PETERS, H., WALTER, T., STOJKOVIC, P., EVANS, J., STOJKOVIC, M. & LAKO, M. 2006. The role of PI3K/AKT, MAPK/ERK and NFkappabeta signalling in the maintenance of human embryonic stem cell pluripotency and viability highlighted by transcriptional profiling and functional analysis. *Hum Mol Genet,* 15**,** 1894-913.

AVERY, S., HIRST, A. J., BAKER, D., LIM, C. Y., ALAGARATNAM, S., SKOTHEIM, R. I., LOTHE, R. A., PERA, M. F., COLMAN, A., ROBSON, P., ANDREWS, P. W. & KNOWLES, B. B. 2013. BCL-XL mediates the strong

selective advantage of a 20q11.21 amplification commonly found in human embryonic stem cell cultures. *Stem Cell Reports,* 1**,** 379-86.

BAILLON, L. & BASLER, K. 2014. Reflections on cell competition. *Semin Cell Dev Biol,* 32**,** 137-44.

BAKER, D., HIRST, A. J., GOKHALE, P. J., JUAREZ, M. A., WILLIAMS, S., WHEELER, M., BEAN, K., ALLISON, T. F., MOORE, H. D., ANDREWS, P. W. & BARBARIC, I. 2016. Detecting Genetic Mosaicism in Cultures of Human Pluripotent Stem Cells. *Stem Cell Reports,* 7**,** 998-1012.

BAKER, D. E., HARRISON, N. J., MALTBY, E., SMITH, K., MOORE, H. D., SHAW, P. J., HEATH, P. R., HOLDEN, H. & ANDREWS, P. W. 2007. Adaptation to culture of human embryonic stem cells and oncogenesis in vivo. *Nat Biotechnol,* 25**,** 207-15.

BALLESTEROS-ARIAS, L., SAAVEDRA, V. & MORATA, G. 2014. Cell competition may function either as tumour-suppressing or as tumour-stimulating factor in Drosophila. *Oncogene,* 33**,** 4377-84.

BARBARIC, I., BIGA, V., GOKHALE, P. J., JONES, M., STAVISH, D., GLEN, A., COCA, D. & ANDREWS, P. W. 2014. Time-lapse analysis of human embryonic stem cells reveals multiple bottlenecks restricting colony formation and their relief upon culture adaptation. *Stem Cell Reports,* 3**,** 142-55.

BARBARIC, I., GOKHALE, P. J., JONES, M., GLEN, A., BAKER, D. & ANDREWS, P. W. 2010. Novel regulators of stem cell fates identified by a multivariate phenotype screen of small compounds on human embryonic stem cell colonies. *Stem Cell Res,* 5**,** 104-19.

BARNES, J. M., PRZYBYLA, L. & WEAVER, V. M. 2017. Tissue mechanics regulate brain development, homeostasis and disease. *J Cell Sci,* 130**,** 71-82.

BEATTIE, G. M., LOPEZ, A. D., BUCAY, N., HINTON, A., FIRPO, M. T., KING, C. C. & HAYEK, A. 2005. Activin A maintains pluripotency of human embryonic stem cells in the absence of feeder layers. *Stem Cells,* 23**,** 489-95.

BECKER, K. A., GHULE, P. N., THERRIEN, J. A., LIAN, J. B., STEIN, J. L., VAN WIJNEN, A. J. & STEIN, G. S. 2006. Self-renewal of human embryonic stem cells is supported by a shortened G1 cell cycle phase. *J Cell Physiol,* 209**,** 883-93.

BEN-DAVID, U., ARAD, G., WEISSBEIN, U., MANDEFRO, B., MAIMON, A., GOLAN-LEV, T., NARWANI, K., CLARK, A. T., ANDREWS, P. W., BENVENISTY, N. & CARLOS BIANCOTTI, J. 2014. Aneuploidy induces profound changes in gene expression, proliferation and tumorigenicity of human pluripotent stem cells. *Nat Commun,* 5**,** 4825.

BEN-DAVID, U., COWELL, I. G., AUSTIN, C. A. & BENVENISTY, N. 2015. Brief reports: Controlling the survival of human pluripotent stem cells by small molecule-based targeting of topoisomerase II alpha. *Stem Cells,* 33**,** 1013-9.

BEN-DAVID, U., GAN, Q. F., GOLAN-LEV, T., ARORA, P., YANUKA, O., OREN, Y. S., LEIKIN-FRENKEL, A., GRAF, M., GARIPPA, R., BOEHRINGER, M., GROMO, G. & BENVENISTY, N. 2013. Selective elimination of human pluripotent stem cells by an oleate synthesis inhibitor discovered in a high-throughput screen. *Cell Stem Cell,* 12**,** 167-79.

BOCK, C., KISKINIS, E., VERSTAPPEN, G., GU, H., BOULTING, G., SMITH, Z. D., ZILLER, M., CROFT, G. F., AMOROSO, M. W., OAKLEY, D. H., GNIRKE, A., EGGAN, K. & MEISSNER, A. 2011. Reference Maps of human ES and iPS cell variation enable high-throughput characterization of pluripotent cell lines. *Cell,* 144**,** 439-52.

BONDAR, T. & MEDZHITOV, R. 2010. p53-mediated hematopoietic stem and progenitor cell competition. *Cell Stem Cell,* 6**,** 309-22.

BOUMA, M. J., VAN ITERSON, M., JANSSEN, B., MUMMERY, C. L., SALVATORI, D. C. F. & FREUND, C. 2017. Differentiation-Defective Human Induced Pluripotent Stem Cells Reveal Strengths and Limitations of the Teratoma Assay and In Vitro Pluripotency Assays. *Stem Cell Reports,* 8**,** 1340-1353.

BOVE, A., GRADECI, D., FUJITA, Y., BANERJEE, S., CHARRAS, G. & LOWE, A. R. 2017. Local cellular neighborhood controls proliferation in cell competition. *Mol Biol Cell,* 28**,** 3215-3228.

BOWLING, S., DI GREGORIO, A., SANCHO, M., POZZI, S., AARTS, M., SIGNORE, M., M, D. S., BARBERA, J. P. M., GIL, J. & RODRIGUEZ, T. A. 2018. P53 and mTOR signalling determine fitness selection through cell competition during early mouse embryonic development. *Nat Commun,* 9**,** 1763.

BOYER, L. A., LEE, T. I., COLE, M. F., JOHNSTONE, S. E., LEVINE, S. S., ZUCKER, J. P., GUENTHER, M. G., KUMAR, R. M., MURRAY, H. L., JENNER, R. G., GIFFORD, D. K., MELTON, D. A., JAENISCH, R. & YOUNG, R. A. 2005. Core transcriptional regulatory circuitry in human embryonic stem cells. *Cell,* 122**,** 947-56.

BRAS-PEREIRA, C. & MORENO, E. 2018. Mechanical cell competition. *Curr Opin Cell Biol,* 51**,** 15-21.

BROKER, L. E., KRUYT, F. A. & GIACCONE, G. 2005. Cell death independent of caspases: a review. *Clin Cancer Res,* 11**,** 3155-62.

BROUWER, M., ZHOU, H. & NADIF KASRI, N. 2016. Choices for Induction of Pluripotency: Recent Developments in Human Induced Pluripotent Stem Cell Reprogramming Strategies. *Stem Cell Rev,* 12**,** 54-72.

BRUMBY, A. M. & RICHARDSON, H. E. 2003. scribble mutants cooperate with oncogenic Ras or Notch to cause neoplastic overgrowth in Drosophila. *EMBO J,* 22**,** 5769-79.

CALDER, A., ROTH-ALBIN, I., BHATIA, S., PILQUIL, C., LEE, J. H., BHATIA, M., LEVADOUX-MARTIN, M., MCNICOL, J., RUSSELL, J., COLLINS, T. & DRAPER, J. S. 2013. Lengthened G1 phase indicates differentiation status in human embryonic stem cells. *Stem Cells Dev,* 22**,** 279-95.

CARMENA, M., WHEELOCK, M., FUNABIKI, H. & EARNSHAW, W. C. 2012. The chromosomal passenger complex (CPC): from easy rider to the godfather of mitosis. *Nat Rev Mol Cell Biol,* 13**,** 789-803.

CARPENTER, A. E., JONES, T. R., LAMPRECHT, M. R., CLARKE, C., KANG, I. H., FRIMAN, O., GUERTIN, D. A., CHANG, J. H., LINDQUIST, R. A., MOFFAT, J., GOLLAND, P. & SABATINI, D. M. 2006. CellProfiler: image analysis software for identifying and quantifying cell phenotypes. *Genome Biol,* 7**,** R100.

CHANG, H. H. Y., PANNUNZIO, N. R., ADACHI, N. & LIEBER, M. R. 2017. Non-homologous DNA end joining and alternative pathways to double-strand break repair. *Nat Rev Mol Cell Biol,* 18**,** 495-506.

CHAUVIER, D., ANKRI, S., CHARRIAUT-MARLANGUE, C., CASIMIR, R. & JACOTOT, E. 2007. Broad-spectrum caspase inhibitors: from myth to reality? *Cell Death Differ,* 14**,** 387-91.

CHEN, G., HOU, Z., GULBRANSON, D. R. & THOMSON, J. A. 2010. Actin-myosin contractility is responsible for the reduced viability of dissociated human embryonic stem cells. *Cell Stem Cell,* 7**,** 240-8.

CHIN, M. H., MASON, M. J., XIE, W., VOLINIA, S., SINGER, M., PETERSON, C., AMBARTSUMYAN, G., AIMIUWU, O., RICHTER, L., ZHANG, J., KHVOROSTOV, I., OTT, V., GRUNSTEIN, M., LAVON, N., BENVENISTY, N., CROCE, C. M., CLARK, A. T., BAXTER, T., PYLE, A. D., TEITELL, M. A., PELEGRINI, M., PLATH, K. & LOWRY, W. E. 2009. Induced pluripotent stem cells and embryonic stem cells are distinguished by gene expression signatures. *Cell Stem Cell,* 5**,** 111-23.

CLAVERIA, C., GIOVINAZZO, G., SIERRA, R. & TORRES, M. 2013. Myc-driven endogenous cell competition in the early mammalian embryo. *Nature,* 500**,** 39-44.

COMPTON, D. A. 2011. Mechanisms of aneuploidy. *Curr Opin Cell Biol,* 23**,** 109-13.

CORTI, S., FARAVELLI, I., CARDANO, M. & CONTI, L. 2015. Human pluripotent stem cells as tools for neurodegenerative and neurodevelopmental disease modeling and drug discovery. *Expert Opin Drug Discov,* 10**,** 615-29.

COWAN, C. A., KLIMANSKAYA, I., MCMAHON, J., ATIENZA, J., WITMYER, J., ZUCKER, J. P., WANG, S., MORTON, C. C., MCMAHON, A. P., POWERS, D. & MELTON, D. A. 2004. Derivation of embryonic stem-cell lines from human blastocysts. *N Engl J Med,* 350**,** 1353-6.

DAMJANOV, I. & ANDREWS, P. W. 2016. Teratomas produced from human pluripotent stem cells xenografted into immunodeficient mice - a histopathology atlas. *Int J Dev Biol,* 60**,** 337-419.

DE LA COVA, C., ABRIL, M., BELLOSTA, P., GALLANT, P. & JOHNSTON, L. A. 2004. Drosophila myc regulates organ size by inducing cell competition. *Cell,* 117**,** 107-16.

DEIGNAN, L., PINHEIRO, M. T., SUTCLIFFE, C., SAUNDERS, A., WILCOCKSON, S. G., ZEEF, L. A., DONALDSON, I. J. & ASHE, H. L. 2016. Regulation of the BMP Signaling-Responsive Transcriptional Network in the Drosophila Embryo. *PLoS Genet,* 12**,** e1006164.

DESMARAIS, J. A., HOFFMANN, M. J., BINGHAM, G., GAGOU, M. E., MEUTH, M. & ANDREWS, P. W. 2012. Human embryonic stem cells fail to activate CHK1 and commit to apoptosis in response to DNA replication stress. *Stem Cells,* 30**,** 1385-93.

DI GREGORIO, A., BOWLING, S. & RODRIGUEZ, T. A. 2016. Cell Competition and Its Role in the Regulation of Cell Fitness from Development to Cancer. *Dev Cell,* 38**,** 621-34.

DIAZ-DIAZ, C., FERNANDEZ DE MANUEL, L., JIMENEZ-CARRETERO, D., MONTOYA, M. C., CLAVERIA, C. & TORRES, M. 2017. Pluripotency Surveillance by Myc-Driven Competitive Elimination of Differentiating Cells. *Dev Cell,* 42**,** 585-599 e4.

DITCHFIELD, C., JOHNSON, V. L., TIGHE, A., ELLSTON, R., HAWORTH, C., JOHNSON, T., MORTLOCK, A., KEEN, N. & TAYLOR, S. S. 2003. Aurora B couples chromosome alignment with anaphase by targeting BubR1, Mad2, and Cenp-E to kinetochores. *J Cell Biol,* 161**,** 267-80.

DRAPER, J. S., PIGOTT, C., THOMSON, J. A. & ANDREWS, P. W. 2002. Surface antigens of human embryonic stem cells: changes upon differentiation in culture. *J Anat,* 200**,** 249-58.

DRAPER, J. S., SMITH, K., GOKHALE, P., MOORE, H. D., MALTBY, E., JOHNSON, J., MEISNER, L., ZWAKA, T. P., THOMSON, J. A. & ANDREWS, P. W. 2004. Recurrent gain of chromosomes 17q and 12 in cultured human embryonic stem cells. *Nat Biotechnol,* 22**,** 53-4.

DUMITRU, R., GAMA, V., FAGAN, B. M., BOWER, J. J., SWAHARI, V., PEVNY, L. H. & DESHMUKH, M. 2012. Human embryonic stem cells have constitutively active Bax at the Golgi and are primed to undergo rapid apoptosis. *Mol Cell,* 46**,** 573-83.

EAKIN, G. S., HADJANTONAKIS, A. K., PAPAIOANNOU, V. E. & BEHRINGER, R. R. 2005. Developmental potential and behavior of tetraploid cells in the mouse embryo. *Dev Biol,* 288**,** 150-9.

ENVER, T., SONEJI, S., JOSHI, C., BROWN, J., IBORRA, F., ORNTOFT, T., THYKJAER, T., MALTBY, E., SMITH, K., ABU DAWUD, R., JONES, M., MATIN, M., GOKHALE, P., DRAPER, J. & ANDREWS, P. W. 2005. Cellular differentiation hierarchies in normal and culture-adapted human embryonic stem cells. *Hum Mol Genet,* 14**,** 3129-40.

FAZELI, A., LIEW, C. G., MATIN, M. M., ELLIOTT, S., JEANMEURE, L. F., WRIGHT, P. C., MOORE, H. & ANDREWS, P. W. 2011. Altered patterns of differentiation in karyotypically abnormal human embryonic stem cells. *Int J Dev Biol,* 55**,** 175-80.

FENDERSON, B. A., ANDREWS, P. W., NUDELMAN, E., CLAUSEN, H. & HAKOMORI, S. 1987. Glycolipid core structure switching from globo- to lacto- and ganglio-series during retinoic acid-induced differentiation of TERA-2-derived human embryonal carcinoma cells. *Dev Biol,* 122**,** 21-34.

FILION, T. M., QIAO, M., GHULE, P. N., MANDEVILLE, M., VAN WIJNEN, A. J., STEIN, J. L., LIAN, J. B., ALTIERI, D. C. & STEIN, G. S. 2009. Survival responses of human embryonic stem cells to DNA damage. *J Cell Physiol,* 220**,** 586-92.

FOLMES, C. D., NELSON, T. J., MARTINEZ-FERNANDEZ, A., ARRELL, D. K., LINDOR, J. Z., DZEJA, P. P., IKEDA, Y., PEREZ-TERZIC, C. & TERZIC, A. 2011. Somatic oxidative bioenergetics transitions into pluripotency-dependent glycolysis to facilitate nuclear reprogramming. *Cell Metab,* 14**,** 264-71.

FORBES, S. J. & NEWSOME, P. N. 2016. Liver regeneration - mechanisms and models to clinical application. *Nat Rev Gastroenterol Hepatol,* 13**,** 473-85.

FRAGA, A. M., SOUZA DE ARAUJO, E. S., STABELLINI, R., VERGANI, N. & PEREIRA, L. V. 2011. A survey of parameters involved in the establishment of new lines of human embryonic stem cells. *Stem Cell Rev,* 7**,** 775-81.

FRASCHINI, R., BERETTA, A., SIRONI, L., MUSACCHIO, A., LUCCHINI, G. & PIATTI, S. 2001. Bub3 interaction with Mad2, Mad3 and Cdc20 is mediated by WD40 repeats and does not require intact kinetochores. *EMBO J,* 20**,** 6648-59.

GADUE, P., HUBER, T. L., PADDISON, P. J. & KELLER, G. M. 2006. Wnt and TGF-beta signaling are required for the induction of an in vitro model of primitive streak formation using embryonic stem cells. *Proc Natl Acad Sci U S A,* 103**,** 16806-11.

GANEM, N. J. & PELLMAN, D. 2012. Linking abnormal mitosis to the acquisition of DNA damage. *J Cell Biol,* 199**,** 871-81.

GARITAONANDIA, I., AMIR, H., BOSCOLO, F. S., WAMBUA, G. K., SCHULTHEISZ, H. L., SABATINI, K., MOREY, R., WALTZ, S., WANG, Y. C., TRAN, H., LEONARDO, T. R., NAZOR, K., SLAVIN, I., LYNCH, C., LI, Y., COLEMAN, R., GALLEGO ROMERO, I., ALTUN, G., REYNOLDS, D., DALTON, S., PARAST, M., LORING, J. F. & LAURENT, L. C. 2015. Increased risk of genetic and epigenetic instability in human embryonic stem cells associated with specific culture conditions. *PLoS One,* 10**,** e0118307.

GHEZRAOUI, H., PIGANEAU, M., RENOUF, B., RENAUD, J. B., SALLMYR, A., RUIS, B., OH, S., TOMKINSON, A. E., HENDRICKSON, E. A., GIOVANNANGELI, C., JASIN, M. & BRUNET, E. 2014. Chromosomal translocations in human cells are generated by canonical nonhomologous end-joining. *Mol Cell,* 55**,** 829-842.

GHULE, P. N., MEDINA, R., LENGNER, C. J., MANDEVILLE, M., QIAO, M., DOMINSKI, Z., LIAN, J. B., STEIN, J. L., VAN WIJNEN, A. J. & STEIN, G. S. 2011. Reprogramming the pluripotent cell cycle: restoration of an abbreviated G1 phase in human induced pluripotent stem (iPS) cells. *J Cell Physiol,* 226**,** 1149-56.

GOKHALE, P. J., AU-YOUNG, J. K., DADI, S., KEYS, D. N., HARRISON, N. J., JONES, M., SONEJI, S., ENVER, T., SHERLOCK, J. K. & ANDREWS, P. W. 2015. Culture adaptation alters transcriptional hierarchies among single human embryonic stem cells reflecting altered patterns of differentiation. *PLoS One,* 10**,** e0123467.

GORDON, D. J., RESIO, B. & PELLMAN, D. 2012. Causes and consequences of aneuploidy in cancer. *Nat Rev Genet,* 13**,** 189-203.

GREGAN, J., POLAKOVA, S., ZHANG, L., TOLIC-NORRELYKKE, I. M. & CIMINI, D. 2011. Merotelic kinetochore attachment: causes and effects. *Trends Cell Biol,* 21**,** 374-81.

GU, W., ZHANG, F. & LUPSKI, J. R. 2008. Mechanisms for human genomic rearrangements. *Pathogenetics,* 1**,** 4.

GUENTHER, M. G., FRAMPTON, G. M., SOLDNER, F., HOCKEMEYER, D., MITALIPOVA, M., JAENISCH, R. & YOUNG, R. A. 2010. Chromatin structure and gene expression programs of human embryonic and induced pluripotent stem cells. *Cell Stem Cell,* 7**,** 249-57.

GUMBINER, B. M. & KIM, N. G. 2014. The Hippo-YAP signaling pathway and contact inhibition of growth. *J Cell Sci,* 127**,** 709-17.

HARDWICK, K. G., JOHNSTON, R. C., SMITH, D. L. & MURRAY, A. W. 2000. MAD3 encodes a novel component of the spindle checkpoint which interacts with Bub3p, Cdc20p, and Mad2p. *J Cell Biol,* 148**,** 871-82.

HARRISON, N. J., BAKER, D. & ANDREWS, P. W. 2007. Culture adaptation of embryonic stem cells echoes germ cell malignancy. *Int J Androl,* 30**,** 275-81; discussion 281.

HAUF, S., COLE, R. W., LATERRA, S., ZIMMER, C., SCHNAPP, G., WALTER, R., HECKEL, A., VAN MEEL, J., RIEDER, C. L. & PETERS, J. M. 2003. The small molecule Hesperadin reveals a role for Aurora B in correcting kinetochore-microtubule attachment and in maintaining the spindle assembly checkpoint. *J Cell Biol,* 161**,** 281-94.

HEESTAND, G. M., SCHWAEDERLE, M., GATALICA, Z., ARGUELLO, D. & KURZROCK, R. 2017. Topoisomerase expression and amplification in solid tumours: Analysis of 24,262 patients. *Eur J Cancer,* 83**,** 80-87.

HENDERSON, J. K., DRAPER, J. S., BAILLIE, H. S., FISHEL, S., THOMSON, J. A., MOORE, H. & ANDREWS, P. W. 2002. Preimplantation human embryos and embryonic stem cells show comparable expression of stage-specific embryonic antigens. *Stem Cells,* 20**,** 329-37.

HINCK, A. P. 2012. Structural studies of the TGF-betas and their receptors - insights into evolution of the TGF-beta superfamily. *FEBS Lett,* 586**,** 1860-70.

HOGAN, C., DUPRE-CROCHET, S., NORMAN, M., KAJITA, M., ZIMMERMANN, C., PELLING, A. E., PIDDINI, E., BAENA-LOPEZ, L. A., VINCENT, J. P., ITOH, Y., HOSOYA, H., PICHAUD, F. & FUJITA, Y. 2009. Characterization of the interface between normal and transformed epithelial cells. *Nat Cell Biol,* 11**,** 460-7.

HUMINIECKI, L., GOLDOVSKY, L., FREILICH, S., MOUSTAKAS, A., OUZOUNIS, C. & HELDIN, C. H. 2009. Emergence, development and diversification of the TGF-beta signalling pathway within the animal kingdom. *BMC Evol Biol,* 9**,** 28.

IAROVAIA, O. V., RUBTSOV, M., IOUDINKOVA, E., TSFASMAN, T., RAZIN, S. V. & VASSETZKY, Y. S. 2014. Dynamics of double strand breaks and chromosomal translocations. *Mol Cancer,* 13**,** 249.

INTERNATIONAL STEM CELL, I. 2018. Assessment of established techniques to determine developmental and malignant potential of human pluripotent stem cells. *Nat Commun,* 9**,** 1925.

INTERNATIONAL STEM CELL, I., ADEWUMI, O., AFLATOONIAN, B., AHRLUND-RICHTER, L., AMIT, M., ANDREWS, P. W., BEIGHTON, G., BELLO, P. A., BENVENISTY, N., BERRY, L. S., BEVAN, S., BLUM, B., BROOKING, J., CHEN, K. G., CHOO, A. B., CHURCHILL, G. A., CORBEL, M., DAMJANOV, I., DRAPER, J. S., DVORAK, P., EMANUELSSON, K., FLECK, R. A., FORD, A., GERTOW, K., GERTSENSTEIN, M., GOKHALE, P. J., HAMILTON, R. S., HAMPL, A., HEALY, L. E., HOVATTA, O., HYLLNER, J., IMREH, M. P., ITSKOVITZ-ELDOR, J., JACKSON, J., JOHNSON, J. L., JONES, M., KEE, K., KING, B. L., KNOWLES, B. B., LAKO, M., LEBRIN, F., MALLON, B. S., MANNING, D., MAYSHAR, Y., MCKAY, R. D., MICHALSKA, A. E., MIKKOLA, M., MILEIKOVSKY, M., MINGER, S. L., MOORE, H. D., MUMMERY, C. L., NAGY, A., NAKATSUJI, N., O'BRIEN, C. M., OH, S. K., OLSSON, C., OTONKOSKI, T., PARK, K. Y., PASSIER, R., PATEL, H., PATEL, M., PEDERSEN, R., PERA, M. F., PIEKARCZYK, M. S., PERA, R. A., REUBINOFF, B. E., ROBINS, A. J., ROSSANT, J., RUGG-GUNN, P., SCHULZ, T. C., SEMB, H., SHERRER, E. S., SIEMEN, H., STACEY, G. N., STOJKOVIC, M., SUEMORI, H., SZATKIEWICZ, J., TURETSKY, T., TUURI, T., VAN DEN BRINK, S., VINTERSTEN, K., VUORISTO, S., WARD, D., WEAVER, T. A., YOUNG, L. A. & ZHANG, W. 2007. Characterization of human embryonic stem cell lines by the International Stem Cell Initiative. *Nat Biotechnol,* 25**,** 803-16.

JACOBS, K., ZAMBELLI, F., MERTZANIDOU, A., SMOLDERS, I., GEENS, M., NGUYEN, H. T., BARBE, L., SERMON, K. & SPITS, C. 2016. Higher-Density Culture in Human Embryonic Stem Cells Results in DNA Damage and Genome Instability. *Stem Cell Reports,* 6**,** 330-41.

JAMES, D., LEVINE, A. J., BESSER, D. & HEMMATI-BRIVANLOU, A. 2005. TGFbeta/activin/nodal signaling is necessary for the maintenance of pluripotency in human embryonic stem cells. *Development,* 132**,** 1273-82.

JOHNSTON, L. A. 2014. Socializing with MYC: cell competition in development and as a model for premalignant cancer. *Cold Spring Harb Perspect Med,* 4**,** a014274.

KAJITA, M. & FUJITA, Y. 2015. EDAC: Epithelial defence against cancer-cell competition between normal and transformed epithelial cells in mammals. *J Biochem,* 158**,** 15-23.

KAJITA, M., HOGAN, C., HARRIS, A. R., DUPRE-CROCHET, S., ITASAKI, N., KAWAKAMI, K., CHARRAS, G., TADA, M. & FUJITA, Y. 2010. Interaction with surrounding normal epithelial cells influences signalling pathways and behaviour of Src-transformed cells. *J Cell Sci,* 123**,** 171-80.

KANEHISA, M., GOTO, S., FURUMICHI, M., TANABE, M. & HIRAKAWA, M. 2010. KEGG for representation and analysis of molecular networks involving diseases and drugs. *Nucleic Acids Res,* 38**,** D355-60.

KANNAGI, R., COCHRAN, N. A., ISHIGAMI, F., HAKOMORI, S., ANDREWS, P. W., KNOWLES, B. B. & SOLTER, D. 1983. Stage-specific embryonic antigens (SSEA-3 and -4) are epitopes of a unique globo-series ganglioside isolated from human teratocarcinoma cells. *EMBO J,* 2**,** 2355-61.

KELLER, A., DZIEDZICKA, D., ZAMBELLI, F., MARKOULI, C., SERMON, K., SPITS, C. & GEENS, M. 2018. Genetic and epigenetic factors which modulate differentiation propensity in human pluripotent stem cells. *Hum Reprod Update*.

KEMPF, H., OLMER, R., HAASE, A., FRANKE, A., BOLESANI, E., SCHWANKE, K., ROBLES-DIAZ, D., COFFEE, M., GOHRING, G., DRAGER, G., POTZ, O., JOOS, T., MARTINEZ-HACKERT, E., HAVERICH, A., BUETTNER, F. F., MARTIN, U. & ZWEIGERDT, R. 2016. Bulk cell density and Wnt/TGFbeta signalling regulate mesendodermal patterning of human pluripotent stem cells. *Nat Commun,* 7**,** 13602.

KIM, K., DOI, A., WEN, B., NG, K., ZHAO, R., CAHAN, P., KIM, J., ARYEE, M. J., JI, H., EHRLICH, L. I., YABUUCHI, A., TAKEUCHI, A., CUNNIFF, K. C., HONGGUANG, H., MCKINNEY-FREEMAN, S., NAVEIRAS, O., YOON, T. J., IRIZARRY, R. A., JUNG, N., SEITA, J., HANNA, J., MURAKAMI, P., JAENISCH, R., WEISSLEDER, R., ORKIN, S. H., WEISSMAN, I. L., FEINBERG, A. P. & DALEY, G. Q. 2010. Epigenetic memory in induced pluripotent stem cells. *Nature,* 467**,** 285-90.

KIMBREL, E. A. & LANZA, R. 2016. Pluripotent stem cells: the last 10 years. *Regen Med,* 11**,** 831-847.

KNOWLTON, A. L., LAN, W. & STUKENBERG, P. T. 2006. Aurora B is enriched at merotelic attachment sites, where it regulates MCAK. *Curr Biol,* 16**,** 1705-10.

KNUUTILA, S., BJORKQVIST, A. M., AUTIO, K., TARKKANEN, M., WOLF, M., MONNI, O., SZYMANSKA, J., LARRAMENDY, M. L., TAPPER, J., PERE, H., EL-RIFAI, W., HEMMER, S., WASENIUS, V. M., VIDGREN, V. & ZHU, Y. 1998. DNA copy number amplifications in human neoplasms: review of comparative genomic hybridization studies. *Am J Pathol,* 152**,** 1107-23.

KOHLER, G. & MILSTEIN, C. 1975. Continuous cultures of fused cells secreting antibody of predefined specificity. *Nature,* 256**,** 495-7.

KOLAHGAR, G., SUIJKERBUIJK, S. J., KUCINSKI, I., POIRIER, E. Z., MANSOUR, S., SIMONS, B. D. & PIDDINI, E. 2015. Cell Competition Modifies Adult Stem Cell and Tissue Population Dynamics in a JAK-STAT-Dependent Manner. *Dev Cell,* 34**,** 297-309.

KON, S. 2018. Physiological and pathological relevance of cell competition in fly to mammals. *Dev Growth Differ,* 60**,** 14-20.

KUCINSKI, I., DINAN, M., KOLAHGAR, G. & PIDDINI, E. 2017. Chronic activation of JNK JAK/STAT and oxidative stress signalling causes the loser cell status. *Nat Commun,* 8**,** 136.

KUREK, D., NEAGU, A., TASTEMEL, M., TUYSUZ, N., LEHMANN, J., VAN DE WERKEN, H. J., PHILIPSEN, S., VAN DER LINDEN, R., MAAS, A., VAN, I. W. F., DRUKKER, M. & TEN BERGE, D. 2015. Endogenous WNT signals mediate BMP-induced and spontaneous differentiation of epiblast stem cells and human embryonic stem cells. *Stem Cell Reports,* 4**,** 114-28.

KURTZ, A., SELTMANN, S., BAIROCH, A., BITTNER, M. S., BRUCE, K., CAPES-DAVIS, A., CLARKE, L., CROOK, J. M., DAHERON, L., DEWENDER, J., FAULCONBRIDGE, A., FUJIBUCHI, W., GUTTERIDGE, A., HEI, D. J., KIM, Y. O., KIM, J. H., KOKOCINSKI, A. K., LEKSCHAS, F., LOMAX, G. P., LORING, J. F., LUDWIG, T., MAH, N., MATSUI, T., MULLER, R., PARKINSON, H., SHELDON, M., SMITH, K., STACHELSCHEID, H., STACEY, G., STREETER, I., VEIGA, A. & XU, R. H. 2018. A Standard Nomenclature for Referencing and Authentication of Pluripotent Stem Cells. *Stem Cell Reports,* 10**,** 1-6.

LAMPSON, M. A., RENDUCHITALA, K., KHODJAKOV, A. & KAPOOR, T. M. 2004. Correcting improper chromosome-spindle attachments during cell division. *Nat Cell Biol,* 6**,** 232-7.

LEE, C. T., BENDRIEM, R. M., KINDBERG, A. A., WORDEN, L. T., WILLIAMS, M. P., DRGON, T., MALLON, B. S., HARVEY, B. K., RICHIE, C. T., HAMILTON, R. S., CHEN, J., ERRICO, S. L., TSAI, S. Y., UHL, G. R. & FREED, W. J. 2015. Functional consequences of 17q21.31/WNT3-WNT9B amplification in hPSCs with respect to neural differentiation. *Cell Rep,* 10**,** 616-32.

LEFORT, N., FEYEUX, M., BAS, C., FERAUD, O., BENNACEUR-GRISCELLI, A., TACHDJIAN, G., PESCHANSKI, M. & PERRIER, A. L. 2008. Human embryonic stem cells reveal recurrent genomic instability at 20q11.21. *Nat Biotechnol,* 26**,** 1364-6.

LEGOFF, L. & LECUIT, T. 2015. Mechanical Forces and Growth in Animal Tissues. *Cold Spring Harb Perspect Biol,* 8**,** a019232.

LEVAYER, R., DUPONT, C. & MORENO, E. 2016. Tissue Crowding Induces Caspase-Dependent Competition for Space. *Curr Biol,* 26**,** 670-7.

LEVAYER, R., HAUERT, B. & MORENO, E. 2015. Cell mixing induced by myc is required for competitive tissue invasion and destruction. *Nature,* 524**,** 476-80.

LEVENSTEIN, M. E., LUDWIG, T. E., XU, R. H., LLANAS, R. A., VANDENHEUVEL-KRAMER, K., MANNING, D. & THOMSON, J. A. 2006. Basic fibroblast growth factor support of human embryonic stem cell self-renewal. *Stem Cells,* 24**,** 568-74.

LI, M. & BELMONTE, J. C. 2017. Ground rules of the pluripotency gene regulatory network. *Nat Rev Genet,* 18**,** 180-191.

LIEW, C. G., DRAPER, J. S., WALSH, J., MOORE, H. & ANDREWS, P. W. 2007. Transient and stable transgene expression in human embryonic stem cells. *Stem Cells,* 25**,** 1521-8.

LOTZ, S., GODERIE, S., TOKAS, N., HIRSCH, S. E., AHMAD, F., CORNEO, B., LE, S., BANERJEE, A., KANE, R. S., STERN, J. H., TEMPLE, S. & FASANO, C. A. 2013. Sustained levels of FGF2 maintain undifferentiated stem cell cultures with biweekly feeding. *PLoS One,* 8**,** e56289.

LYTTON, J., WESTLIN, M. & HANLEY, M. R. 1991. Thapsigargin inhibits the sarcoplasmic or endoplasmic reticulum Ca-ATPase family of calcium pumps. *J Biol Chem,* 266**,** 17067-71.

MADAN, E., GOGNA, R. & MORENO, E. 2018. Cell competition in development: information from flies and vertebrates. *Curr Opin Cell Biol,* 55**,** 150-157.

MANDAL, S., LINDGREN, A. G., SRIVASTAVA, A. S., CLARK, A. T. & BANERJEE, U. 2011. Mitochondrial function controls proliferation and early differentiation potential of embryonic stem cells. *Stem Cells,* 29**,** 486-95.

MAO, Z., BOZZELLA, M., SELUANOV, A. & GORBUNOVA, V. 2008. DNA repair by nonhomologous end joining and homologous recombination during cell cycle in human cells. *Cell Cycle,* 7**,** 2902-6.

MARCHETTO, M. C., YEO, G. W., KAINOHANA, O., MARSALA, M., GAGE, F. H. & MUOTRI, A. R. 2009. Transcriptional signature and memory retention of human-induced pluripotent stem cells. *PLoS One,* 4**,** e7076.

MARINARI, E., MEHONIC, A., CURRAN, S., GALE, J., DUKE, T. & BAUM, B. 2012. Live-cell delamination counterbalances epithelial growth to limit tissue overcrowding. *Nature,* 484**,** 542-5.

MARTIN, F. A., HERRERA, S. C. & MORATA, G. 2009. Cell competition, growth and size control in the Drosophila wing imaginal disc. *Development,* 136**,** 3747-56.

MARTIN, G. R. & EVANS, M. J. 1975. Differentiation of clonal lines of teratocarcinoma cells: formation of embryoid bodies in vitro. *Proc Natl Acad Sci U S A,* 72**,** 1441-5.

MARTIN, U. 2017. Therapeutic Application of Pluripotent Stem Cells: Challenges and Risks. *Front Med (Lausanne),* 4**,** 229.

MARTINEZ, Y., BENA, F., GIMELLI, S., TIREFORT, D., DUBOIS-DAUPHIN, M., KRAUSE, K. H. & PREYNAT-SEAUVE, O. 2012. Cellular diversity within embryonic stem cells: pluripotent clonal sublines show distinct differentiation potential. *J Cell Mol Med,* 16**,** 456-67.

MARTINS, V. C., BUSCH, K., JURAEVA, D., BLUM, C., LUDWIG, C., RASCHE, V., LASITSCHKA, F., MASTITSKY, S. E., BRORS, B., HIELSCHER, T., FEHLING, H. J. & RODEWALD, H. R. 2014. Cell competition is a tumour suppressor mechanism in the thymus. *Nature,* 509**,** 465-70.

MARTINS-TAYLOR, K., NISLER, B. S., TAAPKEN, S. M., COMPTON, T., CRANDALL, L., MONTGOMERY, K. D., LALANDE, M. & XU, R. H. 2011. Recurrent copy number variations in human induced pluripotent stem cells. *Nat Biotechnol,* 29**,** 488-91.

MASSAGUE, J., SEOANE, J. & WOTTON, D. 2005. Smad transcription factors. *Genes Dev,* 19**,** 2783-810.

MENG, Z., MOROISHI, T. & GUAN, K. L. 2016. Mechanisms of Hippo pathway regulation. *Genes Dev,* 30**,** 1-17.

MERINO, M. M., LEVAYER, R. & MORENO, E. 2016. Survival of the Fittest: Essential Roles of Cell Competition in Development, Aging, and Cancer. *Trends Cell Biol,* 26**,** 776-788.

MERINO, M. M., RHINER, C., PORTELA, M. & MORENO, E. 2013. "Fitness fingerprints" mediate physiological culling of unwanted neurons in Drosophila. *Curr Biol,* 23**,** 1300-9.

MERKLE, F. T., GHOSH, S., KAMITAKI, N., MITCHELL, J., AVIOR, Y., MELLO, C., KASHIN, S., MEKHOUBAD, S., ILIC, D., CHARLTON, M., SAPHIER, G., HANDSAKER, R. E., GENOVESE, G., BAR, S., BENVENISTY, N., MCCARROLL, S. A. & EGGAN, K. 2017. Human pluripotent stem cells recurrently acquire and expand dominant negative P53 mutations. *Nature,* 545**,** 229-233.

MEYER, S. N., AMOYEL, M., BERGANTINOS, C., DE LA COVA, C., SCHERTEL, C., BASLER, K. & JOHNSTON, L. A. 2014. An ancient defense system eliminates unfit cells from developing tissues during cell competition. *Science,* 346**,** 1258236.

MI, H., HUANG, X., MURUGANUJAN, A., TANG, H., MILLS, C., KANG, D. & THOMAS, P. D. 2017. PANTHER version 11: expanded annotation data from Gene Ontology and Reactome pathways, and data analysis tool enhancements. *Nucleic Acids Res,* 45**,** D183-D189.

MITELMAN, F., MERTENS, F. & JOHANSSON, B. 1997. A breakpoint map of recurrent chromosomal rearrangements in human neoplasia. *Nat Genet,* 15 Spec No**,** 417-74.

MORATA, G. & RIPOLL, P. 1975. Minutes: mutants of drosophila autonomously affecting cell division rate. *Dev Biol,* 42**,** 211-21.

MORENO, E. & BASLER, K. 2004. dMyc transforms cells into super-competitors. *Cell,* 117**,** 117-29.

MORENO, E., BASLER, K. & MORATA, G. 2002. Cells compete for decapentaplegic survival factor to prevent apoptosis in Drosophila wing development. *Nature,* 416**,** 755-9.

MORENO, E., FERNANDEZ-MARRERO, Y., MEYER, P. & RHINER, C. 2015. Brain regeneration in Drosophila involves comparison of neuronal fitness. *Curr Biol,* 25**,** 955-63.

MOUSTAKAS, A. & HELDIN, C. H. 2009. The regulation of TGFbeta signal transduction. *Development,* 136**,** 3699-714.

MULLEN, A. C., ORLANDO, D. A., NEWMAN, J. J., LOVEN, J., KUMAR, R. M., BILODEAU, S., REDDY, J., GUENTHER, M. G., DEKOTER, R. P. & YOUNG, R. A. 2011. Master transcription factors determine cell-type-specific responses to TGF-beta signaling. *Cell,* 147**,** 565-76.

MUSACCHIO, A. 2015. The Molecular Biology of Spindle Assembly Checkpoint Signaling Dynamics. *Curr Biol,* 25**,** R1002-18.

NAKAO, A., IMAMURA, T., SOUCHELNYTSKYI, S., KAWABATA, M., ISHISAKI, A., OEDA, E., TAMAKI, K., HANAI, J., HELDIN, C. H., MIYAZONO, K. & TEN DIJKE, P. 1997. TGF-beta receptor-mediated signalling through Smad2, Smad3 and Smad4. *EMBO J,* 16**,** 5353-62.

NARVA, E., AUTIO, R., RAHKONEN, N., KONG, L., HARRISON, N., KITSBERG, D., BORGHESE, L., ITSKOVITZ-ELDOR, J., RASOOL, O., DVORAK, P., HOVATTA, O., OTONKOSKI, T., TUURI, T., CUI, W., BRUSTLE, O., BAKER, D., MALTBY, E., MOORE, H. D., BENVENISTY, N., ANDREWS, P. W., YLI-HARJA, O. & LAHESMAA, R. 2010. High-resolution DNA analysis of human embryonic stem cell lines reveals culture-induced copy number changes and loss of heterozygosity. *Nat Biotechnol,* 28**,** 371-7.

NG, E. S., DAVIS, R. P., AZZOLA, L., STANLEY, E. G. & ELEFANTY, A. G. 2005. Forced aggregation of defined numbers of human embryonic stem cells into embryoid bodies fosters robust, reproducible hematopoietic differentiation. *Blood,* 106**,** 1601-3.

NGUYEN, H. T., GEENS, M. & SPITS, C. 2013. Genetic and epigenetic instability in human pluripotent stem cells. *Hum Reprod Update,* 19**,** 187-205.

NORMAN, M., WISNIEWSKA, K. A., LAWRENSON, K., GARCIA-MIRANDA, P., TADA, M., KAJITA, M., MANO, H., ISHIKAWA, S., IKEGAWA, M., SHIMADA, T. & FUJITA, Y. 2012. Loss of Scribble causes cell competition in mammalian cells. *J Cell Sci,* 125**,** 59-66.

NUSSE, R. & CLEVERS, H. 2017. Wnt/beta-Catenin Signaling, Disease, and Emerging Therapeutic Modalities. *Cell,* 169**,** 985-999.

OERTEL, M., MENTHENA, A., DABEVA, M. D. & SHAFRITZ, D. A. 2006. Cell competition leads to a high level of normal liver reconstitution by transplanted fetal liver stem/progenitor cells. *Gastroenterology,* 130**,** 507-20; quiz 590.

OHGUSHI, M., MATSUMURA, M., EIRAKU, M., MURAKAMI, K., ARAMAKI, T., NISHIYAMA, A., MUGURUMA, K., NAKANO, T., SUGA, H., UENO, M., ISHIZAKI, T., SUEMORI, H., NARUMIYA, S., NIWA, H. & SASAI, Y. 2010. Molecular pathway and cell state responsible for dissociation-induced apoptosis in human pluripotent stem cells. *Cell Stem Cell,* 7**,** 225-39.

OHSAWA, S., SUGIMURA, K., TAKINO, K., XU, T., MIYAWAKI, A. & IGAKI, T. 2011. Elimination of oncogenic neighbors by JNK-mediated engulfment in Drosophila. *Dev Cell,* 20**,** 315-28.

OKA, M., TAGOKU, K., RUSSELL, T. L., NAKANO, Y., HAMAZAKI, T., MEYER, E. M., YOKOTA, T. & TERADA, N. 2002. CD9 is associated with leukemia inhibitory factor-mediated maintenance of embryonic stem cells. *Mol Biol Cell,* 13**,** 1274-81.

OLARIU, V., HARRISON, N. J., COCA, D., GOKHALE, P. J., BAKER, D., BILLINGS, S., KADIRKAMANATHAN, V. & ANDREWS, P. W. 2010. Modeling the evolution of culture-adapted human embryonic stem cells. *Stem Cell Res,* 4**,** 50-6.

OLTERSDORF, T., ELMORE, S. W., SHOEMAKER, A. R., ARMSTRONG, R. C., AUGERI, D. J., BELLI, B. A., BRUNCKO, M., DECKWERTH, T. L., DINGES, J., HAJDUK, P. J., JOSEPH, M. K., KITADA, S., KORSMEYER, S. J., KUNZER, A. R., LETAI, A., LI, C., MITTEN, M. J., NETTESHEIM, D. G., NG, S., NIMMER, P. M., O'CONNOR, J. M., OLEKSIJEW, A., PETROS, A. M., REED, J. C., SHEN, W., TAHIR, S. K., THOMPSON, C. B., TOMASELLI, K. J., WANG, B., WENDT, M. D., ZHANG, H., FESIK, S. W. & ROSENBERG, S. H. 2005. An inhibitor of Bcl-2 family proteins induces regression of solid tumours. *Nature,* 435**,** 677-81.

OMOLE, A. E. & FAKOYA, A. O. J. 2018. Ten years of progress and promise of induced pluripotent stem cells: historical origins, characteristics, mechanisms, limitations, and potential applications. *PeerJ,* 6**,** e4370.

ORR, B., GODEK, K. M. & COMPTON, D. 2015. Aneuploidy. *Curr Biol,* 25**,** R538-42.

ORSETTI, B., NUGOLI, M., CERVERA, N., LASORSA, L., CHUCHANA, P., URSULE, L., NGUYEN, C., REDON, R., DU MANOIR, S., RODRIGUEZ, C. & THEILLET, C. 2004. Genomic and expression profiling of chromosome 17 in breast cancer reveals complex patterns of alterations and novel candidate genes. *Cancer Res,* 64**,** 6453-60.

OSLOWSKI, C. M. & URANO, F. 2011. Measuring ER stress and the unfolded protein response using mammalian tissue culture system. *Methods Enzymol,* 490**,** 71-92.

PANOPOULOS, A. D., YANES, O., RUIZ, S., KIDA, Y. S., DIEP, D., TAUTENHAHN, R., HERRERIAS, A., BATCHELDER, E. M., PLONGTHONGKUM, N., LUTZ, M., BERGGREN, W. T., ZHANG, K., EVANS, R. M., SIUZDAK, G. & IZPISUA BELMONTE, J. C. 2012. The metabolome of induced pluripotent stem cells reveals metabolic changes occurring in somatic cell reprogramming. *Cell Res,* 22**,** 168-77.

PARK, J. H., SHIN, J. E. & PARK, H. W. 2018. The Role of Hippo Pathway in Cancer Stem Cell Biology. *Mol Cells,* 41**,** 83-92.

PENZO-MENDEZ, A. I., CHEN, Y. J., LI, J., WITZE, E. S. & STANGER, B. Z. 2015. Spontaneous Cell Competition in Immortalized Mammalian Cell Lines. *PLoS One,* 10**,** e0132437.

PETERS, J. M. 2002. The anaphase-promoting complex: proteolysis in mitosis and beyond. *Mol Cell,* 9**,** 931-43.

PETERSON, S. E., GARITAONANDIA, I. & LORING, J. F. 2016. The tumorigenic potential of pluripotent stem cells: What can we do to minimize it? *Bioessays,* 38 Suppl 1**,** S86-95.

PURI L, S. J. 2014. Getting a Clue from 1q: Gain of Chromosome 1q in Cancer. . *J Cancer Biol Res* 2**,** 1053.

QIN, H., YU, T., QING, T., LIU, Y., ZHAO, Y., CAI, J., LI, J., SONG, Z., QU, X., ZHOU, P., WU, J., DING, M. & DENG, H. 2007. Regulation of apoptosis and differentiation by p53 in human embryonic stem cells. *J Biol Chem,* 282**,** 5842-52.

RAO, J. & GREBER, B. 2017. Concise Review: Signaling Control of Early Fate Decisions Around the Human Pluripotent Stem Cell State. *Stem Cells,* 35**,** 277-283.

REUBINOFF, B. E., PERA, M. F., FONG, C. Y., TROUNSON, A. & BONGSO, A. 2000. Embryonic stem cell lines from human blastocysts: somatic differentiation in vitro. *Nat Biotechnol,* 18**,** 399-404.

RHINER, C., LOPEZ-GAY, J. M., SOLDINI, D., CASAS-TINTO, S., MARTIN, F. A., LOMBARDIA, L. & MORENO, E. 2010. Flower forms an extracellular code that reveals the fitness of a cell to its neighbors in Drosophila. *Dev Cell,* 18**,** 985-98.

RINKENBERGER, J. L., HORNING, S., KLOCKE, B., ROTH, K. & KORSMEYER, S. J. 2000. Mcl-1 deficiency results in peri-implantation embryonic lethality. *Genes Dev,* 14**,** 23-7.

RODRIGUEZ, E., HOULDSWORTH, J., REUTER, V. E., MELTZER, P., ZHANG, J., TRENT, J. M., BOSL, G. J. & CHAGANTI, R. S. 1993. Molecular cytogenetic analysis of i(12p)-negative human male germ cell tumors. *Genes Chromosomes Cancer,* 8**,** 230-6.

ROSEN, C., SHEZEN, E., ARONOVICH, A., KLIONSKY, Y. Z., YAAKOV, Y., ASSAYAG, M., BITON, I. E., TAL, O., SHAKHAR, G., BEN-HUR, H., SHNEIDER, D., VAKNIN, Z., SADAN, O., EVRON, S., FREUD, E., SHOSEYOV, D., WILSCHANSKI, M., BERKMAN, N., FIBBE, W. E., HAGIN, D., HILLEL-KARNIEL, C., KRENTSIS, I. M., BACHAR-LUSTIG, E. & REISNER, Y. 2015. Preconditioning allows engraftment of mouse and human embryonic lung cells, enabling lung repair in mice. *Nat Med,* 21**,** 869-79.

ROSLER, E. S., FISK, G. J., ARES, X., IRVING, J., MIURA, T., RAO, M. S. & CARPENTER, M. K. 2004. Long-term culture of human embryonic stem cells in feeder-free conditions. *Dev Dyn,* 229**,** 259-74.

RUCHAUD, S., CARMENA, M. & EARNSHAW, W. C. 2007. Chromosomal passengers: conducting cell division. *Nat Rev Mol Cell Biol,* 8**,** 798-812.

SAHAI, E. & MARSHALL, C. J. 2003. Differing modes of tumour cell invasion have distinct requirements for Rho/ROCK signalling and extracellular proteolysis. *Nat Cell Biol,* 5**,** 711-9.

SAITO-OHARA, F., IMOTO, I., INOUE, J., HOSOI, H., NAKAGAWARA, A., SUGIMOTO, T. & INAZAWA, J. 2003. PPM1D is a potential target for 17q gain in neuroblastoma. *Cancer Res,* 63**,** 1876-83.

SAKAKI-YUMOTO, M., LIU, J., RAMALHO-SANTOS, M., YOSHIDA, N. & DERYNCK, R. 2013. Smad2 is essential for maintenance of the human and mouse primed pluripotent stem cell state. *J Biol Chem,* 288**,** 18546-60.

SANCAR, A., LINDSEY-BOLTZ, L. A., UNSAL-KACMAZ, K. & LINN, S. 2004. Molecular mechanisms of mammalian DNA repair and the DNA damage checkpoints. *Annu Rev Biochem,* 73**,** 39-85.

SANCHO, M., DI-GREGORIO, A., GEORGE, N., POZZI, S., SANCHEZ, J. M., PERNAUTE, B. & RODRIGUEZ, T. A. 2013. Competitive interactions eliminate unfit embryonic stem cells at the onset of differentiation. *Dev Cell,* 26**,** 19-30.

SANO, R. & REED, J. C. 2013. ER stress-induced cell death mechanisms. *Biochim Biophys Acta,* 1833**,** 3460-3470.

SANTAGUIDA, S. & AMON, A. 2015. Short- and long-term effects of chromosome mis-segregation and aneuploidy. *Nat Rev Mol Cell Biol,* 16**,** 473-85.

SASAKI, A., NAGATAKE, T., EGAMI, R., GU, G., TAKIGAWA, I., IKEDA, W., NAKATANI, T., KUNISAWA, J. & FUJITA, Y. 2018. Obesity Suppresses Cell-Competition-Mediated Apical Elimination of RasV12-Transformed Cells from Epithelial Tissues. *Cell Rep,* 23**,** 974-982.

SELTMANN, S., LEKSCHAS, F., MULLER, R., STACHELSCHEID, H., BITTNER, M. S., ZHANG, W., KIDANE, L., SERIOLA, A., VEIGA, A., STACEY, G. & KURTZ, A. 2016. hPSCreg--the human pluripotent stem cell registry. *Nucleic Acids Res,* 44**,** D757-63.

SHALTIEL, I. A., KRENNING, L., BRUINSMA, W. & MEDEMA, R. H. 2015. The same, only different - DNA damage checkpoints and their reversal throughout the cell cycle. *J Cell Sci,* 128**,** 607-20.

SHAMAS-DIN, A., KALE, J., LEBER, B. & ANDREWS, D. W. 2013. Mechanisms of action of Bcl-2 family proteins. *Cold Spring Harb Perspect Biol,* 5**,** a008714.

SHEVINSKY, L. H., KNOWLES, B. B., DAMJANOV, I. & SOLTER, D. 1982. Monoclonal antibody to murine embryos defines a stage-specific embryonic antigen expressed on mouse embryos and human teratocarcinoma cells. *Cell,* 30**,** 697-705.

SHRAIMAN, B. I. 2005. Mechanical feedback as a possible regulator of tissue growth. *Proc Natl Acad Sci U S A,* 102**,** 3318-23.

SIMPSON, P. & MORATA, G. 1981. Differential mitotic rates and patterns of growth in compartments in the Drosophila wing. *Dev Biol,* 85**,** 299-308.

SINGH, A. M., REYNOLDS, D., CLIFF, T., OHTSUKA, S., MATTHEYSES, A. L., SUN, Y., MENENDEZ, L., KULIK, M. & DALTON, S. 2012. Signaling network crosstalk in human pluripotent cells: a Smad2/3-regulated switch that controls the balance between self-renewal and differentiation. *Cell Stem Cell,* 10**,** 312-26.

SMITH, J. R., VALLIER, L., LUPO, G., ALEXANDER, M., HARRIS, W. A. & PEDERSEN, R. A. 2008. Inhibition of Activin/Nodal signaling promotes specification of human embryonic stem cells into neuroectoderm. *Dev Biol,* 313**,** 107-17.

SPITS, C., MATEIZEL, I., GEENS, M., MERTZANIDOU, A., STAESSEN, C., VANDESKELDE, Y., VAN DER ELST, J., LIEBAERS, I. & SERMON, K. 2008. Recurrent chromosomal abnormalities in human embryonic stem cells. *Nat Biotechnol,* 26**,** 1361-3.

STEIN, C., BARDET, A. F., ROMA, G., BERGLING, S., CLAY, I., RUCHTI, A., AGARINIS, C., SCHMELZLE, T., BOUWMEESTER, T., SCHUBELER, D. & BAUER, A. 2015. YAP1 Exerts Its Transcriptional Control via TEAD-Mediated Activation of Enhancers. *PLoS Genet,* 11**,** e1005465.

SUDAKIN, V., CHAN, G. K. & YEN, T. J. 2001. Checkpoint inhibition of the APC/C in HeLa cells is mediated by a complex of BUBR1, BUB3, CDC20, and MAD2. *J Cell Biol,* 154**,** 925-36.

SUIJKERBUIJK, S. J., KOLAHGAR, G., KUCINSKI, I. & PIDDINI, E. 2016. Cell Competition Drives the Growth of Intestinal Adenomas in Drosophila. *Curr Biol,* 26**,** 428-38.

SUN, Q., LUO, T., REN, Y., FLOREY, O., SHIRASAWA, S., SASAZUKI, T., ROBINSON, D. N. & OVERHOLTZER, M. 2014. Competition between human cells by entosis. *Cell Res,* 24**,** 1299-310.

SUN, Y., LIU, W. Z., LIU, T., FENG, X., YANG, N. & ZHOU, H. F. 2015. Signaling pathway of MAPK/ERK in cell proliferation, differentiation, migration, senescence and apoptosis. *J Recept Signal Transduct Res,* 35**,** 600-4.

SUPEK, F., BOSNJAK, M., SKUNCA, N. & SMUC, T. 2011. REVIGO summarizes and visualizes long lists of gene ontology terms. *PLoS One,* 6**,** e21800.

TAIT, S. W., ICHIM, G. & GREEN, D. R. 2014. Die another way--non-apoptotic mechanisms of cell death. *J Cell Sci,* 127**,** 2135-44.

TAKAHASHI, K., TANABE, K., OHNUKI, M., NARITA, M., ICHISAKA, T., TOMODA, K. & YAMANAKA, S. 2007. Induction of pluripotent stem cells from adult human fibroblasts by defined factors. *Cell,* 131**,** 861-72.

TAKAHASHI, K. & YAMANAKA, S. 2006. Induction of pluripotent stem cells from mouse embryonic and adult fibroblast cultures by defined factors. *Cell,* 126**,** 663-76.

TAMORI, Y., BIALUCHA, C. U., TIAN, A. G., KAJITA, M., HUANG, Y. C., NORMAN, M., HARRISON, N., POULTON, J., IVANOVITCH, K., DISCH, L., LIU, T., DENG, W. M. & FUJITA, Y. 2010. Involvement of Lgl and Mahjong/VprBP in cell competition. *PLoS Biol,* 8**,** e1000422.

TATENO, H., HIEMORI, K., HIRAYASU, K., SOUGAWA, N., FUKUDA, M., WARASHINA, M., AMANO, M., FUNAKOSHI, T., SADAMURA, Y., MIYAGAWA, S., SAITO, A., SAWA, Y., SHOFUDA, T., SUMIDA, M., KANEMURA, Y., NAKAMURA, M., OKANO, H., ONUMA, Y., ITO, Y., ASASHIMA, M. & HIRABAYASHI, J.

2017. Development of a practical sandwich assay to detect human pluripotent stem cells using cell culture media. *Regen Ther,* 6**,** 1-8.

TEO, A. K., ALI, Y., WONG, K. Y., CHIPPERFIELD, H., SADASIVAM, A., POOBALAN, Y., TAN, E. K., WANG, S. T., ABRAHAM, S., TSUNEYOSHI, N., STANTON, L. W. & DUNN, N. R. 2012. Activin and BMP4 synergistically promote formation of definitive endoderm in human embryonic stem cells. *Stem Cells,* 30**,** 631-42.

TERRYN, J., TRICOT, T., GAJJAR, M. & VERFAILLIE, C. 2018. Recent advances in lineage differentiation from stem cells: hurdles and opportunities? *F1000Res,* 7**,** 220.

THEISSEN, J., OBERTHUER, A., HOMBACH, A., VOLLAND, R., HERTWIG, F., FISCHER, M., SPITZ, R., ZAPATKA, M., BRORS, B., ORTMANN, M., SIMON, T., HERO, B. & BERTHOLD, F. 2014. Chromosome 17/17q gain and unaltered profiles in high resolution array-CGH are prognostically informative in neuroblastoma. *Genes Chromosomes Cancer,* 53**,** 639-49.

THEUNISSEN, T. W. & JAENISCH, R. 2017. Mechanisms of gene regulation in human embryos and pluripotent stem cells. *Development,* 144**,** 4496-4509.

THIES, R. S. & MURRY, C. E. 2015. The advancement of human pluripotent stem cell-derived therapies into the clinic. *Development,* 142**,** 3077-84.

THOMSON, J. A., ITSKOVITZ-ELDOR, J., SHAPIRO, S. S., WAKNITZ, M. A., SWIERGIEL, J. J., MARSHALL, V. S. & JONES, J. M. 1998. Embryonic stem cell lines derived from human blastocysts. *Science,* 282**,** 1145-7.

TICHY, E. D. 2011. Mechanisms maintaining genomic integrity in embryonic stem cells and induced pluripotent stem cells. *Exp Biol Med (Maywood),* 236**,** 987-96.

TONGE, P. D., SHIGETA, M., SCHROEDER, T. & ANDREWS, P. W. 2011. Functionally defined substates within the human embryonic stem cell compartment. *Stem Cell Res,* 7**,** 145-53.

TSANKOV, A. M., AKOPIAN, V., POP, R., CHETTY, S., GIFFORD, C. A., DAHERON, L., TSANKOVA, N. M. & MEISSNER, A. 2015. A qPCR ScoreCard quantifies the differentiation potential of human pluripotent stem cells. *Nat Biotechnol,* 33**,** 1182-92.

TSUBOI, A., OHSAWA, S., UMETSU, D., SANDO, Y., KURANAGA, E., IGAKI, T. & FUJIMOTO, K. 2018. Competition for Space Is Controlled by Apoptosis-Induced Change of Local Epithelial Topology. *Curr Biol,* 28**,** 2115-2128 e5.

TSUKAZAKI, T., CHIANG, T. A., DAVISON, A. F., ATTISANO, L. & WRANA, J. L. 1998. SARA, a FYVE domain protein that recruits Smad2 to the TGFbeta receptor. *Cell,* 95**,** 779-91.

UNGER, C., SKOTTMAN, H., BLOMBERG, P., DILBER, M. S. & HOVATTA, O. 2008. Good manufacturing practice and clinical-grade human embryonic stem cell lines. *Hum Mol Genet,* 17**,** R48-53.

URYU, K., NISHIMURA, R., KATAOKA, K., SATO, Y., NAKAZAWA, A., SUZUKI, H., YOSHIDA, K., SEKI, M., HIWATARI, M., ISOBE, T., SHIRAISHI, Y., CHIBA, K., TANAKA, H., MIYANO, S., KOH, K., HANADA, R., OKA, A., HAYASHI, Y., OHIRA, M., KAMIJO, T., NAGASE, H., TAKIMOTO, T., TAJIRI, T., NAKAGAWARA, A., OGAWA, S. & TAKITA, J. 2017. Identification of the genetic and clinical characteristics of neuroblastomas using genome-wide analysis. *Oncotarget,* 8**,** 107513-107529.

VALLIER, L., ALEXANDER, M. & PEDERSEN, R. A. 2005. Activin/Nodal and FGF pathways cooperate to maintain pluripotency of human embryonic stem cells. *J Cell Sci,* 118**,** 4495-509.

VALLIER, L., TOUBOUL, T., CHNG, Z., BRIMPARI, M., HANNAN, N., MILLAN, E., SMITHERS, L. E., TROTTER, M., RUGG-GUNN, P., WEBER, A. & PEDERSEN, R. A. 2009. Early cell fate decisions of human embryonic stem cells and mouse epiblast stem cells are controlled by the same signalling pathways. *PLoS One,* 4**,** e6082.

VAN DER WAAL, M. S., HENGEVELD, R. C., VAN DER HORST, A. & LENS, S. M. 2012. Cell division control by the Chromosomal Passenger Complex. *Exp Cell Res,* 318**,** 1407-20.

VAN JAARSVELD, R. H. & KOPS, G. 2016. Difference Makers: Chromosomal Instability versus Aneuploidy in Cancer. *Trends Cancer,* 2**,** 561-571.

VANDER HEIDEN, M. G., CANTLEY, L. C. & THOMPSON, C. B. 2009. Understanding the Warburg effect: the metabolic requirements of cell proliferation. *Science,* 324**,** 1029-33.

VARELA, C., DENIS, J. A., POLENTES, J., FEYEUX, M., AUBERT, S., CHAMPON, B., PIETU, G., PESCHANSKI, M. & LEFORT, N. 2012. Recurrent genomic instability of chromosome 1q in neural derivatives of human embryonic stem cells. *J Clin Invest,* 122**,** 569-74.

VILLA DEL CAMPO, C., CLAVERIA, C., SIERRA, R. & TORRES, M. 2014. Cell competition promotes phenotypically silent cardiomyocyte replacement in the mammalian heart. *Cell Rep,* 8**,** 1741-1751.

VINCENT, J. P., FLETCHER, A. G. & BAENA-LOPEZ, L. A. 2013. Mechanisms and mechanics of cell competition in epithelia. *Nat Rev Mol Cell Biol,* 14**,** 581-91.

VLEUGEL, M., HOOGENDOORN, E., SNEL, B. & KOPS, G. J. 2012. Evolution and function of the mitotic checkpoint. *Dev Cell,* 23**,** 239-50.

VOLAREVIC, V., MARKOVIC, B. S., GAZDIC, M., VOLAREVIC, A., JOVICIC, N., ARSENIJEVIC, N., ARMSTRONG, L., DJONOV, V., LAKO, M. & STOJKOVIC, M. 2018. Ethical and Safety Issues of Stem Cell-Based Therapy. *Int J Med Sci,* 15**,** 36-45.

WAGSTAFF, L., GOSCHORSKA, M., KOZYRSKA, K., DUCLOS, G., KUCINSKI, I., CHESSEL, A., HAMPTON-O'NEIL, L., BRADSHAW, C. R., ALLEN, G. E., RAWLINS, E. L., SILBERZAN, P., CARAZO SALAS, R. E. & PIDDINI, E. 2016. Mechanical cell competition kills cells via induction of lethal p53 levels. *Nat Commun,* 7**,** 11373.

WATANABE, K., UENO, M., KAMIYA, D., NISHIYAMA, A., MATSUMURA, M., WATAYA, T., TAKAHASHI, J. B., NISHIKAWA, S., NISHIKAWA, S., MUGURUMA, K. & SASAI, Y. 2007. A ROCK inhibitor permits survival of dissociated human embryonic stem cells. *Nat Biotechnol,* 25**,** 681-6.

WEAVER, B. A. & CLEVELAND, D. W. 2005. Decoding the links between mitosis, cancer, and chemotherapy: The mitotic checkpoint, adaptation, and cell death. *Cancer Cell,* 8**,** 7-12.

WECKSELBLATT, B., HERMETZ, K. E. & RUDD, M. K. 2015. Unbalanced translocations arise from diverse mutational mechanisms including chromothripsis. *Genome Res,* 25**,** 937-47.

WEISSBEIN, U., BENVENISTY, N. & BEN-DAVID, U. 2014. Quality control: Genome maintenance in pluripotent stem cells. *J Cell Biol,* 204**,** 153-63.

WERBOWETSKI-OGILVIE, T. E., BOSSE, M., STEWART, M., SCHNERCH, A., RAMOS-MEJIA, V., ROULEAU, A., WYNDER, T., SMITH, M. J., DINGWALL, S., CARTER, T., WILLIAMS, C., HARRIS, C., DOLLING, J., WYNDER, C., BOREHAM, D. & BHATIA, M. 2009. Characterization of human embryonic stem cells with features of neoplastic progression. *Nat Biotechnol,* 27**,** 91-7.

WERBOWETSKI-OGILVIE, T. E., SCHNERCH, A., RAMPALLI, S., MILLS, C. E., LEE, J. B., HONG, S. H., LEVADOUX-MARTIN, M. & BHATIA, M. 2011. Evidence for the transmission of neoplastic properties from transformed to normal human stem cells. *Oncogene,* 30**,** 4632-44.

WILLIAMS, B. P., DANIELS, G. L., PYM, B., SHEER, D., POVEY, S., OKUBO, Y., ANDREWS, P. W. & GOODFELLOW, P. N. 1988. Biochemical and genetic analysis of the OKa blood group antigen. *Immunogenetics,* 27**,** 322-9.

XU, C., ROSLER, E., JIANG, J., LEBKOWSKI, J. S., GOLD, J. D., O'SULLIVAN, C., DELAVAN-BOORSMA, K., MOK, M., BRONSTEIN, A. & CARPENTER, M. K. 2005. Basic fibroblast growth factor supports undifferentiated human embryonic stem cell growth without conditioned medium. *Stem Cells,* 23**,** 315-23.

XU, R. H., SAMPSELL-BARRON, T. L., GU, F., ROOT, S., PECK, R. M., PAN, G., YU, J., ANTOSIEWICZ-BOURGET, J., TIAN, S., STEWART, R. & THOMSON, J. A. 2008. NANOG is a direct target of TGFbeta/activin-mediated SMAD signaling in human ESCs. *Cell Stem Cell,* 3**,** 196-206.

YANG, S., LIN, G., TAN, Y. Q., DENG, L. Y., YUAN, D. & LU, G. X. 2010. Differences between karyotypically normal and abnormal human embryonic stem cells. *Cell Prolif,* 43**,** 195-206.

YANG, S., LIN, G., TAN, Y. Q., ZHOU, D., DENG, L. Y., CHENG, D. H., LUO, S. W., LIU, T. C., ZHOU, X. Y., SUN, Z., XIANG, Y., CHEN, T. J., WEN, J. F. & LU, G. X. 2008. Tumor progression of culture-adapted human embryonic stem cells during long-term culture. *Genes Chromosomes Cancer,* 47**,** 665-79.

YE, J., BATES, N., SOTERIOU, D., GRADY, L., EDMOND, C., ROSS, A., KERBY, A., LEWIS, P. A., ADENIYI, T., WRIGHT, R., POULTON, K. V., LOWE, M., KIMBER, S. J. & BRISON, D. R. 2017. High quality clinical grade human embryonic stem cell lines derived from fresh discarded embryos. *Stem Cell Res Ther,* 8**,** 128.

ZHANG, J. H. & XU, M. 2000. DNA fragmentation in apoptosis. *Cell Res,* 10**,** 205-11.

ZHANG, L. & SHAY, J. W. 2017. Multiple Roles of APC and its Therapeutic Implications in Colorectal Cancer. *J Natl Cancer Inst,* 109.

ZHANG, W. & YU, Y. 2011. The important molecular markers on chromosome 17 and their clinical impact in breast cancer. *Int J Mol Sci,* 12**,** 5672-83.

ZHU, Z. & HUANGFU, D. 2013. Human pluripotent stem cells: an emerging model in developmental biology. *Development,* 140**,** 705-17.

ZUBA-SURMA, E. K., JOZKOWICZ, A. & DULAK, J. 2011. Stem cells in pharmaceutical biotechnology. *Curr Pharm Biotechnol,* 12**,** 1760-73.

ZUBA-SURMA, E. K., WOJAKOWSKI, W., MADEJA, Z. & RATAJCZAK, M. Z. 2012. Stem cells as a novel tool for drug screening and treatment of degenerative diseases. *Curr Pharm Des,* 18**,** 2644-56.
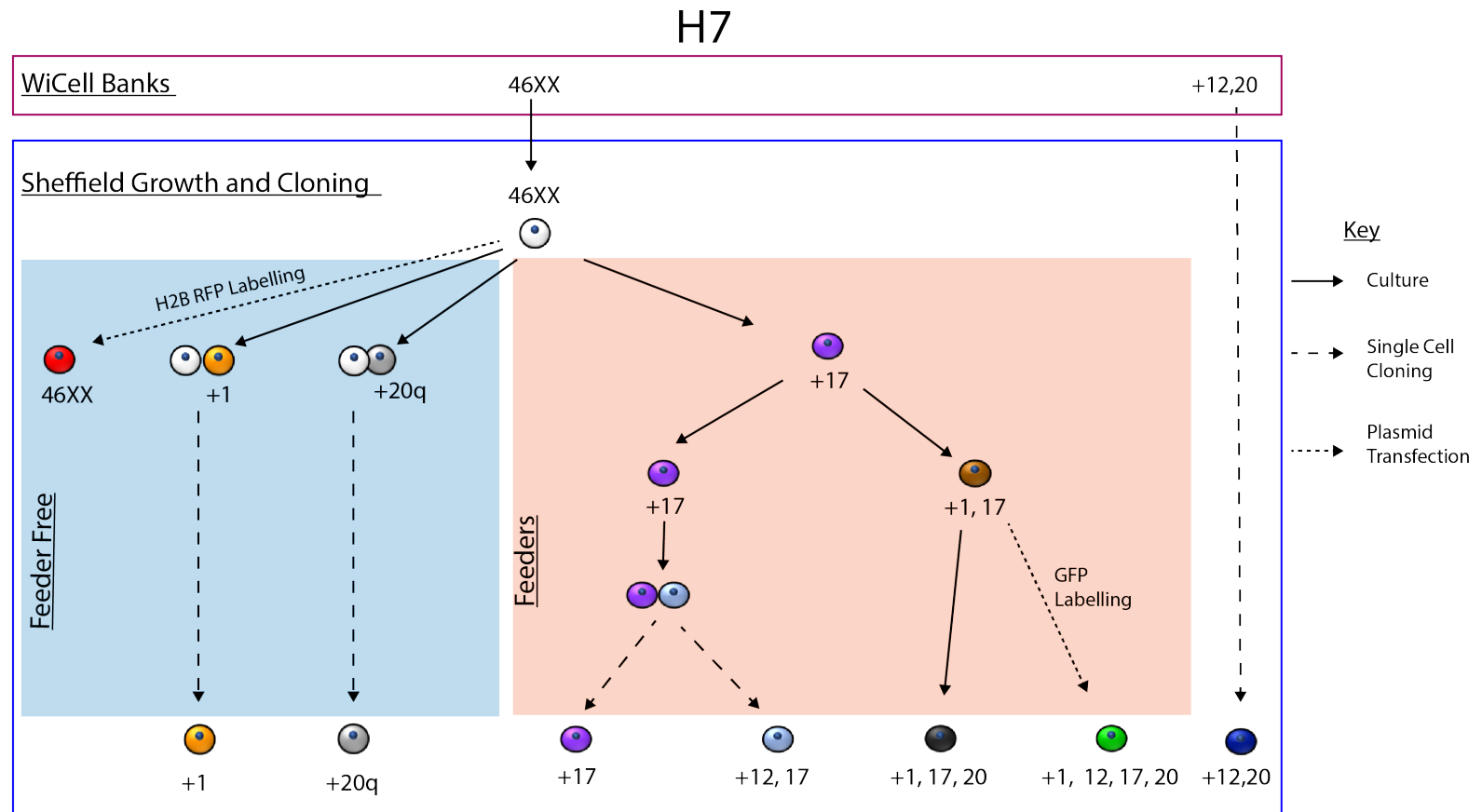
Figure 9.1 Schematic diagram of the appearance and isolation of variant hPSC lines used within this study

Karyotypically normal H7 (46,XX) hPSCs were originally acquired from WiCell. During the subsequent culture at the Centre for Stem Cell Biology in Sheffield variants with karyotypic abnormalities spontaneously arose during culture and were cloned out following their detection by either G-banding or FISH. Where known, the culture conditions cells were grown in is indicated by the background shading.

A

$$y_1(t) = Ae^{k_1 t} \qquad\qquad y_2(t) = Be^{k_2 t}$$

$t = time\ (hours)$

$A = Ratio\ of\ cell\ population\ 1\ at\ t(0)$

$B = Ratio\ of\ cell\ population\ 2\ at\ t(0)$

$$k = \frac{\ln(2)}{cell\ cycle\ time\ (hours)}$$

B

Equation for normal hPSCs   Equation for variant hPSCs
                                  + gain of chromsome 17

$$y_1(t) = 9e^{\frac{\ln(2)}{16}t} \qquad\qquad y_2(t) = e^{\frac{\ln(2)}{14}t}$$

C

Days in Culture	Time in hours	Number of normal hPSCS	Number of variant hPSCs + gain of chromosome 17	Percentage of variant cells
Day 0	0	9	1	10.00%
Day 1	24	25	3	11.42%
Day 2	48	72	11	13.01%
Day 3	72	204	35	14.78%
Day 4	96	576	116	16.75%
Day 5	120	1,629	380	18.93%
Day 6	144	4,608	1,248	21.32%
Day 7	168	13,033	4,096	23.91%
Day 8	192	36,864	13,440	26.72%
Day 9	216	104,267	44,102	29.72%
Day 10	240	294,912	144,715	32.92%
Day 11	264	834,137	474,860	36.28%
Day 12	288	2,359,296	1,558,178	39.78%
Day 13	312	6,673,097	5,122,914	43.43%
Day 14	336	18,874,368	16,777,216	47.06%
Day 15	360	53,384,774	55,051,774	50.77%
Day 16	384	150,994,944	180,643,666	54.47%
Day 17	408	427,078,195	592,753,544	58.12%
Day 18	432	1,207,959,552	1,945,026,759	61.69%
Day 19	456	3,416,625,562	6,382,296,874	65.13%
Day 20	480	9,663,676,416	20,942,249,511	68.43%

Figure 9.2 Simulated data of population growth based on cell cycle time only relating to Figure 3.8

(A) The exponential growth rate equations used to model the population doubling time of two different cell populations **(B)** Exponential growth rate equations used to calculate the population growth rates of normal hPSCs and variant hPSCs possessing gain of chromosome 17 starting at a 9:1 ratio. **(C)** Table of results from the modelling of normal and variant hPSCs population growth using the equations described in *(B)*.
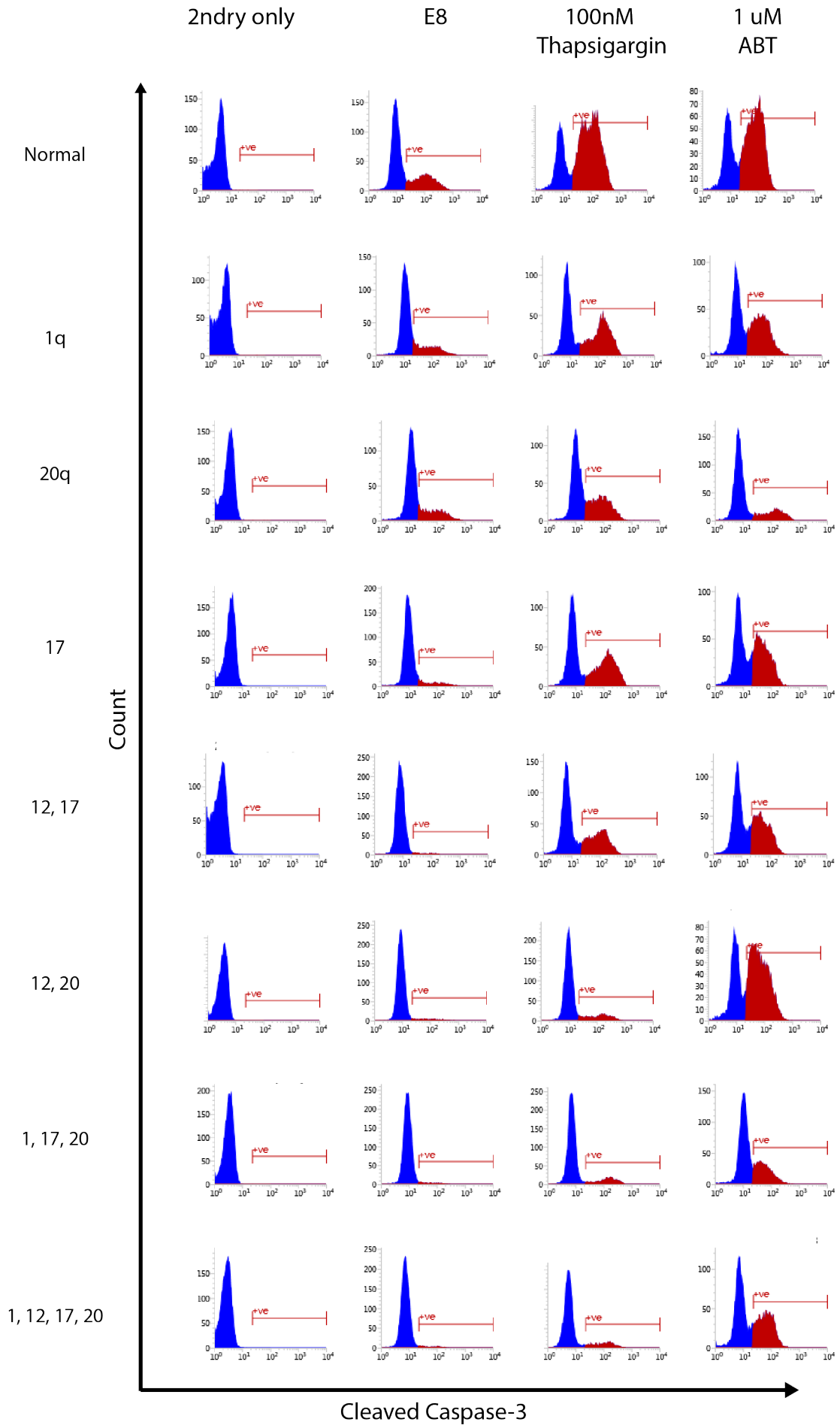
Figure 9.3 Representative Flow Cytometric histograms of cleaved caspase staining relating to Figure 3.10

Flow cytometric histograms for cleaved caspase-3 staining in normal and variant hPSC lines grown either in E8, E8 supplemented with 100nM Thapsigargin or E8 supplemented with 1μM ABT. In all histograms blue represents negative staining, and red indicates positive antibody staining.
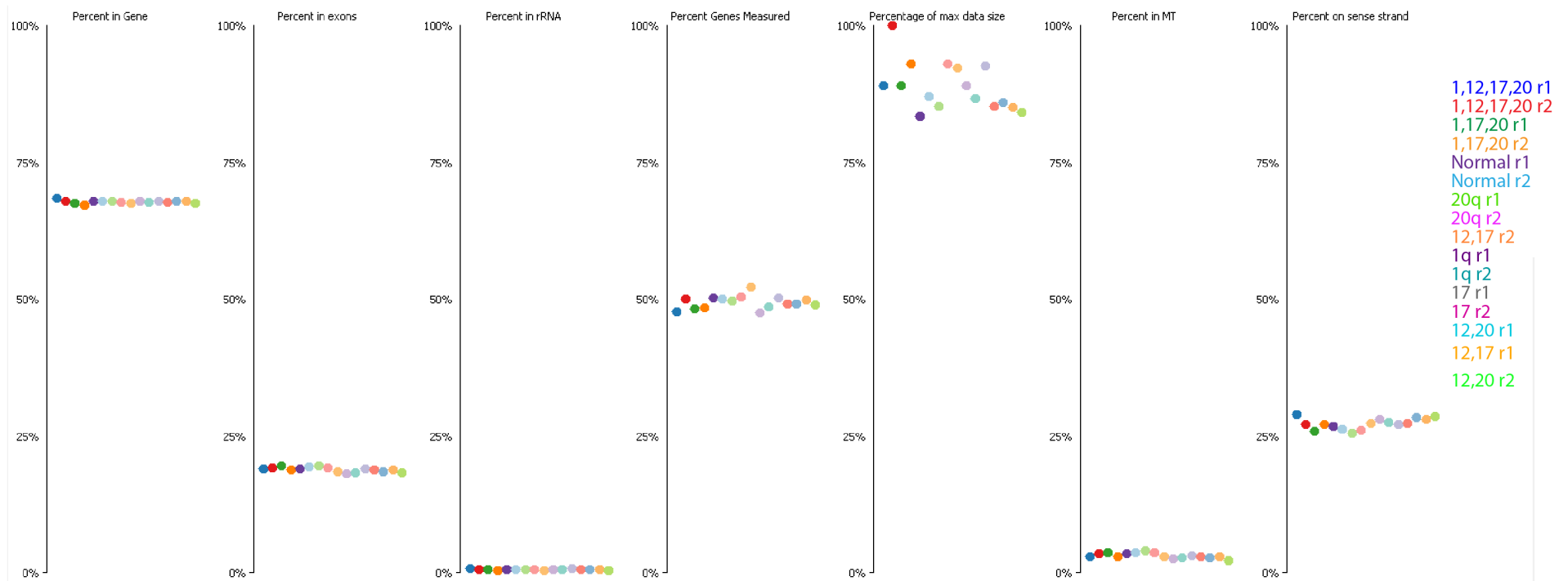
Figure 9.4 RNA sequencing quality control analysis

Quality control analysis of RNA sequencing data from normal and karyotypically variant hPSC samples. Each coloured dot represents the corresponding sample in the list on the right-hand side of the plot. Samples are organised horizontally in the same order as they appear vertically in the sample list.